Use of baculovirus surface display for characterization of AHSV4-VP2 antigenic structure

Mine Aksular

A thesis submitted in partial fulfilment of the requirements of Oxford Brookes University for the degree of

Doctor of Philosophy

This research programme was carried out in collaboration with Oxford Expression Technologies Ltd and The Pirbright Institute

OXFORD BROOKES UNIVERSITY

OXFORD EXPRESSION TECHNOLOGIES

THE Pirbright INSTITUTE

January 2017

Abstract

African horse sickness is an infectious, non-contagious, insect vector-borne disease of equids. It is highly lethal and mortality rates can exceed 90% in susceptible populations. The disease is caused by African horse sickness virus (AHSV), which is mostly endemic in sub-Saharan Africa. However, occasional outbreaks have occurred outside Africa, such as the devastating AHSV-9 outbreak in 1959 reaching India and Pakistan or the European outbreaks caused by serotype 4 (AHSV4) between 1987 and 1993. AHS is an OIE (World Organisation for Animal Health) listed disease for its impact on animal health economy and international trade of equids.

The prevention of disease is mainly dependent on an efficient vaccination regime. However, the current live-attenuated vaccines are not considered safe for use in non-endemic regions. Sub-unit protein vaccines expressed from recombinant baculoviruses are an option for generating safe vaccines due to the absence of pre-existing immunity, non-toxicity in mammalian systems and their inability to replicate in mammalian cells. In addition, the fact that AHSV replicates in insect cells during its transmission to a mammalian host, makes the baculovirus insect cell expression system very advantageous for the production of correctly-folded AHSV proteins. Baculoviruses can also be used to display foreign antigens on the baculovirus envelope surface, which is very beneficial for studying protein-protein interactions.

The AHSV major outer capsid protein, VP2, is a good target for subunit vaccine studies as it has been shown to be the main-serotype specific antigen, carrying virus neutralising (VN) epitopes. This thesis focused on investigating the antigenic structure of AHSV4-VP2. Full-length AHSV-VP2 and eleven subdomains thereof were expressed using standard baculovirus expression systems and a baculovirus surface display approach. The antigenic properties of these proteins were studied using a range of techniques including; immunoblotting and ELISA in order to gain further understanding of the properties of VN epitopes. Understanding the antigenic structure of this major immunogenic protein is paramount for generating more efficient, safe vaccines.

This thesis demonstrated the benefits of using TnHi5 cells for the production of full-length VP2. In addition, polyhistidine-tag affinity-purified VP2 was shown to retain biological functions, generating VNAbs in mice, unlike the purified VP2 indicated in the literature.

All eleven VP2 subdomains were successfully produced by baculoviruses, however, the surface display constructs greatly improved the yield of these proteins when compared to their synthesis as individual proteins. The antigenicity of VP2 subdomains was investigated by several *in vitro* binding assays using AHSV4-VP2-specific antibodies and a vaccination study in mice.

Although previous studies found the amino terminal half of the protein to be more antigenic, this thesis provided evidence that the carboxy terminus might play a role in the formation of important antigenic epitopes, including those involved in virus neutralisation. It was also demonstrated that VN epitopes of VP2 are highly conformational and difficult to mimic using individual subdomains. These results raised the question whether AHSV neutralisation is a multifunctional process and whether trimerisation is a critical factor in the formation of VNAb epitopes and the induction of VNAb when VP2-based vaccines are used. Additional studies aimed at advancing further our knowledge of AHSV-VP2 were suggested.

Presentations

The work described in this thesis has been presented at international conferences and seminars in the form of posters and oral presentations.

Posters

Aksular, M, Chambers A. C., Castillo-Olivares, J., King, L. A. (2014) Recombinant vaccines for African horse sickness based on baculovirus pseudotyping and transduction. Student Day, The Pirbright Institute, Woking, UK.

Aksular, M, Chambers A. C., Castillo-Olivares, J., King, L. A. (2015) Recombinant vaccines against African horse sickness based on baculovirus expression and pseudotyping. Postgraduate Research Student Symposium, Oxford Brookes University, Oxford, UK.

Aksular, M, Chambers A. C., Castillo-Olivares, J., King, L. A. (2015) Recombinant vaccines against African horse sickness based on baculovirus expression and pseudotyping. Impact Conference, Oxford Brookes University, Oxford, UK

Aksular, M, Chambers A. C., Castillo-Olivares, J., R. D. Possee, King, L. A. (2016). Improving Baculovirus Surface Display System. 49th Annual Meeting of the Society for Invertebrate Pathology, Tours, France. **Winner of 2nd place prize for best student poster presentation.**

Oral Presentations

Aksular, M, Chambers A. C., Castillo-Olivares, J., King, L. A. (2013) Recombinant vaccines for African horse sickness based on baculovirus pseudotyping and transduction. Student seminar series. The Pirbright Institute, Woking, UK.

Aksular, M, Chambers A. C., Castillo-Olivares, J., King, L. A. (2014) Recombinant vaccines for African horse sickness based on baculovirus pseudotyping and transduction. Postgraduate Research Student Symposium, Oxford Brookes University, Oxford, UK.

Aksular, M, Chambers A. C., Castillo-Olivares, J., King, L. A. (2014) Recombinant vaccines for African horse sickness based on baculovirus pseudotyping and transduction. Student seminar series. The Pirbright Institute, Woking, UK.

Aksular, M, Chambers A. C., Castillo-Olivares, J., King, L. A. (2014) Recombinant vaccines for African horse sickness based on baculovirus pseudotyping and transduction. Lunch time seminar series. The Pirbright Institute, Woking, UK.

Aksular, M, Chambers A. C., Castillo-Olivares, J., King, L. A. (2015) Recombinant vaccines for African horse sickness based on baculovirus pseudotyping and transduction. Seminar series. The Pirbright Institute, Woking, UK.

Aksular, M, Chambers A. C., Castillo-Olivares, J., King, L. A. (2015) Use of baculovirus pseudotyping to characterise the antigenic structure of AHSV-VP2. Student Day. The Pirbright Institute, Woking, UK.

Aksular, M, Chambers A. C., Castillo-Olivares, J., King, L. A. (2016) Use of baculovirus pseudotyping to characterise the antigenic structure of AHSV-VP2. Biomedical and Medical Sciences Seminar Series. Oxford Brookes University, Oxford, UK.

Flash Presentations

(5 minute oral presentation and a poster presentation)

Aksular, M, Chambers A. C., Castillo-Olivares, J., King, L. A. (2016). Use of baculovirus pseudotyping to characterise the antigenic structure of AHSV-VP2. 10th Annual Meeting EPIZONE, Madrid, Spain.

Acknowledgements

The last four years of my life have been an incredible learning journey. As well as science, I have learnt so much about life, being more patient, having to carry on even at hardest times and experiencing the joy of achievements. This journey could not have been completed without certain people and I have long waited to write this section of my thesis to take the opportunity to thank you all.

Initially, I would like to thank my supervisors Professor Linda King and Dr Javier Castillo-Olivares for giving me the opportunity to carry out this project but also their support and guidance throughout these four years-well appreciated! I would like to use this opportunity to thank Oxford Brookes University, Oxford Expression Technologies and The Pirbright Institute, who were the three collaborators of my PhD, for providing the studentship.

Next, I would like to thank all the members of IVRG; Leo, Sarah, Carina, Raquel, Riyadh and all the members of Oxford Expression Technologies for their continuing support and making these four years even more enjoyable! ☺. A special thanks goes to Olga for all her help for protein purification and also to Bob, for all the helpful discussions and wise guidance in general lab work! I also would like to thank Dr Eva Calvo, Dr Javier Ortego and all people involved at CISA-INIA, Madrid, Spain for carrying out the mice vaccination experiments.

Now I would like to move on and thank to all my friends, especially 'bocx'; Gun, Mel and Fik, and also Deniz, my childhood friend, for always being there and supporting me. Thank you for all the spirit-lifting conversations, your understanding and sorry if I weren't myself as a friend especially during the last stages of the PhD.

Now moving on to the people who were physically far far apart but the ones closest to the heart-my family! Your unconditional love, support and belief in me was the one thing that always kept me going. There were times I was at the edge, questioning whether I could do it. And it was your love and the thought of not disappointing you gave me the strength to carry on. My sister gave me a special present during my PhD, which was the birth of my lovely nephew, Demir. It's incredible how the smile of a baby on a camera lifts your spirit and makes you forget everything you are worrying about! So glad to have a sunshine like you in my life teyzecigim!. And now couple of sentences in Turkish for you all. Canim ailem, sizin sevginiz, desteginiz ve bana olan inanciniz olmasa, asla ve asla buralara gelemezdim. En zor anlarda bile, sizin varliginiz ve inanciniz bana guc verdi. Sizin gibi bir ailem oldugu icin dunyadaki en sansli insanim gercekten! Size ne kadar tesekkur etsem az-iyiki varsiniz, hepinizi cok ama cok seviyorum. Ayrica bahsetmeliyim ki, sen daha

minicik olsan da farkinda olmadan bana bu doktora surecinde en buyuk desdegi verenlerden biriydin Demir, senin bir gulusunun bana ne kadar huzur ve devam etme gucu verdigini tahmin bile edemezsin. Seni cok seviyorum teyzecigim.

And now the one and only person who I do not even know where to start thanking, **Adam**. There are no words to describe how much I appreciated your support, help and guidance throughout this whole time. You are the one person that has gone through this with me every single day at work and at home. There were times I could not even bear myself, and yet you were still there listening, helping and supporting me. I really think I couldn't have come this far if you weren't this understanding, loving and supporting. Thank you ever so much canim, my husband to be, for being in my life and for being you. I am the luckiest girl-love you so so much!

I am also grateful to Adam's family for their support during this period.

Finally, I should also mention that my love for music and passion for playing the piano helped smoothen the roads of this pebbly journey!

Thank you all!

Contents Page

Abstract i
Presentations ii
Acknowledgements iv
Contents Page vi
Figures xi
Tables xiii
Abbreviations xiv
Chapter 1 Introduction 1
1.1 African horse sickness 2
1.1.1 History of African horse sickness 2
1.1.2 Epidemiology 2
1.1.2a Host species 2
1.1.2b Transmission 3
1.1.2c Transmission vectors 3
1.1.2d African horse sickness outbreaks 4
1.1.2e Clinical symptoms of African horse sickness 6
1.1.3 Structure of African horse sickness virus 7
1.1.3a Structural proteins 7
Outer capsid proteins: VP2 and VP5 7
Major core proteins: VP7 and VP3 9
Minor core proteins: VP1, VP4 and VP6 10
1.1.3b Non-structural proteins 11
1.1.4 Virus replication 13
1.1.5 Laboratory Diagnosis 14
1.1.6 Control Measures 16
1.1.6a AHS movement policy in South Africa 16
1.1.6b Vaccination 18
1.2 Baculoviruses 21
1.2.1 Characteristics of baculoviruses 21
1.2.2 Baculovirus GP64 envelope protein 24
1.2.3 Baculoviruses as tools for biotechnological and pharmaceutical applications 25
1.2.3a Baculovirus expression vector system 25
1.2.3b Baculovirus based vaccines 31

1.3 Project Focus and Aims 34
Chapter 2 Materials and Methods 37
2.1 Materials 38
2.2 Cells and Viruses 40
2.2.1 Cells 40
2.2.2 Virus amplification 40
2.2.3 Generation of recombinant viruses by co-transfection of insect cells 41
2.2.4 Titration of virus stocks 41
2.2.4a Plaque Assay 41
2.2.5 Purification of budded virus 42
2.2.6 Budded virus fractionation 42
2.3 Bacteria Protocols 43
2.3.1 Preparation of ultra-competent *Escherichia coli* cells (DH5α strain) 43
2.3.2 Transformation of competent *E.coli* cells 43
2.3.3 Plasmid DNA purification from transformed *E.coli* cells 43
2.4 Molecular Biology Protocols 44
2.4.1 Restriction enzyme digests 44
2.4.2 Agarose gel electrophoresis 44
2.4.2a Gel purification of DNA 44
2.4.3 DNA vector dephosphorylation 44
2.4.4 DNA ligation 45
2.4.5 Polymerase chain reaction (PCR) 45
2.4.6 Cloning PCR fragments into pGEM-T and pGEM-T Easy vectors 48
2.4.7 DNA sequencing 48
2.5 Protein Analysis Protocols 48
2.5.1 Infecting insect cells 48
2.5.2 SDS-PAGE analysis of proteins 49
2.5.2a Coomassie staining 49
2.5.2b Western blot analysis 49
2.5.3 Protein assays 50
2.5.3a BCA assay 50
2.5.3b Bradford assay 50
2.5.4 Analysis of post-translational modifications 51
2.5.5 Immunofluorescence 51
2.6 Protein purification 52

2.6.1 Protein solubilisation 52
2.7 Enzyme-linked immunosorbent assay (ELISA) 53
2.8 Statistical analysis 54
2.9 Vaccination experiments 54
Chapter 3 Characterizing the antigenicity of AHSV4 VP2 and the subdomains produced in insect cells 55
3.1 Introduction 56
3.2 Selection of VP2 subdomains 56
3.3 Construction of transfer vectors 59
3.3.1 Construction of pOET1_VP2$^{HIS/N}$ 59
3.3.2 Construction of pOET1_VP2-H$^{HIS/N}$ 59
3.3.3 Construction of the remaining VP2 subdomain transfer vectors 62
3.4 Generation of recombinant baculoviruses 64
3.5 Characterization of AcVP2$^{HIS/N}$ and AcVP2-H$^{HIS/N}$ in insect cells 65
3.6 Characterization of AcVP2-A$^{HIS/N}$ to AcVP2-Z$^{HIS/N}$ in insect cells 66
3.7 Purification of VP2 and the subdomains 69
3.8 Solubilisation and purification of VP2 subdomains 71
3.9 Optimizing purification of full-length VP2 73
3.10 Antigenic characteristics of full-length AHSV4-VP2 75
3.11 Discussion 77
3.12 Conclusion 82
Chapter 4 Optimization of baculovirus surface display for the production of AHSV4-VP2 and the subdomains 83
4.1 Introduction 84
4.2 Construction of pBACsurf-1_*p6.9* and pBACsurf-1_*gp64* 84
4.3 Cloning of full-length VP2 and fragment H into pBACsurf-1, pBACsurf-1_*p6.9* and pBACsurf-1_*gp64* 85
4.4 Generation of full-length VP2 and fragment H surface display viruses 87
4.5 Characterization of full-length VP2 and fragment H surface display viruses 89
4.6 Truncating the GP64 in pBACsurf-1 91
4.7 Cloning of enhanced green fluorescent protein into pBACsurf-1 and pBACsurf-1$^{GP64/F463}$ 93
4.8 Generation of AcSurf_EGFP and AcSurf_EGFP^{TRUN} 93
4.9 Characterization of AcSurf_EGFP and AcSurf_EGFP^{TRUN} 93
4.10 Construction of pBACsurf-1_VP2$^{GP64/F463}$ and pBACsurf-1_VP2-H$^{GP64/F463}$ 102
4.11 Generation of AcSurf_VP2^{TRUN} and AcSurf_VP2-H^{TRUN} 103
4.12 Characterization of AcSurf_VP2^{TRUN} and AcSurf_VP2-H^{TRUN} 103

by SDS-PAGE 103
4.12.1 Difference of plaque profile between AcSurf_VP2-H and 104
AcSurf_VP2-H^{TRUN} 104
4.13 Discussion 106
4.14 Conclusion 112
Chapter 5 Displaying VP2 Subdomains on BV surface 113
5.1 Introduction 114
5.2 Constructing surface display transfer vectors for VP2 subdomains 114
5.3 Generating VP2 subdomain surface display viruses 115
5.4 Characterizing VP2 subdomain surface display viruses 117
5.5 Post-translational modification analysis of VP2 subdomain chimeric proteins 124
5.6 Budded virus fractionation analysis 126
5.7 Discussion 128
5.8 Conclusion 131
Chapter 6 Antigenic characterization of VP2 subdomains 133
6.1 Introduction 134
6.2 Binding of VP2 subdomains to AHSV4-VP2-specific monoclonal antibodies 134
6.3 Binding of VP2 subdomains to antibodies from MVA-VP2 post-vaccination serum 139
6.4 Vaccination studies 141
6.4.1 Antigen preparation 143
6.4.1a Preparation of test and negative control vaccine antigens 144
6.4.1b Preparation of positive control vaccine antigens 145
6.4.2 Immunization of mice 147
6.4.3 Analysis of post-vaccination serum antibodies by ELISA 148
6.4.4 Analysing the virus neutralization capacity of post-vaccination serum antibodies by plaque reduction neutralization test 149
6.5 Discussion 151
6.5.1 Analysis with non-neutralising monoclonal antibodies 152
6.5.2 Analysis with neutralising monoclonal antibodies 153
6.5.3 Analysis with MVA-VP2 post-vaccination equine serum 154
6.5.4 Analysis of post-vaccination serum from mice 155
6.5.4a Immunogenicity of full-length VP2 155
6.5.4b Immunogenicity of fragment E 156
6.6 Conclusion 157
Chapter 7 Final Discussion and Future Work 159
7.1 Introduction 160

7.2 Discussion of results and future work 161
7.2.1 Analysis of full-length VP2 161
7.2.2 Analysing VP2 subdomains 162
7.2.2a Production of VP2 subdomains 162
7.2.2b Characterization of VP2 subdomains 164
7.3 Concluding remarks 166
References 167
Appendix 185
Appendix 1: Raw data for Figure 3.11 186
Appendix 2: Raw data for Figure 3.12 187
Appendix 3: Raw data for Figure 4.9 188
Appendix 4: Raw data for Figure 4.12 189
Appendix 5: Raw data for Table 6.1 190
Appendix 5: Raw data for Table 6.1 continued 191
Appendix 6: Raw data for Figure 6.3 192
Appendix 7: Raw data for Figure 6.10A 193
Appendix 7: Raw data for Figure 6.10B 194

Figures

Figure 1.1. Schematic representation of AHSV biological transmission 4
Figure 1.2 Map of AHS outbreaks in Africa between 2004 and 2016 5
Figure 1.3 Clinical signs of AHS in infected horses 7
Figure 1.4 African horse sickness virus structure 8
Figure 1.5 African horse sickness virus core like particles 10
Figure 1.6 Negative contrast electron micrograph of African horse sickness virus NS1 11
Figure 1.7 Schematic representation of African horse sickness virus replication cycle 14
Figure 1.8: AHS control area map of South Africa 17
Figure 1.9: Schematic representation of the two distinct forms of baculoviruses 22
Figure 1.10 Schematic representations of baculovirus gene expression phases and the life cycle 22
Figure 1.11: Cryo-EM images of AcMNPV budded virus 25
Figure 1.12 Schematic representation of recombinant baculovirus production 27
Figure 1.13 Schematic representation of the BacPAK6 28
Figure 1.14 Schematic representation of the Bac-to-Bac® system 29
Figure 1.15 Schematic representation of flashBAC™ system 30
Figure 1.16 *flash*BAC™ time line compared to other baculovirus expression vector systems 30
Figure 3.1 Schematic representation of the *flash*BAC system using *flash*BACULTRA DNA 57
Figure 3.2 Schematic representations of the full-length VP2 structure and the location of its subdomains 58
Figure 3.3 Construction of pOET1_VP2$^{HIS/N}$ 60
Figure 3.4 Construction of pOET1_VP2-H$^{HIS/N}$ 61
Figure 3.5 Generation of transfer plasmids for the remaining VP2 subdomains 62
Figure 3.6 Characterization of AcVP2$^{HIS/N}$ and AcVP2-H$^{HIS/N}$ in TnHi5 cells 67
Figure 3.7 Western blot analyses of AcVP2-A$^{HIS/N}$, AcVP2-B$^{HIS/N}$, AcVP2-C$^{HIS/N}$, AcVP2-D$^{HIS/N}$, AcVP2-E$^{HIS/N}$, AcVP2-F$^{HIS/N}$, AcVP2-G$^{HIS/N}$, AcVP2-I$^{HIS/N}$, AcVP2-J$^{HIS/N}$ and AcVP2-Z$^{HIS/N}$ in TnHi5 cells 68
Figure 3.8 Western blot analysis of protein purification from TnHi5 cells infected with AcVP2$^{HIS/N}$, AcVP2-A$^{HIS/N}$, AcVP2-B$^{HIS/N}$ and AcVP2-D$^{HIS/N}$. 70
Figure 3.9 Western blot analysis of VP2 subdomain solubilisation and purification from TnHi5 cells 72
Figure 3.10 Western blot and coomassie staining analysis of VP2 purification optimization 74
Figure 3.11 Reactivity of AHSV4-VP2-specific MAbs with purified VP2 76
Figure 3.12 Reactivity of MVA-VP2 post vaccination serum from ponies to baculovirus-expressed purified VP2 76
Figure 4.1 Construction of pBACsurf-1_*p6.9* and pBACsurf-1_*gp64* 86
Figure 4.2 Cloning of full-length VP2 and fragment H into pBACsurf-1, pBACsurf-1_*p6.9* and pBACsurf-1_*gp64* 89
Figure 4.3 Characterization of fragment H surface display viruses 90
Figure 4.4 Truncating GP64 in pBACsurf-1 92
Figure 4.5 Cloning of EGFP into pBACsurf-1 and pBACsurf-1$^{GP64/F463}$ 94
Figure 4.6 Characterization of AcSurf_EGFP and AcSurf_EGFP^{TRUN} by western blotting and Coomassie staining 96
Figure 4.7 Characterization of AcSurf_EGFP and AcSurf_EGFP^{TRUN} by fluorescence microscopy 97

Figure 4.8A Characterization of AcSurf_EGFP and AcSurf_EGFP^{TRUN} in Sf9 cells by Confocal microscopy 98
Figure 4.8B Characterization of AcSurf_EGFP and AcSurf_EGFPTRUN in TnHi5 cells by Confocal microscop 99
Figure 4.9 Quantitative analysis of EGFP chimeric protein production in Sf9 and TnHi5 cells 101
Figure 4.10 Restriction digest analysis of pBACsurf-1_VP2$^{GP64/F463}$ and pBACsurf-1_VP2-H$^{GP64/F463}$ 102
Figure 4.11 Characterization of Acsurf_VP2-H and Acsurf_VP2-H^{TRUN} by SDS-PAGE 104
Figure 4.12 Plaque formation analyses of AcSurf_VP2-H and AcSurf_VP2-H^{TRUN} 105
Figure 5.1 Constructing surface display transfer vectors for VP2 subdomains 117
Figure 5.2 Characterizing VP2 subdomain surface display viruses by SDS-PAGE 121
Figure 5.3 Characterizing purified VP2 subdomain surface display viruses by western blotting ... 122
Figure 5.4 De-glycosylation of fragments C, D and E-GP64^{TRUN} chimeric proteins 125
Figure 5.5 Budded virus fractionation of Acsurf_VP2-E^{TRUN}, Acsurf_VP2-F^{TRUN}, Acsurf_VP2-H^{TRUN} and Acsurf_VP2-J^{TRUN} 127
Figure 6.1 Schematic representation of monoclonal antibody binding sites within VP2 137
Figure 6.2 Western blot analyses of full-length VP2 using AHSV4-specific monoclonal antibodies 139
Figure 6.3 Binding of antibodies from MVA-VP2 post-vaccination serum to VP2 subdomains 140
Figure 6.4 Western blot analysis of VP2 subdomains with MVA-VP2 post vaccination serum 141
Figure 6.5 Schematic representation of antigens used in the pilot vaccination 143
Figure 6.6 SDS-PAGE analysis of fragment E-GP64^{TRUN} production from TnHi5 cells infected with 0.1 vs 5 MOI 144
Figure 6.7 Western blot analyses of purified Acsurf^{TRUN} and Acsurf_VP2-E^{TRUN} 145
Figure 6.8 Western blot analysis of AcVP2$^{HIS/N}$-infected TnHi5 cells vaccine antigen 146
Figure 6.9 SDS-PAGE analysis of purified VP2$^{HIS/N}$ vaccine antigen 147
Figure 6.10 Analysis of post-vaccination serum antibodies by ELISA 149

Tables

Table 1.1 The functions and the benefits of AcMNPV genes deleted from *flash*BAC™ variants 32
Table 1.2 BEVS products approved for commercial use 33
Table 2.1 Plasmids 38
Table 2.1 (continued) Plasmids 39
Table 2.2 Viruses 39
Table 2.2 (continued) Viruses 40
Table 2.3 *E. coli* strains 40
Table 2.4 Bacmids 40
Table 2.5 Primers used in this thesis 46
Table 2.5 (continued) Primers used in this thesis 47
Table 2.5 (continued) Primers used in this thesis 48
Table 2.6 Antibodies used for western blotting 50
Table 2.7 Antibodies used for immunofluorescence 52
Table 3.1: Summary of VP2 and the subdomains cloning information 64
Table 3.2: Summary of viruses 65
Table 3.3 Summary of VP2 and its subdomains' production in insect cells 69
Table 3.4 Reactivity of MAbs with VP2 from Martinez Torrecuadrada et al.(1996) 81
Table 4.1 Summary of fragment H and full-length VP2 surface display viruses with different promoters 87
Table 5.1: Summary of VP2 subdomain surface display viruses 115
Table 5.2 Summary of chimeric protein expression results 123
Table 6.1 Summary of VP2 subdomain binding to AHSV4-VP2-specific MAbs in an indirect ELISA 138
Table 6.2 Antigens and doses used for mice immunization 147
Table 6.3 Average plaque count from each antigen group 150
Table 6.4 Virus plaque reduction percentages of pooled post-vaccination serum samples from vaccinated mice 150

Abbreviations

aa: amino acid

AcMNPV: Autographa californica multicapsid nucleopolyhedrovirus

AHS: African horse sickness

AHSV: African horse sickness virus

AHSV3: African horse sickness virus serotype 3

AHSV4: African horse sickness virus serotype 4

AHSV5: African horse sickness virus serotype 5

BAC: bacterial artificial chromosome

BEVS: Baculovirus expression vector systems

bp: base pairs

BTV: Bluetongue virus

BTV10: Bluetongue virus serotype 10

BSA: bovine serum albumin

BV: Budded virus

CMV: Cytomegalovirus

DNA: deoxyribonucleic acid

dNTP: deoxynucleotide triphosphate

dpi: days post infection

dsDNA: double stranded deoxyribonucleic acid

ECL: Enhanced chemiluminescence

EGFP: Enhanced green fluorescent protein

ELISA: Enzyme-linked immunosorbent assay

FB: flashBAC™

FBG: flashBACGOLD™

FBU: flashBACULTRA™

FBS: foetal bovine serum

hpi: Hours post infection

HRP: horseradish peroxidase

ie1: immediate early 1

MAb: Monoclonal antibody

moi: multiplicity of infection

OBs: occlusion bodies

ODV: occlusion-derived virus

PCR: polymerase chain reaction

pfu: plaque forming units

polh: polyhedrin

RNA: ribonucleic acid

rpm: rotations per minute

SDS: sodium dodecyl sulfate

SDS-PAGE: sodium dodecyl sulfate polyacrylamide gel electrophoresis

Sf: *Spodoptera frugiperda*

TMD: transmembrane domain

Tni: *Trichoplusi ni*

VNAb: virus neutralising antibody

VN: virus neutralisation

Wt: wild-type

-'ve cont: Negative control

Chapter 1
Introduction

1.1 African horse sickness

1.1.1 History of African horse sickness

African horse sickness (AHS) is a lethal, non-contagious disease of equids, which is also an Office International des Epizooties (OIE)-listed disease due to its severity and ability for rapid and unexpected expansion (Mellor and Hamblin, 2004). The disease has a very ancient history, being first reported in Yemen in 1327. Following this, Father Monclaro, a travel story writer, also reported AHS-like disease in horses from the journey of Francisco Barro to East Africa in 1569 (reviewed by Vandenbergh, 2010). As reviewed by Coetzer and Guthrie (2005), after the introduction of horses and donkeys to Africa, several AHS outbreaks occurred in South Africa over the years. One of the most devastating AHS outbreaks occurred in 1855 in the Cape of Good Hope, where 70,000 horses, which accounted more than 40% of the horse population, died (Vandenbergh, 2010). This had a dreadful impact on the community as horses were widely used for transportation, military operations and for draught power in agriculture and mining (Coetzer and Guthrie, 2005) . Following this, extensive research on AHS was carried out in South Africa over the years.

The causative agent of AHS was demonstrated by M'Fadyean (1900) to be a virus (AHSV), after the successful transmission of the disease with a bacteria-free filtrate of blood obtained from an infected animal (reviewed by Coetzer and Guthrie, 2005, Verwoerd, 2012). Sir Arnold Theiler, a veterinarian researching AHS, discovered that immunised horses were not always protected against infection with AHSV, which suggested the presence of multiple virus serotypes (reviewed by Coetzer and Guthrie, 2005, Verwoerd, 2012). Subsequent research by McIntosh (1958) and Howell (1962) collectively identified the currently accepted nine antigenically distinct serotypes of AHSV (Verwoerd, 2012).

1.1.2 Epidemiology

1.1.2a Host species

Although AHSV is capable of infecting all equids, the highest mortality rates are seen in horses (up to 95%) and occasionally in mules. On the other hand, zebras have long been accepted as the natural reservoir host as they rarely show clinical signs of AHSV infection (Mellor and Hamblin, 2004). In addition, zebras are native species of Africa and their presence in the country has been correlated with the frequent outbreaks observed in this continent. For example, a decline in the zebra population through hunting also reduced the number of AHS outbreaks observed in the South Africa (Barnard, 1998). Furthermore, the duration of viremia in zebra blood has been shown to be significantly longer than in

horses (Barnard *et al.*, 1994), which therefore, makes the distribution of this asymptomatic AHSV host species into AHS-free zones very dangerous.

In addition to equids, AHSV-specific antibodies have also been detected in elephants and African carnivores (Binepal *et al.*, 1992, Alexander *et al.*, 1995). AHSV infection in dogs has also been reported to result in death due to the effects of the virus. The majority of these incidents are thought to be related to ingestion of AHSV-infected meat, however, death without ingestion of infected meat has also been reported (Van Sittert *et al.*, 2013). Although the level of viremia and duration is not very clear, transmission of AHSV from a carnivore is yet to be documented in the wild (Wilson *et al.*, 2009).

1.1.2b Transmission

At the start of the 19th century, there were strong suggestions that an insect vector might play a role in the transmission of AHSV, as effective disease prevention was observed by protecting horses from flying insects (Pitchford and Theiler, 1903). Later in 1944, Du Toit established a light trap to catch substantial numbers of insects and by analysing the transmission of virus into susceptible hosts from these insects, it was proven that the biting midge of *Culicoides* species was the transmitting vector for both bluetongue virus (BTV) and AHSV (Du Toit, 1944).

For biological transmission to occur, AHSV should be accessible to the blood-feeding adult female midges in the host skin surface or peripheral blood vessels. Once ingested by the vector midges, the virus initially infects the gut wall cells then spreads through the cells and tissues to reach the salivary glands. Infection of the salivary glands enables the horizontal transmission to another vertebrate host during a consequent blood meal (Figure 1.1). During this period, minimal pathogenesis occurs to allow the vector to be effective for viral transmission (Wilson *et al.*, 2009).

1.1.2c Transmission vectors

Culicoides imicola has been accepted as the major vector for the transmission of AHSV and it has been shown to account for about 94% of infected species in a field outbreak (Meiswinkel, 1998). As reviewed by Mellor and Hamblin (2004), *C. imicola* is widely distributed throughout Africa and South East Asia, however, in 1982 it was also recorded in Europe and found to be widespread across the majority of the southern continent including Spain, Portugal, Greece and several Mediterranean islands. *C. imicola* breeding habitats are located in areas of damp and enriched soil (Nevill and Anderson, 1972) and it is generally present in warm areas where heavy summer rainfall occurs but found to be very rare in areas of cold and high-land places (Venter and Meiswinkel, 1994). In 1998, a second species, *C. bolitinos,* was shown to be involved in the field transmission of AHSV

(Meiswinkel and Paweska, 2003). *C. bolitinos* was shown to be the major species present in the colder, high-land parts of South Africa (Venter and Meiswinkel, 1994). This increases the risk of AHSV spreading to areas where the primary vector, *C. imicola* is absent.

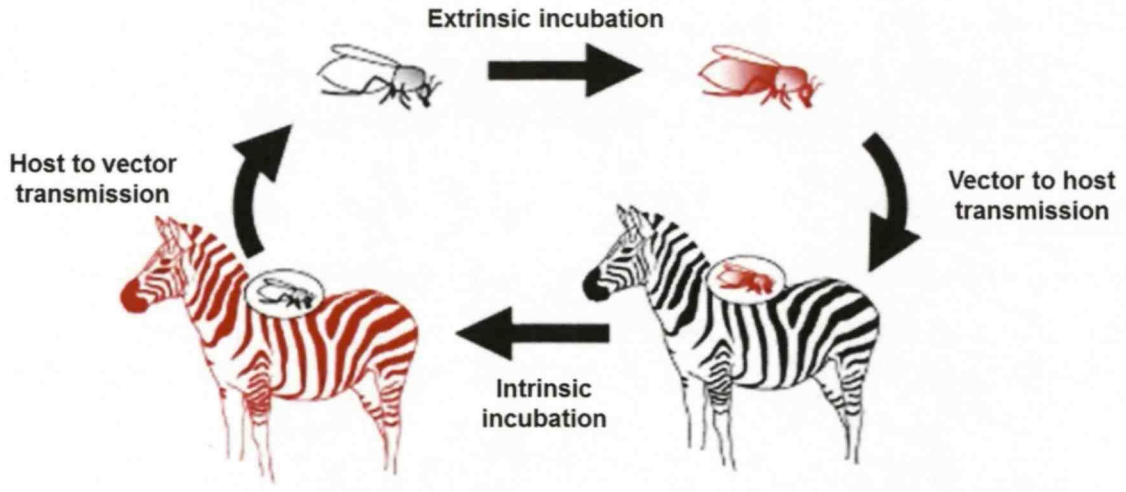


Figure 1.1. Schematic representation of AHSV biological transmission

Vectors feed on the infected host blood through peripherial blood vessels or the skin surface and goes through an extrinsic incubation period where the virus replicates to high levels in the vector body. Subsequently the infected vector bites a non-infected host transmitting the virus. The period where the virus replicates within the horse is called the intrinsic incubation (adapted from Wilson *et al.*, 2009).

Blood-sucking female adult *Culicoides* midges require flight activity to feed, mate and lay eggs in suitable habitats. The flying range of these midges is generally short, up to a maximum of 5km, however, they have also been shown to be distributed very long distances by wind (Mellor *et al.*, 2000, Elbers *et al.*, 2015). Furthermore, dispersal of biting midges by warm wind has been shown to be the possible causes of several vector-borne virus outbreaks in non-endemic regions, such as AHS from Morocco to Spain, and Turkey to Cyprus (Sellers *et al.*, 1977) or BTV8 in Sweden (Ågren *et al.*, 2010).

1.1.2d African horse sickness outbreaks

Although AHS is mainly endemic in Sub-Saharan Africa, during the period of 1959-1961 serotype 9 caused outbreaks in Afghanistan, Pakistan, Syria, Lebanon, Jordon, Iraq, Turkey, Cyprus and India. This outbreak ended after an extensive vaccination regime and the death of 300,000 animals (Howell, 1960, Mellor, 1993). Following this, serotype 9 made another appearance outside its traditional region of Sub-Saharan Africa and caused outbreaks in North Africa (Morocco, Algeria, and Tunisia) and Spain during 1965-1966.

While the virus was eliminated from Spain within three weeks by intense vaccination and a slaughter approach, it remained in North Africa throughout the whole period (Montilla and Martí, 1967, Mellor, 1993).

Following these excursions, AHS was confined in Sub-Saharan Africa for about 20 years, however, serotype 4 (AHSV4) then commenced an outbreak in central Spain in 1987. This outbreak was believed to be due to the importation of infected zebra from Namibia to a safari park located about 50km South West of Madrid, which became the first site of confirmed AHS cases in Spain (Lubroth, 1988). Occurrence of outbreaks carried on during subsequent years of 1987-1991 in Spain (Mellor *et al.*, 1990, Rodriguez *et al.*, 1992), Iberian Peninsula (Rawlings and Mellor, 1994), Portugal (Portas *et al.*, 1999) and Morocco (Bouayoune *et al.*, 1998).

Furthermore, the unexpected spread of serotypes two and seven was also observed within East and West Africa, where AHSV9 was the predominant serotype circulating within the region until 2007 (Diouf *et al.*, 2013). In addition, unexpected AHS outbreaks occurred in 1999, 2004, 2011, 2013, 2014 and 2016 within AHS regions of Africa. AHS surveillance and control is ongoing in these areas (Sinclair *et al.*, 2006, Grewar *et al.*, 2013, WAHID, 2016, Figure 1.2).

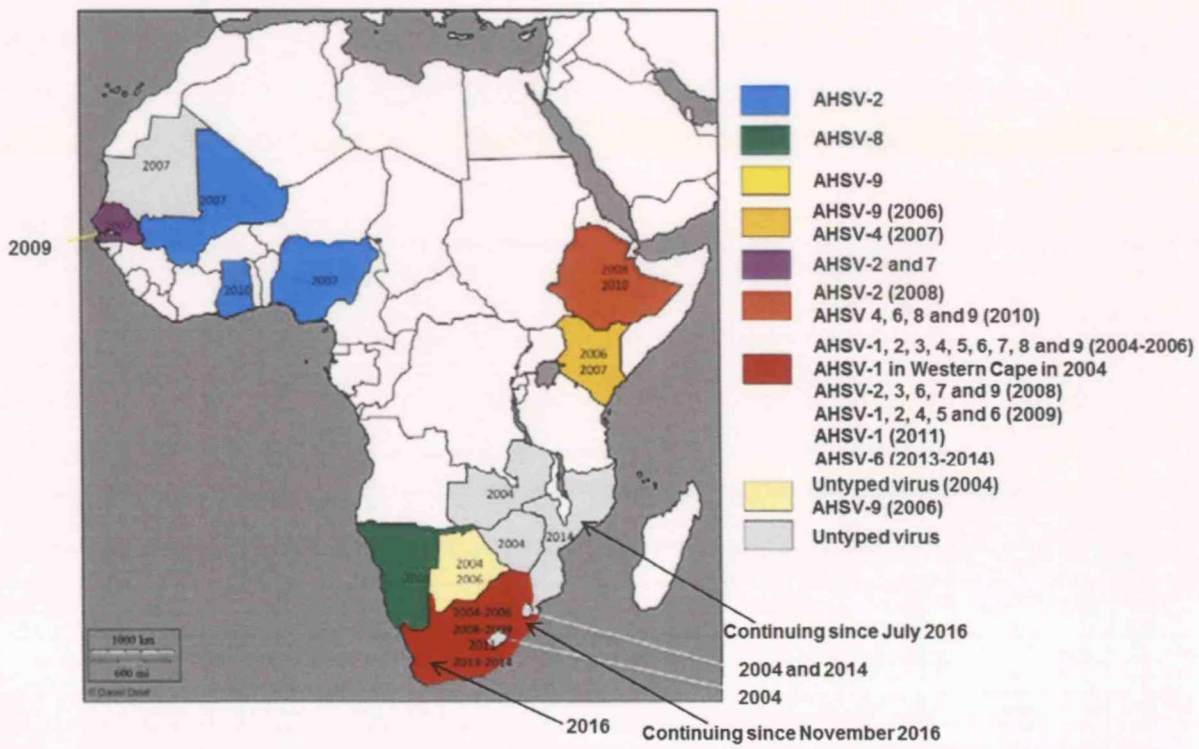


Figure 1.2 Map of AHS outbreaks in Africa between 2004 and 2016

This map is an updated version from Zientara *et al.* (2015) using the information from World Animal Health Information Database, OIE, 2016.

1.1.2e Clinical symptoms of African horse sickness

Once an animal is bitten by an infected midge vector, the virus first replicates in the regional lymph nodes from where it then gets distributed to the target organs (heart, lung lymphoid tissue and spleen) by the bloodstream. The incubation period of the disease varies from three to fifteen days and, based on the virulence of infecting virus, AHS is classified into four clinical forms: horse sickness fever, cardiac form, mixed form and pulmonary form (Burrage and Laegreid, 1994).

Horsesickness fever

This is the mildest form of AHS that causes no mortality and is the only form seen in African donkeys and zebra. The clinical signs are very rare; onset of temperature (up to 40°C) is observed over a period of four to five days, which is followed by recovery (Long and Guthrie, 2014).

Cardiac form

The incubation period for the cardiac form to develop is between five to seven days, which is followed by increase in temperature (39-41°C). Typical clinical signs include oedema of the head, neck and chest, which can result in difficulty in breathing (dyspnea). Conjunctivitis in the eyes and haemorrhages on the tongue can develop, which become apparent shortly before death (Figure 1.3 A). Severe and fluctuating abdominal pains may also be experienced by some animals. After the onset of temperature, death usually occurs after four to eight days and the mortality rates of cardiac form are more than 50% (Long and Guthrie, 2014).

Mixed form

This form of AHS is most common and the mortality rates are about 70%. The clinical signs are a mixture of the cardiac and the pulmonary forms of the disease. In some cases, subclinical signs of the pulmonary form are followed by oedema and death occurs due to cardiac failure. In other cases, mild clinical signs of the cardiac form are followed by rapid onset of dyspnea and other signs of the pulmonary form, which leads to death (Long and Guthrie, 2014).

Pulmonary form

This is the per-acute form of AHS, with more than 95% mortality rates in fully susceptible horses. The incubation period is short, between three to four days, which is followed by a rapid increase in the temperature (40-41°C). Fast and progressive respiratory failure is the main characteristic of the disease, where respiratory rate may increase to more than 50 breaths per minute. Extended head, dilated nostrils, heavy sweating and discharge of

frothy liquid from the nostrils is very common (Figure 1.3B). Death usually occurs within 30 minutes to a few hours after the onset of a very sudden dyspnea. It is also observed that healthy-looking animals may suddenly develop a severe dyspnea and die, which is why it is referred as the per-acute form of AHS (Long and Guthrie, 2014).

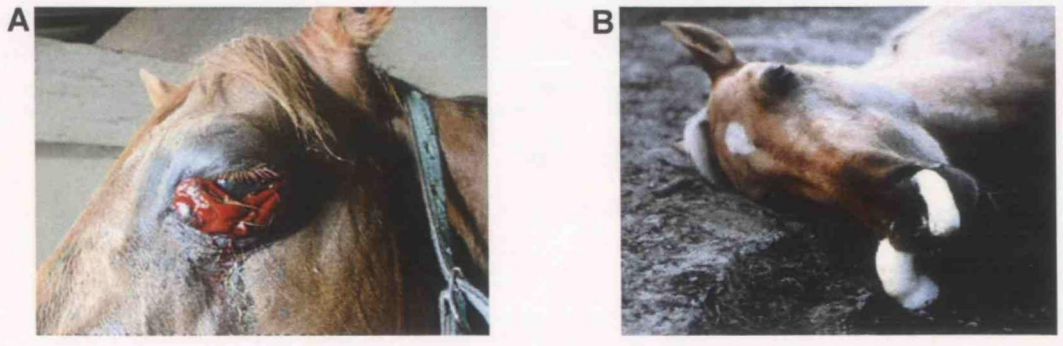


Figure 1.3 Clinical signs of AHS in infected horses

A: Horse affected by the cardiac form of AHS suffering from oedema in the head and conjunctivitis in the eyes (UC Davis Center, 2008).

B: A deceased horse that has suffered from the pulmonary form of AHS showing the discharge of frothy liquid from the nostrils (Horsetalk, 2013).

1.1.3 Structure of African horse sickness virus

African horse sickness virus belongs to the genus *Orbivirus* within the *Reoviridae* family (Verwoerd *et al.*, 1979). Similar to the prototype BTV from the same genus, it has an icosahedral shape that is formed by three concentric protein layers (Oellermann *et al.*, 1970, Roy *et al.*, 1994b, Stuart *et al.*, 1998, Manole *et al.*, 2012). The virus genome consists of ten double-stranded RNA segments that encodes seven structural (VP1-7) and five non-structural proteins (NS1, NS2, NS3/NS3A and NS4) (Oellermann, 1970, Bremer, 1976, Roy *et al.*, 1994b, Mertens *et al.*, 2005, Zwart *et al.*, 2015) (Figure 1.4).

1.1.3a Structural proteins

Outer capsid proteins: VP2 and VP5

Early research on the characterization and the cloning of the AHSV genome has shown that segment two was the least conserved genome segment among all nine AHSV serotypes, which strongly suggested it encoded the serotype-specific, outer capsid protein VP2 (Bremer *et al.*, 1990). It was shown by the use of a panel of AHSV-specific monoclonal antibodies that the virus neutralizing epitopes are located on this outer capsid protein (Ranz *et al.*, 1992, Burrage *et al.*, 1993). This characteristic has made VP2 a primary target for the development of sub-unit protein vaccines.

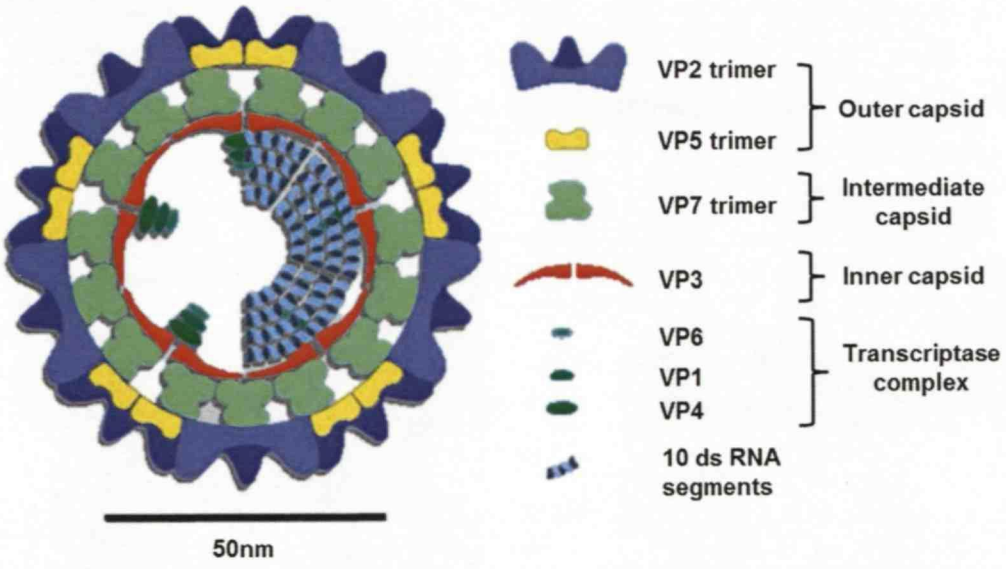


Figure 1.4 African horse sickness virus structure

Schematic representation of the virus structure illustrating the dsRNA genome enclosed in three concentric protein layers (adapted from Mertens and Diprose, 2004)

Expression of several VP2 subdomains in *Escherichia coli* revealed that the amino terminal half of the protein is more antigenic (Martinez-Torrecuadrada and Casal, 1995, Bentley *et al.*, 2000). Investigations by Martinez-Torrecuadrada *et al.* (1995) narrowed the main antigenic determinant of the protein to be located between the amino acid regions 200-414. A more recent study has suggested that the central domain of VP2 monomers interact with each other in the VP2 trimer in an independent structural subdomain that contains most of the linear peptides defined so far (Martinez-Torrecuadrada and Casal, 1995, Bentley *et al.*, 2000, Manole *et al.*, 2012, Figure 3.2).

VP5, which is encoded by genome segment six, is the other major protein constituting the AHSV outer capsid formation. Despite this, it is less exposed on the surface compared to VP2 (Figure 1.4) and relatively more conserved among other orbiviruses such as BTV and epizootic haemorrhagic disease virus-1 (EHDV) (Roy *et al.*, 1994b) and even more with other AHSV serotypes (du Plessis and Nel, 1997, Williams *et al.*, 1998). On the other hand, VP5 was found to be one of the earliest serological markers for the identification of the disease in experimentally infected horses (Martinez-Torrecuadrada *et al.*, 1997). Although the role of VP5 in virus neutralization is not clearly established, its presence together with VP2 was shown to enhance the immune responses achieved against both BTV (Roy *et al.*, 1990, Mohd Jaafar *et al.*, 2014) and AHSV (Martinez-Torrecuadrada *et al.*, 1996). Furthermore, AHSV4 VP5 was shown to generate low levels of virus neutralizing antibodies in rabbits in the absence of VP2 (Martínez-Torrecuadrada *et al.*,

1999), however this was not the case for BTV10 VP5, where antibodies generated in the absence of VP2 could not neutralize virus infectivity *in vitro* (Marshall and Roy, 1990).

A recent study, based on the cytotoxicity activity of baculovirus-expressed AHSV VP5 in Sf9 insect cells, reported that VP5 serves as a membrane permeabilisation protein. Analysis of various deletion constructs revealed that the N-terminal amphipathic α-helices were the structural features responsible for this outcome (Stassen *et al.*, 2011). This suggested an important role for VP5 in the early stages of virus entry into cells. A very similar analysis for BTV VP5 confirmed the cytotoxic feature of VP5 permeabilizing both mammalian and *Culicoides* insect cells. The same study showed, by microscopy analysis, that VP5 successfully attaches to the mammalian cell surface but does not get internalized, whereas the VP2 capsid protein does, suggesting that the role of VP5 is to initiate cellular entry by de-stabilizing the membrane (Hassan *et al.*, 2001)

Major core proteins: VP7 and VP3

AHSV genome segments three and seven encode the major inner core capsid proteins VP3 and VP7, respectively and both of these proteins hold group-specific antigenic determinants (Roy *et al.*, 1994b). Baculovirus-expressed VP7 was reported to form crystal structures in Sf9 cells that could be purified. Use of purified VP7 crystals in an indirect ELISA showed that VP7 was recognized by polyclonal equine sera from nine AHSV serotypes but elicited minimal cross-reactivity with anti-BTV and anti-EHDV serum. This demonstrated that VP7 is highly conserved among all nine AHSV serotypes, which makes it a very good target for diagnosing AHSV infection despite the virus serotype (Chuma *et al.*, 1992).

VP3 was found to be highly conserved among three orbiviruses; AHSV, BTV and EHDV (Iwata *et al.*, 1992). Analysis of the atomic structure of BTV core has shown that VP3 forms a thin layer of scaffold for VP7 and also interacts with the minor proteins in the inner core (Grimes *et al.*, 1998). In addition, VP3 and VP7 of both AHSV and BTV were shown to form core-like particles (CLPs) in insect cells when co-expressed by recombinant baculoviruses (French and Roy, 1990, Maree *et al.*, 1998, Maree *et al.*, 2016, Figure 1.5).

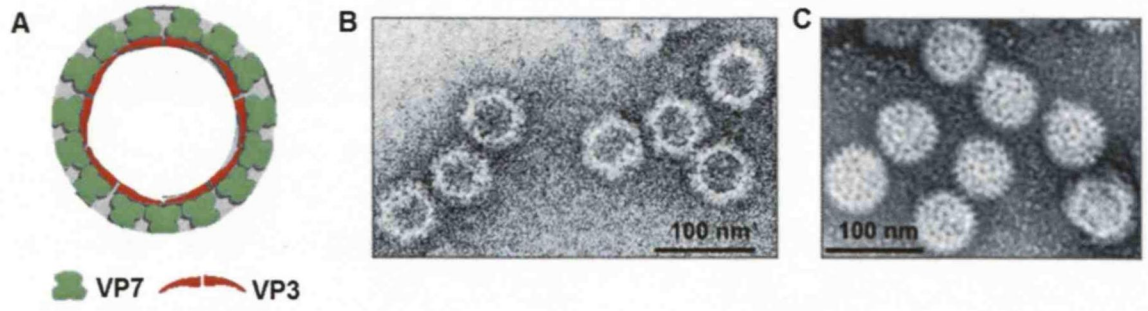


Figure 1.5 African horse sickness virus core like particles

A: Schematic representation of AHSV CLPs (adapted from Mertens and Diprose, 2004)

B: Transmission electron micrographs (TEM) of 72nm AHSV CLPs purified from Sf9 cells co-synthesizing recombinant AHSV VP3 and VP7

C: TEM of purified authentic AHSV cores (CLPs).

B and **C** are taken from (Maree *et al.*, 2016) based on the permission rights granted from Elsevier (RightsLink®).

Minor core proteins: VP1, VP4 and VP6

Minor core proteins of orbiviruses have been associated with enzymatic actions for RNA transcription and replication and the majority of work to demonstrate these putative functions has been carried out with BTV (reviewed by Mertens *et al.*, 2004). Although the roles of these proteins are expected to be the same, minimal work has been done on AHSV minor core proteins.

Viral Protein 1 (VP1)

Analysis of AHSV9 VP1 gene sequence suggested that the putative role of this protein is a viral RNA polymerase (Vreede and Huismans, 1998). VP1 protein of the prototype BTV was also associated with RNA polymerase activity when expressed by recombinant baculoviruses and analysed by polymerase activity (Urakawa *et al.*, 1989).

Viral Protein 4 (VP4)

Recombinant BTV VP4 was demonstrated to have the enzymatic activities associated with RNA capping, which is necessary for downstream gene expression (Ramadevi *et al.*, 1998). In the case of AHSV, sequence analysis of the gene segment that encodes VP4 was also suggested to have a possible RNA capping enzyme role, however, due to problems encountered with the solubility of recombinant AHSV VP4, the enzymatic activity of the protein has not been demonstrated to date (Van den Bout, 2005).

Viral Protein 6 (VP6)

BTV VP6 protein, encoded by genome segment nine, was expressed by recombinant baculoviruses. Purified VP6 was shown to bind ATP and catalyse the unwinding of double-stranded RNA segments demonstrating a helicase function (Stäuber *et al.*, 1997). The genome segment encoding VP6 of AHSV has been cloned, sequenced and found to be 95% similar between AHSV3 and AHSV6 but only 29% amino acid similarity with BTV10 (Turnbull *et al.*, 1996). When partially purified recombinant VP6 of AHSV was analysed, it was reported to bind both single- (ss) and double-stranded (ds) RNA and DNA, where the binding to ds RNA was suggested to depend on net charge of the protein (de Waal and Huismans, 2005). Furthermore, AHSV VP6 was shown to be crucial for the generation of infectious virus particles as the deletion of this protein resulted in viruses that were replication-incompetent (Lulla *et al.*, 2016).

1.1.3b Non-structural proteins

Non Structural protein 1 (NS1)

Synthesis of tubular structures in infected cells has been shown to be characteristic of infection with orbiviruses such as AHSV, BTV and EHDV (Huismans and Els, 1979). Studies carried out using recombinant baculovirus expression have demonstrated that NS1 is responsible for the formation of the tubule structures (Figure 1.6 Maree and Huismans, 1997). Furthermore, NS1 was shown to be highly conserved among AHSV serotypes four, six and nine (Maree and Huismans, 1997) as well as among eight attenuated AHSV vaccine strains, suggesting that NS1 has a potential to be used as diagnostic reagent for AHSV infection (Mizukoshi *et al.*, 1992).

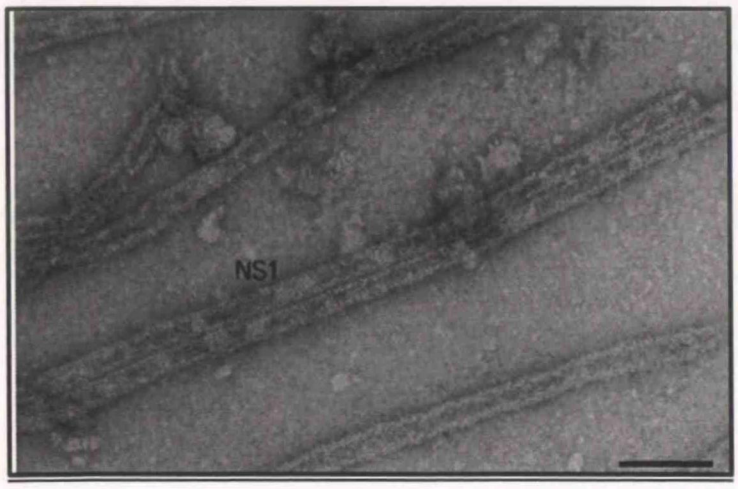


Figure 1.6 Negative contrast electron micrograph of African horse sickness virus NS1

Sucrose-gradient purified, baculovirus-expressed NS1 tubules. This image is taken from (Maree and Huismans, 1997) based on the permission rights granted by Microbiology society (RightsLink®). The scale bar represents 100nm.

Non Structural protein 2 (NS2)

NS2 protein of BTV, AHSV and EHDV was characterized by using recombinant baculoviruses in insect cells. The results showed that the recombinant NS2 protein of all viruses is phosphorylated, forms multimers and presents non-specific binding to ss RNA with decreasing affinities in the order of BTV, EHDV and AHSV, respectively. In addition, all three viral NS2 proteins were shown to accumulate in virus inclusion body (VIB)-like structures in infected cells (Uitenweerde *et al.*, 1995). In a previous study, VIBs formed during BTV infection were demonstrated to be the site for BTV synthesis and assembly (Brookes *et al.*, 1993). Therefore, it is highly likely that the VIB formed by AHSV NS2 protein also serves as the location of virus assembly in infected cells.

Non Structural protein 3/A (NS3/NS3A)

The smallest genome segment of AHSV (S10) was shown to encode for two non-structural proteins, NS3 and NS3A, which is due to the presence of two in-frame translation initiation codons in this gene (van Staden and Huismans, 1991). Genome segment analysis has revealed that the conservation of NS3 gene (S10) among AHSV serotypes is relatively low (Bremer *et al.*, 1990, van Staden *et al.*, 1995) unlike with BTV, where S10 was found to be highly conserved among different BTV serotypes (Pierce *et al.*, 1998). The low similarity observed between S10 gene of AHSV serotypes has suggested a possible association of this protein with virus virulence and pathogenesis. This association was demonstrated in a genome reassortment study between virulent and avirulent viruses, where the NS3 gene was shown to influence the virulence of progeny virus (O'Hara *et al.*, 1998).

Recombinant NS3 expressed by baculoviruses was shown to have a cytotoxic effect on Sf9 cells, increasing cell permeability (van Staden *et al.*, 1995). Furthermore, the location of NS3 was shown to be associated with disrupted plasma membrane of recombinant NS3 expressing baculovirus-infected Sf9 cells (Stoltz *et al.*, 1996). Expressing AHSV NS3 mutants in Sf9 cells using recombinant baculoviruses suggested that the cytotoxicity is associated with two hydrophobic regions of the protein that enables membrane anchorage (van Niekerk *et al.*, 2001). Overall, these characteristics of NS3 protein suggested a putative role in viral pathogenesis and release from infected cells. van de Water *et al.* (2015) demonstrated that NS3/NS3A is not required for AHSV replication *in vitro* but is crucial for the release of viruses from cultured insect cells and involved in causing a cytopathic effect in mammalian cells.

Non Structural protein 4 (NS4)

Bioinformatic analysis revealed that segment nine (S9) of the Orbivirus genome, which normally encodes for the minor core protein VP6, also has an overlapping open reading frame (ORF) designated as ORFx (Firth, 2008). After several analyses with BTV and Great Island Virus (GIV), ORFx was demonstrated to encode for a new non-structural orbivirus protein named as NS4 (Belhouchet *et al.*, 2011). Furthermore Belchouchet *et al.* (2011) showed by western blot analysis using NS4-specific rabbit antiserum that NS4 was detected from orbivirus-infected cells but not purified virus particles confirming that this protein is non-structural. In addition their confocal microscopy analysis demonstrated the accumulation of this protein in the cytoplasm and the nucleus of the cells as early as four hours post infection suggesting an early role in virus replication cycle. Later on during the infection the protein was detected from the plasma membrane suggesting a possible involvement in virus exit (Belhouchet *et al.*, 2011).

Zwart *et al.* (2015) characterized the S9 of all AHSV serotypes and demonstrated that two types of NS4 protein were expressed in cultured mammalian and infected host cells, NS4-I and NS4-II, which differed in length and amino acid sequence. Localization of AHSV NS4 was demonstrated to be in the cytoplasm and nucleus as reported before but not in the plasma membrane at any time during infection, unlike BTV and GIV (Belhouchet *et al.*, 2011, Zwart *et al.*, 2015). Although the expression and localization of AHSV NS4 was demonstrated, its function in the virus replication cycle is yet to be identified.

1.1.4 Virus replication

The replication cycle of AHSV is thought to be very similar to the replication of the prototype virus BTV. Although the majority of work has been done with BTV, it was recently suggested that the entry route for AHSV is based on micropinocytosis (Vermaak *et al.*, 2016). During cell entry, outer capsid proteins VP2 and VP5 disassociate and the transcriptionally active core particle is released into the cytoplasm, where the virus replication takes place (Mertens *et al.*, 2004, Matsuo *et al.*, 2010). Multiple ss RNA segments are produced that act as a messenger RNA for viral protein production and a template for dsRNA genome synthesis. Core virus particles are thought to assemble within the VIB, located in the cytoplasm of infected cells and the outer capsid proteins are added as the core leaves the VIBs. Progeny virus exit from the cells occur either by budding, where the envelope acquired during this process disappears soon after the exit, or by cell lysis (Mertens *et al.*, 2004, Figure 1.7).

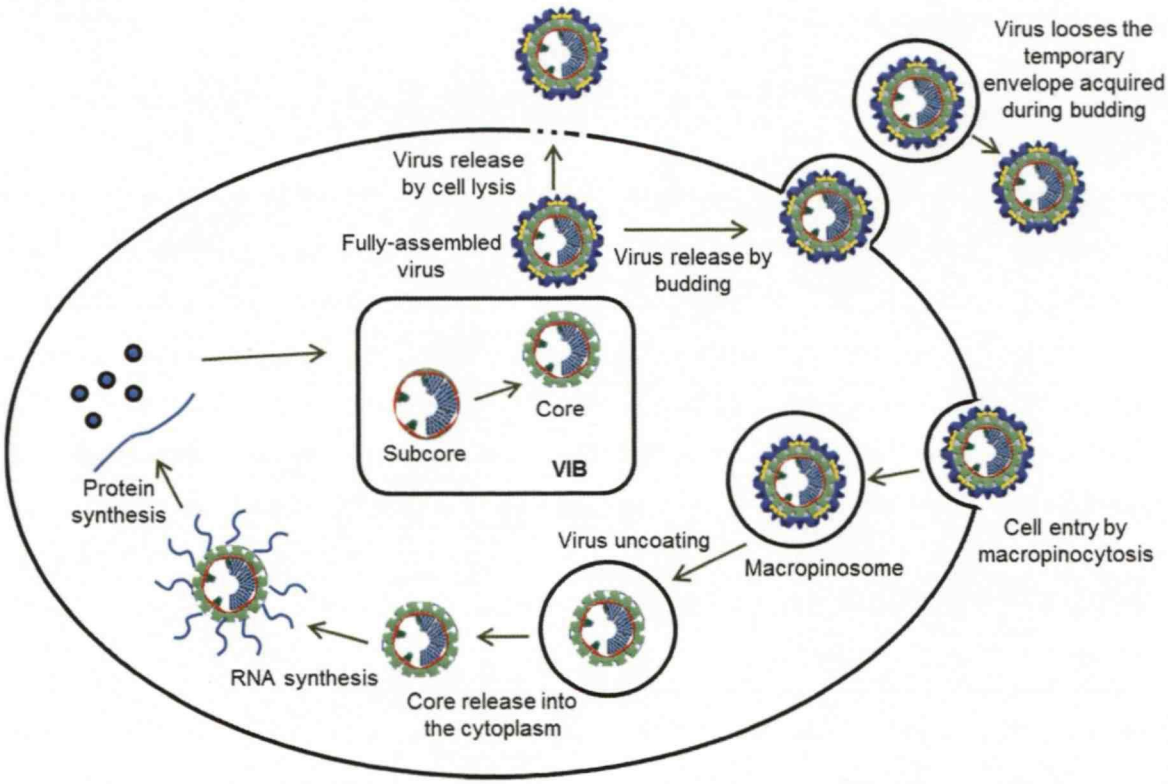


Figure 1.7 Schematic representation of African horse sickness virus replication cycle.

Simplified diagram of AHSV replication based on the general understanding of orbivirus replication cycle. VIB: virus inclusion bodies located in the cytoplasm.

1.1.5 Laboratory Diagnosis

Clinical signs of AHS, (section 1.1.5) can be helpful in making provisional diagnosis of the disease however, laboratory diagnosis is essential for correct and confirmatory identification of AHSV infection. Several serological assays are used for the identification of AHSV infection such as complement fixation test, immunoblotting, virus neutralization (VN) test and enzyme-linked immunosorbent assay (ELISA) (House *et al.*, 1990) and all are approved by OIE. Furthermore, a new duplex lateral flow assay was developed by Costa *et al.* (2016) that can simultaneously detect antibodies against AHSV and equine infectious anaemia virus (EIAV). This assay was shown to be successful in the rapid diagnosis of two diseases that might present similar clinical signs and proven to be advantageous for field use due to its practicality and rapid outcome (Costa *et al.*, 2016).

Over the years, several ELISAs have been developed and widely used to detect AHSV group-specific antigens. Majority of these ELISAs were based on the highly conserved AHSV structural protein, VP7 (Laviada *et al.*, 1992, Wade-Evans *et al.*, 1993, Kweon *et al.*, 2003, Maree and Paweska, 2005). An ELISA based on the detection of AHSV NS3 was also developed with the aim of differentiating infected animals from animals vaccinated with a purified, inactivated vaccine (Laviada *et al.*, 1995). In contrast, another

study has shown that NS3 could not be used as a marker for such differentiation as some horses still developed NS3 antibodies after vaccination with purified, inactivated vaccines. However, this was suggested to be due to insufficient purification of the inactivated vaccine (Idrissi *et al.*, 1999).

Serological tests are very useful for epidemiological surveillance of the virus. However, virus identification techniques provide better AHS diagnosis as the antibody generation can only be detected 10 to 14 days post infection and most animals will succumb to the disease before this point. In addition, interpreting the results of serological assays in areas of routine vaccination can be complicated (Zientara *et al.*, 2015). Therefore, assays for the rapid identification of viruses such as reverse transcriptase polymerase chain reaction (RT-PCR) are more favourable in laboratories. Several RT-PCR assays have been developed to identify AHSV infection regardless of the virus serotype by targeting highly conserved genome segments such as S7 (VP7) (Zientara *et al.*, 1994, Aguero *et al.*, 2008, Fernandez-Pinero *et al.*, 2009), S5 (NS1) (Rodriguez-Sanchez *et al.*, 2008), S8 (NS2) (Monaco *et al.*, 2011) and S1 (VP1) and S3 (VP3) (Bachanek-Bankowska *et al.*, 2014). Furthermore, development of RT-PCR for the amplification of S2, encoding the serotype-specific outer capsid protein, VP2, enabled the identification and distinction of nine AHSV serotypes (Sailleau *et al.*, 2000, Bachanek-Bankowska *et al.*, 2014). This type of assay has crucial importance in the occurrence of an outbreak to rapidly identify the causative serotype, unlike the traditional virus neutralization test, which can take up to seven to 14 days for virus identification.

Currently, RT-PCR-based assays are applicable only in laboratory settings and inappropriate storage of samples during the transport from field to designated laboratories may result in unreliable results. In addition, the risk of delay in obtaining the results due to the transport time is unfavourable in an outbreak scenario. Recently, a novel reverse transcription loop-mediated isothermal amplification (LAMP) assay was developed for rapid AHSV detection with promising field use (Fowler *et al.*, 2016). The basis of LAMP assays is the amplification of DNA at a constant temperature without the requirement of thermocyclers (Notomi *et al.*, 2000). In addition, the assay was shown to be very sensitive, rapid and eligible for coupling with a simple and disposable detection device making it even more favourable for field use (Notomi *et al.*, 2000, Waters *et al.*, 2014). The AHSV-based RT-LAMP assay developed by Fowler *et al.* (2016) was very promising where the results were comparable to the ones obtained by standard RT-PCR (Aguero *et al.*, 2008). Therefore, as the authors suggested, the assay can be further developed to be used in the field for AHSV detection.

The detection of AHSV infection by serological assays has also been improved recently by the development of luminex-based assays (Sanchez-Matamoros *et al.*, 2016a, 2016b).

Initially, Sanchez-Matamoros *et al* (2016a) developed a monoplex assay where fluorescent micro-sphere beads were coated with recombinant AHSV VP7 protein and was shown to be successful in detecting VP7-specific antibodies of all nine AHSV serotypes from horse serum. In addition, this assay was shown to be rapid, specific and even more sensitive than the conventional ELISA (Sanchez-Matamoros *et al.*, 2016a). Furthermore, an extended study has developed a multiplex assay targeting both VP7 and NS3 proteins of AHSV, aiming to differentiate infected from vaccinated animals (DIVA) similar to the concept developed by Laviada *et al.* (1995) (Sanchez-Matamoros *et al.*, 2016b). However, the platform developed by Sanchez-Matamoros *et al.* (2016b) is more advantageous as both viral proteins can be detected simultaneously from a very small sample, whereas in the conventional ELISA, detection of only a single target could be achieved. Therefore, luminex-based DIVA assay is very promising for AHS disease surveillance and for differentiation of uninfected, infected and vaccinated animals if the appropriate proteins and vaccines were used during the assay set-up and screening.

1.1.6 Control Measures

As AHSV can only be transmitted by infected vector bites, a number of control measures can play an important role in preventing disease spread and initiation of new infection foci. For instance, the major transmission vector *C. imicola* is exophilic suggesting that stabling susceptible animals indoors during times of high vector activity could reduce biting rates of these midges. In addition, minimizing vector entry into animal housing by netting the windows and doors was shown to reduce the numbers of the two major AHSV field vectors; *C. imicola* and *C. bolitinos* in animal housing by 14-fold (Meiswinkel *et al.*, 2000). Apart from husbandry modifications, use of insecticides and repellents can provide protection up to a degree. However, it is almost impossible to completely eliminate the vector populations and there is no treatment for the disease therefore, other measures including animal movement restrictions and more importantly vaccination are considered the most effective ways for disease control. Slaughter of viraemic animals is also considered very early in an epidemic to prevent bigger losses if ethical approval is granted (Mellor and Hamblin, 2004).

1.1.6a AHS movement policy in South Africa

In order to establish an AHS-free zone in Cape peninsula, a protocol was submitted to the European Union (EU) in 1993. The establishment of a tightly controlled AHS-free zone would enable the movement of certified horses from South Africa to EU and other AHS-free countries (Bosman *et al.*, 1995). In 1997, a movement policy was established in the Western Cape based on the regulations and guidelines inclined by the EU, OIE and the South African veterinary authority for the movement of equids within the AHS controlled

area. Western Cape Province, which is the AHS control area of South Africa consist of free, surveillance and protection zones as it can be seen in the map (Bosman *et al.*, 1995, Figure 1.8, African Horse Sickness Trust, 2016b).

Horses moving from the direction of infected to free zone require an official movement permit and a health certificate given by a veterinarian no longer than 48 hours before travelling. Further quarantine rules apply to horses coming from high-risk infected areas. Regarding to vaccinations, horses from infected zone must be vaccinated with an approved AHSV vaccine no longer than 24 months ago and not less than 40 days ago, prior to travelling. On the other hand, vaccination of horses within the controlled area must only be carried out with permission from the veterinary authority (African Horse Sickness Trust, 2016a, b, Buhrmann, 2016). The regulations and the boundaries of the AHS controlled area can be altered in case of an AHS outbreak occurring within these regions. For instance, a further containment zone was established in the surveillance area after a confirmed AHS death case was detected in Paarl on 2 April 2016. Following an immediate action of control measures, testing campaign and movement restrictions, the outbreak was contained and the regulations reverted to normal in the surveillance zone (Jooste, 2016)

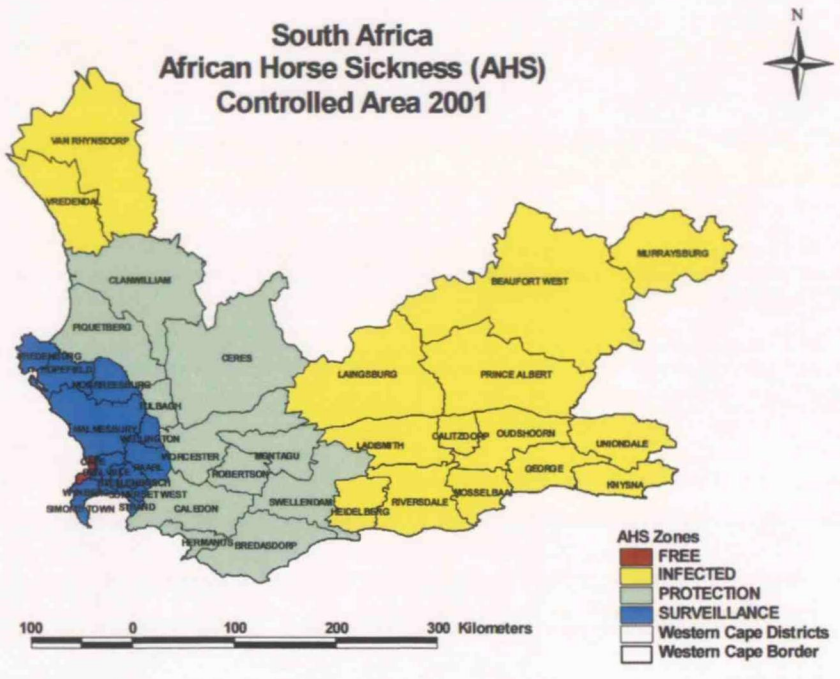


Figure 1.8: AHS control area map of South Africa

Colour-coded map of AHS control area in South Africa indicating free (red), surveillance (turquoise), protection (mint green) and infected zones (yellow) (African Horse Sickness Trust, 2016b).

1.1.6b Vaccination

The very early research on the generation of vaccines for AHS has shown that cerebral passaging of the virus in mice and guinea pigs effectively reduces its virulence. In addition, this attenuation was shown not to affect the antigenicity of the virus hence generating a solid immunity in horses against homologous virus (Alexander and Du Toit, 1934). As reviewed by Zientara *et al.* (2015), immunizations carried out using virus that is attenuated in mice brain occasionally caused fatal encephalitis in horses and donkeys. However, using cell-culture based attenuation instead was shown to minimize the problems encountered (Zientara *et al.*, 2015). Currently used live-attenuated vaccines are based on the selection of large plaques from Vero cell cultures, which were shown by Erasmus in 1976 to be non-pathogenic (OIE, 2016). These vaccines are generated by Onderstepoort Biological Products (OBP) in South Africa and are provided in two polyvalent vials; vial 1`consisting of AHSV1, 3 and 4, and the second covering AHSV2, 6, 7 and 8. The two vials are suggested to be given to the animals two to three weeks apart and annual vaccination is highly recommended as repeated immunisations are required for gaining immunity against all serotypes (OBP, 2016).

AHSV5 and AHSV9 were excluded from the polyvalent OBP-LAVs, due to safety concerns and low prevalence, respectively (Robin *et al.*, 2016). However, both sequence homology analysis (Potgieter *et al.*, 2003) and *in vivo* studies (von Teichman *et al.*, 2010) have demonstrated cross-reactivity and cross-protection, respectively for serotypes five and eight and serotypes six and nine. Therefore, the current OBP-LAVs are thought to protect animals against all serotypes. On the other hand, monovalent LAV vaccine for AHSV nine is used in West Africa, as this was the only serotype circulating in this region until 2007 (Diouf *et al.*, 2013).

Although the success of LAV for protecting against AHSV is established in endemic regions, there are safety concerns especially for use in disease-free areas due to the nature of the vaccine. For instance, as AHSV has a segmented genome, there is always a risk of re-assortment, which is the exchange of genome segments that can generate new genotype with novel biological characteristics (including increased pathogenicity). In fact, a study investigating the source of outbreaks that occurred in the controlled region of Africa has shown that reversion to virulence and re-assortment was responsible for the outbreaks under investigation (Weyer *et al.*, 2016). In addition, a farm study located in an AHS-endemic region, Namibia, demonstrated that even after repeated vaccination with OBP-LAV, AHS cases occurred in the farm with fatalities seen in horses under age two (Molini *et al.*, 2015).

Moreover, the two major AHSV field vectors, *C. imicola* and *C. bolitinos* were shown to be orally susceptible to infection with live-attenuated vaccine strains. In addition, AHSV4 and AHSV7 vaccine strains were shown to replicate in these midges to titres permissive for virus transmission during a blood meal (Paweska *et al.*, 2003). Although LAVs do not cause sufficient viremia in the host to allow vector transmission, the risks of reversion to virulence and the fact that the midges are susceptible to infection raises concerns about these vaccines. There are other supplementary concerns about the use of LAVs as covered by Mellor and Hamblin *et al.* (2004) and Zientara *et al.* (2015). These include the risk of introducing new virus topotypes into non-endemic regions as the current LAV are generated from viruses of South African origin. Additionally, possible teratogenic effects of the current vaccines are foreseen hence not recommended for use in pregnant mares (Mellor and Hamblin, 2004, Zientara *et al.*, 2015).

As the OBP-LAV are the only commercial vaccines available for AHS and their safety is a big concern, development of safer vaccines for AHS has been a major focus over the years. Inactivated vaccines in comparison to LAV are considered safer as the virus is essentially made inactive with chemicals that abort viral replication. This approach has been tried with AHS vaccines, where formalin- (Mirchamsy and Taslimi, 1968) and bromoethylenimine hydrobromide-inactivated AHSV9 vaccine (Lelli *et al.*, 2013) protected the horses against homologous virus challenge under experimental conditions. Furthermore, a commercially produced, formalin-inactivated AHSV4 vaccine apparently was used to control the outbreaks in Spain, Portugal and Morocco during 1987-1991. However, soon after the eradication of AHSV, this vaccine was withdrawn from the market and is no longer available. The drawbacks of the inactivated vaccines can include expensive production and insufficient inactivation leading to viral replication and subsequent viremia causing disease (Mellor and Hamblin, 2004, Zientara *et al.*, 2015).

On the other hand, subunit recombinant vaccines could be the safest approach as they are based on using only the immunogenic proteins instead of the whole virus particles. Moreover, use of subunit vaccines would enable DIVA, which is crucial for animal movement regulations, using the current well-established diagnostic assays (Chuma *et al.*, 1992, Zientara *et al.*, 1994, Sanchez-Matamoros *et al.*, 2016b), unlike with OBP-LAV.

Over the years, extensive research has been carried out for the production of subunit AHSV vaccines mainly based on the expression of AHSV outer capsid proteins, VP2 and VP5, using different platforms. Use of modified vaccinia Ankara virus (MVA) expressing AHSV VP2 has been shown to induce virus neutralizing antibodies (VNAbs) that are sufficient for protection against lethal AHSV challenge both in mice (Castillo-Olivares *et al.*, 2011, Calvo-Pinilla *et al.*, 2014, Calvo-Pinilla *et al.*, 2015) and horses (Stone-Marschat *et al.*, 1996, Chiam *et al.*, 2009, Alberca *et al.*, 2014). On the other hand, Guthrie *et al.*

(2009) showed that horses could be protected against AHSV when immunized with a recombinant canarypox vectored vaccine expressing both outer capsid proteins VP2 and VP5. Furthermore, use of baculovirus expression was proven to be an efficient platform to generate AHSV vaccines that confer protection in horses (Roy *et al.*, 1996, Scanlen *et al.*, 2002). Despite the experimental success achieved with these various subunit vaccine candidates, currently they are yet to be commercialized.

Recently, use of reverse genetics system has been very attractive for the generation of orbivirus vaccine candidates. One of the concepts using reverse genetics is to develop disabled infectious single animal (DISA) vaccine platform. This has been applied to BTV, where DISA viruses were generated by introducing deletion mutants into the NS3/NS3a ORF that caused a completely avirulent virus, which can only replicate locally in vivo but not cause detectable viremia. In addition, BTV DISA vaccine candidate was shown to protect sheep against virulent BTV challenge (Feenstra *et al.*, 2014). Based on the similar concept, van de Water *et al.* (2015) demonstrated the viability of AHS DISA vaccine platform by deleting AHSV NS3/NS3A. Additionally, this group combined the deletion of NS3/NS3A with the exchange of VP2 genome segment proposing a platform for AHSV DISA vaccines against all nine serotypes (van de Water *et al.*, 2015). Although, no viremia was detected with BTV DISA vaccine candidates, the fact that these viruses are still capable of replicating locally *in vivo*, there is still risk of reassortment and reversion to virulence.

The reverse genetics was also applied to generate disabled infectious single cycle (DISC) viruses for orbiviruses. This approach was initially established with the prototype BTV, where Matsuo *et al.* (2011) created a BTV DISC by deleting a replication-essential gene, encoding VP6 protein. DISC BTV was shown to be incapable of producing infectious virus particles unless VP6 was provided by a complementing cell line resulting in high yield infectious viruses. As DISC viruses can only enter a single replication cycle in normal cells, it can trigger immune responses without causing a viremia, which was also demonstrated by the protection of sheep against virulent BTV challenge after vaccination with BTV DISC (Matsuo *et al.*, 2011).

Based on the same technology, Lulla *et al.* (2016) generated a VP6-defective AHSV1 DISC virus and a VP6-expressing complimentary cell line. This was further extended to construct defective viruses of all nine AHSV serotypes by the exchange of two to five RNA genome segments. All DISC viruses generated were incapable of replicating in either mammalian or insect cell lines unless complemented with VP6 expression. Furthermore, immunization with these replication-incompetent viruses was shown to be highly protective in an AHSV mouse model against a homologous lethal virus challenge (Lulla *et al.*, 2016). The use of reverse genetics to generate DISC viruses seems like a promising

vaccine generation platform, which is safer than the DISA vaccine approach due to the absence of infectious virus production.

1.2 Baculoviruses

1.2.1 Characteristics of baculoviruses

Baculoviruses are arthropod-specific viruses that belong to the family *Baculoviridae*. They infect more than 600 host species found in a number of different orders: Lepidoptera (butterflies and moths); Hymenoptera (wasps); and Diptera (mosquitoes) (Herniou *et al.*, 2003, Possee *et al.*, 2010). Autographa californica multiple nucleopolyhedrovirus (AcMNPV), isolated from the Alfafa looper in 1971 (Vail, 1971), is the prototype baculovirus that belongs to the genus Alphabaculoviruses. The common rod-shaped nucleocapsid of baculoviruses encloses a double-stranded, circular supercoiled DNA genome, which is between 80-180 kbp in size (Funk *et al.*, 1997). The prototype AcMNPV was the first baculovirus to be sequenced completely and was found to be 134kbp in size and harbour 154 ORFs (Ayres *et al.*, 1994). It is also the basis of the expression vectors used in this thesis.

Baculoviruses have a bi-phasic replication cycle, which is driven by the two structurally distinct forms of the virus; budded virus (BV) and the occlusion-derived virus (ODV) (Figure 1.9). Primary infection is initiated by ODV within the larval midgut cells and BV, produced after this phase, initiates the secondary infection to spread the virus throughout the host cells and tissues (reviewed by Possee *et al.*, 2010). It is also the form that is used in cell culture as it has been shown to be about 1,800-fold more infectious than ODV (Volkman *et al.*, 1976). DNA replication, synthesis of structural proteins and the expression of viral genes occurs during four successive phases in the nucleus (Figure 1.10A), which is also the location of the new progeny virus formation (reviewed by Slack and Arif, 2006, Romanowski, 2013). While ODV is formed in the nucleus together with its envelope, BV obtains its envelope when the nucleocapsids bud through the infected cell plasma membrane after exiting the nucleus and crossing the cytoplasm (Figure 1.10B). The GP64 envelope protein is acquired during the budding stage and is the major protein for BV attachment, fusion and budding (reviewed by Rohrmann, 2008).

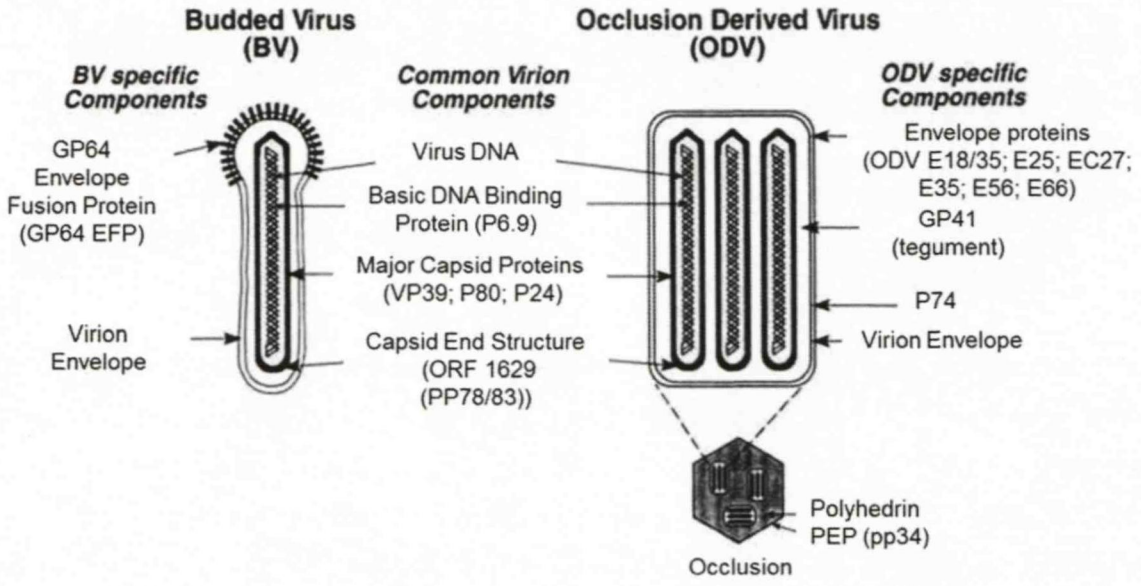


Figure 1.9: Schematic representation of the two distinct forms of baculoviruses

Two functionally distinct forms of baculoviruses share identical nucleocapsids and DNA genome. The major feature that distinguishes BV (left) and ODV (right) are their envelope proteins (Modified from Federici, 1997)

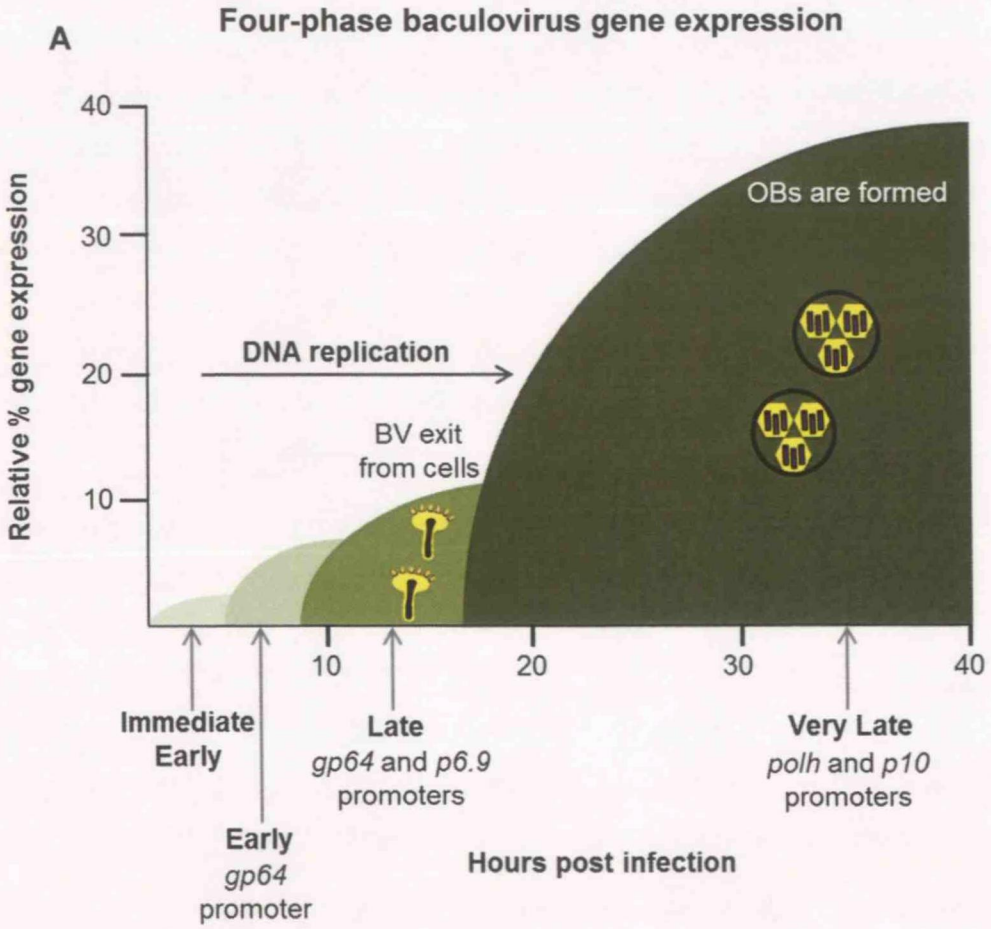
Figure 1.10 Schematic representations of baculovirus gene expression phases and the life cycle

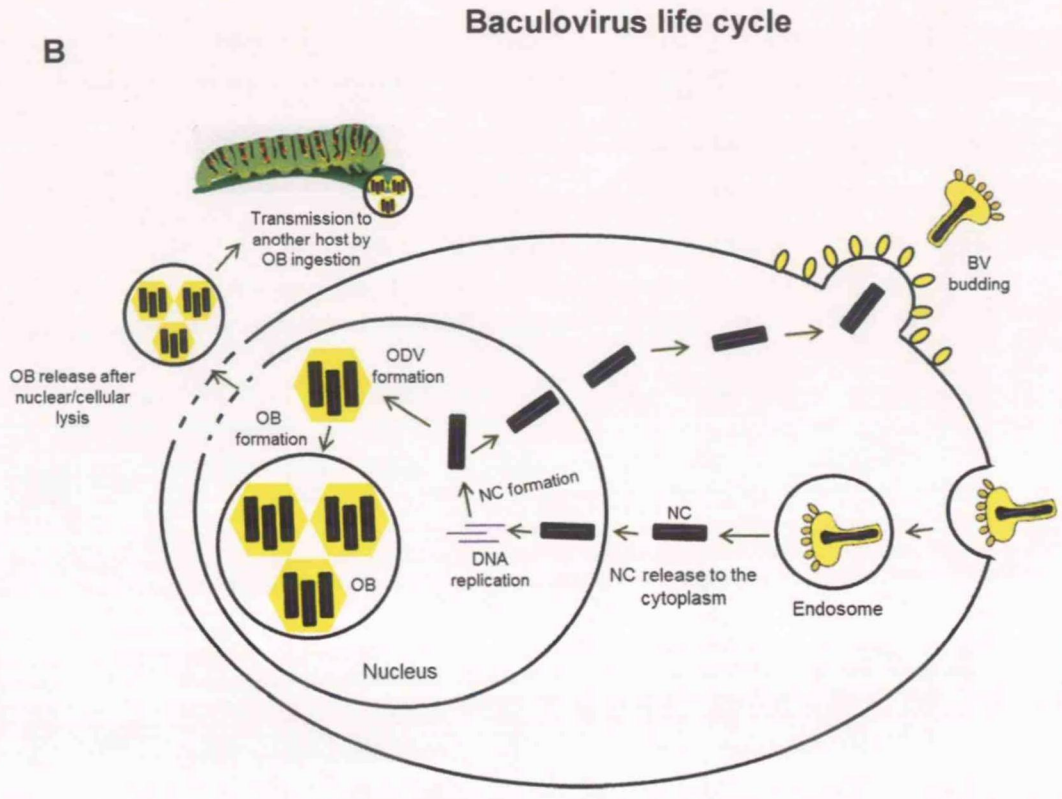
A: Four-phase baculovirus gene expression

Baculoviruses have four successive phases of gene expression namely; immediate early, early, late and very late. At the very early stages of the infection the gene transcription is dependent on the host RNA polymerase, which is then switched to the viral RNA polymerase after viral DNA replication. BV production occurs after the transcription of late genes between six to 24 hours, whereas ODV is produced after the transcription of very late genes, which is from 18 hours onwards. The examples of gene promoters active at different phases of the infection are also indicated on the graph: *gp64* promoter is active during both early and late phases of infection whereas *p6.9* promoter that drives the expression of DNA-binding protein is activated during the late stages. On the other hand, *polh* and *p10* promoters are activated at the very late stages of the infection as they are associated with OB formation and nuclear lysis, respectively.

B: Baculovirus life cycle

BV entry into the cells occurs by clathrin-mediated endocytosis. The GP64 envelope protein enables this entry by binding to a yet unknown receptor. Once internalized into the endosomes, nucleocapsid is released into the cytoplasm, where it gets transported to the nucleus by actin microfilaments. DNA replication and progeny virus formation occurs in the nucleus. BV form of the virus leaves the nucleus and travels to the plasma membrane, where it acquires the GP64-containing envelope from the plasma membrane during cell exit. BV spreads the infection to surrounding cells and tissues in the host and in cell culture. Later in the infection, nucleocapsids gain an envelope in the nucleus forming ODVs, which are then enclosed into occlusion bodies (OBs) surrounded by polyhedrin protein. ODV-containing OBs are released by cell lysis and are very stable in the environment transmitting the infection to other hosts.


A
Four-phase baculovirus gene expression
Relative % gene expression
40
30
20
10
OBs are formed
DNA replication
BV exit
from cells
10
20
30
40
Immediate
Early
Late
gp64 and p6.9
promoters
Very Late
polh and p10
promoters
Early
gp64
promoter
Hours post infection


B
Baculovirus life cycle
Transmission to
another host by
OB ingestion
BV
budding
OB release after
nuclear/cellular
lysis
ODV
formation
OB
formation
NC formation
NC
DNA
replication
NC release to the
cytoplasm
Endosome
OB
Nucleus

1.2.2 Baculovirus GP64 envelope protein

After the infectivity of AcMNPV BV was shown to be specifically neutralized by monoclonal antibody AcV1 (Hohmann and Faulkner, 1983), immunoprecipitation analysis using this antibody has identified that GP64 was the target glycoprotein responsible for BV infectivity (Volkman *et al.*, 1984). The importance of GP64 in BV infectivity was also demonstrated by Monsma *et al.* (1996) with the generation of a GP64-null virus, which failed to disseminate the infection *in vitro* unless provided with GP64 in a complementary cell line. Furthermore, GP64-null virus was shown to form native ODV that was infectious *in vivo* but the subsequently produced BV was unable to disseminate the infection through the cells and tissues of the larvae (Monsma *et al.*, 1996). In addition, GP64 was also shown to be crucial for budding from the cells (Oomens and Blissard, 1999).

Gene sequence (Whitford *et al.*, 1989) and *in vitro* biosynthesis (Jarvis and Garcia, 1994) analysis demonstrated that AcMNPV GP64 is expressed during both early and late phases of infection. Biosynthesis analysis also revealed that GP64 has N-linked glycosylation, which was demonstrated to be important for its cell surface expression and the production of infectious BV particles (Stiles *et al.*, 1983, Charlton and Volkman, 1986, Jarvis and Garcia, 1994). Furthermore, GP64 was shown to form oligomers including dimers and trimers under non-reducing conditions (Volkman and Goldsmith, 1984).

The location of GP64 was found to be in the plasma membrane of infected cells prior to BV budding in the form of spikes and was also shown to be incorporated into BV envelope surface being mainly concentrated at one apical end (Volkman *et al.*, 1984). Concentration of envelope proteins to one end of the rod-shaped BV was also supported by ultrastructural analysis of AcMNPV using electron microscopy (EM) (Fraser, 1986). However, a recent study by Wang *et al.* (2016) contradicted these findings when they demonstrated using cryo-EM that GP64 spikes are mainly concentrated on both apical ends of the virion. In addition, they have suggested that BV has an ovoid shape structure where the envelope is closely associated at the two apical ends with large lateral spaces between the nucleocapsid and the envelope, unlike previous findings where envelope was shown to coat the nucleocapsid in a rod-shape structure (Figure 1.11, Wang *et al.*, 2016).

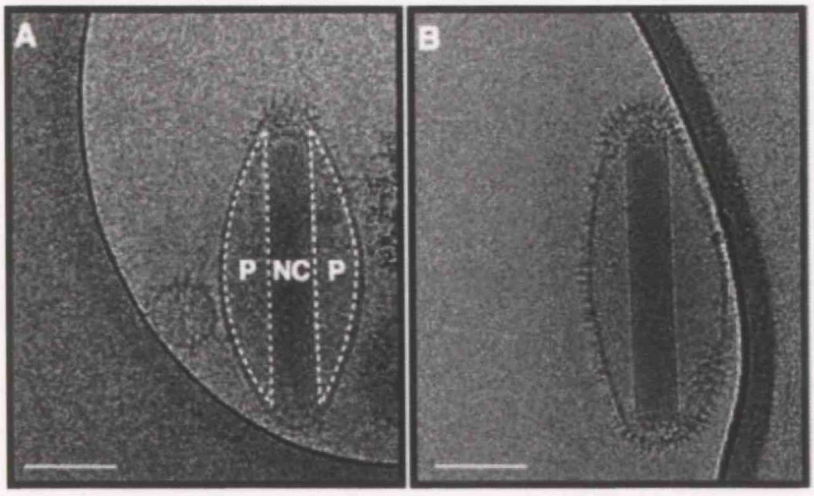


Figure 1.11: Cryo-EM images of AcMNPV budded virus

Recently demonstrated ovoid-shaped structure of AcMNPV BV harbouring GP64 spikes at both apical ends. This image is taken from (Wang *et al.*, 2016) based on the permission rights obtained from ScienceDirect. NC, nucleocapsid; P, pocket at lateral sides.

1.2.3 Baculoviruses as tools for biotechnological and pharmaceutical applications

The increase in understanding the biology of baculoviruses has led to their use in various applications. For instance, baculoviruses have been widely used as biological pesticides due to their host specificity and safety for environment and human health (Bonning and Hammock, 1992). Another widely used application of baculoviruses is the production of recombinant proteins in insect cells, which was developed in the mid 1980's and termed as baculovirus expression vector system (BEVS; Summers, 2006). Over the years, the BEVS gone through several advancements for improved protein expression, which is explained in more detail below. Further development of baculovirus technology has enabled their use beyond just recombinant protein expression in insect cells. These include the delivery of target genes to mammalian cells for gene therapy purposes, which is achieved by the generation of baculovirus vectors containing expression cassettes with mammalian cell promoters (Kost *et al.*, 2005, Airenne *et al.*, 2013). In addition, baculovirus surface display strategy became very attractive to study protein-protein interactions and generation of target-specific immune responses (Oker-Blom *et al.*, 2003). Moreover, baculovirus expression technology has been utilized for the generation of commercially available vaccines (Felberbaum, 2015).

1.2.3a Baculovirus expression vector system

After it was demonstrated that *polyhedrin (polh)*, the major structural component of OBs, is not essential for infectious BV production in cell culture (Smith *et al.*, 1983a), this information was used to generate a eukaryotic expression vector for the production of

recombinant proteins (Figure 1.12). The human β-interferon was the first protein that was successfully produced to high yields when inserted in place of the *polh* coding region in the AcMNPV genome (Smith *et al.*, 1983b). In addition, the *p10* gene locus was also demonstrated to be useful for foreign gene expression due to its non-essential requirement for infectious BV production in cell culture (Vlak *et al.*, 1988, Vlak *et al.*, 1990). The *polh* (Possee and Howard, 1987) and *p10* (Knebel *et al.*, 1985) genes have very strong promoters that drive high-yield protein expression very late in infection, which is also very beneficial to the BEVS. Moreover, the insect host cells used for BEVS have the capacity for recognizing and processing signal peptides, oligomerisation and post-translational modifications such as glycosylation, acylation, phosphorylation and disulphide bond formation, hence enabling the correct formation of authentic eukaryotic proteins (Klenk, 1996, Geisler and Jarvis, 2009).

As the baculoviruses have a very large genome, insertion of a foreign gene can only occur after recombination between the virus genome and a transfer vector carrying the gene of interest, which is also the basis of BEVS (Figure 1.12) (reviewed by King *et al.*, 2007). Initially, recombinant viruses were identified by a polh-negative phenotype (absence of OBs) in insect cells, which was followed by several rounds of plaque purification for virus isolation; a long and tedious process (Smith *et al.*, 1983b). Although Smith *et al.* (1983b) successfully demonstrated the feasibility of recombinant protein expression using BEVS, the rate of detecting recombinant viruses was very low (~0.5%). Linearization of the AcMNPV genome with a single *Bsu361* site introduced at the *polh* locus was shown to reduce the parental virus background as linear virus cannot replicate. Hence, the detection of recombinant viruses was enhanced up to 30%, which was a step forward for improving the efficiency of BEVS (Kitts *et al.*, 1990).

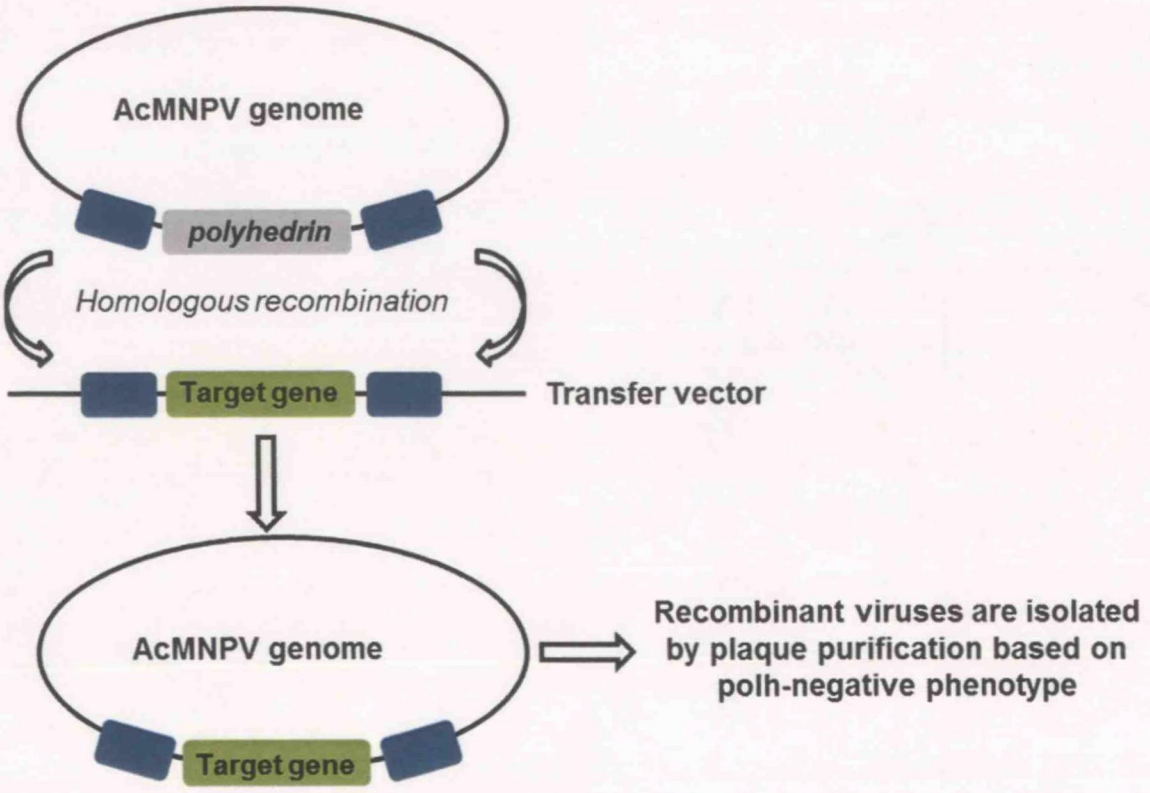


Figure 1.12 Schematic representation of recombinant baculovirus production

The gene of interest is inserted in place of the *polh* coding region in insect cells as a result of homologous recombination between the AcmNPV genome and a transfer vector carrying the target gene. Recombinant viruses are isolated by plaque purification based on polh-negative phenotype in insect cells.

The major improvement to BEVS' efficiency was however achieved by the generation of the BacPAK6 system, which relies on a triple *Bsu361*-cut AcMNPV genome that contains *lacZ* at the *polh* locus (Kitts and Possee, 1993). The *Bsu361* sites are located in the *lacZ* itself and the two flanking genes, one being the essential ORF1629. Linearization results in the removal of *lac*Z gene together with a fragment of ORF1629 producing a virus genome that is replication incompetent. Simultaneous transfection of insect cells with linearized DNA and the transfer vector containing the gene of interest results in a restored ORF1629 function and the re-circularization of DNA, generating a replication-competent recombinant virus (Figure 1.13). This method greatly decreased the parental virus background, improving the efficiency of recombinant virus production up to 90%. However, it is impossible to be certain of the triple *Bsu361*-digestion of the entire DNA present in the sample and any partially-digested DNA can re-circularize to replicate in the culture causing a parental background. Therefore, screening of viruses using plaque purification based on blue/white selection is still required (Kitts and Possee, 1993). The BacPAK6 system is commercially available from Oxford Expression Technologies (OET) Ltd alongside other commercial systems.

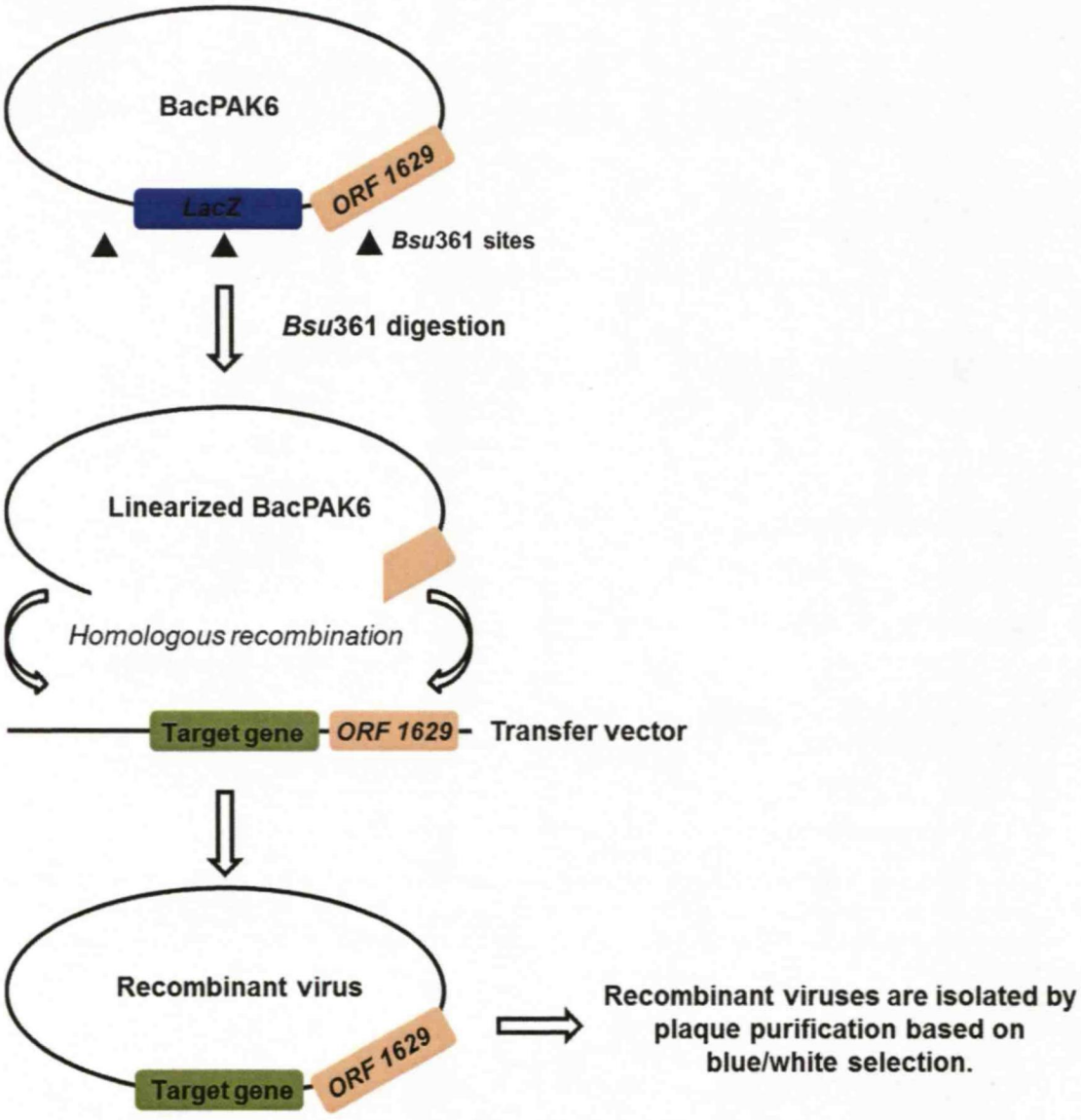


Figure 1.13 Schematic representation of the BacPAK6

The BacPAK6 system is based on the linearization of the AcMNPV genome by triple *Bsu*361 digestion, which results in the impairment of the replication-essential ORF1629 gene. When the target gene is inserted into the AcMNPV genome after homologues recombination in insect cells, the function of the ORF1629 is restored enabling recombinant virus replication. Recombinant viruses are isolated by plaque purification in insect cells based on blue/white selection in the presence of X-gal. White plaques indicate recombinant viruses.

A major improvement to avoid the isolation of recombinant viruses by plaque purification was the generation of an AcMNPV bacmid that can be modified in *E.coli* but also is infectious in insect cells (Luckow *et al.*, 1993). This bacmid contains *lacZ* as a selection marker and Tn7 transposition sites. The other major element of this system is a transfer vector that contains the gene of interest flanked by Tn7 transposition sites. When the transfer vector is introduced into the *E.coli* containing the AcMNPV bacmid, a site-directed transposition occurs between the bacmid genome and the transfer vector inserting the gene of interest into the *polh* locus disrupting the *lacZ* sequence (Figure 1.14). Once the

recombinant bacmid is identified, based on antibiotic resistance and blue/white selection on agar plates, it is amplified, isolated and introduced into insect cells for BV production (Luckow *et al.*, 1993). Although this system removes the requirement of plaque-purification, there are still several steps carried out in *E. coli* before recombinant viruses can be generated in the insect cells. This system is designated as Bac-to-Bac® and is commercially available from Invitrogen Ltd.

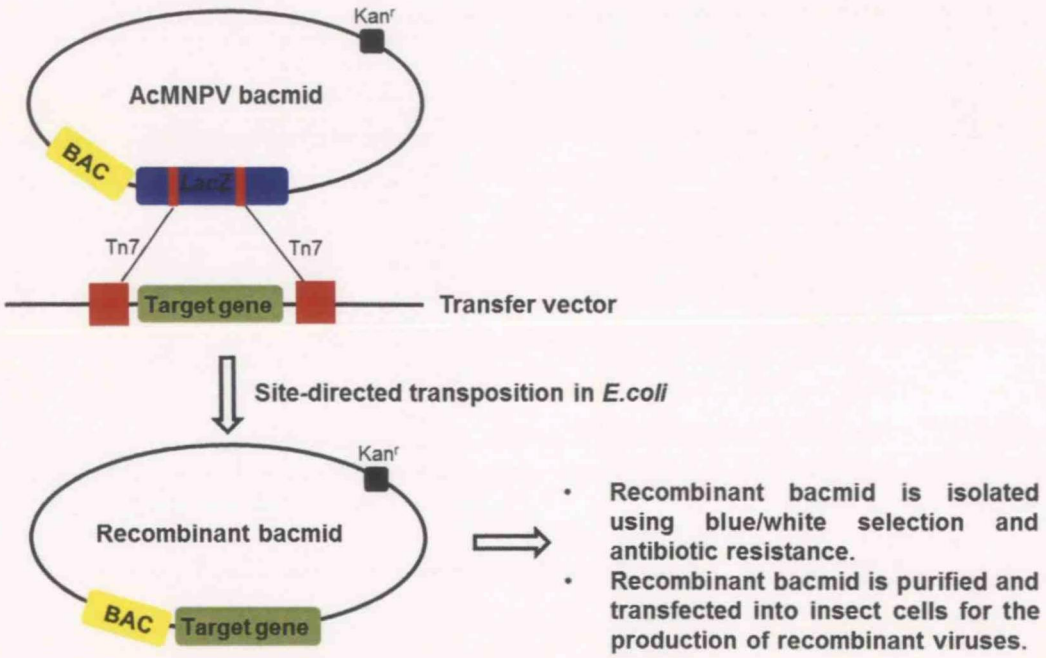


Figure 1.14 Schematic representation of the Bac-to-Bac® system

AcmNPV bacmid contains a *lacZ* reporter gene (blue), Tn7 transposition sites (red) and Kanamycin resistance gene (black). The target gene is inserted into the AcMNPV bacmid in DH10Bac™ *E.coli* cells by Tn7 site-directed transposition. Recombinant bacmid is isolated by *kanamycin* resistance and blue/white selection in bacterial cells (white colonies indicate the recombinant bacmids). Once isolated, recombinant bacmid is amplified and then transfected into insect cells for the production of recombinant viruses.

The final improvement of BEVS was the development of a novel platform for the rapid production of recombinant baculoviruses. This platform is based on AcMNPV genome that contains part of an essential gene, ORF1629 that can only be restored after successful homologous recombination with an appropriate transfer vector in insect cells, hence removing the requirement of plaque purification. In addition, a bacterial artificial chromosome (BAC) is added to the AcMNPV, enabling its maintenance in *E.coli*, hence removing the requirement of DNA linearization prior to recombination (Figure 1.15)(Je *et al.*, 2001, Possee *et al.*, 2008). This platform was shown to be superior to other BEVS due to its ability for one-step generation of high throughput baculovirus expression vectors very rapidly (Possee *et al.*, 2008, Figure 1.16). The *flashBAC*™(FB) system was developed based on this platform (Possee *et al.*, 2008) and is commercialized by OET Ltd.

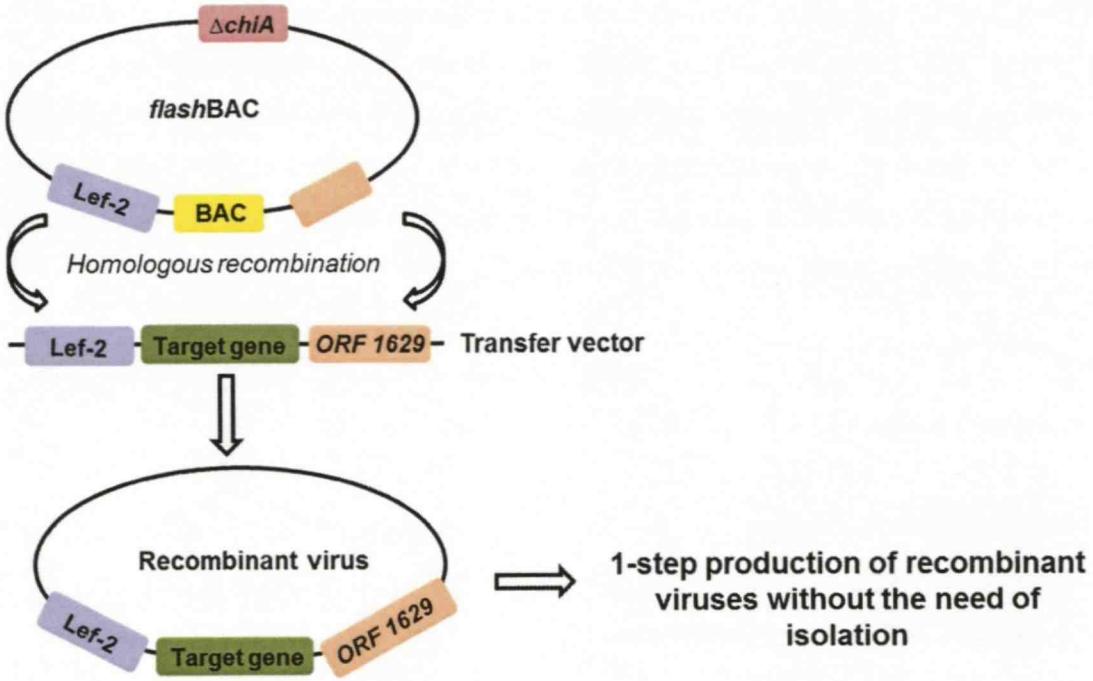


Figure 1.15 Schematic representation of flashBAC™ system

AcMNPV genome contains a BAC (yellow) and lacks part of an essential gene ORF1629 (beige). The target gene is inserted into the AcMNPV genome in insect cells by homologous recombination between the transfer vector and the genome, which restores the function of ORF1629. Only recombinant viruses can replicate hence no isolation is required.

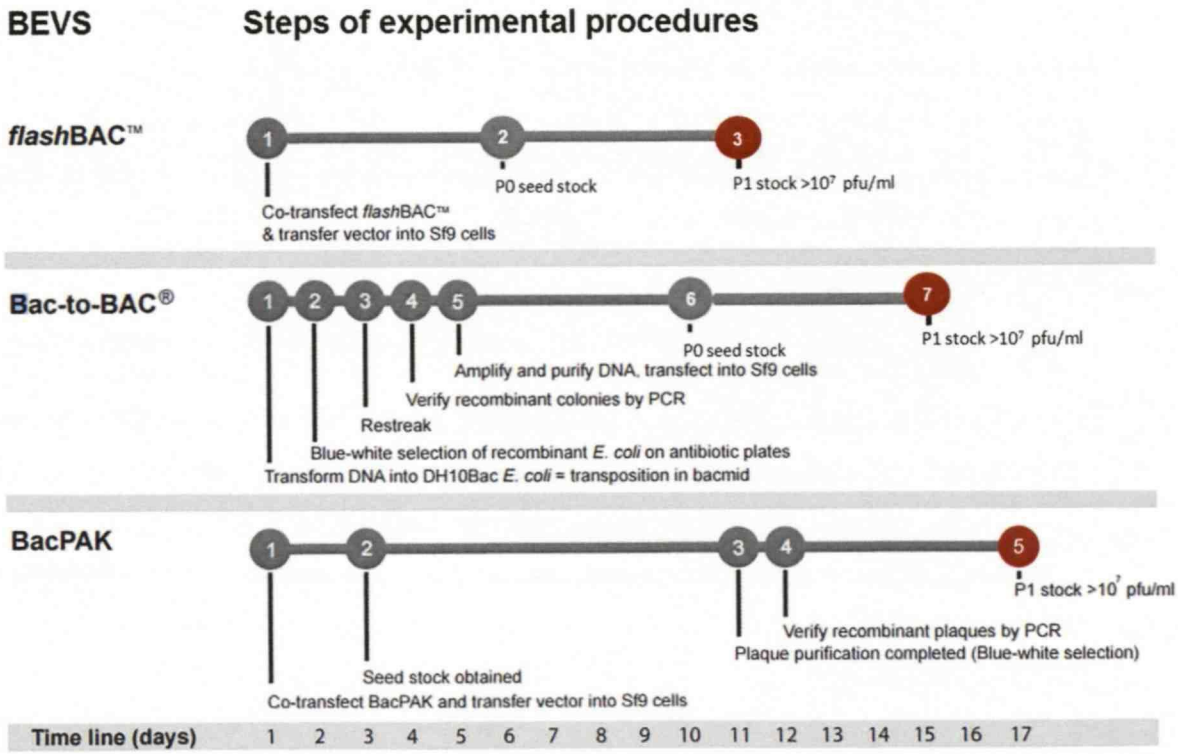


Figure 1.16 *flash*BAC™ time line compared to other baculovirus expression vector systems (modified from Oxford Expression Technologies Ltd, 2016).

The *flash*BAC™ system was taken a step forward by improving the recombinant protein yield and quality by the additional deletion of non-essential virus genes. This resulted in the two sub-forms of the system namely; *flash*BACGOLD™ (FBG) (Hitchman *et al.*, 2010b) and *flash*BACULTRA™ (FBU) (Hitchman *et al.*, 2010a), which are also marketed by OET Ltd. The details of gene deletions in these systems and their functions are summarized in Table 1.1.

1.2.3b Baculovirus based vaccines

The technology provided by BEVS can also be used as a vaccine generation platform due to the advantageous characteristics offered such as safety and the rapid, correctly folded high-yield production of recombinant proteins. The time required to generate a vaccine is especially important during an outbreak of an emerging disease. For instance, in the case of the common human pathogen, influenza, it takes at least six months to generate an influenza vaccine using the traditional egg-based manufacturing (Wong and Webby, 2013). On the other hand, it was shown that a clinical batch of an Ebola virus vaccine was generated in half of that time (three months) using the baculovirus expression platform (Hahn *et al.*, 2015).

Regarding their safety, baculoviruses have a very specific invertebrate host range as mentioned above, which has resulted in their use as biopesticides in the environment for a long time (Bonning and Hammock, 1992). They were also shown to be incapable of replication in mammalian cells or produce recombinant proteins unless the expression is driven by a mammalian cell promoter (Kost *et al.*, 2005). In addition, baculoviruses are generally found on fresh, green vegetables; hence they are daily consumed by individuals as part of their diet (Heimpel *et al.*, 1973). Furthermore, due to their invertebrate specificity, there is no concern for the pre-existing immunity with the use of baculoviruses as vaccine vectors in mammalian systems, unlike other viral vectors such as adenoviruses and poxviruses, which are frequently found in human populations (Madhan *et al.*, 2010) The safe use of baculoviruses as a vaccine generation platform is also proven by the approval of several commercial veterinary and human vaccines as well as human therapeutics agents as summarized in Table 1.2 (Cox, 2012, Felberbaum, 2015, van Oers *et al.*, 2015).

Table 1.1 The functions and the benefits of AcMNPV genes deleted from *flash*BAC™ variants

Gene	Platform it is deleted from	Function	Advantages to BEVS		Reference
Chitinase (chiA)	FB, FBG, FBU	Is expressed late in infection and functions as endo- and exo-chitinolytic enzyme, which breaks down chitin, major component of the arthropod exoskeleton. It is partly involved in the liquefaction of the host, enabling horizontal transmission of the virus to other hosts. It contains a signal peptide and a C-terminal endoplasmic reticulum (ER) retention signal (KDEL), which causes its accumulation in ER blocking the secretory pathway.	Improved production of membrane-bound and secreted recombinant proteins in insect cells.		Hawtin *et al.*, 1995 Thomas *et al.*, 1998 Possee *et al.*, 1999 Hawtin *et al.*, 1997 Possee *et al.*, 2008
Cathepsin (v-cath)	FBG, FBU	Is a cysteine proteinase that is expressed late in infection and degrades proteins with target sequences. It is involved in host liquefaction together with *chiA*. *proV-cath* was demonstrated to interact with *chitinase*, which aids its retention in the ER.	Enhanced yield and stability of recombinant proteins by preventing their degradation.		Slack *et al.*, 1995 Hodgson *et al.*, 2011 Kaba *et al.*, 2004 Hitchman *et al.*, 2010b
p10	FBU	Is abundantly expressed very late in infection just like polyhedrin. It has an unknown function but is thought to play a role in the nuclear/cellular lysis for the release of OBs and is non-essential for cell culture infection.	Enhances *polh* promoter activity Also improves cellular and nuclear stability, providing a longer time frame for recombinant protein production.	Removes unnecessary genetic load from recombinant viruses, hence enables more access to cellular resources for recombinant protein production.	Smith *et al.*, 1983c Carpentier *et al.*, 2008 Williams *et al.*, 1989
p26	FBU	Early gene with an unknown function. Shown to be non-essential for virus replication *in vitro* or *in vivo*.	-		Simon *et al.*, 2008
p74	FBU	Crucial gene of ODVs for the establishment of primary infection in the midgut cells of the larvae. It is non-essential in cell culture.	Enhanced biosafety profile of recombinant baculoviruses in the environment		Faulkner *et al.*, 1997 Hitchman *et al.*, 2010a

Table 1.2 BEVS products approved for commercial use

Target Disease/Virus	Product name (Manufacturer)	Target protein	Product type	Reference
Veterinary vaccines				
Classical swine fever	Porcilis® Pesti (MSD Animal Health)	E2 glycoprotein	Subunit vaccine	Moormann *et al.*, 2000
Porcine circovirus type 2 (PCV2)	Porcilis® PCV (MSD Animal Health)	ORF2 capsid protein	Subunit vaccine (VLP)	Blanchard *et al.*, 2003
	Ingelvac® CircoFLEX™ (Boehringer Ingelheim Vetmedica)	ORF2 capsid protein	Subunit vaccine (VLP)	Fachinger et al 2008
	Circumvent® PCV (Merck Animal Health)	ORF2 capsid protein	Subunit vaccine (VLP)	Kristensen *et al.*, 2011
Human vaccines				
Human papilloma virus (HPV)	Cervarix® (GlaxoSmithKline)	L1 capsid proteins of HPV serotypes 16 and 18	Subunit vaccine (VLP)	Paavonen *et al.*, 2007
Influenza	Flublok® (Protein Sciences Corporation)	Hemagglutinin of three or four seasonal influenza strains	Subunit vaccine	McPherson, 2008
Human Therapeutics				
Prostate cancer	Provenge® (Dendreon)	Fusion protein of human prostatic acid phosphatase (PAP) and Granulocyte macrophage colony-stimulating factor (GM-CSF)	Immunotherapy	Small *et al.*, 2000
Lipoprotein lipase deficiency (LPLD)	Glybera® (UniQure)	Adeno associated virus vector with human LPL variant *	Gene therapy	Guadet *et al.*, 2012

* The vector used in gene therapy is adeno associated virus vector, which is produced using baculovirus expression technology.

In addition to safety, the affordable costs of BEVS platform for vaccines is also attractive for commercial manufacturing. One of the reasons for lower costs is the high yield protein production in BEVS. This is exemplified by Cox (2012), showing that four to seven times higher hemagglutinin (HA) yield is produced in BEVS than Madin-Darby Canine Kidney Epithelial Cells (MDCK), automatically reducing the costing for influenza vaccine production. Moreover, as reviewed by Felberbaum *et al* (2015), once a BEVS facility is established, it can be used for the generation of various different products, which also makes the platform more cost effective. Furthermore, no live agents are used for antigen production in BEVS hence, the costs of providing and maintaining biocontainment facilities are also removed (Felberbaum, 2015).

1.3 Project Focus and Aims

The horse industry has a major role in the economy of mainland Europe and the United Kingdom. For example, National Equestrian Survey conducted by The British Equestrian Trade Association in 2015 estimated that the economic value of the equestrian sector is about £4.3 billion, which is an increase from £3.8 billion in 2011 (BETA, 2016). European Horse Network evaluates this figure to be more than €100 billion a year in Europe (EHN, 2016). Therefore, an AHSV outbreak in these non-endemic regions would have a considerable impact on sporting events, trade and animal health, which collectively affects the economy of a country. Climate change, the vast presence of *Culicoides species* in Europe and most importantly the recent, unexpected incursion of BTV into Europe, which shares similar midge vectors, raises huge concerns that AHSV could follow the same pattern (reviewed by Zientara *et al.*, 2015, Robin *et al.*, 2016).

As the virus is transmitted by *Culicoides* species, it replicates in the cells and tissues of its arthropod vector before it can be transmitted into another host (Du Toit, 1944, Boorman *et al.*, 1975, Mellor *et al.*, 1975). This characteristic of arboviruses makes baculovirus-insect cell expression system very advantageous for the production of correctly folded arboviral proteins.

The focus of this thesis was to investigate the antigenic structure of AHSV4 VP2 further by expressing the full-length protein and eleven subdomains thereof using baculovirus expression and surface display strategies. Understanding the antigenic structure of this protein, which is the target of VNAbs, contributes to generating more efficient and safe vaccines. Moreover, these baculovirus constructs would also serve as potential vaccine candidates for AHSV. In order to achieve the overall goal of this thesis, each chapter has focused on a different aim with the details being described below:

- Initial aim of this thesis, which was the basis of Chapter three, was to construct recombinant baculoviruses that express the full-length VP2 and its eleven subdomains in two different insect cell lines. Hence, the competence of their expression in this system would be evaluated. Additionally, these proteins were designed to contain a histidine tag to enable affinity-based purification. Purified proteins would facilitate a comparison between the conformation of the virus neutralizing epitopes of the protein when they are expressed individually and when they are displayed on the baculovirus envelope surface.

- Chapter four focused on optimizing the baculovirus surface display, which is the other strategy this thesis adopted for the expression of AHSV4 VP2 and its subdomains. Optimizations included the testing of three different AcMNPV

promoters for the expression of full-length VP2 and one of the subdomains, fragment H. Additionally, truncation of GP64 TMD was analysed for possible improvement of fusion protein production. This was achieved by comparing constructs that were generated to express a reporter gene, enhanced green fluorescent protein (EGFP).

- Having identified the optimum conditions for baculovirus surface display in Chapter four, the focus of Chapter five was to generate baculovirus constructs that display all VP2 subdomains on their envelope surface and characterize the expression of the fusion proteins.

- Chapter six aimed to investigate the antigenicity of the subdomains produced by the recombinant baculoviruses constructed in Chapter three and five by several *in vitro* binding assays using a panel of AHSV4-specific monoclonal antibodies (MAbs), AHSV4 virus neutralizing serum and vaccination studies in mice. In doing so, the knowledge of VP2 antigenic structure will be expanded.

- The aim of the final Chapter seven was to summarize all the major findings of this thesis and mainly focus on the future work that could be carried out to take this project forward.

Chapter 2
Materials and Methods

2.1 Materials

General chemicals were purchased from the following companies unless stated otherwise: BDH Chemicals Ltd, Fisher Scientific or Sigma-Aldrich. Molecular biology reagents were purchased from Invitrogen, New England Biolabs (NEB), Fermentas or Promega. Cell culture media was supplied by Gibco and Oxford Expression Technologies Ltd (OET).

All internally prepared solutions were sterilized either by autoclaving for 15 minutes (15 pounds per square inch (p.s.i.)) or by filtration using 0.45 or 0.2µm filters. All reagent percentages are w/v unless otherwise stated.

The plasmids used in this thesis are listed in Table 2.1, the viruses used are listed in Table 2.2, *Escherichia coli* (*E. coli*) strains used for cloning are listed in Table 2.3 and bacmids used are listed in Table 2.4.

Table 2.1 Plasmids

Plasmid	Source	Chapter
pSC11 VP2	Dr Javier Castillo-Olivares, The Pirbright Institute	3, 4 and 5
pOET1	OET Ltd	3
pOET-1N	OET Ltd	3
pOET3	OET Ltd	4
pBACsurf-1	Novagen	4 and 5
pGEM-T	Promega	3 and 4
pGEM-T Easy	Promega	3 and 4
pBac-1_CMV	Dr Elisabetta Hitchman, Oxford Brookes University	3
pEGFP-N1	Clontech	4
pBacPAKgp64dsred	Dr John Danquah, Oxford Brookes University	4
pOET1_VP2$^{HIS/N}$	Mine Aksular, this thesis	3
pOET1_VP2-H$^{HIS/N}$	Mine Aksular, this thesis	3
pOET1N_VP2-A$^{HIS/N}$	Mine Aksular, this thesis	3
pOET1N_VP2-B$^{HIS/N}$	Mine Aksular, this thesis	3
pOET1N_VP2-C$^{HIS/N}$	Mine Aksular, this thesis	3
pOET1N_VP2-D$^{HIS/N}$	Mine Aksular, this thesis	3
pOET1N_VP2-E$^{HIS/N}$	Mine Aksular, this thesis	3
pOET1N_VP2-F$^{HIS/N}$	Mine Aksular, this thesis	3
pOET1N_VP2-G$^{HIS/N}$	Mine Aksular, this thesis	3
pOET1N_VP2-I$^{HIS/N}$	Mine Aksular, this thesis	3
pOET1N_VP2-J$^{HIS/N}$	Mine Aksular, this thesis	3
pOET1N_VP2-Z$^{HIS/N}$	Mine Aksular, this thesis	3
pBACsurf-1_p6.9	Mine Aksular, this thesis	4
pBACsurf-1_gp64	Mine Aksular, this thesis	4
pBACsurf-1_*polh*_VP2-H	Mine Aksular, this thesis	4
pBACsurf-1_*polh*_VP2-H^{HIS}	Mine Aksular, this thesis	4
pBACsurf-1_*p6.9*_VP2-H	Mine Aksular, this thesis	4
pBACsurf-1_*p6.9*_VP2-H^{HIS}	Mine Aksular, this thesis	4
pBACsurf-1_*gp64*_VP2-H	Mine Aksular, this thesis	4
pBACsurf-1_*gp64*_VP2-H^{HIS}	Mine Aksular, this thesis	4

Table 2.1 (continued) Plasmids

Plasmid	Source	Chapter
pBACsurf-1_*p6.9*_VP2^{HIS}	Mine Aksular, this thesis	4
pBACsurf-1_*gp64*_VP2	Mine Aksular, this thesis	4
pBACsurf-1$^{GP64/F463}$	Mine Aksular, this thesis	4
pBACsurf-1_EGFP	Mine Aksular, this thesis	4
pBACsurf-1_EGFP$^{GP64/F463}$	Mine Aksular, this thesis	4
pBACsurf-1_VP2$^{GP64/F463}$	Mine Aksular, this thesis	4
pBACsurf-1_VP2-H$^{GP64/F463}$	Mine Aksular, this thesis	4
pBACsurf-1_VP2-A$^{GP64/F463}$	Mine Aksular, this thesis	5
pBACsurf-1_VP2-B$^{GP64/F463}$	Mine Aksular, this thesis	5
pBACsurf-1_VP2-C$^{GP64/F463}$	Mine Aksular, this thesis	5
pBACsurf-1_VP2-D$^{GP64/F463}$	Mine Aksular, this thesis	5
pBACsurf-1_VP2-E$^{GP64/F463}$	Mine Aksular, this thesis	5
pBACsurf-1_VP2-F$^{GP64/F463}$	Mine Aksular, this thesis	5
pBACsurf-1_VP2-G$^{GP64/F463}$	Mine Aksular, this thesis	5
pBACsurf-1_VP2-I$^{GP64/F463}$	Mine Aksular, this thesis	5
pBACsurf-1_VP2-J$^{GP64/F463}$	Mine Aksular, this thesis	5
pBACsurf-1_VP2-Z$^{GP64/F463}$	Mine Aksular, this thesis	5

Table 2.2 Viruses

Virus	Source	Chapter
WT AcMNPV	Prof Robert Possee, OET Ltd	3 and 5
AcVP2$^{HIS/N}$	Mine Aksular, this thesis	3, 4 and 6
AcVP2-H$^{HIS/N}$	Mine Aksular, this thesis	3, 4, 5 and 6
AcVP2-A$^{HIS/N}$	Mine Aksular, this thesis	3
AcVP2-B$^{HIS/N}$	Mine Aksular, this thesis	3
AcVP2-C$^{N\text{-}HIS}$	Mine Aksular, this thesis	3
AcVP2-D$^{HIS/N}$	Mine Aksular, this thesis	3
AcVP2-E$^{HIS/N}$	Mine Aksular, this thesis	3
AcVP2-F$^{HIS/N}$	Mine Aksular, this thesis	3
AcVP2-G$^{HIS/N}$	Mine Aksular, this thesis	3
AcVP2-I$^{HIS/N}$	Mine Aksular, this thesis	3
AcVP2-J$^{HIS/N}$	Mine Aksular, this thesis	3
AcVP2-Z$^{HIS/N}$	Mine Aksular, this thesis	3
AcSurf_VP2-H	Mine Aksular, this thesis	4
AcSurf_VP2-H^{HIS}	Mine Aksular, this thesis	4
AcSurf_VP2-H$^{p6.9}$	Mine Aksular, this thesis	4
AcSurf_VP2-H$^{p6.9/HIS}$	Mine Aksular, this thesis	4
AcSurf_VP2-H^{gp64}	Mine Aksular, this thesis	4
AcSurf_VP2-H$^{gp64/HIS}$	Mine Aksular, this thesis	4
AcSurf_VP2$^{p6.9/HIS}$	Mine Aksular, this thesis	4
AcSurf_VP2^{gp64}	Mine Aksular, this thesis	4
AcSurf_EGFP	Mine Aksular, this thesis	4 and 5
AcSurf_EGFP^{TRUN}	Mine Aksular, this thesis	4 and 5
AcEGFP^{wssv}	Mine Aksular, this thesis	4
Acsurf_VP2^{TRUN}	Mine Aksular, this thesis	4
Acsurf_VP2-H^{TRUN}	Mine Aksular, this thesis	4, 5 and 6
Acsurf_VP2-A^{TRUN}	Mine Aksular, this thesis	5 and 6

Table 2.2 (continued) Viruses

Virus	Source	Chapter
Acsurf_VP2-B^{TRUN}	Mine Aksular, this thesis	5 and 6
Acsurf_VP2-C^{TRUN}	Mine Aksular, this thesis	5 and 6
Acsurf_VP2-D^{TRUN}	Mine Aksular, this thesis	5 and 6
Acsurf_VP2-E^{TRUN}	Mine Aksular, this thesis	5 and 6
Acsurf_VP2-F^{TRUN}	Mine Aksular, this thesis	5 and 6
Acsurf_VP2-G^{TRUN}	Mine Aksular, this thesis	5 and 6
Acsurf_VP2-I^{TRUN}	Mine Aksular, this thesis	5 and 6
Acsurf_VP2-J^{TRUN}	Mine Aksular, this thesis	5 and 6
Acsurf_VP2-Z^{TRUN}	Mine Aksular, this thesis	5 and 6
Acsurf^{TRUN}	Mine Aksular, this thesis	6

Table 2.3 *E. coli* strains

E. coli strain	Genotype	Source
DH5α	F$^-$ Φ80*lac*ZΔM15 Δ(*lac*ZYA-*arg*F) U169 *rec*A1 *end*A1 *hsd*R17(r_k^-, m_k^+) *pho*A *sup*E44 *thi*-1 *gyr*A96 *rel*A1 λ$^-$	Thermo Fisher Scientific

Table 2.4 Bacmids

Bacmid	Genotype	Source
*flash*BAC ULTRA	*Δp74, Δp10, Δp26, Δv-cath, ΔchiA*	OET Ltd

2.2 Cells and Viruses

2.2.1 Cells

The cell lines used throughout this project to either propagate viruses or to produce proteins were: *Trichoplusia ni* (TnHi5) (Wickham *et al.*, 1992, Wickham and Nemerow, 1993), *Spodoptera frugiperda* (Sf21 and Sf9) (Vaughn *et al.*, 1977). Both Insectogrow (Corning®) and ESF 921 (Expression Systems) serum-free media were used to maintain Sf9 cells over the course of this project. TnHi5 cells were maintained in ESF 921 serum-free media and Sf21 cells were maintained in TC100 (Gibco) medium supplemented with 10% (v/v) foetal bovine serum (FBS) as described in King and Possee (1992).

2.2.2 Virus amplification

In order to amplify virus stocks, Sf9 cells at a density of $2x10^6$ cells/ml were seeded in shaker cultures. The cells were infected with the corresponding virus at multiplicity of infection (MOI) 0.1 pfu/cell and incubated at 28°C. After 5 days post-infection (dpi), the

infected culture was centrifuged at 4000 rpm for 20 minutes (4°C) to pellet the cells (TY-JS 4.2 rotor, J6-MI Beckman centrifuge). The clarified culture media containing the budded virus (BV) particles were then stored in sterile tubes in the dark at 4°C. The virus stocks were supplemented with 2% (v/v) FBS to preserve titres as high as possible over long-term storage. Several 1ml aliquots were also stored at -80°C.

2.2.3 Generation of recombinant viruses by co-transfection of insect cells

Recombinant viruses were generated using the *flash*BAC™ system following the supplier's protocol (Oxford Expression Technologies Ltd; Possee *et al.*, 2008). Sf9 cells were co-transfected with virus DNA (100ng) and the transfer plasmid containing the gene of interest (500ng) using the liposome-mediated transfection method (Lipofectin™, Invitrogen). Briefly, virus and the transfer plasmid DNA were added to 1ml of TC100 medium in 7ml bijoux tubes, which were then mixed with 1ml TC100 containing 10µl lipofectin. This mixture was incubated at room temperature for 30 minutes before adding it to duplicate 35mm dishes seeded with $0.7x10^6$ cells/dish of Sf9 cells. The cells were incubated at 28°C for 5 hours or overnight before the addition of 1ml Insectogrow medium containing 200U/ml of penicillin/streptomycin (Gibco). Following 5 days of incubation at 28°C, culture media containing the recombinant virus was harvested. This sample was generally referred to as the P0 virus stock, which was then used to amplify a larger stock of P1 virus as described in section 2.2.2.

2.2.4 Titration of virus stocks

Virus stocks were titrated using either the standard plaque assay technique that is described in detail by King and Possee (1992) or a qPCR based titration system using the *baculo*QUANT™ ALL-IN-ONE by following the supplier's protocol (Oxford Expression Technologies Ltd; Hitchman *et al.*, 2007b).

2.2.4a Plaque Assay

Sf21 cells were seeded at a density of $1.4x10^6$ cells/well or $0.5x10^6$ cells/well in 6-well or 12-well plate, respectively and placed on a flat surface for 1 hour at 28°C to settle. For each virus stock to be titrated, ten-fold serial dilutions were prepared in serum-supplemented medium. Then the medium overlay from the seeded plates was replaced with 100µl virus inoculum at the appropriate dilution and incubated on a rocking table for 1 hour at room temperature. Following this incubation, virus inoculum was removed and replaced with 2ml (or 1ml for 12-well plates) of 1% low gelling temperature (LGT) agarose, which is obtained by diluting a 2% LGT solution with an equal volume of appropriate insect culture medium. The agarose was then allowed to solidify at room temperature for approximately 20 minutes. After the agarose had set, 1ml of serum-supplemented

medium overlay containing 200U/ml penicillin/streptomycin was added to each well and incubated at 28°C. Once the cell monolayer reached confluency, at approximately 4-5 dpi, 1ml Neutral red was added to each well to stain the live cells (1:15 dilution of 0.5% Neutral red in PBS). After 4 hours or overnight incubation at 28°C, the stain was discarded into 1% Virkon disinfectant and the plates were incubated inverted at room temperature in the dark. The next day, clear plaques were counted manually on a light box and the virus titres were calculated based on the virus dilution and the volume of virus inoculate used during the assay. Virus titres were generally in the range 1-2x10^8 pfu/ml.

2.2.5 Purification of budded virus

The required volume (50-1000ml) of Sf9 or TniHi5 cell cultures in shake flasks were seeded at a density of 2x10^6 cells/ml or 1x10^6 cells/ml, respectively, and infected with virus stocks to be purified at 0.1 or 5 MOI. Following 5 dpi (for 0.1 MOI cultures) or 3 dpi (for 5 MOI cultures), cultures were centrifuged at 4000 rpm for 20 minutes at 4°C to pellet the cells (TY-JS 4.2 rotor, J6-MI Beckman centrifuge). The clarified culture media containing the BV was centrifuged further at 14000 rpm (30074g) for 1 hour at 4°C (JA-14 rotor, Avanti J-25i Beckman centrifuge) to pellet the virus particles. The culture media from this stage was discarded and the BV pellet was soaked in 1x TE buffer (10mM Tris-HCl, pH 8.0; 1 mM EDTA) overnight at 4°C prior to resuspension. The next day, the virus suspension was loaded on to a 10%-50% discontinuous sucrose gradient buffered in 1xTE in ultra-clear tubes. The tubes were topped with a layer of liquid paraffin and centrifuged at 26000 rpm for 1 hour at 4°C (SW32TI rotor, Optima LE-80K Beckman Ultracentrifuge). The band representing the BV fraction after ultracentrifugation was then gently harvested from the gradient using a p1000 pipette into a 7ml bijoux. BV particles were then dialysed against 500ml 1x TE buffer (for analysis) or 1x PBS (for vaccination) stirring at 4°C for 2-4 days in the dark to remove the contaminating sucrose. The surrounding TE buffer or PBS was replaced every 24 hours and once the purified BV was harvested, it was stored at 4°C.

2.2.6 Budded virus fractionation

A glycerol gradient (30-70% v/v in 10% steps) buffered in 1xTE was set up in 5ml ultra-clear tubes by slowly adding 850µl of each glycerol concentration. These were allowed to fuse overnight at 4°C to form a continuous gradient. The following day, 200µg of sucrose-gradient purified BV particles were treated in 1% (v/v) NP-40 in 10mM Tris-HCl, pH 8.5 at room temperature for 30 minutes with gentle agitation. The treated BV particles were then loaded onto the 30-70% (v/v) continuous glycerol gradient and centrifuged at 35000 rpm for 1 hour, 4°C (SW55TI rotor, Optima XPN-80K Beckman Ultracentrifuge). Envelope

fractions were collected from the top of the gradient and dialysed against 10mM Tris-HCl, pH 7.4, overnight at 4 °C.

2.3 Bacteria Protocols

2.3.1 Preparation of ultra-competent *Escherichia coli* cells (DH5α strain)

A single bacterial colony was picked from a fresh plate of *E.coli* cells and grown in 25 ml SOB medium (20g Bacto-tryptone, 5g yeast extract, 0.5g NaCl dissolved in 1L distilled water (dH_2O), 10ml 250mM KCl added, pH adjusted to 7.0, autoclaved and 5ml 2M $MgCl_2$ added) for 6-8 hours at 37°C, shaking at 200 rpm. This culture was then used to inoculate three starter cultures with 250ml SOB in each flask receiving 2 ml, 4ml or 10ml of the bacterial culture. All three flasks were then incubated overnight at 18°C, shaking at 180 rpm. The culture cell density was monitored using a spectrophotometer (DU 730, Beckman) until one of them reached 0.55 at OD_{600}. The culture with a 0.55 reading was then chilled in an ice-water bath for 10 minutes and the cells were harvested by centrifuging at 3000 rpm for 10 minutes (4°C). Following this, the culture media was discarded and the cells were re-suspended gently in 80ml ice-cold Inoue transformation buffer (55mM $MnCl_2$, 15mM $CaCl_2$, 250mM KCl, 10mM PIPES, pH6.7). The cells were then pelleted again and re-suspended for the final time in 20ml ice-cold Inoue buffer. After the addition of 1.5ml DMSO, the cells were aliquoted into 1.5ml (v/v) Eppendorf tubes (250-750µl) and snap-frozen immediately by immersing into liquid nitrogen. These aliquots were stored at -70◦C until used.

2.3.2 Transformation of competent *E.coli* cells

Competent *E.coli* cells prepared from section 2.3.1 were thawed on ice and for each reaction, 50µl of cells were mixed with either 2µl of ligation mix or 1-10ng of plasmid DNA. This mixture was incubated on ice for 30 minutes and then heat-shocked at 42°C for 45 seconds. Following this, 1ml of SOC medium (SOB medium + 20µl/ml 1M glucose) was added to each tube and incubated for 1 hour at 37°C on a horizontally shaking platform at 200 rpm. After 1 hour incubation, 100µl cells were added on to the Luria broth (LB) nutrient agar plates containing the appropriate antibiotic based on the plasmid resistance (50µg/ml ampicillin, Sigma) and spread across the agarose surface using disposable plastic spreaders. These plates were then inverted and incubated at 37°C overnight.

2.3.3 Plasmid DNA purification from transformed *E.coli* cells

A single bacterial colony was picked from agarose plates (section 2.3.2) and grown overnight in 3ml LB medium at 37°C, with shaking (180 rpm). The plasmid DNA from

these cultures was purified using QIAprep Spin Miniprep kit, following the supplier's protocol (Qiagen).

2.4 Molecular Biology Protocols

2.4.1 Restriction enzyme digests

Restriction enzyme (RE) digests were carried out to either check or aid DNA cloning. Generally 2µL of DNA for checking and 10µl of DNA for cloning were digested using the enzymes, buffers and the protocols provided by the supplier (New England Biolabs). Unless otherwise stated, the reactions were incubated at 37°C for 1-4 hours or sometimes overnight if the DNA was to be used for cloning. The reactions were stopped by the addition of 1:5 volumes of 5x loading buffer (40% sucrose, 5x TAE (40 mM Tris-Acetate, 1 mM EDTA), 2.5% SDS, and 0.1% bromophenol blue dye). The samples were then applied into agarose gels for electrophoresis (section 2.4.2) to analyse or isolate DNA for downstream cloning experiments.

2.4.2 Agarose gel electrophoresis

High gelling temperature agarose (Fisher Scientific) was used with varying concentrations of 0.8-3% depending on the size of the DNA to be analysed. The agarose gel contained 0.5µg/ml ethidium bromide (EBr) to stain the DNA and was completely submerged in 1x TAE buffer during electrophoresis. The samples to be analysed on the gel were prepared to contain 1:5 volumes of the 5x loading buffer (section 2.4.1). Agarose gels were run horizontally at 40-100 volts (V) for 1-4 hours and then the DNA was visualized using a UV transilluminator (Bio Rad, Chemi Doc ™ Imaging Systems). EBr was absorbed from the electrophoresis buffers using de-staining tea bags (Fisher chemicals), which were then disposed into cytotoxic waste for incineration off-site alongside with EBr-containing gels.

2.4.2a Gel purification of DNA

RE digested DNA to be purified was separated by electrophoresis on 1% agarose gel at 40V as described in section 2.4.2. Following the electrophoresis, DNA fragments were briefly visualized using the UV transilluminator and the appropriate fragments were carefully excised from the gel using a scalpel. DNA from the excised gels was then purified using the QIAquick™ Gel Extraction Kit, following the suppliers protocol (Qiagen).

2.4.3 DNA vector dephosphorylation

Following gel purification, vector DNA was dephosphorylated in order to improve cloning outcomes by preventing self-ligation. Dephosphorylation was carried out by the addition of 1µl Antarctic Phosphatase (AnP) and 1:10 volumes of the AnP reaction buffer (New

England Biolabs) to the eluted sample from the purification and these were incubated at 37°C for 15-60 minutes. After the incubation, AnP was heat-inactivated at 70°C for 5 minutes.

2.4.4 DNA ligation

Ligation reactions were carried out using 50ng vector DNA and various concentrations of insert DNA using molar ratios of vector: insert of 1:1, 1:3, 3:1. These calculations were achieved by using the Promega Biomath Calculator website. The reactions were carried out by the addition of 0.4µl T4 DNA ligase and 1µl ligase buffer (Promega) to the calculated volumes of vector and insert DNA. The total volume of 10µl was achieved by the addition of dH_2O when required. These reactions were generally incubated at room temperature for minimum 2 hours or occasionally at 4°C overnight before proceeding with bacterial transformation as described in section 2.3.2.

2.4.5 Polymerase chain reaction (PCR)

Primers to be used in the PCR reactions were specifically designed by the author except for RDP213/214 and synthesized as synthetic oligonucleotides by Eurofins MWG Operon. They were supplied as freeze-dried pellets and upon receipt, were re-suspended in dH_2O to a stock concentration of 100pmol/µl. Stock primers were stored at -20°C. The list of primers used in this thesis can be found in Table 2.5.

Each PCR reaction contained 2pmol of the individual primers (forward and reverse), 10mM dNTPs, 1:10 volumes of polymerase buffer, 0.2-0.5µl DNA template, and the required amount of either Taq polymerase (New England Biolabs) or Herculase (Agilent Technologies) enzyme. The choice of enzyme depended on the requirement for proofreading activity, which only Herculase enzyme provided. The total reaction volume was brought up to 50µl by the addition of dH_2O. Each set of reaction contained a negative control, which was the addition of dH_2O instead of template DNA. PCR amplifications were then carried out in a thermocycler (RoboCycler gradient 96, Stratagene) based on a programme set out using the protocol provided by the enzyme supplier. At the end of the cycles, 5µl of PCR sample was mixed with 5µl dH_2O and 2.5µl loading buffer and analysed on an agarose gel following the protocol from section 2.4.2. If the results from the agarose gel showed the anticipated amplification, PCR products were then purified using QIAquick PCR purification kit following the supplier's protocol (Qiagen).

Table 2.5 Primers used in this thesis

Primer Name	Primer sequence (5'-3')
Chapter 3	
VP2 F	ACCGCGGGTACCATGGCGTCCGAGTTTGGAATATTGATGAC
VP2 His Rd1 F	ACCATCACGCTGCAGCGGCGTCCGAGTTTGGAATATTGATGAC
VP2 His Rd2 F	ACCTAAGGTACCATGCATCACCATCACCATCACGCTGCAGCGGC G
VP2 R	TTAGGTCCCGGGCTATTCCGTTTTTGCGAGTAACTTCGACAACAA G
VP2-H F	ACCTAGGGTACCATGAAAGCTTCTGCTATGTATTCTGGA
VP2-H His Rd1 F	CATCACGCTGCAGCGAAAGCTTCTGCTATGTATTCTGGAAAA
VP2-H His Rd2 F	ACCTAGGGTACCATGCATCACCATCACCATCACGCTGCAGCGAA A
VP2-H R	TTAGGTCCCGGGCTAATCGATCGACACTTGGCATGG
VP2-A F	ACCGCGGGATCCGCGTCCGAGTTTGG
VP2-A R	ACCGCGGCGGCCGCTTACGCATCTCTCCATTG
VP2-B R	ACCGCGGCGGCCGCTTATAAATCATCCCGCTC
VP2-C R	ACCGCGGCGGCCGCTTATCCACGCGTGATTTT
VP2-D R	ACCGCGGCGGCCGCTTACACTTGGCATGGTTG
VP2-E R	ACCGCGGCGGCCGCTTATCTTAAAACCCCAAC
VP2-F R	ACCGCGGCGGCCGCTTAATACGTGGTTTCCGC
VP2-G F	ACCGCGGGATCCTCGGAAAGAGAAACG
VP2-G R	ACCGCGGCGGCCGCTTAGTTCGAACCGATCCA
VP2-I F	ACCGCGTCTAGAAGCGGTTAATGAAAGG
VP2-I R	ACCGCGGCGGCCGCTTAGATCCCCAACTCTCC
VP2-J F	ACCGCGGGATCCAAGCTTGATCGGATT
VP2-J R	ACCGCGGCGGCCGCTTAATCGATCGACACTTG
VP2-Z F	CGCACCAAGCTTGAAGATTACGGAGAA
VP2-Z R	ACCGCGGCGGCCGCTTATTCCGTTTTTGCGAG

Table 2.5 (continued) Primers used in this thesis

Primer Name	Primer sequence (5'-3')
Chapter 4	
*p6.9*P F	TTGCTGATATCGGGAGTTCAGTCGTCGAATG
*p6.9*P R	CGCGGCACTAGTGAGCTCGTTTAAATTGTGTAATTTATG
*gp64*P F	GACTACGATATCTGAGCGTCCGTGTTCATGATC
*gp64*P R	GCAAGTGAGCTCCTTGCTTGTGTGTTCC
VP2-H Surf F	ACCTAGCTGCAGGTAAAAGCTTCTGCTATGTATTCT
VP2-H Surf His Rd1 F	ACCATCACGCAGCTGCGAAAGCTTCTGCTATGTATTC
VP2-H Surf His Rd2 F	GATCTGCAGGTACATCACCATCACCATCACGCAGCTGCGAA
VP2-H Surf R	TTAGGTCCCGGGGATCGATCGACACTTG
VP2 Surf F	ACCTAGCTGCAGGTAGCGTCCGAGTTTGGAATATTGA
VP2 Surf His Rd1 F	CATCACGCAGCTGCGGCGTCCGAGTTTGGAATATTG
VP2 Surf His Rd2 F	ACCTAACTGCAGGTACATCACCATCACCATCACGCAGCTGC
VP2 Surf R	GGCGGTCCCGGGGTTCCGTTTTTGCGAGTAA
Chapter 5	
Trun GP64 F	ACCTAGCCCGGGCGTTCATGTTTGGTCATGTAGTTA
Trun GP64 R	GAATTATTAAAATACGTACAACAATTGTCTG
EGFP surf F	GCCACCCTGCAGGTGAGCAAGGGCGA
EGFP surf R	CCGCTTTACCCGGGCTTGTACAGCTCGT
VP2-A Surf F	ACCGCCCTGCAGGTAGCGTCCGAGTTTGGAA
VP2-A Surf R	ACCGCGCCCGGGGCGCATCTCTCCATTGT
VP2-B Surf R	ACCGCGCCCGGGGTAAATCATCCCGCTCA
VP2-C Surf R	ACCGCGCCCGGGGTCCACGCGTGATTTTC
VP2-D Surf R	ACCGCGCCCGGGGCACTTGGCATGGTTGT
VP2-E Surf R	ACCGCGCCCGGGGTCTTAAAACCCCAACT
VP2-F Surf R	ACCGCGCCCGGGGATACGTGGTTTCCGCC
VP2-G Surf F	ACCGCCCTGCAGGTATCGGAAAGAGAAACGT
VP2-G Surf R	ACCGCGCCCGGGGGTTCGAACCGATCCAT
VP2-I Surf F	ACCGCCCTGCAGGTAGCGGTTAATGAAAGGA

Table 2.5 (continued) Primers used in this thesis

VP2-I Surf R	ACCGCGCCCGGGGGATCCCCAACTCTCCA
VP2-J Surf F	ACCGCCCTGCAGGTAAAGCTTGATCGGATTC
VP2-J Surf R	ACCGCGCCCGGGGATCGATCGACACTTGG
VP2-Z Surf F	ACCGCCCTGCAGGTAGAAGATTACGGAGAAA
VP2-Z Surf R	ACCGCGCCCGGGGTTCCGTTTTTGCGAGT
Sequencing primers	
RDP213	TGAGACGCACAAACTAATATCAC
RDP214	ATACGTACAACAATTGTCTGTAAATC
MA seq F	TCACGGAACCGACATTATCT
MA seq R	CAAACGTTTAGTTTGTACAACC
MA seq Z R	AAAACAATCCACAGCAGAAA

2.4.6 Cloning PCR fragments into pGEM-T and pGEM-T Easy vectors

If difficulties were encountered directly cloning the PCR fragments into the desired plasmids, they were first sub-cloned into pGEMT-T/pGEM-T easy vectors. The ligation reactions for inserting the PCR fragments into these T-vectors were carried out following the supplier's protocol (Promega). For T-vectors, PCR fragments are required to contain a single 3' adenosine (A) overhang, which occurs when the fragments are amplified using *Taq* polymerase. However, when proofreading enzyme such as Herculase was used for the PCR amplification, the Adenosine residue was added by incubating PCR fragments with 0.2mM dATP (Promega) and non-proofreading enzyme, *Taq* polymerase (5u/µl) at 70°C, for 30 minutes.

2.4.7 DNA sequencing

All DNA sequencing was outsourced to Source Bioscience, and the resultant sequencing data was analysed by using the SnapGene® software.

2.5 Protein Analysis Protocols

2.5.1 Infecting insect cells

Test expressions were regularly carried out in Sf9/TniHi5 cells to examine the production of recombinant proteins. In order to do this, the cells were seeded at $0.5x10^6$cells/well for TniHi5 or $1x10^6$cells/well for Sf9 cells in a 6-well plate. After the cells had settled down,

they were infected with 5 moi of the corresponding virus diluted in culture medium to a final volume of 100µl/well. Cells were incubated with the virus inoculum for 1 hour at room temperature on a rocking table. Following the incubation, the virus inoculum was removed and replaced by 2ml of the appropriate growth culture medium. The infections were incubated at 28°C until the required time of harvest.

Crude cell pellets were harvested by centrifugation at 13000 rpm for 5 minutes and BV particles were harvested from the culture medium by spinning at 13000 rpm for 30 minutes, at 4◦C.

2.5.2 SDS-PAGE analysis of proteins

Protein samples were analysed using the standard dodecyl sulphate polyacryamide gel electrophoresis (SDS-PAGE) as described in Sambrook and Russell (2001). SDS-PAGE gels were hand-casted at various percentages from 6 to 12%, based on the size of the proteins to be analysed, using the protocol described by Sambrook and Russel (2001). Proteins were analysed from a variety of different samples such as infected whole cell lysates, culture supernatants, purified proteins or BV particles. These samples were mixed with $1/5^{th}$ volume of 6X Laemmli SDS-PAGE loading buffer (250mM Tris-HCl pH 6.8, 10% SDS, 50% (v/v) glycerol, 0.05-0.5% bromophenol blue and 25% (v/v) β-mercaptoethanol, added just before use), boiled for 5 minutes and were analysed on SDS-PAGE gels using the mini-PROTEAN vertical gel electrophoresis system (Bio-Rad) at 150-180V. Following this, the gels were either stained by Coomassie (2.5.2a) or processed further for western blotting (2.5.2b).

2.5.2a Coomassie staining

For Coomassie staining the gels were immersed into 0.25% Coomassie Brilliant Blue R-250 dissolved in 50% (v/v) methanol, 10% (v/v) glacial acetic acid for three or more hours. They were then de-stained with 30% (v/v) methanol, 10% (v/v) glacial acetic acid until a clear gel background was obtained. Once the desired destaining was achieved, the gels were washed with dH_2O and imaged using a Bio Rad, Chemi Doc ™ Imaging System.

2.5.2b Western blot analysis

For western blotting, the proteins from the SDS-PAGE gel were transferred onto a nitrocellulose membrane using Towbin transfer buffer (25mM Tris, 192mM glycine and 20% (v/v) methanol) and the Trans-Blot Turbo blotting system, following the supplier's instructions (Bio Rad). Once the proteins were transferred, the membrane was incubated in 10ml blocking buffer (5% skimmed milk powder in PBS-T (PBS+ 0.1% (v/v) Tween 20)) for 30 minutes at room temperature on a horizontally rotating platform. Then the

membrane was incubated in 5-10ml blocking buffer containing the primary antibody at the required dilution (Table 2.6) for 1 hour at room temperature. Following this, the membrane was washed every ten minutes for four times with 12ml of PBS-T. After the washes, the membrane was incubated with 5-10ml of blocking buffer containing the corresponding secondary antibody at the required dilution (Table 2.6) for 1 hour at room temperature. The membrane was washed four times for 40 minutes with 12ml PBS-T and then developed using Clarity western ECL blotting substrate kit following the supplier's instructions (Bio Rad). Developed membranes were then visualized and imaged by using the Bio Rad, Chemi Doc ™ Imaging System.

Table 2.6 Antibodies used for western blotting

Antibody target	Source species	Working dilution	Supplier
Anti-6xhis-tag	Mouse	1:1000	Biorad
Anti-gp64 AcV5-tag	Mouse	1:1000	Sigma
Anti-GFP	Rabbit	1:3000	Abcam
Anti-AHSV4-VP2 (R190)	Rabbit	1:1000	Genscript
Anti-AHSV4-VP2 (R189)	Rabbit	1:1000	Genscript
Anti-AHSV4-VP2 (Rabbit B)	Rabbit	1:200	The Pirbright Institute
Anti-AHSV4-VP2 (pony 9204)	Pony	1:1000	The Pirbright Institute
Anti-mouse IgG conjugated to horseradish peroxidase (HRP)	Goat	1:50000	Jackson ImmunoResearch
Anti-rabbit IgG conjugated to HRP	Goat	1:50000	Sigma
Anti-horse IgG conjugated to HRP	Goat	1:50000	Jackson ImmunoResearch

2.5.3 Protein assays

2.5.3a BCA assay

Protein concentrations were measured by the BCA protein assay using the standard micro-scale assay format, following the supplier's instructions (Novagen). A range of six bovine serum albumin (BSA) standards were used (1000, 500, 250, 125, 25, 0µg/ml). The absorbance was then measured using the BCA protein assay format of a DU730 Beckman spectrophotometer at 562 nm wavelength and the results were converted to concentrations at µg/ml automatically. The protein samples were diluted accordingly to be in the linear range of the standards.

2.5.3b Bradford assay

Protein concentrations were measured by the Quick Start Bradford protein assay, using the standard 1ml cuvette assay following the supplier's instructions (Biorad). Seven

concentrations of BSA were used as standards (2, 1.5, 1, 0.75, 0.5, 0.25 and 0.125 mg/ml). Bradford assay settings were used from the spectrophotometer (DU 730, Beckman Coulter), where the absorbance values were measured at 595nm wavelength and concentrations were automatically calculated from the standard curve obtained at the start of the assay. The protein samples were diluted accordingly to be in the linear range of the standards.

2.5.4 Analysis of post-translational modifications

Duplicate samples of sucrose gradient-purified BV particles (200µl) were pelleted on a bench-top centrifuge at 13000rpm for 15 minutes. While one set of samples were re-suspended in PBS to be used as a negative control in the analysis, the other set was processed with corresponding buffers of specific enzymatic treatments following the supplier's protocol (NEB). De-glycosylation analysis was carried out using either *Endo* H or *PNG*ase F enzymes and de-phosphorylation analysis was carried out using Lambda Protein Phosphatase.

2.5.5 Immunofluorescence

Immunofluorescence analysis was carried out on cells that were seeded on sterile coverslips in 6-well plates. The cells were infected with the virus of interest following the same protocol in section 2.5.1. At the required time post-infection, the culture medium was removed and the cells were washed twice with 2ml 1xPBS. Following the washes, the cells were fixed for 1 hour at room temperature by adding 1ml 4% (v/v) paraformaldehyde diluted in PBS. Fixed samples were washed twice with 1ml 1xPBS. After the washes, cells were permeabilised by a 10 minute treatment with 1ml PBS-BSA (PBS containing 1% BSA (Sigma Aldrich)) containing 0.1% (v/v) Triton X-100. Next the cells were washed twice with 2ml PBS and blocked by 2ml PBS-BSA for 20 minutes. After blocking, 200µl of corresponding primary antibody (Table 2.7) was added. Following the 1 hour primary antibody incubation at room temperature, the cells were washed three times with 2ml of PBS-BSA. After the washes, 200µl corresponding secondary antibody was added and the cells were incubated at room temperature for 1 hour. Secondary antibody was washed five times with 2ml PBS-BSA and the cover slips were mounted on to microscope slides with Vectashield (Vector laboratories), a glycerol based mounting media. The edges of coverslips were sealed with clear nail vanish and the samples were stored at 4°C, protected from light until visualisation by fluorescence or confocal microscopes.

Table 2.7 Antibodies used for immunofluorescence

Antibody target	Source species	Working dilution	Supplier
SMAA (AHSV4 VP2 MAb)	Mouse	1:100	Ingenasa
6DF4 (AHSV4 VP2 MAb)	Mouse	1:100	Ingenasa
Anti-GP64 AcV5-tag	Mouse	1:200	Sigma
Anti-mouse IgG conjugated to Alexa Fluor 488	Goat	1:200	Life technologies

2.6 Protein purification

Cell pellets containing the histidine-tagged protein of interest were re-suspended in 15-20ml of Buffer A (20mM Tris-HCl, pH 8.0, 0.3M NaCl, 10mM imidazole) and lysed by sonication using the 10-second interval pulsar cycle timer (XL2020 ultrasonic liquid processor). Depending on the experimental requirements, the cell pellets were alternatively lysed in 1% NP-40 lysis buffer (10mM Tris-HCl, pH 8.0, 0.15M NaCl, 1mM EDTA and 1% (v/v) NP-40) by incubating on ice for 1-2 hours. Protease inhibitor cocktail (Calbiochem) was added to the lysed cells to minimize protein degradation. Following cell lysis, the medium was clarified by centrifuging at 20000rpm for 20 minutes, at 4°C. If NP40 lysis was used, 0.15M NaCl and 10mM imidazole were added at this stage to match the conditions of purification buffer A. The presence of imidazole was important to prevent non-specific binding. Clarified medium was then incubated with nickel-coated sepharose beads (GE Healthcare) on a rotating platform at 4°C for 1-2 hours to enable binding of proteins to the beads. After the incubation, the samples were centrifuged at 1000rpm for 1 minute and then the beads were transferred onto Proteus 1-step batch midi spin columns (Generon). The beads were washed in the columns three times using Buffer A. Excess wash buffer was removed by centrifuging at 1000rpm for 1 minute. The columns were transferred into clean collection tubes and the proteins were eluted from the beads with purification Buffer B (300mM imidazole, 20mM Tris-HCl, pH 8.0 and 0.3M NaCl).

2.6.1 Protein solubilisation

Cell pellets containing the insoluble proteins were re-suspended in 15ml solubilisation buffer (50mM Tris-HCl, pH8.0, 0.5% (v/v) glycerol and 2M guanidinium hydrochloride) in the presence of a protease inhibitor cocktail (Calbiochem). The re-suspended cells were incubated on ice for 15 minutes and then lysed by sonication. Lysed cells were centrifuged at 20000 rpm for 20 minutes, at 4°C, to clarify the soluble fraction. Small aliquots of the total lysate and the clarified medium were dialysed against a tris-based buffer (50mM Tris-HCl, pH 8.0, 0.5% (v/v) glycerol, 1M NaCl) to enable SDS-PAGE

analysis as guanidinium is not compatible with SDS-PAGE. The remainder of the clarified medium was processed further to purify the proteins following the protocol in section 2.6. To enhance the recovery of correctly-folded soluble proteins after purification, decreasing concentrations of urea (6M, 3M and 1M) were included in purification buffer A for washes and 1M urea was included in the final elution buffer.

2.7 Enzyme-linked immunosorbent assay (ELISA)

An indirect ELISA was used to detect AHSV4-VP2-specific antibodies. 96-well, polystyrene, non-tissue culture-treated assay plates were coated overnight at 4ºC with baculovirus-expressed, purified VP2 (100µl at 15ng/well) diluted in 0.05M carbonate/bicarbonate buffer, pH9.6 (Sigma, C3041). The following day, VP2-coated plates were washed four times with 200µl PBS+0.05% (v/v) Tween 20 using a microplate washer (LT-3500). Immediately after the washes, the wells were blocked with 200µl/well 5% milk in PBS+0.05% Tween 20, for 1 hour at 37ºC to prevent non-specific binding. Blocking was followed by the addition of primary antibody (either monoclonal antibody (MAb) or equine serum at 1 in 100 dilution, 50-100µl/well), which was incubated for 1 hour at 37ºC. Primary antibody was washed from the wells four times with 200µl PBS+0.05% (v/v) Tween 20. HRP-conjugated secondary antibody was then added (100µl) and incubated for 1 hour at 37ºC. The secondary antibodies were: anti-horse HRP at a dilution of 1 in 15000 and anti-mouse HRP at a dilution of 1 in 2000 (Jackson Immunoresearch). Secondary antibody was washed four times with 200µl PBS+0.05% (v/v) Tween 20. The washes were followed with the addition of 50µl/well of TMB substrate (3, 3′,5 ,5′-Tetramethylbenzidine Liquid Supersensitive Substrate, T4444 Sigma). The plates were incubated for 5 minutes in the dark at room temperature and the reaction was stopped with the addition of 50µl/well sulfuric acid stop solution (N600, Thermo Scientific). The absorbance was read at 450nm using a microplate reader (LT-4500).

The results were represented in the form of graphs or colour-coded table, depending on the size of experimental data. In some cases data were normalized by subtracting the mean OD of negative control for each particular experiment (pre-immunisation serum, null-infected crude cell lysates, blank wells) from the mean OD of test samples. Sample sizes differed between duplicates and quadruplicates, which is clearly indicated in the figure legend of each particular experiment. Raw data for each experiment is included in the appendix. Statistical analysis was carried out to compare and evaluate the data from the experiments following section 2.8.

2.8 Statistical analysis

T-test was carried out for the statistical analysis of experimental outcomes using the Graphpad Prism software and the results were interpreted based on the *p* value outcome of the test. Error bars included in the mean datasets of replicate samples (duplicates-quadruplicates) represent either ±3 SD (standard deviation) or the standard error and were calculated using the corresponding standard deviation of each sample.

2.9 Vaccination experiments

Vaccination experiments in mice and the analysis of serum post-vaccination were carried out by Dr Eva Calvo at CISA-INIA (Research Centre for Animal Health) in Valdeolmos, Spain through collaboration with the Pirbright institute.

For this experiment 30 female, six week-old Balb/c mice were used in total. Upon receipt of the mice, they were separated into six different antigen groups (5 mice/group) and were acclimatized to the new environment for five days prior to the start of immunisations. The antigens were injected into the mice by subcutaneous route (200µl), within the presence of Imject Alum adjuvant (Thermo Fisher, 1:1 antigen:adjuvant ratio). Pre-vaccination serum (0 dpv) and post-vaccination serum (21 dpv and 35 dpv) were collected by venepuncture. Mice were checked twice daily for their well-being throughout the experiment and were euthanized with overdose of anaesthesia followed by exposure to CO_2 and dislocation of the neck at the end.

Chapter 3
Characterizing the antigenicity of AHSV4 VP2 and the subdomains produced in insect cells

3.1 Introduction

African horse sickness virus (AHSV) causes a lethal equine disease and currently there is no licenced vaccine that can be used safely in non-endemic regions. The AHSV major outer capsid protein, VP2, has been shown to be the main-serotype specific antigen, carrying the virus neutralizing epitopes (Burrage *et al.*, 1993). Therefore, VP2 is the optimum target for subunit vaccine studies. AHSV has nine serotypes and VP2 from serotype four (AHSV4-VP2) was the focus of this project as this serotype was responsible for the outbreaks in Spain and Portugal (Lubroth, 1988, Mellor *et al.*, 1990, Mellor and Hamblin, 2004) in 1987 - 1993.

The project initially examined the expression of VP2 and its subdomains within insect cells to confirm the competence of their expression by recombinant baculoviruses. There are several different insect cell lines, but Sf9 and TnHi5 are the most commonly used for recombinant protein production and expression profile of proteins may differ greatly in these two cell lines because of unknown reasons. Therefore, both cell lines were used throughout this project.

The *flash*BAC system was used to generate these recombinant baculoviruses in a single step, without the need of isolation from the parental background. *flash*BAC is based on a modified AcMNPV genome, which contains a bacterial artificial chromosome (BAC) in place of the polyhedrin gene and part of an essential gene, ORF1629. In order to generate the recombinant baculoviruses, insect cells are transfected with the *flash*BAC DNA and the transfer vector that contains the gene of interest. This leads to homologous recombination, where the BAC is replaced with the gene of interest and the function of ORF1629 is restored enabling the virus DNA to replicate and produce recombinant baculoviruses (Figure 3.1). The *flash*BAC system has been further developed into two sub-forms; *flash*BACGOLD where *chiA* and *v-cath* are removed and *flash*BACULTRA where *p10, p74, p26, chiA* and *v-cath* are removed from the genome (Hitchman *et al.*, 2011). Both forms take the *flash*BAC system a step further by improving recombinant protein yield and quality by deletion of non-essential virus genes (Hitchman *et al.*, 2007a, 2009, Hitchman *et al.*, 2010b).

3.2 Selection of VP2 subdomains

Initially this project investigated the expression of full-length VP2 and a single subdomain; fragment H, which contains the linear virus neutralisation domain of VP2 identified by Martinez-Torrecuadrada and Casal (1995). Following the preliminary results, it was decided to explore ten more VP2 subdomains, hence to cover a wide range across the protein. Previous studies on the antigenic structure of VP2, especially the study by Manole

et al. (2012) determined the selection of the ten subdomains for this project. This study suggested that the central domain of VP2 trimers forms an independent structural subdomain that contains most of the immunogenic linear peptides of the protein defined so far (Figure 3.2A). Using this information, ten subdomains were identified to investigate VP2 antigenic structure by expression using recombinant baculoviruses. The schematic representation of the full-length VP2 and its subdomains are illustrated in Figure 3.2B. This figure also shows the peptides used to generate the main VP2-specific antibodies, R189 and R190, used in this project. The location of these peptides indicates that these antibodies should detect all but subdomains A, B and G (Figure 3.2B).

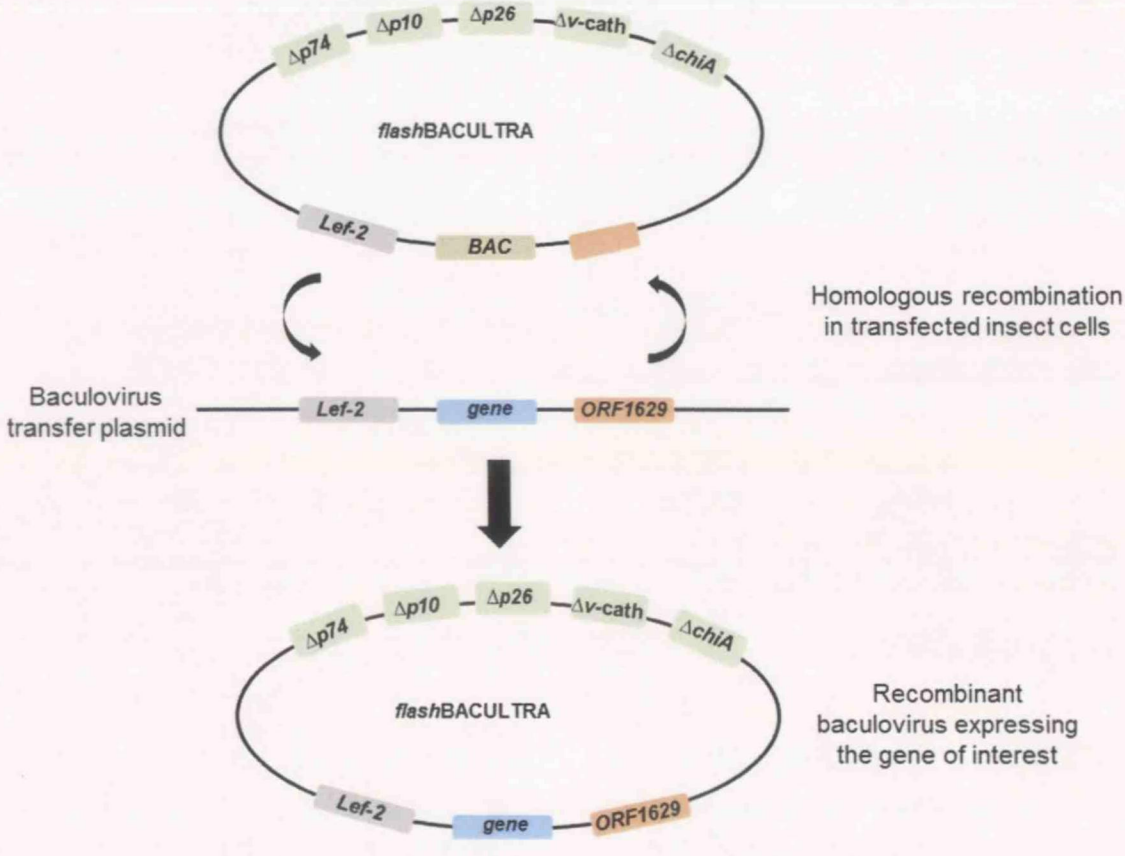


Figure 3.1 Schematic representation of the *flash*BAC system using *flash*BACULTRA DNA

Insect cells are transfected with *flash*BACULTRA DNA and the baculovirus transfer plasmid containing the gene of interest. As a result of homologous recombination, the BAC is replaced with the gene of interest and the function of ORF1629 is restored in transfected insect cells. This enables the virus DNA to replicate and produce recombinant baculoviruses expressing the gene of interest.

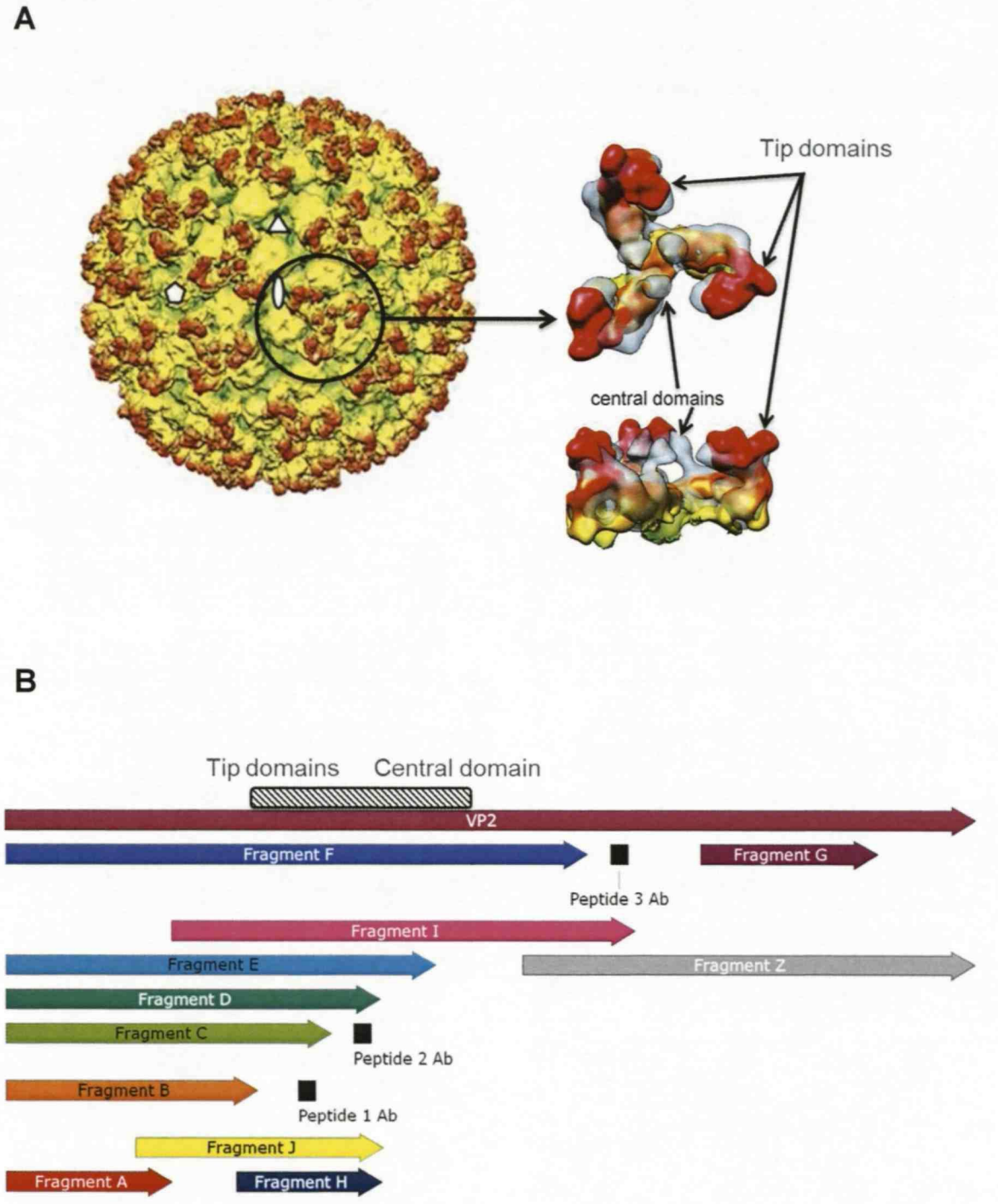


Figure 3.2 Schematic representations of the full-length VP2 structure and the location of its subdomains

A: Trimers of AHSV4-VP2 associated with the viral capsid (left) and as individual protein structure (right). Central domain of VP2 trimers form a structural subdomain, which contains the linear epitopes identified so far, viewed from above (top right) and side (bottom right). Reproduced by permission of the journal (Manole *et al.*, 2012).

B: Gene sequences of the subdomains were individually highlighted from the full-length VP2 sequence to generate this schematic representation using the SnapGene® software. Each subdomain is colour-coded and shown by a single arrow indicating their location in the full-length protein. Black squares indicate the peptides used to generate the VP2 specific antibodies, R189 and R190. Colour codes are used throughout this thesis.

3.3 Construction of transfer vectors

The first stage of generating recombinant baculoviruses using the *flash*BAC system is the insertion of genes into the transfer plasmids (Figure 3.1). For each subdomain to be expressed, an individual baculovirus transfer vector was generated using the standard cloning techniques described in sections 2.3 and 2.4. Initially, full-length VP2 and fragment H were designed to contain a polyhistidine tag (6xhis) at either the amino- or carboxy-terminals to enable protein purification. However, preliminary results showed that the addition of 6xhis tag at the carboxy-terminus inhibited the generation of recombinant baculoviruses (data not shown). Therefore, all the proteins were designed to contain 6xhis tag at their amino-terminus only and the transfer vectors were constructed to drive the expression of the target genes by the strong polyhedrin gene promoter.

3.3.1 Construction of pOET1_VP2$^{HIS/N}$

Nucleotide sequences encoding AHSV4-VP2 were amplified by PCR from the template vector pSC11-AHSV-4-VP2 (obtained from The Pirbright Institute) using gene-specific primers. The 6xHis tag was added to the 5' terminus of the VP2 sequence during two rounds of amplification. The final PCR product, VP2$^{HIS/N}$, from Figure 3.3B (3.1kbp fragment) was sub-cloned into the pGEM T Easy vector through TA cloning (section 2.4.6). VP2$^{HIS/N}$ was excised using *Not*I and *Sca*I enzymes and gel purified before ligating into the pOET1 vector, at the *Not*I restriction sites, to generate pOET1_VP2$^{HIS/N}$ (Figure 3.3A). The success of the cloning was confirmed by single restriction digests using the enzymes *Not*I and *EcoR*V. *Not*I digest resulted in two fragments of 4.5kbp and 3.1kbp, which confirmed the presence of VP2$^{HIS/N}$ in the vector. Digestion with *EcoR*V, which has a site in the vector and a site in VP2$^{HIS/N}$, confirmed the correct orientation of VP2$^{HIS/N}$ within the plasmid (Figure 3.3C).

3.3.2 Construction of pOET1_VP2-H$^{HIS/N}$

Gene-specific primers were used to PCR-amplify the fragment H subdomain of AHSV4-VP2 from the template vector pSC11-AHSV-4-VP2. Similar to the full-length VP2, 6xhis tag was added to the 5' terminus by using two rounds of PCR amplification. The final PCR product, VP2-H$^{HIS/N}$, from Figure 3.4B (500bp), was sub-cloned into the baculovirus transfer vector, pBac-1_CMV[1] (E. Locanto thesis, Oxford Brookes University) using *Kpn*I and *Sma*I restriction sites. Fragment H was excised using *Kpn*I and *Not*I enzymes, gel purified and inserted into the pOET1 vector (Figure 3.4). Plasmid DNA was purified from several colonies and screened with *Not*I and *Kpn*I restriction digests that confirmed the successful construction of pOET1_VP2-H$^{HIS/N}$. (Figure3.4C).

[1] Fragment H was initially cloned into this vector to enable expression in mammalian cells, however, this aspect of the project was not continued as the expression of these genes could not be achieved.

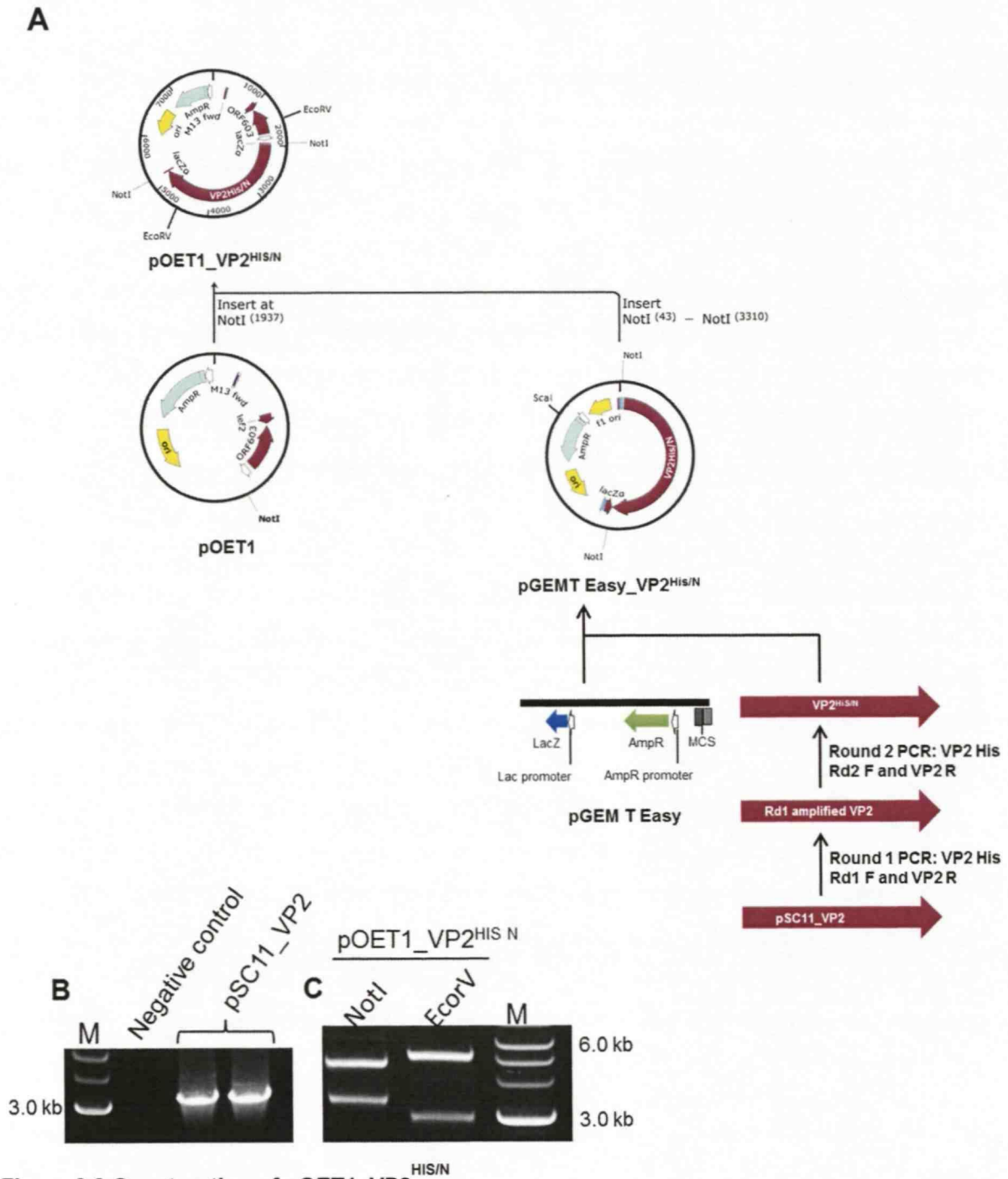


Figure 3.3 Construction of pOET1_VP2$^{HIS/N}$

A: Schematic representation of cloning strategy generated by the SnapGene software. Full length VP2 was amplified from the pSC11_VP2 vector during two rounds of PCR, using the primers; VP2 His Rd1 F, VP2 His Rd2 F and VP2 R. Final PCR product, VP2$^{HIS/N}$, was then sub-cloned into the pGEM T Easy vector through TA cloning, to generate pGEMT Easy_VP2$^{HIS/N}$. VP2$^{HIS/N}$ was then excised from the pGEMT Easy_VP2$^{HIS/N}$ using *Not*I and *Sca*I restriction enzymes, which then enabled its ligation into the pOET1 vector, to generate the transfer plasmid pOET1_VP2$^{HIS/N}$ through NotI restriction sites.
B: Analysis of VP2$^{HIS/N}$ PCR amplification from pSC11_VP2 vector on a 1% agarose gel. VP2$^{HIS/N}$ was amplified as duplicate reaction and both were run on the gel. M: 2-log ladder, Negative control: dH_2O as the template in PCR.
C: Restriction digest analysis of pOET1_VP2$^{HIS/N}$ purified from a colony pick in 1% agarose gel. 2µl of pOET1_VP2$^{HIS/N}$ was individually digested either with *Not*I or *Eco*RV restriction enzymes for 2 hours at 37°C, prior to analysis.

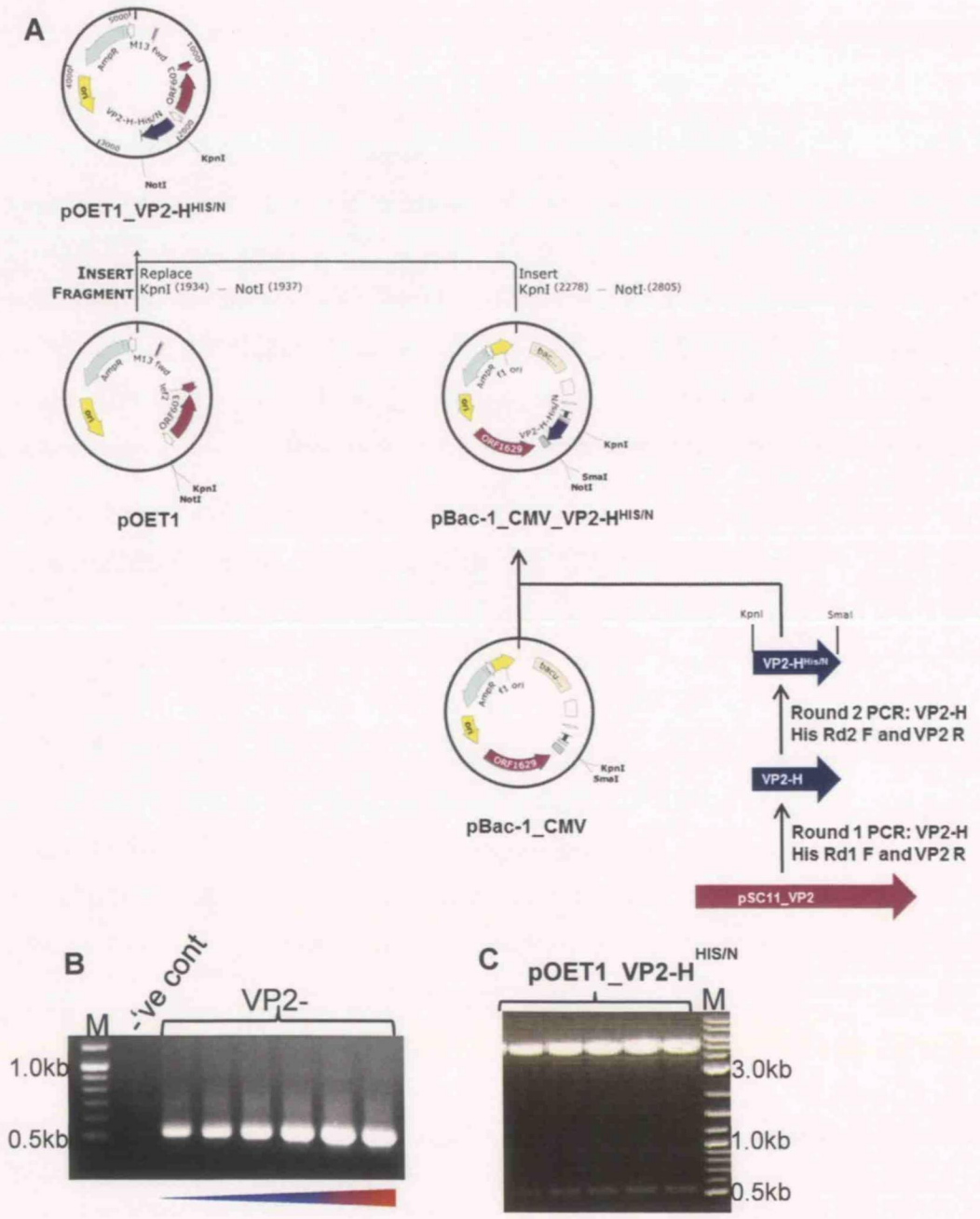


Figure 3.4 Construction of pOET1_VP2-H$^{HIS/N}$

A: Schematic representation of cloning strategy generated by the SnapGene software. Fragment H subdomain of VP2 was amplified from the pSC11_VP2 vector during two rounds of PCR, using the primers; VP2-H His Rd1 F, VP2-H His Rd2 and VP2-H R. Final PCR product was sub-cloned into the pBac-1_CMV vector using the KpnI and SmaI restriction sites to generate pBac-1_CMV_VP2-H$^{HIS/N}$. VP2-H$^{HIS/N}$ was excised using KpnI and NotI restriction sites, which enabled its ligation into the pOET1 vector to generate the transfer plasmid pOET1_VP2-H$^{HIS/N}$.

B: Analysis of PCR amplified VP2-H$^{HIS/N}$ from pSC11_VP2 on a 1% agarose gel. During PCR amplification, a gradient of 6 increasing temperatures were used and all samples were analysed on the gel with the order of lowest to highest temperature from left to right, respectively. M: 2-log ladder, -'ve cont: dH_2O as template in the PCR. Coloured arrow beneath the gel indicates increasing temperature.

C: Restriction digest analysis of pOET1_VP2-H$^{HIS/N}$ plasmids purified from 5 colony picks in 1% agarose gel. 2µl of each pOET1_VP2-H$^{HIS/N}$ was digested using *Kpn*I and *Not*I enzymes for 2 hours at 37°C, prior to analysis.

3.3.3 Construction of the remaining VP2 subdomain transfer vectors

Transfer vectors for all the remaining VP2 subdomains (fragments A, B, C, D, E, F, I, J and Z) were generated using the same cloning strategy that is illustrated in Figure 3.5A. Initially, fragments were PCR amplified using gene-specific primers from the template vector pSC11-AHSV-4-VP2. Fragments A, B, C, D, E and F shared the same forward primer with individual reverse primers as they all started from the same 5' nucleotide sequence. Unlike the full-length VP2 and fragment H, the 6xhis tag at the 5' terminus of the proteins was derived from the host plasmid, pOET1N 6x His. This approach saved time and resources due to the application of only one round of PCR.

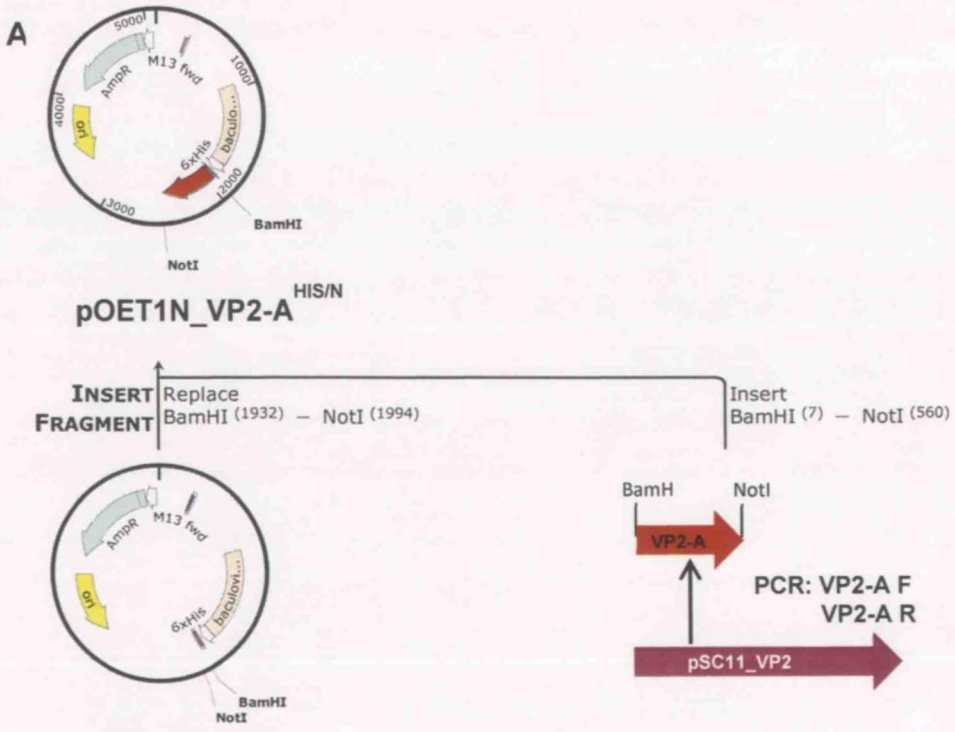
Once the individual nucleotide sequences were amplified at their expected sizes (Figure 3.5B-G), they were cloned into the pOET1N 6x His vector. The required restriction sites were incorporated into the primers used to amplify each fragment. All the subdomains, apart from fragment I and Z, were cloned using *BamH*I and *Not*I restriction sites. For fragment I, *Xba*I-*Not*I and for fragment Z, *Hind*III-*Not*I sites were used, because the sequences contained internal *BamH*I restriction sites. Following ligation and transformation of *E.coli* (section 2.4.4 and 2.3.2) plasmids from three colonies for each construct were screened with the corresponding restriction enzymes. Restriction digest analysis of each fragment resulted in two fragments at expected sizes, confirming the presence of the target gene inserts in pOET1N 6x His vector (Figure 3.5 I&J). A summary of the cloning information for all the target genes is shown in Table 3.1.

Figure 3.5 Generation of transfer plasmids for the remaining VP2 subdomains

A: Representative schematic illustration of the cloning strategy for all the remaining VP2 subdomains shown by the cloning of fragment A. The target gene was PCR amplified using corresponding primers adding the desired restriction sites on each terminus. Following a restriction digest, they were ligated into the pOET1N 6x His vector to generate the individual baculovirus transfer vectors listed in table 3.1.

B-G: Analysis of the PCR amplifications in 1% agarose gel. M:2-log ladder, -'ve cont: dH_2O as template in PCR, panel B: amplification of VP2-$A^{HIS/N}$, panel C: amplification of VP2-$B^{HIS/N}$, panel D: amplification of VP2-$C^{HIS/N}$, panel E: amplification of VP2-$D^{HIS/N}$, VP2-$E^{HIS/N}$ and VP2-$F^{HIS/N}$ respectively, panel F: amplification of VP2-$G^{HIS/N}$ and VP2-$J^{HIS/N}$ respectively and panel G: VP2-$I^{HIS/N}$ and VP2-$Z^{HIS/N}$ respectively. In panels B, C, E, F and G, a gradient of 6 temperatures were used in the annealing stage of the PCR to amplify the corresponding products and all temperature samples were analysed on the agarose gel with the order of lowest to highest temperature from left to right, respectively. In panel D, duplicate sample of a single temperature was used to amplify the PCR product and both samples were analysed on the gel. Coloured arrows beneath the gels indicate increasing temperature.

I&J: Restriction digest analysis of the constructed baculovirus transfer vectors, purified from colony picks (3 colonies/construct) in 1% agarose gel. Transfer vectors for fragments A, B, C, D, E, F, G and J were digested with *BamH*I and NotI enzymes, whereas *Hind*III and *Not*I enzymes for fragment Z, and *Xba*I and *Not*I enzymes for fragment I were used. 2µl of each plasmid was digested with the corresponding enzymes and incubated at 37°C for 2 hours, prior to running on the agarose gel. (M: 2-log ladder).


A
5000
1000
2000
3000
4000
AmpR
M13 fwd
ori
6xHis
baculo...
BamHI
NotI
pOET1N_VP2-A HIS/N
INSERT FRAGMENT
Replace
BamHI (1932) – NotI (1994)
Insert
BamHI (7) – NotI (560)
BamH
NotI
VP2-A
PCR: VP2-A F
VP2-A R
pSC11_VP2
AmpR
M13 fwd
ori
6xHis
baculovi...
BamHI
NotI
pOET1N 6x His

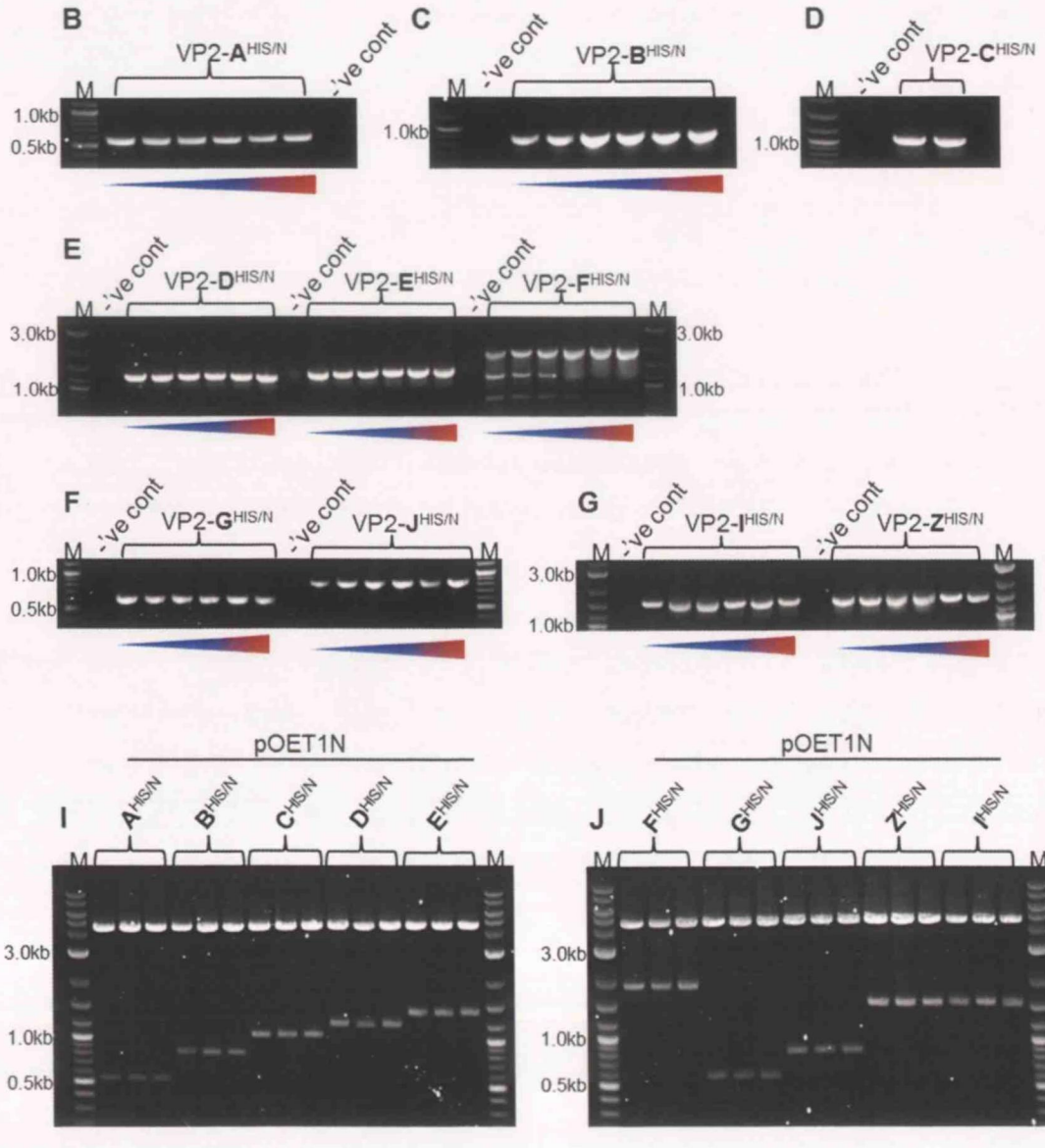

B
VP2-A HIS/N
-ve cont
M
1.0kb
0.5kb
C
-ve cont
VP2-B HIS/N
M
1.0kb
D
-ve cont
VP2-C HIS/N
M
1.0kb
E
-ve cont
VP2-D HIS/N
-ve cont
VP2-E HIS/N
-ve cont
VP2-F HIS/N
M
3.0kb
1.0kb
F
-ve cont
VP2-G HIS/N
-ve cont
VP2-J HIS/N
M
1.0kb
0.5kb
G
-ve cont
VP2-I HIS/N
-ve cont
VP2-Z HIS/N
M
3.0kb
1.0kb
pOET1N
I
A HIS/N
B HIS/N
C HIS/N
D HIS/N
E HIS/N
M
3.0kb
1.0kb
0.5kb
pOET1N
J
F HIS/N
G HIS/N
J HIS/N
Z HIS/N
I HIS/N
M
3.0kb
1.0kb
0.5kb

Table 3.1: Summary of VP2 and the subdomains cloning information

Target	Plasmid name	Position (aa)	Size (bp)
VP2	pOET1_VP2$^{HIS/N}$	1-1061	3183
Fragment H	pOET1_VP2-H$^{HIS/N}$	253-413	480
Fragment A	pOET1N_VP2-A$^{HIS/N}$	1-182	543
Fragment B	pOET1N_VP2-B$^{HIS/N}$	1-276	825
Fragment C	pOET1N_VP2-C$^{HIS/N}$	1-357	1068
Fragment D	pOET1N_VP2-D$^{HIS/N}$	1-411	1230
Fragment E	pOET1N_VP2-E$^{HIS/N}$	1-472	1413
Fragment F	pOET1N_VP2-F$^{HIS/N}$	1-637	1908
Fragment G	pOET1N_VP2-G$^{HIS/N}$	760-955	582
Fragment I	pOET1N_VP2-I$^{HIS/N}$	182-689	1524
Fragment J	pOET1N_VP2-J$^{HIS/N}$	143-414	816
Fragment Z	pOET1N_VP2-Z$^{HIS/N}$	566-1060	1482

3.4 Generation of recombinant baculoviruses

Following the construction of the baculovirus transfer vectors described in section 3.3, twelve recombinant baculoviruses expressing the full-length VP2 and its subdomains were generated using the *flash*BACULTRA system (Figure 3.1), following the protocol from section 2.2.3. After virus seed stocks were generated, 50ml P1 virus stocks were amplified in Sf9 insect cells and titrated by QPCR as described in sections 2.2.2 and 2.2.4, respectively. This titration method is based on QPCR, which allows rapid virus titration using a set of primers and a probe specifically designed to amplify a small region of the baculovirus genome from DNA extracted from budded virus. The increase in the amplification correlates to the genome copy number. This technique is only efficient for viruses not older than three months. A summary of all the viruses generated in this chapter is shown in Table 3.2.

Table 3.2: Summary of viruses

Target	Virus Name	P1 virus stock titre (pfu/ml)	Predicted protein size (kDa)
VP2	AcVP2$^{HIS/N}$	7.5x10^{7}	124
Fragment H	AcVP2-H$^{HIS/N}$	3.9x10^{8}	19
Fragment A	AcVP2-A$^{HIS/N}$	7.1x10^{7}	21.7
Fragment B	AcVP2-B$^{HIS/N}$	7.9x10^{7}	32.6
Fragment C	AcVP2-C$^{N\text{-}HIS}$	3.2x10^{8}	41.9
Fragment D	AcVP2-D$^{HIS/N}$	2.4x10^{8}	48.1
Fragment E	AcVP2-E$^{HIS/N}$	8.6x10^{7}	55
Fragment F	AcVP2-F$^{HIS/N}$	1x10^{8}	74.3
Fragment G	AcVP2-G$^{HIS/N}$	1.1x10^{8}	23.2
Fragment I	AcVP2-I$^{HIS/N}$	1x10^{8}	58.9
Fragment J	AcVP2-J$^{HIS/N}$	1x10^{8}	31.7
Fragment Z	AcVP2-Z$^{HIS/N}$	6.9x10^{7}	58

3.5 Characterization of AcVP2$^{HIS/N}$ and AcVP2-H$^{HIS/N}$ in insect cells

Following the generation of the recombinant baculoviruses, the first step was to characterize protein production in insect cells. Initially, the production of full-length VP2 and fragment H was analysed from their corresponding viruses AcVP2$^{HIS/N}$ and AcVP2-H$^{HIS/N}$, respectively, in Sf9 and TnHi5 cells. Briefly, Sf9 (1x10^{6} cells/well) and TnHi5 (0.5x10^{6} cells/well) were infected with AcVP2$^{HIS/N}$ and AcVP2-H$^{HIS/N}$ using a multiplicity of infection of 5 pfu/cell (moi 5); and mock-infected cells were included as negative control. After incubation at 28ºC for 72 hours, crude cell lysates were harvested and analysed by SDS-PAGE. The proteins were separated on different percentage SDS-PAGE gels based on their sizes; for fragment H, 12% and for full-length VP2, 6% SDS-PAGE gels were used. After SDS-PAGE, the gels were either stained with Coomassie blue or the proteins were transferred onto a PVDF membrane for western blot analysis, using histidine and VP2-specific antibodies, following the protocols described in section 2.5.

Full-length VP2 (124 kDa) and fragment H (19kDa) expressed in TnHi5 cells were detected by western blotting using histidine- and VP2-specific antibodies (Figure 3.6A-D). No recombinant proteins were detected by Coomassie blue staining and no proteins were detected in Sf9 cells (data not shown).

TnHi5 cells were also infected to characterize protein production by immunofluorescence (IF) using VP2-specific monoclonal antibodies (MAbs); SMAA and 6DF4. In order to do this $0.5x10^6$ cells/dish of TnHi5 cells were infected with 5 moi of $AcVP2^{HIS/N}$ or AcVP2-$H^{HIS/N}$. Mock-infected cells and wild-type AcMNPV-infected cells were used as negative controls for this analysis. At 72 hpi, the cells were fixed with 4% formaldehyde and stained with 6DF4 and SMAA MAbs followed by anti-mouse Alexa fluor 488 secondary antibody as described in section 2.5.5 After the staining, several images were taken using a Zeiss fluorescent microscope (Axiovert 135). VP2 was detected by both MAbs, but fewer fluorescent cells were observed with 6DF4 suggesting that it is less sensitive than SMAA antibody (Figure 3.6E). No fluorescence was detected in AcVP2-H-infected TnHi5 cells, suggesting that these antibodies do not recognize any epitopes on the fragment H.

3.6 Characterization of AcVP2-$A^{HIS/N}$ to AcVP2-$Z^{HIS/N}$ in insect cells

In order to characterize the recombinant baculoviruses expressing the remaining VP2 subdomains in Sf9 and TnHi5 insect cells, the same approach was applied as in section 3.5. Virus-infected crude cell lysates were harvested at 72 hpi and analysed by SDS-PAGE gels (10%), Coomassie staining and western blotting using VP2 and histidine antibodies as described. Wild-type AcMNPV-infected and mock-infected cells were used as negative controls during the experiment and purified VP2 protein was used as a positive control for the antibodies on the gels.

Fragments A, B and G were detected with the histidine antibody and all the remaining subdomains were detected with the VP2 antibody at their predicted sizes on a western blot (Figure 3.7). However, no distinctive bands were identified for any of the proteins by Coomassie staining (data not shown). As with full-length VP2 and fragment H no proteins were detected in virus-infected Sf9 cells. The results of the protein production are summarized in Table 3.3.

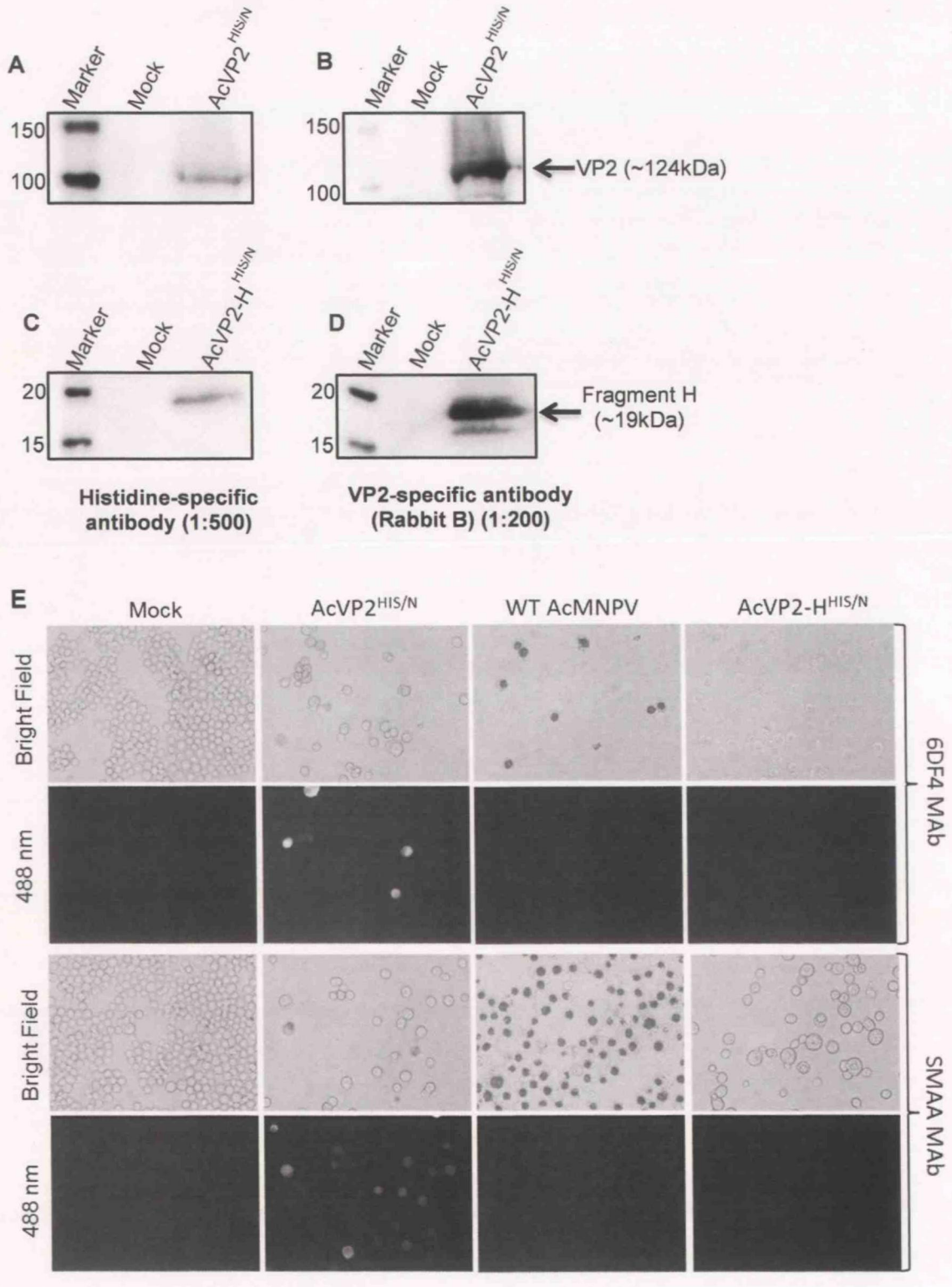


Figure 3.6 Characterization of AcVP2$^{HIS/N}$ and AcVP2-H$^{HIS/N}$ in TnHi5 cells

0.5x10^6 cells/well of TnHi5 were infected with AcVP2$^{HIS/N}$ and AcVP2-H$^{HIS/N}$ using 5 moi.

A-D: Crude cell lysates were harvested at 72 hpi, and separated on 6% and 12% SDS-PAGE gels for AcVP2$^{HIS/N}$ (124kDa) (A&B) and AcVP2-H$^{HIS/N}$ (19 kDa) (C&D) respectively. Western blotting was carried out using histidine (A&C) and VP2 (B&D) antibodies. Mock: non-infected cells, Marker: Precision plus protein Western C standard, Biorad.

E: Cells were fixed with 4% formaldehyde at 72 hpi and stained with 6DF4 and SMAA MAb followed by anti-mouse Alexa fluor 488 antibodies. The images were taken at 100x magnification using Zeiss fluorescent microscope. Mock: non-infected cells.

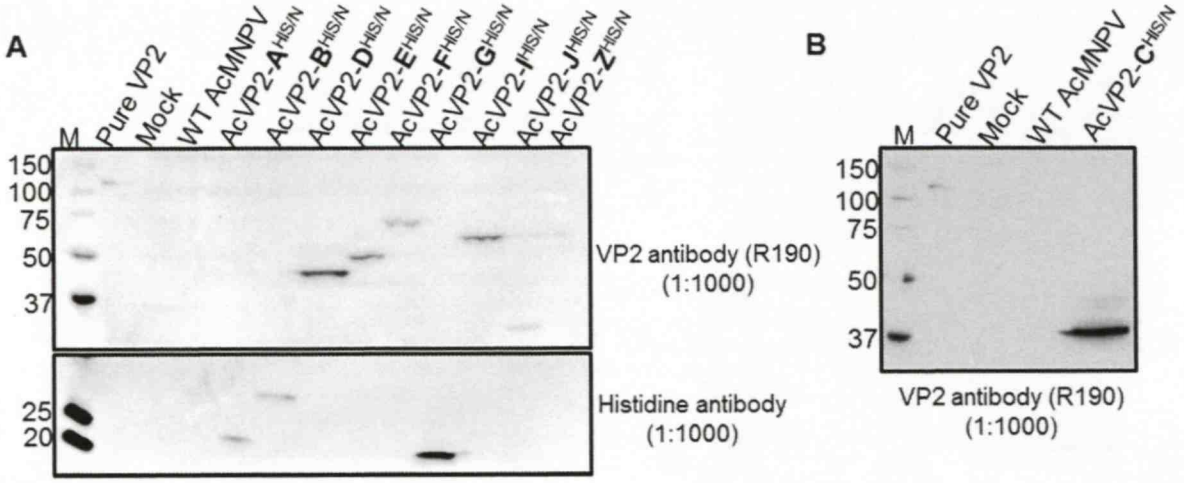


Figure 3.7 Western blot analyses of AcVP2-A$^{HIS/N}$, AcVP2-B$^{HIS/N}$, AcVP2-C$^{HIS/N}$, AcVP2-D$^{HIS/N}$, AcVP2-E$^{HIS/N}$, AcVP2-F$^{HIS/N}$, AcVP2-G$^{HIS/N}$, AcVP2-I$^{HIS/N}$, AcVP2-J$^{HIS/N}$ and AcVP2-Z$^{HIS/N}$ in TnHi5 cells

0.5x10^6 cells/well of TnHi5 were infected with the corresponding recombinant viruses using 5 moi and crude cell lysates were harvested at 72 hpi for western blot analysis. Mock: non-infected cells, Pure VP2: purified VP2, WT: wild-type AcMNPV, Marker: Precision plus protein Western C standard, Biorad

A: Analysis of AcVP2-A$^{HIS/N}$ (21.7kDa), AcVP2-B$^{HIS/N}$ (32.6 kDa), AcVP2-D$^{HIS/N}$ (48.1 kDa), AcVP2-E$^{HIS/N}$ (55 kDa), AcVP2-F$^{HIS/N}$ (74.3 kDa), AcVP2-G$^{HIS/N}$ (23.2 kDa), AcVP2-I$^{HIS/N}$ (58.9 kDa), AcVP2-J$^{HIS/N}$ (31.7 kDa) and AcVP2-Z$^{HIS/N}$ (58 kDa) with VP2 antibody (top) and histidine antibody (bottom)

B: Analysis of AcVP2-C$^{HIS/N}$ (41.9) with VP2 antibody

Table 3.3 Summary of VP2 and its subdomains' production in insect cells

VP2 subdomains	Sample type	Sf9 cells			TnHi5 cells		
		WB	*Coomassie*	*IF*	*WB*	*Coomassie*	*IF*
$A^{HIS/N}$	*Crude cell lysates*	x	x	Not tested	✓ (His-tag)	x	Not tested
$B^{HIS/N}$	*Crude cell lysates*	x	x	Not tested	✓ (His-tag)	x	Not tested
$C^{HIS/N}$	*Crude cell lysates*	x	x	Not tested	✓ (R190)	x	Not tested
$D^{HIS/N}$	*Crude cell lysates*	x	x	Not tested	✓ (R190)	x	Not tested
$E^{HIS/N}$	*Crude cell lysates*	x	x	Not tested	✓ (R190)	x	Not tested
$F^{HIS/N}$	*Crude cell lysates*	x	x	Not tested	✓ (R190)	x	Not tested
$G^{HIS/N}$	*Crude cell lysates*	x	x	Not tested	✓ (His-tag)	x	Not tested
$I^{HIS/N}$	*Crude cell lysates*	x	x	Not tested	✓ (R190)	x	Not tested
$J^{HIS/N}$	*Crude cell lysates*	x	x	Not tested	✓ (R190)	x	Not tested
$Z^{HIS/N}$	*Crude cell lysates*	x	x	Not tested	✓ (R190)	x	Not tested
$H^{HIS/N}$	*Crude cell lysates*	x	x	Not tested	✓ (R190)	x	x (6DF4) x (SMAA)
$VP2^{HIS/N}$	*Crude cell lysates*	x	x	Not tested	✓ (R190)	x	✓(6DF4) ✓ (SMAA)

3.7 Purification of VP2 and the subdomains

After characterizing the viruses and confirming the production of VP2 and its subdomains in TnHi5 cells, the next step was to purify the individual proteins using poly-histidine tag affinity purification. Initially, a small-scale purification was carried out from the cells infected in 6-well plates. However, after the purification, only a very faint band for VP2 was detected on the western blot and no bands were detected for any of the subdomains (data not shown).

Larger scale experiments were performed in order to determine whether the absence of proteins after purification was due to the low yield obtained from the small-scale or due to problems of protein solubility. Shake cultures of TnHi5 cells (90 ml) were set up and infected with 5 moi of $AcVP2^{HIS/N}$, $AcVP2\text{-}A^{HIS/N}$, $AcVP2\text{-}B^{HIS/N}$ or $AcVP2\text{-}D^{HIS/N}$. After 72 hpi, 1ml aliquots were taken to check the presence of protein expression in the cells prior to sonication or purification treatment. These cell pellet samples were lysed with dH_2O prior to running on SDS-PAGE. The cells from the remaining culture were then harvested

and lysed by sonication to purify the proteins using nickel-coated sepharose beads as described in section 2.6. The purification fractions were separated by SDS-PAGE (10% gel) and analysed by western blotting using VP2 and histidine antibodies. Fragments A, B and D were only detected in the total cell lysates and not in the clear supernatant or elution fractions, suggesting that these subdomains were insoluble. However, full-length VP2 could be clearly detected in the elution fraction after purification, suggesting that it was soluble and was able to be purified (Figure 3.8).

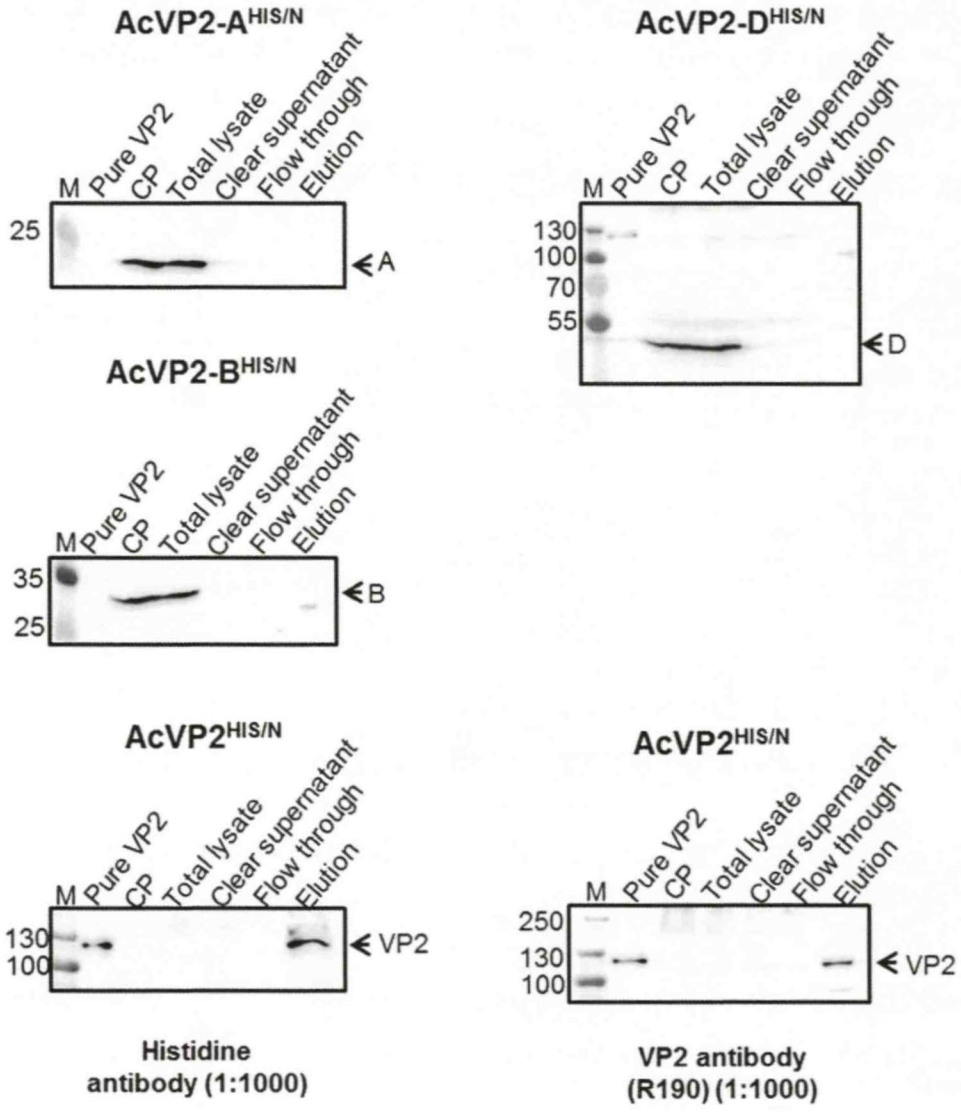


Figure 3.8 Western blot analysis of protein purification from TnHi5 cells infected with AcVP2$^{HIS/N}$, AcVP2-A$^{HIS/N}$, AcVP2-B$^{HIS/N}$ and AcVP2-D$^{HIS/N}$.

90ml cultures of TnHi5 cells were infected with AcVP2$^{HIS/N}$ (124kDa), AcVP2-A$^{HIS/N}$ (21.7 kDa), AcVP2-B$^{HIS/N}$ (32.6 kDa) and AcVP2-D$^{HIS/N}$ (48.1 kDa) at 5 moi. At 72hpi, the cells were harvested, lysed by sonication and processed for purification using nickel-coated sepharose beads. The total lysate, clear supernatant, flow through and final elution fractions of the purification were separated by SDS-PAGE (10% gel) and analysed by western blotting using histidine (left) and VP2 antibodies (right). M: PageRuler plus prestained protein ladder. Pure VP2: previously purified VP2 as positive control on the blots. CP: cell pellet from 1 ml aliquot lysed with dH_2O and not sonication.

3.8 Solubilisation and purification of VP2 subdomains

Since it was found that all the VP2 subdomains were insoluble and could not be purified, the next stage was to try and solubilise the proteins to see whether this would help with their purification. Initial solubilisation testing was carried out with fragments A, B and D and in order to do this, 45ml cultures of TnHi5 cells were infected at 5 moi and the infected cells were harvested at 72 hpi. The proteins were solubilised by incubating the cells with 2M guanidine hydrochloride buffer on ice for 15 minutes. The cells were then lysed by sonication and clarified by high-speed centrifugation at 20000rpm, for 20 minutes. In order to analyse the samples by SDS-PAGE and western blotting, the guanidine had to be removed by dialysis as it is not compatible with SDS-PAGE. Following dialysis, the total lysates and clear supernatants were analysed by western blots using histidine and VP2 antibodies, which demonstrated that fragments A, B and D were successfully solubilized (data not shown). Solubilisation was further optimized by replacing the guanidine hydrochloride with 1M urea at the dialysis stage.

Once the solubility of fragments A, B and D had been confirmed, the soluble fractions were then incubated with nickel-coated sepharose beads for purification; full length VP2 was used as a purification control. The beads were washed with decreasing concentrations of urea (6M, 3M and 1M, respectively) to remove guanidine hydrochloride and proteins were eluted in the presence of 1M urea, which is compatible with SDS-PAGE. Following this, the purification fractions were separated in 10% SDS-PAGE gels and analysed by western blotting using histidine and VP2 antibodies. While fragments A, B and D were all soluble when the sepharose beads were added (shown by the relevant band in the clear supernatant fractions), only fragment D was successfully purified and detected in the elution fraction (48.1kDa; Figure 3.9A).

The same approach used for fragments A, B and D was applied to solubilise and purify the remaining VP2 subdomains. The purification fractions for these fragments were analysed by SDS-PAGE, followed by western blotting using VP2 and histidine antibodies. The results showed that fragments C, H, I and J could be solubilized and among these, fragment C was the only one that could not be purified (data not shown). Following this, the elution fractions for all the VP2 subdomains were separated in a 10% SDS-PAGE gel and analysed by Coomassie staining and western blotting using VP2 and histidine antibodies. Varying intensities of bands were detected at the predicted sizes for fragments D, H, I and J, using the VP2 antibody on the western blot, confirming purification of these subdomains (Figure 3.9B). No bands were detected from the histidine antibody blot confirming that fragments A, B and G were not able to be purified. None of the

subdomains could be detected by Coomassie staining, suggesting that the yield of the purified proteins was very low (data not shown).

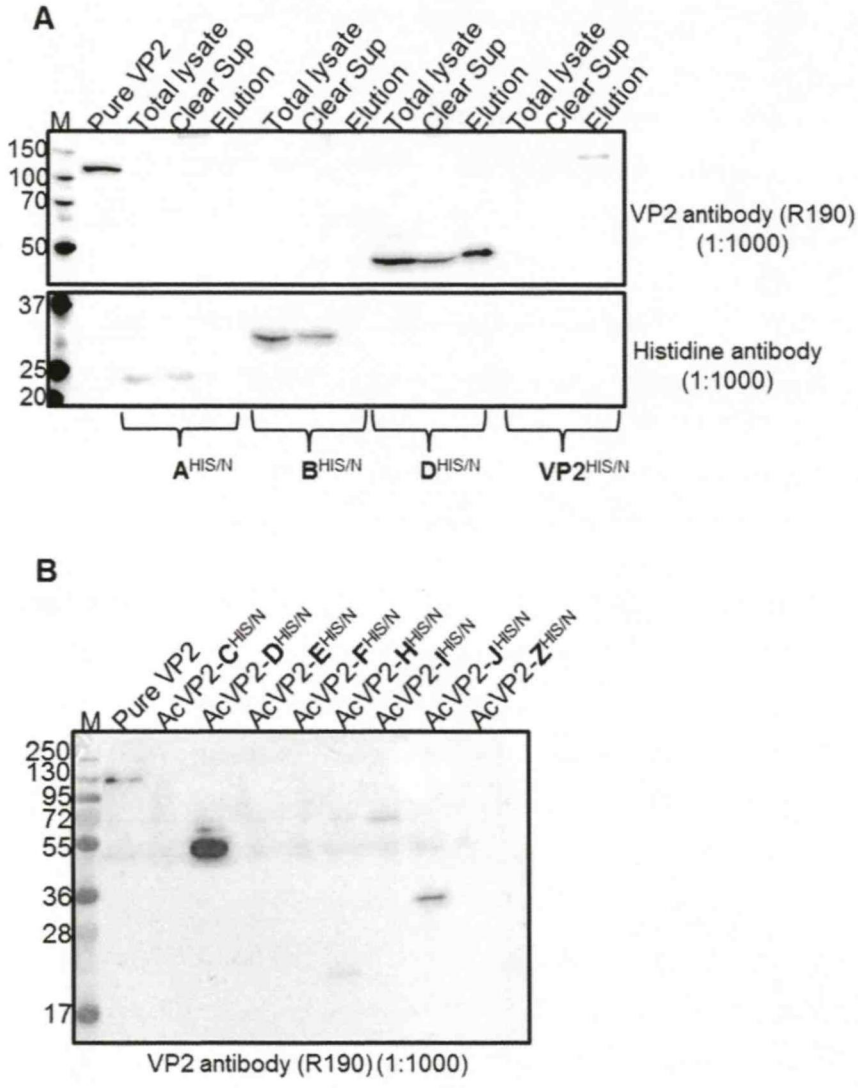


Figure 3.9 Western blot analysis of VP2 subdomain solubilisation and purification from TnHi5 cells

45ml cultures of TnHi5 cells were infected with corresponding viruses of VP2 subdomains using 5 moi and the cells were harvested at 72 hpi. The proteins were solubilised using 2M guanidine hydrochloride prior to purification using nickel-coated sepharose beads. Purification fractions were then separated by SDS-PAGE (10% gel) and analysed by western blotting. Pure VP2: previously purified VP2 as a positive control.

A: Western blot analysis of the purification fractions obtained from AcVP2-$A^{HIS/N}$ (21.7 kDa), AcVP2-$B^{HIS/N}$ (32.6 kDa) and AcVP2-$D^{HIS/N}$ (48.1 kDa) and AcVP2$^{HIS/N}$ (124kDa), using VP2 antibody (top) and histidine antibody (bottom). M: Precision plus protein Western C standard, Biorad.

B: Western blot analysis of the elution fractions of AcVP2-$C^{HIS/N}$ (41.9 kDa), AcVP2-$D^{HIS/N}$ (48.1), AcVP2-$E^{HIS/N}$ (55 kDa), AcVP2-$F^{HIS/N}$ (74.3 kDa), AcVP2-$I^{HIS/N}$ (58.9 kDa), AcVP2-$J^{HIS/N}$ (31.7 kDa) and AcVP2-$Z^{HIS/N}$ (58 kDa) with VP2 antibody. M: PageRuler plus prestained protein ladder.

3.9 Optimizing purification of full-length VP2

The starting point for purification of VP2 was virus-infected TnHi5 cells maintained in shake cultures. However, the fact that purified VP2 was only detected by western blotting and not by Coomassie staining, suggested that the yield obtained from the purification was not very high. In order to try to improve the yield of purified VP2, various protocol variations were tested including incubating the cells in static culture rather than shake cultures and using different cell lysis conditions.

Initially, infecting TnHi5 cells maintained in static culture using two different moi was tested. In order to do this, $2x10^7$ TnHi5 cells seeded in T175 flasks in a total volume of 25ml were infected with $AcVP2^{HIS/N}$ using either 5 or 10 moi (3 flasks/moi). At 72 hpi, the cells were harvested and VP2 was purified using nickel-coated sepharose beads following the protocol described in section 2.6. The purification fractions were then separated in 6% SDS-PAGE gels and analysed by Coomassie staining and western blotting using VP2 and histidine antibodies. VP2 was detected in all the purification fractions using the VP2 antibody but it was only detected in the elution fraction when the histidine antibody was used (Figure 3.10A). However, its presence in the elution fractions confirmed successful purification. In addition, VP2 was detected very clearly by Coomassie staining, suggesting significantly improved yield of purified VP2. Infection of cells at moi 5 gave an increased yield of VP2 (Figure 3.10A).

Even though the yield of purified VP2 was greatly improved, the purity of VP2 was still low, as evidenced by the non-specific proteins observed in the elution fraction by Coomassie staining (Figure 3.10A). In order to try and improve the purity of VP2, the first elution fraction was passed through a superdex 200 column using the AKTA system, but this proved unsuccessful (data not shown).

It is known that the method of cell lysis can affect purity of the final protein, so different lysis methods were compared. Until this point, the cells had been lysed by sonication, which releases the proteins from all the cellular compartments. Instead, 1% NP40 buffer was used, which disrupts the cell membrane and only releases the cytoplasmic proteins. In this way, the nucleus would remain intact so there would be less contaminating proteins involved at the start of the purification. In order to test this, $1.7x10^7$ TnHi5 cells, seeded in static tissue culture dishes in a volume of 25ml/dish, were infected with $AcVP2^{HIS/N}$ at 5 moi. At 72 hpi, the cells were harvested and lysed with 1% NP-40 buffer by incubating on ice for 1 hour. Following this, the usual purification protocol was initially followed as described in section 2.6. At the clear supernatant stage, however, the material was divided into two and incubated with either nickel- or cobalt-coated sepharose beads. The latter have less sensitivity to polyhistidine tags than the nickel. Purification fractions were

then separated in 10% SDS-PAGE gels and analysed by Coomassie staining and western blotting using VP2 antibody. Previously purified VP2 was included in the gel as a positive control. The results of this analysis showed that VP2 could not be purified using the cobalt-coated beads. VP2 from the nickel-coated beads was detected in the two elution fractions tested by both western blotting and Coomassie staining (Figure 3.10B). These results suggested that the purity of VP2 was greatly improved using NP40 lysis rather than sonication (Figure 3.10A).

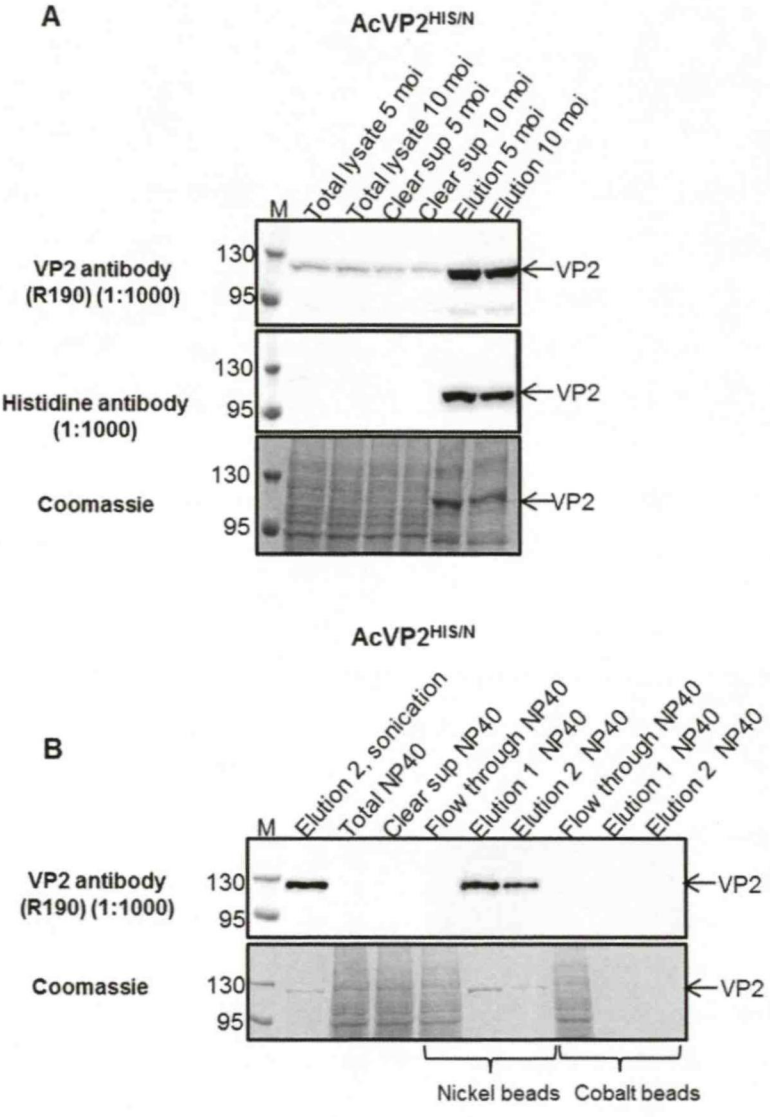


Figure 3.10 Western blot and coomassie staining analysis of VP2 purification optimization

A: $2x10^7$ of TnHi5 cells seeded in T175 flasks were infected with $AcVP2^{HIS/N}$ using 5 and 10 moi and the cells were harvested at 72 hpi. VP2 (124 kDa) was purified using nickel-coated sepharose beads after lysing the cells with sonication. Purification fractions were separated by SDS-PAGE (6% gel) and analysed by coomassie staining (bottom) and western blotting using VP2 (top) and histidine (middle) antibodies. M: PageRuler plus prestained protein ladder.

B: $1.7x10^7$ TnHi5 cells seeded in large tissue culture dishes were infected with $AcVP2^{HIS/N}$ using 5 moi and the cells were harvested at 72hpi. The cells were lysed using 1% NP-40 buffer, prior to VP2 purification using nickel and cobalt-coated sepharose beads. Purification fractions were separated by SDS-PAGE (6% gel) and analysed by coomassie staining (bottom) and western blotting using VP2 antibody (top). M: PageRuler plus prestained protein ladder.

3.10 Antigenic characteristics of full-length AHSV4-VP2

Following the successful purification of AHSV4-VP2, further analysis was carried out to determine its antigenic characteristics. A panel of monoclonal antibodies (MAbs) (INGENASA), previously shown to bind AHSV4 virions (Martinez-Torrecuadrada *et al.*, 1996), were used in an indirect ELISA (section 2.7) to test their reactivity with the AHSV4-VP2 produced and purified in this study. Secondary antibody only sample was used as a negative control in the analysis. All the MAbs bound to the purified VP2 with varying strengths. The lowest binding resulted from 6DF4 antibody with an OD value of 0.5 and the strongest binding resulted from 8AE6 with an OD value of 3.1 (Figure 3.11). Some of these antibodies (8DH3, 10BE7, 10BG7, 10BC12, 10AH5, SMAA and 8CH7) were previously shown to have neutralizing capacity for AHSV4 (Martinez-Torrecuadrada *et al.*, 1996) and among these, 8DH3, 10BC12 and SMAA showed strong binding to the purified VP2 from this thesis with OD values above 1.5 (Figure 3.11). This suggested that the VP2 produced and purified in this study mimics the native conformation of the viral VP2 protein as it binds well to MAbs that bind the virion

Further analysis was carried out by testing the binding of purified VP2 to MVA-VP2 post-vaccination serum from ponies, obtained from The Pirbright Institute. This serum was shown to neutralise the infectivity of AHSV4 virions in a monolayer protection assay (personal communication with Dr Javier Castillo-Olivares). This was carried out by incubating the equine serum with a range of increasing VP2 amounts (50-400ng) for 2 hours at 37ºC, prior to adding to the wells of VP2-coated ELISA plates at the primary antibody stage (section 2.7). Pre-immunization equine serum was used as a negative control in the analysis and the data were normalized by removing the mean OD obtained with this serum.

When the serum only sample was used in the ELISA with the absence of VP2 in the pre-incubation, there was a signal with an OD value of 0.5, confirming the binding of antibodies from MVA-VP2 post-vaccination serum to the purified VP2 (Figure 3.12). Pre-incubation with 50ng VP2 decreased the ELISA signal by 1.7-fold (OD values from 0.5 to 0.3), which was not considered statistically significant (t-test p=0.0741). The magnitude of this decrease was 5-fold when the serum was pre-incubated with 100ng of VP2 (OD values from 0.5 to 0.1) and this difference was considered to be statistically significant (t-test p=0.0004). After this point a linear relationship was observed where there was a further 2-fold decrease in the ELISA signal as the serum was pre-incubated with doubling amounts of VP2. Overall, about 20-fold decrease in the ELISA signal was observed when the maximum amount of VP2 (400ng) was pre-incubated with the serum, which is considered to be extremely statistically significant (t-test p=0.0001). This suggested that

the antibodies from the MVA-VP2 post-vaccination serum were capable of binding the purified VP2 in solution, depleting the ELISA signal (Figure 3.12).

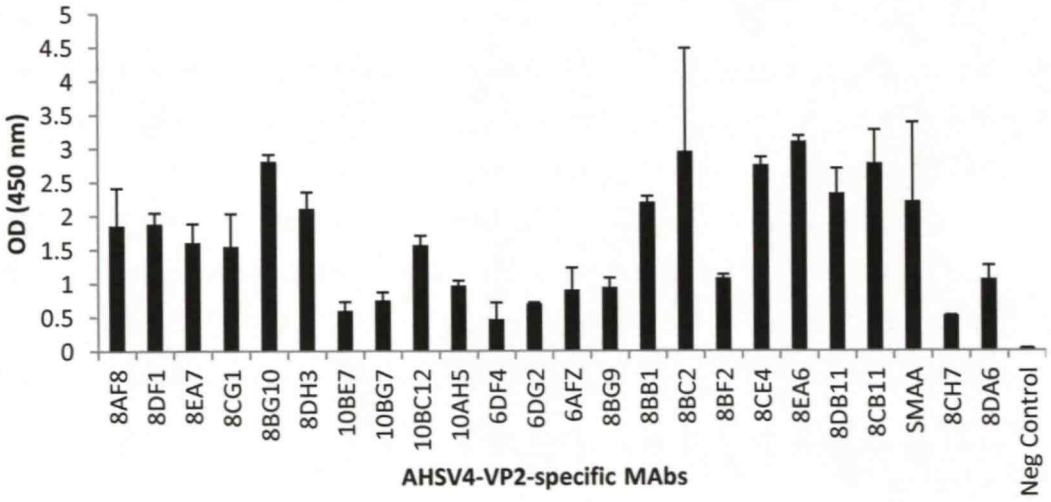


Figure 3.11 Reactivity of AHSV4-VP2-specific MAbs with purified VP2

Assay plates were coated with 15ng baculovirus-expressed purified VP2 overnight at 4°C. MAbs were used with 1 in 100 dilution and HRP-conjugated anti-mouse secondary antibodies were used with 1in2000 dilution. Following the antibody incubations, 50µl of TMB substrate and sulfuric acid stop solution were added respectively and absorbance was measured at 450nm with a microplate reader (LT-4500). The graph was generated using the mean OD values of duplicate samples. Error bars indicate the ±3 standard deviation for each sample. Neg control: secondary antibody only (anti-mouse) sample with a mean OD value of 0.03425. Raw data can be found in Appendix 1.

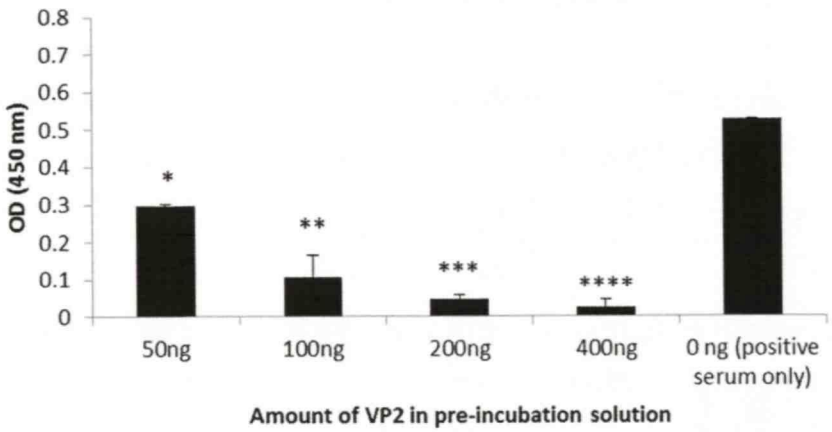


Figure 3.12 Reactivity of MVA-VP2 post vaccination serum from ponies to baculovirus-expressed purified VP2

Assay plates were coated with 15ng of baculovirus-expressed purified VP2 overnight at 4◦C. Equine serum (1 in 100 dilution) was pre-incubated with 50-400ng of VP2 at 37◦C for 2 hours. The serum was directly added to the VP2-coated plates after the incubation. HRP-conjugated anti-horse secondary antibody was used at 1 in 15000. The signal was developed with the addition of TMB substrate (50µl), stopped with sulfuric acid stop solution (50µl) and the absorbance was measured at 450nm using a micro-plate reader (LT-4500). Graph was generated using the mean OD values of quadruplicate samples after subtracting the mean OD values obtained with the pre-immunisation equine serum for each corresponding sample. Error bars indicate the standard error of each sample. Un-paired t-test was carried out using GraphPad software to compare the OD values of each VP2 amount used in the pre-incubation solution to the positive serum only (0ng VP2). *T-test p=0.0741, **t-test p=0.0004), ***t-test p=0.0002, ****t-test p=0.0001. Raw data can be found in Appendix 2.

3.11 Discussion

This project aims to investigate the VP2 antigenic structure by expressing eleven VP2 subdomains using baculovirus vectors. The majority of the subdomains chosen are located on the amino-terminal half of the protein, which has been shown by a previous study to be more antigenic than the carboxy-terminal (Martinez-Torrecuadrada and Casal, 1995). In addition, a recent study by Manole *et al.* (2012) also supports the subdomain choices, as they have shown that the central domain of VP2 trimers forms in itself an independent structural subdomain that contains most of the antigenic domains defined so far, and it is also the most antigenically variable domain of the protein. It should be noted that the proteins used for the antigenic characterization by Martinez-Torrecuadrada and Casal (1995) were generated in *E. coli*. This thesis however, used baculovirus-insect cell expression, which is suggested to be a more advantageous system for the production of correctly-folded arboviral proteins.

The initial aim of this chapter was to generate the recombinant baculoviruses to express the full-length VP2 and the eleven selected subdomains within insect cells. In order to facilitate purification at later stages, a 6xhistidine tag was added to either amino- or carboxy-terminals of the proteins, as it was unknown which terminus would be best for tagging. However, it was immediately discovered that histidine tagging the proteins at the carboxy-terminal inhibited the generation of recombinant baculoviruses (data not shown). The underlying reason for this discovery was not investigated any further as recombinant baculoviruses with proteins tagged at the amino-terminus were successfully generated. However, it could be due to a toxic effect on the transfected Sf9 cells resulting from the product generated by adding the his-tag to the carboxy-terminus.

Following their generation, recombinant baculoviruses were characterized in Sf9 and TnHi5 cell lines to analyse the production of VP2 and the subdomains. The results have shown that the production of VP2 subdomains could only be detected in TnHi5 cells, whereas, the full-length VP2 could be detected from both cell lines. However, the full-length VP2 could be detected from Sf9 cells only after it had been purified using poly-histidine tag affinity column and not from the crude cell lysates (data not shown) suggesting the protein yield from Sf9 cells was very low.

Low-yield production of recombinant VP2 in Sf9 cells was also reported by previous studies for AHSV4 (Martinez-Torrecuadrada *et al.*, 1994) and AHSV5 (Du Plessis *et al.*, 1998). In addition, these studies reported that the majority of VP2 produced in Sf9 cells were insoluble. Interestingly, Martinez-Torrecuadrada *et al.* (1994) observed an improvement in the solubility of VP2 in Sf9 cells, when it was co-expressed with another AHSV capsid protein, VP5, from a dual expression construct. Low-yield production of VP2

observed in Sf9 cells was however, overcome by using an alternative insect cell line, TnHi5 cells, in this thesis. On the other hand, it would be interesting to co-express VP5 in the future to investigate whether this will improve VP2 production further in TnHi5 cells.

The difference in protein expression profiles between these two cell lines has also been observed by several other studies, where TnHi5 cells were favoured for the expression of recombinant proteins and virus-like-particles (Krammer *et al.*, 2010, Wilde *et al.*, 2014). Even though the distinct reason behind this is unknown, it is more likely dependent on the nature of individual proteins and also the fact that these two cell lines originate from different insect species. Sf9 cells are the clonal isolates of a cell line derived from the pupal ovarian tissue of *Spodoptera frugiperda*, the army worm (Vaughn *et al.*, 1977), whereas TnHi5 cells originate from the ovarian cells of *Trichoplusia ni,* which is a cabbage looper (Wickham *et al.*, 1992, Wickham and Nemerow, 1993). Therefore, these two cell lines most likely differ in the way they process the recombinant protein production.

After confirming the production of VP2 and its subdomains in TnHi5 cells, several experiments were carried out to purify the proteins. Purifying these proteins from the insect cells would play an important role in characterizing the antigenicity of these subdomains. They could be used in several biological analyses such as, enzyme-linked immunosorbent assay (ELISA), antibody depletion assays using serum samples containing virus neutralizing antibodies and also in vaccination of animals. In addition, using these subdomains in vaccinations as purified proteins would serve as a control to test the hypothesis that the conformation adopted by baculovirus surface display might play an important role in presenting the virus neutralizing epitopes of the protein, which is investigated in chapters five and six.

The results of the purification studies have shown that apart from full-length VP2, all the subdomains were insoluble, which prevented their purification in the first instance. Misfolded polypeptide chains are one of the main reasons for a protein to become insoluble, which occurs when the regions of the polypeptide chain interact in a way that the hydrophobic amino acid residues are exposed on the surface, causing them to aggregate (Pain, 2000, Radford, 2000, Dobson, 2004). In the majority of cases, molecular chaperones assist the correct folding of polypeptide chains, preventing their aggregation. This is achieved by stabilizing the structures at the intermediate folding stage, which could have hydrophobic residues exposed on the surface, until the folding process is complete (Barral *et al.*, 2004). However, it should be taken into consideration that VP2 subdomains are not produced as individual proteins in the actual host and they are just sections of a large protein. So, when they are expressed as recombinant proteins in insect cells, they are forced to form individual structures, which might result in their aggregation, making

them insoluble. Furthermore, as part of cellular biology, misfolded protein aggregates are one of the favoured targets for degradation by ubiquitin pathway as a defence mechanism against disease (Dobson, 2004). This form of degradation might further explain why the expression of VP2 subdomains could not be detected from Sf9 cells.

In respect of the insolubility of the VP2 subdomains, addition of guanidine hydrochloride and urea was tested to increase solubility; however, this was not very effective. When the subdomains that could be solubilized, such as fragments H, D, I and J, were purified (Figure 3.9 B), it was found out that the yield of correctly folded soluble protein was very low; and insufficient for downstream analysis. The stability and solubility of proteins has been improved previously with the use of fusion tags such as small ubiquitin-related modifier (SUMO) protein (Panavas *et al.*, 2009), however, this has not been investigated further during this project; largely because baculovirus surface display was used as an alternative approach as described in chapters four and five.

In the case of antibody detection, the results have shown that even though they were histidine tagged, the majority of the VP2 subdomains, apart from fragments A, B and G, were not detected by histidine antibody on a western blot (Figure 3.7A). This could not be due to the absence of the histidine tag, as its presence was confirmed both by plasmid sequencing at the cloning stages and also by the purification results. If the histidine tag was not present during the purification, it would not have been possible to purify fragments D, H, I and J following their solubilisation (Figure 3.9B). Therefore, it could be suggested that the efficiency of the histidine antibody was not as high as the VP2 antibody in detecting the proteins.

A similar problem was also encountered in a previous study, where Debeljak *et al.* (2006) tested the presence of their target protein on a western blot using several commercial histidine antibodies and a protein-specific monoclonal antibody. In this study, they showed that the target protein from the test samples and the positive controls were detected by the specific monoclonal antibody and only one of the commercial histidine antibodies. The remaining commercial histidine antibodies only detected the positive controls. They suggested that the variability of the histidine antibody detection could depend on several factors such as: location of the his-tag on the individual protein, length of the his-tag and protein purity (Debeljak *et al.*, 2006). Although, further analysis would be required to confirm the reason behind the variable detection of histidine antibody in this study, concentration and purity of protein is highly likely to play an important role. It has been shown in this chapter that the VP2 subdomains were insoluble and the expression yields were low, and also the full-length VP2 was detected with the histidine antibody only from

the elution fractions after the purification and not from the total lysate or the clear supernatant (Figure 3.10A).

Furthermore in this chapter, VP2 purification was optimized, which has revealed that the final yield could be greatly improved when VP2 was produced in cells of adherent rather than suspension culture, and also when the cells were lysed with NP-40 buffer instead of sonication. The reason for the improved yield using NP-40 lysis is most probably because of the reduced amount of contaminating proteins present at the start of the purification. This is due to the disruption of the cytoplasmic membrane only, where the nucleus is kept intact, resulting in the elimination of several histidine-rich proteins found in the nucleus. On the other hand, the reason behind the improved yield from adherent cultures is much more complicated and requires detailed investigation for further understanding. However, it could be suggested that the amount of oxygen accessible by the cells might play an important role. This is because; while the adherent cells are directly exposed to oxygen, the cells in suspension rely on kinetic energy for aeration of the whole culture. It has been also shown by a previous study that baculovirus-infected cultures have an increased requirement for oxygen compared to non-infected cultures (Wong *et al.*, 1994). In addition, cells in suspension are more prone to shearing due to the kinetic motion, which could also affect the production and/or the stability of the proteins.

Once the full-length VP2 was successfully purified to high concentrations, the next stage was to determine the antigenic nature of the protein. The results showed that a panel of AHSV4-specific MAbs recognized the purified VP2 in an indirect ELISA (Figure 3.11). The strong binding observed by three of the MAbs; 8DH3, 10BC12 and SMAA was of high importance as they previously displayed neutralizing capacity for AHSV4 virions (Martinez-Torrecuadrada *et al.*, 1996). This suggested that the purified VP2 represents the native conformation of AHSV4 virus antigenic epitopes.

A similar analysis was carried out by Martinez-Torrecuadrada *et al.* (1996), where the reactivity of these MAbs was also tested with baculovirus-expressed, purified recombinant VP2. However, their findings did not match to the profile observed in this thesis, as majority of the MAbs did not recognize their purified VP2 (Table. 3.4). The main difference between the two VP2 that could cause such an outcome is probably due to the method used for purification. While VP2 purification was achieved by affinity chromatography using specific antibodies in the study by Martinez Torrecuadrada *et al.* (1996), poly-histidine tag affinity purification was the method used in this thesis. It is known from the literature that antibody affinity chromatography could permanently affect the properties of a protein due to elution stage containing extreme pH conditions (Kimple *et al.*, 2013).

Therefore, it is highly likely that the antibody binding altered the conformation of VP2 during purification.

Virus neutralizing antibodies play an important role in protecting the host against lethal AHSV challenge (Martinez-Torrecuadrada *et al.*, 1996, Alberca *et al.*, 2014, Calvo-Pinilla *et al.*, 2014). Therefore, it was important to confirm the reactivity of purified VP2 with antibodies from MVA-VP2 post-vaccination serum, which was shown to contain VN antibodies generated in equine host. An indirect ELISA demonstrated that antibodies from MVA-VP2 post-vaccination equine serum successfully bound to immobilized purified VP2 in assay plates. In addition, pre-incubation with increasing amounts of VP2 demonstrated that the antibodies could be depleted from the solution by specific antigen binding (Figure 3.12). However, it should be noted that MVA-VP2 post-vaccination serum contains a heterogeneous mix of polyclonal VP2-specific antibodies in which some of them might not be neutralising. Hence, the biological activity of purified VP2 was tested *in vivo* in mice as described in chapter six.

Table 3.4 Reactivity of MAbs with VP2 from Martinez Torrecuadrada et al.(1996)

AHSV4-specific MAb	Purified rVP2	AHSV4
8AF8		
8DF1		
8EA7		
8CG1		
8BG10		
8DH3		
10BE7		
10BG7		
10BC12		
10AH5		
6DF4		
6DG2		
6AFZ		
8BG9		
8BB1		
8BC2		
8BF2		
8CE4		
8EA6		
8DB11		
8CB11		
SMAA		
8CH7		
8DA6		

0-40%
40-60%
60-80%
80-100%

*The table was adapted from Martinez Torrecuadrada *et al.* (1996). The percentage reactivity in the study was expressed as A405/the greatest absorbance value (3.0) at this wavelength.

3.12 Conclusion

Overall in this chapter, it has been shown that TnHi5 cells are the favoured cell line for the production of AHSV4-VP2 and its subdomains. In addition, unlike previous studies poly-histidine tag affinity purification was used successfully to purify VP2 to sufficient quantities. Furthermore, antigenicity analysis has shown that it represents the native conformation of the AHSV4-VP2 antigenic epitopes. On the other hand, VP2 subdomains were produced to low yields and could not be purified due to insolubility. Therefore, the focus of the project was directed towards baculovirus surface display to improve the production of VP2 subdomains, as will be described in chapters four and five.

Chapter 4

Optimization of baculovirus surface display for the production of AHSV4-VP2 and the subdomains

4.1 Introduction

Surface display systems have been widely used to study protein-protein interactions for many years. They have been applied in various platforms for the screening of large peptide libraries, generation of antibodies and potential vaccines using phage (Smith, 1985, McCafferty *et al.*, 1990), bacterial or yeast cell surface display (Boder and Wittrup, 1997, Westerlund-Wikstrom *et al.*, 1997). However, these platforms suffer from disadvantages that limit the type of protein used for display. Phage display is restricted by prokaryotic expression, which lacks post-translational modifications that are crucial for the correct folding of the majority of mammalian and viral proteins (Fiedler and Simons, 1995, Phizicky and Fields, 1995, Oldham, 2012). Yeast surface display can be disadvantageous due to the low recombinant protein yield (Oldham, 2012). The baculovirus expression system, however, is an alternative solution as it provides high recombinant protein yield in insect cells, and mammalian cell-like post-translational modifications for authentic protein folding (Smith *et al.*, 1983b, Luckow and Summers, 1988). Boublik *et al.* (1995) developed a universal eukaryotic vector for the display of foreign proteins on AcMNPV budded virus surface using the glycoprotein, GP64. The site identified for foreign gene insertion was between the GP64 signal peptide and the transmembrane domain (TMD). The modifications were carried out on a second copy of the GP64 gene in a baculovirus transfer vector to retain expression of the native GP64 protein on the virion envelope surface, as this is crucial for virus infectivity (Blissard and Wenz, 1992).

Baculovirus surface display is one of the major interests of this thesis for the investigation of the AHSV4-VP2 antigenic structure. Initially, three different AcMNPV promoters, *polh*, *p6.9* and *gp64* were tested for the optimum expression of full-length VP2 or fragment H subdomain on the baculovirus envelope surface. These promoters drive the expression of the gene of interest at different times during the infection cycle. The *gp64* promoter drives expression during both early and late phases of the infection cycle (Whitford *et al.*, 1989), whereas *p6.9* is a late (Wilson *et al.*, 1987) and *polh* a very late promoter (Possee and Howard, 1987). Once the optimum promoter was identified, further studies compared the effectiveness of a full-length and truncated GP64, as Grabherr *et al.* (1997) and Lin *et al.* (2008) had shown that using a truncated GP64 may increase expression levels. This was carried out by comparing the expression levels of enhanced green fluorescent protein (EGFP) fused to the original or truncated GP64 on the baculovirus envelope surface.

4.2 Construction of pBACsurf-1_*p6.9* and pBACsurf-1_*gp64*

The commercial pBACsurf-1 (Novagen) is based on the baculovirus surface display vector described by Boublik *et al.* (1995), which drives the expression of genes using the *polh* promoter. In this project, pBACsurf-1 was modified to generate two additional surface

display vectors to drive gene expression using the *p6.9* and *gp64* promoters. The cloning strategy for promoter replacement is illustrated in Figure 4.1A. Initially, the *p6.9* promoter was PCR-amplified using gene-specific primers from the pOET3 vector (OET Ltd). Primers were designed to contain 5' *EcoR*V and 3' *Sac*I and *Spe*I restriction site sequences, respectively. The amplified *p6.9* promoter (0.1kbp fragment from Figure 4.1B) was cloned into pBACsurf-1 vector using *EcoR*V and *Spe*I restriction enzymes. This replaced the *polh* promoter, generating pBACsurf-1_*p6.9*. Subsequently, nucleotide sequences encoding the *gp64* promoter were PCR-amplified using gene-specific primers from the pBacPAKgp64dsred vector. The PCR product (211bp fragment from Figure 4.1C) was cloned into pBACsurf-1_*p6.9* vector using *EcoR*V and *Sac*I restriction sites, which replaced the *p6.9* promoter and resulted in the generation of pBACsurf-1_*gp64*. Restriction digestion analysis was carried out to confirm the presence of promoters in their corresponding plasmids. For pBACsurf-1 and pBACsurf-1_*p6.9*, *EcoR*V-*Spe*I, and for pBACsurf-1_*gp64, EcoR*V-*Sac*I was used, which resulted in two fragments indicating the promoters and the remaining plasmid backbone in each case (Figure 4.1D).

4.3 Cloning of full-length VP2 and fragment H into pBACsurf-1, pBACsurf-1_*p6.9* and pBACsurf-1_*gp64*

Nucleotide sequences encoding AHSV4-VP2 and fragment H were PCR-amplified from the template vector pSC11-AHSV-4-VP2 using gene specific primers (Figure 4.2B-D). During the PCR amplification, start and stop codons were removed to enable surface display as a fusion to GP64. In order to test whether histidine tagging the proteins would affect the display on the baculovirus envelope surface, cloning was designed to generate both amino-terminus histidine-tagged and non-tagged versions of the proteins. For non-tagged proteins, genes were generated in a single PCR-amplification whereas a 6xhis tag was added to the 5' sequences during two rounds of amplification. Restriction enzymes (*Pst*I and *Sma*I) incorporated into the genes during the amplification were used to clone the final PCR products into pBACsurf-1, pBACsurf-1_*p6.9* and pBACsurf-1_*gp64* generated in section 4.2.

The overall cloning strategy is shown in Figure 4.2A. Following ligation and transformation of *E.coli* (sections 2.4.4, 2.3.2 and 2.3.3), plasmids from several colonies were screened using *Pst*I and *Sma*I enzymes. Restriction digest analysis confirmed that both non-tagged and 6xhis-tagged fragment H were successfully cloned into all three transfer vectors, shown by the two fragments at the expected sizes in Figure 4.2E. In the case of full-length VP2, only two constructs were successfully generated; non-tagged VP2 in pBACsurf-1_*gp64* and 6xhis-tagged VP2 in pBACsurf-1_*p6.9* (Figure 4.2F).

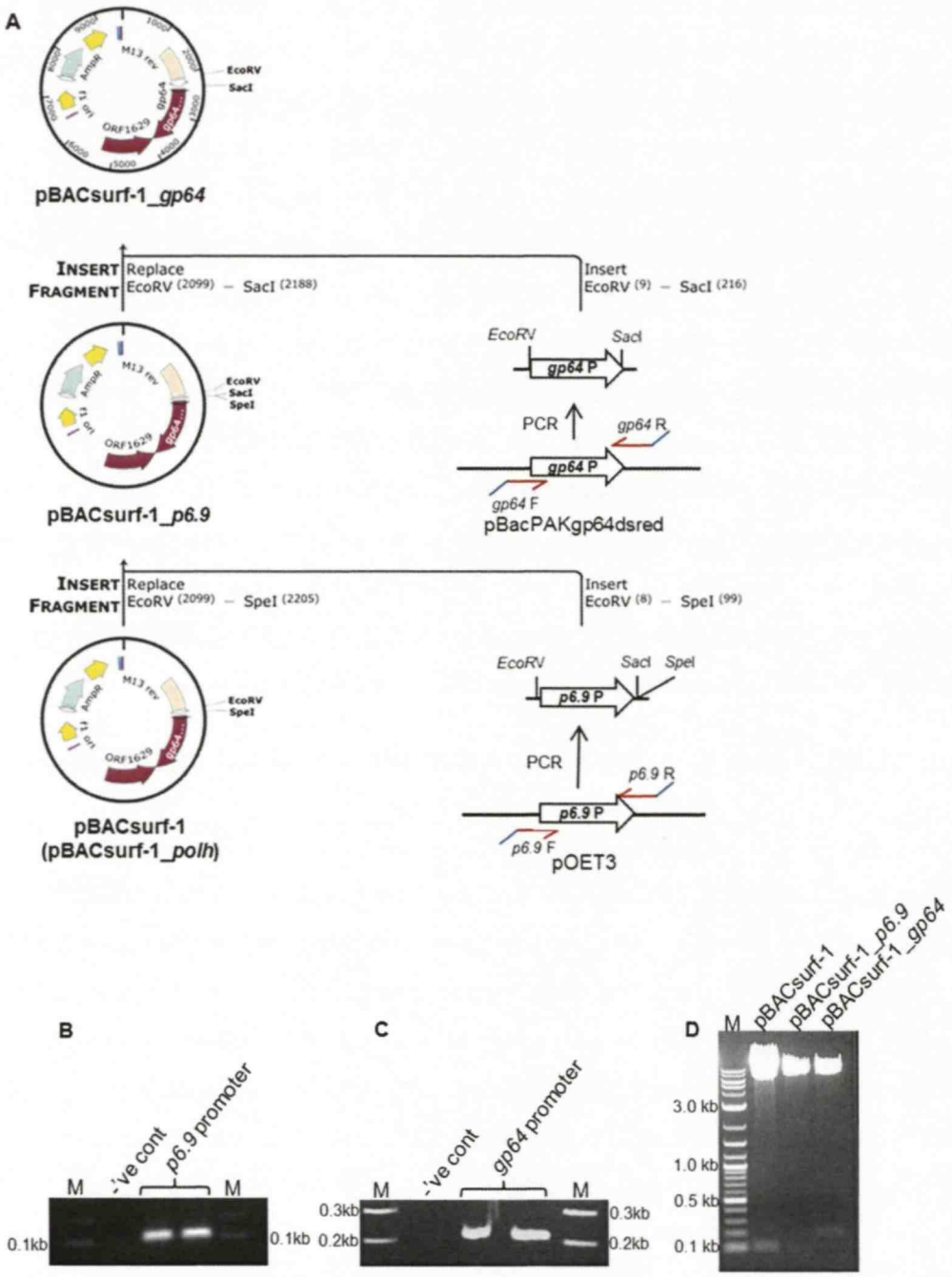


Figure 4.1 Construction of pBACsurf-1_*p6.9* and pBACsurf-1_*gp64*

A: Schematic representation of the cloning strategy generated by SnapGene® software. The *p6.9* promoter was PCR amplified from pOET3 vector using the primers; *p6.9* F and *p6.9* R. The PCR product was cloned into pBACsurf-1 vector using *EcoR*V-*Spe*I restriction sites, which replaced the *polh* promoter to generate pBACsurf-1_*p6.9*. Then, the *gp64* promoter was PCR-amplified from the pBacPAKgp64dsred vector using the primers: *gp64* F and *gp64* R. The PCR product was cloned into pBACsurf-1_*p6.9* using *EcoR*V-*Sac*I sites to replace *p6.9* promoter and generate pBACsurf-1_*gp64*.

B&C: Analysis of PCR amplification of *p6.*9 (B) and *gp64* (C) promoters in 1% and 3% agarose gels, respectively. Duplicate samples were used in the PCR amplification of both promoters and both were run on the agarose gels. M: 2-log ladder, -'ve cont: dH_2O as the template in PCR.

D: Restriction digest analysis of pBACsurf-1 (*EcoR*V-*Spe*I), pBACsurf-1_*p6.9* (*EcoR*V-*Spe*I) and pBACsurf-1_*gp64* (*EcoR*V-*Sac*I) plasmids purified from colony picks in a 1% agarose gel. 2µl of each plasmid was digested with the indicated restriction enzymes for 2 hours at 37°C, prior to analysis.

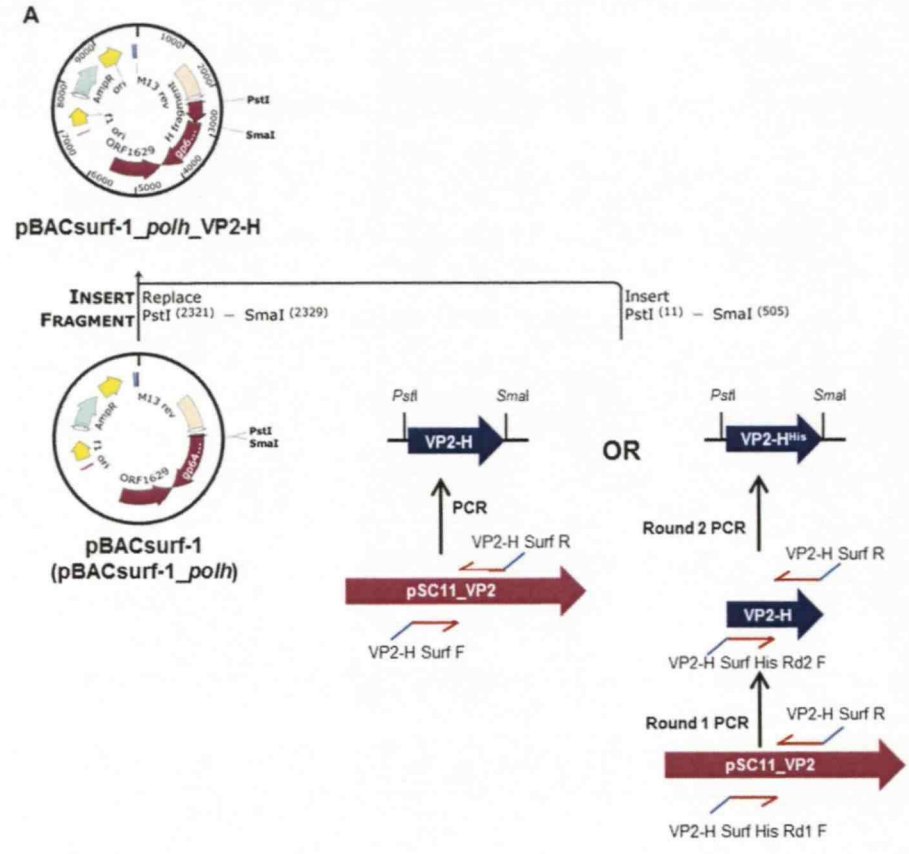
In order to generate the remaining constructs with full-length VP2, several protocol variations were tested, which involved vector dephosphorylation (Section 2.4.3), subcloning into pGEMT vector (Section 2.4.6) and different ligation temperatures, but this proved unsuccessful.

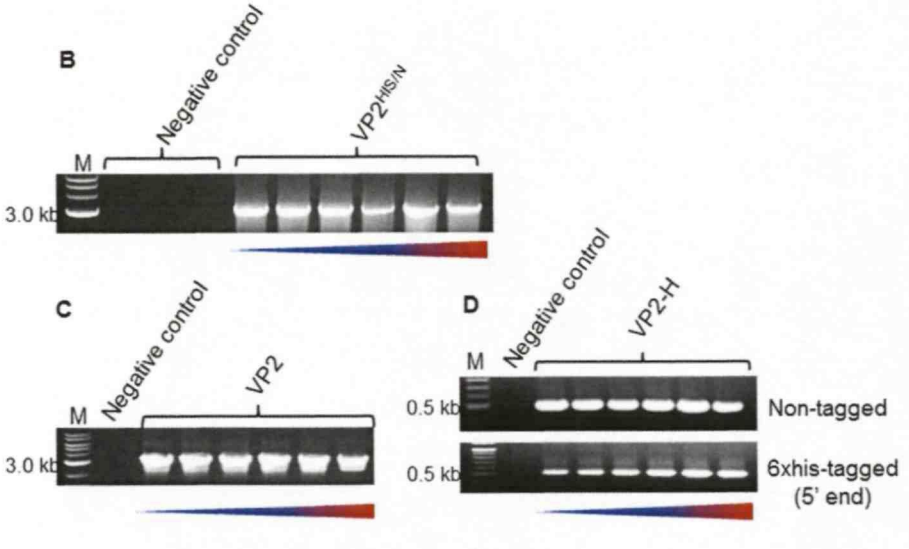
4.4 Generation of full-length VP2 and fragment H surface display viruses

Following the construction of the baculovirus transfer vectors described in section 4.3, eight recombinant baculoviruses were generated using the *flash*BACULTRA system (section 2.2.3). After virus seed stocks were generated, 50ml P1 virus stocks were amplified in Sf9 insect cells and titrated by QPCR following the protocols from sections 2.2.2 and 2.2.4, respectively. A summary of these viruses is shown in Table 4.1.

Table 4.1 Summary of fragment H and full-length VP2 surface display viruses with different promoters

Target	Plasmid name	Virus name	P1 virus stock titre (pfu/ml)	Predicted chimeric protein size (kDa)
Fragment H	pBACsurf-1_*polh*_VP2-H	AcSurf_VP2-H	$5.8x10^8$	75
	pBACsurf-1_*polh*_VP2-H^{HIS}	AcSurf_VP2-H^{HIS}	$2.4x10^8$	75
	pBACsurf-1_*p6.9*_VP2-H	AcSurf_VP2-$H^{p6.9}$	$2.1x10^7$	75
	pBACsurf-1_*p6.9*_VP2-H^{HIS}	AcSurf_VP2-$H^{p6.9/HIS}$	$3.4x10^7$	75
	pBACsurf-1_*gp64*_VP2-H	AcSurf_VP2-H^{gp64}	$1.2x10^8$	75
	pBACsurf-1_*gp64*_VP2-H^{HIS}	AcSurf_VP2-$H^{gp64/HIS}$	$8.6x10^7$	75
VP2	pBACsurf-1_*p6.9*_$VP2^{HIS}$	AcSurf_$VP2^{p6.9/HIS}$	$1.4x10^8$	180
	pBACsurf-1_*gp64*_VP2	AcSurf_$VP2^{gp64}$	$1.7x10^8$	180


A
PstI
SmaI
pBACsurf-1_polh_VP2-H
INSERT FRAGMENT
Replace
PstI (2321) – SmaI (2329)
Insert
PstI (11) – SmaI (505)
pBACsurf-1
(pBACsurf-1_polh)
PstI
SmaI
VP2-H
OR
VP2-H^His
PCR
Round 2 PCR
VP2-H Surf R
pSC11_VP2
VP2-H Surf F
VP2-H Surf His Rd2 F
Round 1 PCR
VP2-H Surf His Rd1 F


B
Negative control
VP2^HIS/N
M
3.0 kb
C
Negative control
VP2
M
3.0 kb
D
Negative control
VP2-H
M
0.5 kb
Non-tagged
0.5 kb
6xhis-tagged
(5' end)

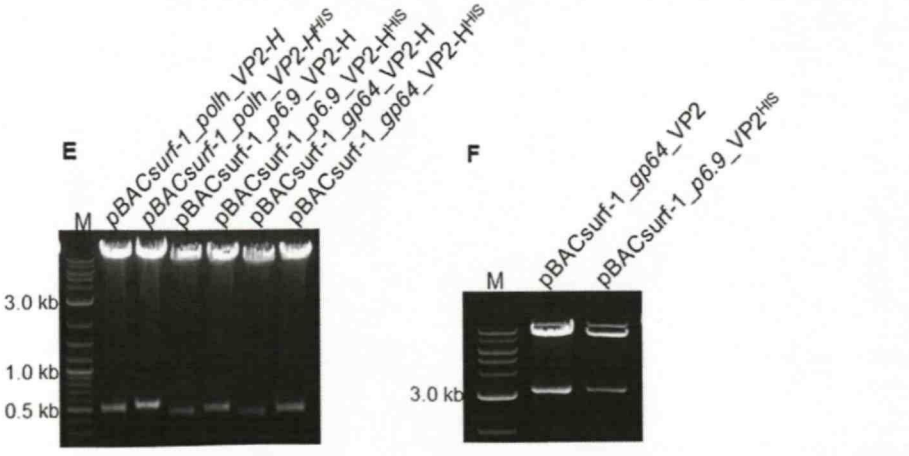

E
M
pBACsurf-1_polh_VP2-H
pBACsurf-1_polh_VP2-H^HIS
pBACsurf-1_p6.9_VP2-H
pBACsurf-1_p6.9_VP2-H^HIS
pBACsurf-1_gp64_VP2-H
pBACsurf-1_gp64_VP2-H^HIS
3.0 kb
1.0 kb
0.5 kb
F
M
pBACsurf-1_gp64_VP2
pBACsurf-1_p6.9_VP2^HIS
3.0 kb

Figure 4.2 Cloning of full-length VP2 and fragment H into pBACsurf-1, pBACsurf-1_*p6.9* and pBACsurf-1_*gp64*

A: Schematic representation of cloning strategy generated by SnapGene® software using the example of 6xhis-tagged and non-tagged fragment H constructs. The same cloning approach was used for all the remaining constructs shown in this figure. Fragment H was PCR-amplified from the template vector pSC11_VP2 using the primers: VP2-H Surf His Rd1 F, VP2-H Surf His Rd2 F, VP2-H Surf F and VP2-H Surf R. Final PCR products were cloned into pBACsurf-1, pBACsurf-1_*p6.9* and pBACsurf-1_*gp64* using the restriction sites *Pst*I and *Sma*I.

B-D: Analysis of PCR-amplified 6xhis-tagged full-length VP2 (B), non-tagged VP2 (C), non-tagged fragment H (D, top) and 6xhis-tagged fragment H (D, bottom) in a 1% agarose gel. A gradient of 6 different temperatures were used in the annealing stage of PCR and all samples were run on the agarose gel with the order of lowest to highest temperature from left to right, respectively. In each gel, the temperature gradient samples were collectively labelled as pSC11_VP2, which is the template vector used in the PCR for amplification. M: 2-log ladder, Negative control: dH_2O as template in the PCR.

E&F: Restriction digest analysis of fragment H (E) and full-length VP2 (F) surface display transfer plasmids isolated from colony picks in a 1% agarose gel. 2µl of each plasmid was digested using *Pst*I and *Sma*I restriction enzymes for 2 hours at 37ºC, prior to analysis. M: 2-log ladder.

4.5 Characterization of full-length VP2 and fragment H surface display viruses

Following the generation of surface display viruses for fragment H and full-length VP2, a small-scale time-course experiment was carried out to test the synthesis of recombinant chimeric proteins. In order to do this, Sf9 cells seeded in 6-well plates ($1x10^6$ cells/well) were infected with the viruses from Table 4.1, using 5 moi. Culture media and the cell lysates were harvested at 24, 48 and 72 hpi, respectively. Culture media were spun at 13000 rpm for 30 minutes in a table-top centrifuge to pellet the budded virus particles. Budded virus fractions and the cell lysates of all time points were run on SDS-PAGE and analysed by western blotting using histidine- and VP2-specific antibodies (sections 2.5.2 and 2.5.2b). The results of this analysis showed no detectable expression of chimeric proteins using either of the antibodies (data not shown).

Larger scale infections were therefore performed to purify budded virus particles for the analysis of chimeric protein synthesis. Shake cultures of Sf9 cells (200 ml at $1.6x10^6$cells/ml) were set up and infected with 0.1 moi of surface display viruses from Table 4.1. $AcVP2^{HIS/N}$ from section 3.4 was used as a negative control for surface display in this experiment. Following five days incubation at 28ºC, culture media was clarified and further processed to purify budded virus particles on a 10-50% (w/v) sucrose gradient (section 2.2.5). Purified budded virus particles were run on SDS-PAGE and analysed by western blotting using VP2 and histidine antibodies. Purified VP2 was included in the gel as positive control for the antibody. Fragment H-GP64 chimeric protein was detected as a

double-band at around 75 kDa using VP2-specific but not the histidine-specific antibody (Figure 4.3). In the samples where H-GP64 chimeric protein was detected, a larger band was observed, whose size suggested it to be a dimer form of the chimeric protein, despite the reducing conditions of SDS-PAGE. However, no bands were detected for the full-length VP2-GP64 chimeric protein. No bands were detected from the control virus, $AcVP2^{HIS/N}$ after purification, as expected; suggesting that the proteins detected are associated with the budded virus particles and are not contamination from the cells.

In addition, the *polh* promoter gave the highest expression levels, followed by the *gp64* promoter with very little expression detected when the *p6.9* promoter was used (Figure 4.3). It was also observed from these results that histidine tagging the proteins lowered the expression levels, indicated by the intensity of the bands in the western blot (Figure 4.3).

It was shown in chapter 3 that the production of full-length VP2 and the subdomains were favoured in TnHi5 cells compared to Sf9 cells. In order to test whether this was valid for the surface display constructs, infections were set up in TnHi5 cells to analyse the production of fragment H-GP64 and VP2-GP64 chimeric proteins. Budded virus particles were pelleted from the infected TnHi5 cultures and then purified using 10-50% sucrose cushion. Both pelleted and sucrose cushion-purified virus particles were analysed by SDS-PAGE and western blotting using VP2 antibody. Fragment H-GP64 chimeric protein was very weakly detected from the *polh* promoter constructs in the pelleted samples; however, no bands were detected from the sucrose cushion-purified samples. No bands were detected for VP2-GP64 chimeric protein, neither from the pelleted nor purified virus particles (data not shown).

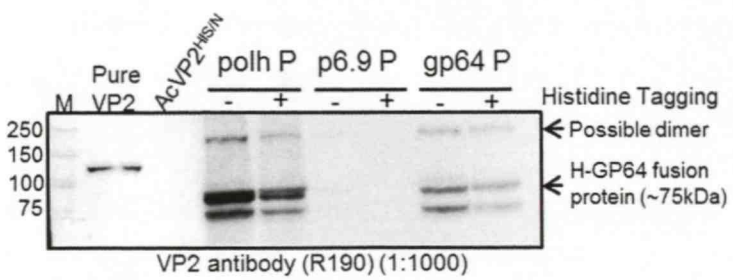


Figure 4.3 Characterization of fragment H surface display viruses.

Shake cultures of Sf9 cells (200ml at $2x10^6$ cells/ml) were infected with the surface display viruses using 0.1 moi. 5 dpi, culture supernatant was harvested and the budded virus particles were pelleted by high-speed centrifugation. Pelleted particles were purified using 10-50% sucrose cushion. Purified viruses were analysed by SDS-PAGE (10%) and western blotting using VP2 antibody (1:1000 dilution). M: Precision Plus Protein WesternC standard. Pure VP2: purified VP2 from chapter 3 as positive control on the blot. $AcVP2^{HIS/N}$: negative control virus for surface display. - + indicates the histidine tagging of the protein.

4.6 Truncating the GP64 in pBACsurf-1

It was shown that full-length VP2-GP64 chimeric protein could not be produced and the synthesis of fragment H-GP64 chimeric protein could only be detected from Sf9 cells after purifying the virus particles. Previous studies have shown that using only the membrane anchorage domain of GP64 at the carboxy terminal was sufficient and could be even more efficient for displaying foreign proteins on the baculovirus envelope surface (Grabherr *et al.*, 1997, Lin *et al.*, 2008). Therefore, it was decided to truncate the GP64 protein in this project to test whether this will allow the synthesis of full-length VP2-GP64 and also improve the yield of fragment H-GP64 chimeric protein.

The cloning strategy for truncating the GP64 is illustrated in Figure 4.4A. Initially, 172bp nucleotide sequence encoding the carboxy-terminal domain of GP64 and part of ORF1629 gene was PCR-amplified from pBACsurf-1 vector using gene-specific primers (Figure 4.4B). pBACsurf-1 vector was digested with *Xma*I and *SnaB*I enzymes, which removed the full-length mature GP64 and part of ORF1629. The PCR product was ligated into the pBACsurf-1 vector restoring the ORF1629 gene. Following ligation and transformation of *E.coli* (sections 2.4.4, 2.3.2 and 2.3.3), plasmids from several colonies were screened using the corresponding enzymes to confirm success of the cloning. All the plasmids, apart from one, resulted in two fragments indicating the truncated GP64, part of ORF1629 (172bp) and the remaining pBACsurf-1 vector (7874bp) (Figure 4.4C). Overall, this truncation reduced the GP64 from 1479 bp (56.6kDa) to 97 bp (3.8 kDa). Therefore, truncated GP64 started at phenylalanine 463 as illustrated in the schematic image of Figure 4.4D and the transfer vector was designated pBACsurf-1$^{GP64/F463}$. The efficiency of truncation was analysed by expressing GFP-GP64 chimeric protein as described below.

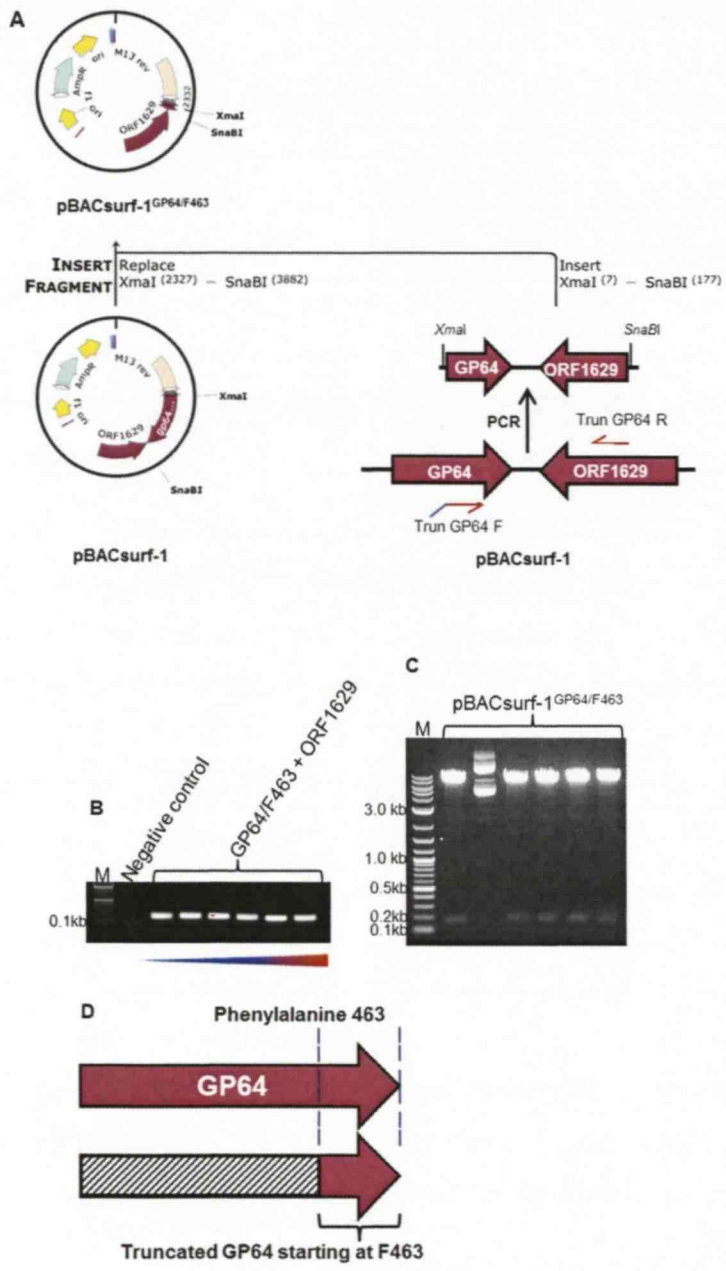


Figure 4.4 Truncating GP64 in pBACsurf-1

A: Schematic representation of the cloning strategy generated by SnapGene® software. The carboxy-terminal domain of GP64 and part of ORF1629 gene was PCR-amplified from pBACsurf-1 vector using the primers Trun GP64 F and Trun GP64 R. The PCR product was ligated into the pBACsurf-1 vector using the restriction enzymes *Xma*I and *SnaB*I to generate the plasmid pBACsurf-1$^{GP64/F463}$.

B: Analysis of PCR-amplified truncated GP64 and part of ORF1629 in a 1% agarose gel. During the PCR, a gradient of 6 different temperatures was used to amplify the product from the pBACsurf-1 transfer vector and all samples were analysed in the gel with the order of lowest to highest temperature from left to right, respectively. M: 2-log ladder, Negative control: dH_2O as template in the PCR

C: Restriction digest analysis of pBACsurf-1$^{GP64/F463}$ plasmids isolated from 6 different colony picks in a 1% agarose gel. 2µl of each plasmid purified was digested using *Xma*I and *SnaB*I restriction enzymes for 2 hours at 37°C, prior to running on the agarose gel. M: 2-log ladder.

D: Schematic representation of GP64 truncation. GP64 was truncated from 1479 bp (56.6kDa) to 97 bp (3.8 kDa). Truncated GP64 started at phenylalanine 463.

4.7 Cloning of enhanced green fluorescent protein into pBACsurf-1 and pBACsurf-1$^{GP64/F463}$

In order to analyse and compare the effect of truncating the GP64 on baculovirus surface display, the EGFP coding region was cloned into pBACsurf-1 and pBACsurf-1$^{GP64/F463}$. The cloning strategy is shown in Figure 4.5A. Initially nucleotide sequences encoding EGFP were PCR-amplified from the template vector pEGFP-N1 using gene specific primers (Figure 4.5B). Amplified product was ligated into pBACsurf-1 and pBACsurf-1$^{GP64/F463}$ using *Pst*I and *Xma*I restriction enzymes (section 2.4.4). Following transformation of *E.coli* (section 2.3.2), plasmids from several colonies were screened with the corresponding restriction enzymes. Restriction digest analysis confirmed the successful cloning of EGFP in both plasmids indicated by the two fragments at the expected sizes of 717bp (EGFP) and 9423bp (pBACsurf-1) or 8040bp (pBACsurf-1$^{GP64/F463}$) as shown in Figure 4.5C.

4.8 Generation of AcSurf_EGFP and AcSurf_EGFP^{TRUN}

Following the construction of transfer vectors pBACsurf-1_EGFP and pBACsurf-1_EGFP$^{GP64/F463}$ in section 4.7, recombinant baculoviruses were generated using the *flash*BACULTRA system (section 2.2.3) to display EGFP on the baculovirus envelope surface. Recombinant baculovirus where EGFP is fused to the native GP64 was named AcSurf_EGFP and the virus producing EGFP as a fusion to the truncated GP64 was named as AcSurf_EGFP^{TRUN}. After virus seed stocks were generated, 50ml P1 virus stocks were amplified in Sf9 insect cells and titrated by QPCR following the protocols from sections 2.2.2 and 2.2.4, respectively. Titres for P1 virus stocks were $1.6x10^8$ pfu/ml and $5x10^7$ pfu/ml for AcSurf_EGFP and AcSurf_EGFP^{TRUN}, respectively.

4.9 Characterization of AcSurf_EGFP and AcSurf_EGFP^{TRUN}

Initial assessment of EGFP production as a fusion to either the native (EGFP-GP64) or truncated GP64 (EGFP-GP64^{TRUN}) for display on virus envelope surface was carried out on pelleted budded virus particles. AcEGFP^{WSSV} was used as a negative control virus for the baculovirus display of EGFP in this analysis[1]. In order to do this, P1 virus stocks of AcSurf_EGFP, AcSurf_EGFP^{TRUN} and AcEGFP^{WSSV} were pelleted to $1x10^8$ pfu on a table-top centrifuge (30 minutes at 13000 rpm) and equally loaded in 10% SDS-PAGE gels. Protein production was analysed by Coomassie staining and western blotting using GFP- and GP64-specific antibodies.

[1]AcEGFP^{WSSV} was generated for analysis of EGFP in mammalian cells under the control of the white spot syndrome virus immediate early 1 promoter, but this aspect of the project was not continued.

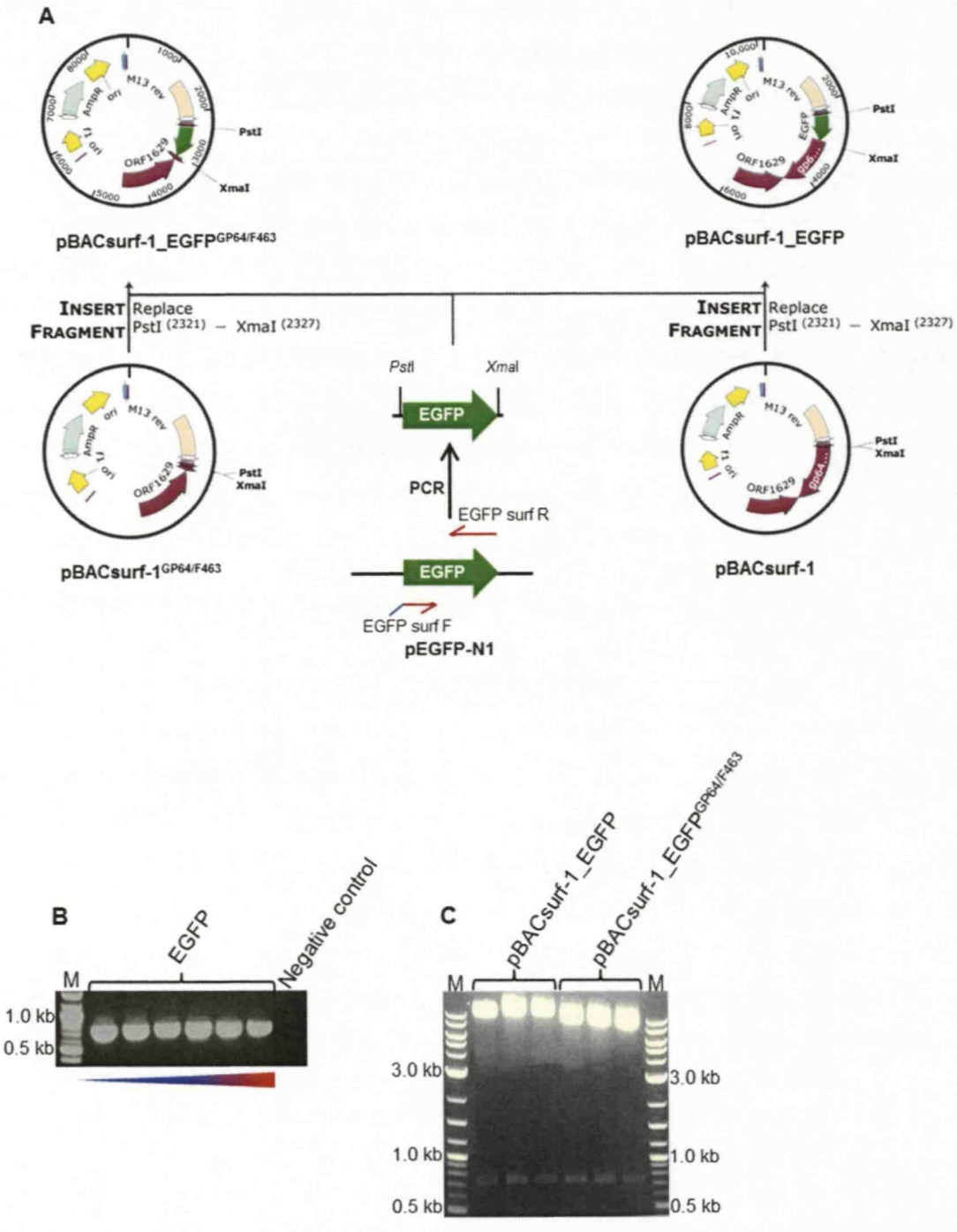


Figure 4.5 Cloning of EGFP into pBACsurf-1 and pBACsurf-1$^{GP64/F463}$

A: Schematic representation of the cloning strategy generated by SnapGene® software. EGFP was PCR-amplified from the pEGFP-N1 vector, using the primers: EGFP surf F and EGFP surf R. PCR product was ligated into pBACsurf-1 (right) and pBACsurf-1$^{GP64/F463}$ (left) using *PstI* and *XmaI* restriction enzymes to generate the transfer vectors pBACsurf-1_EGFP and pBACsurf-1_EGFP$^{GP64/F463}$, respectively.

B: Analysis of PCR-amplified EGFP from pEGFP-N1 vector in a 1% agarose gel. Amplification was carried out using a 6-temperature gradient at the annealing stage and all the samples from lowest to highest temperature were loaded on the gel from left to right, respectively. M: 2-log ladder, Negative control: dH_2O as template in the PCR.

C: Restriction digest analysis of pBACsurf-1_GFP and pBACsurf-1_GFP$^{GP64/F463}$ plasmids isolated from the colony picks (3 colonies/construct) in a 1% agarose gel. 2µl of each vector was digested using *PstI* and *XmaI* restriction enzymes for 2 hours at 37°C, prior to analysis. M: 2-log ladder.

EGFP chimeric proteins with either the native (~84kDa) or truncated GP64 (~30kDa) were clearly detected using GFP-specific antibody from their corresponding pelleted virus samples (Figure 4.6A top panel). In the case of AcEGFP^{WSSV}, non-chimeric EGFP at a lower size was detected as a faint band. Native GP64 protein was detected by both GP64-specific antibody (AcV5-tag) on the western blot and the Coomassie staining in all samples, confirming the presence of budded virus particles in the pelleted samples (Figure 4.6A middle and bottom panels, respectively).

In addition, a larger band was detected using the GP64-specific antibody in Figure 4.6 middle panel, only in the AcSurf-EGFP sample, which corresponds to the chimeric GP64 protein (~84kDa). Coomassie staining showed that the samples were equally loaded as anticipated but also suggested that more native GP64 protein was produced from the AcSurf_EGFP^{TRUN} virus, observed from the intensities of the bands (Figure 4.6A bottom panel).

In order to confirm that the chimeric proteins detected from the pelleted budded virus samples were not due to contamination from the cells, shake culture infections were set up to purify the budded virus particles. In addition, two different moi were also compared. Shake cultures of Sf9 cells (50ml at 2x10^{6}cells/ml) were infected with 5 pfu/cell or 0.1 pfu/cell using AcEGFP^{WSSV}, AcSurf_EGFP or AcSurf_EGFP^{TRUN}. Cultures of 5 pfu/cell infections were harvested at 3dpi and 0.1 pfu/cell cultures were harvested at 5dpi. Budded virus particles were purified using 10%-50% (w/v) sucrose gradient following the protocol from section 2.2.5. Purified virus particles were titrated using QPCR (Section 2.2.4) and then equally loaded on SDS-PAGE gel (10%) to a final amount of 2.8x10^7 pfu/well. Protein production was analysed by Coomassie staining and western blotting using GFP- and GP64-specific antibodies.

EGFP-GP64 and EGFP-GP64^{TRUN} chimeric proteins were clearly detected at their expected sizes from both moi samples using GFP-specific antibody (Figure 4.6B top panel). Coomassie staining confirmed the equal loading of the samples (Figure 4.6B bottom panel) and GP64-specific antibody confirmed the samples to be budded virus particles (Figure 4.6B middle panel). It was shown that using different moi and harvesting time especially for AcSurf_EGFP samples did not affect the level of chimeric protein production as the band intensities on the western blot were very similar. However, it was observed that when the culture was infected with AcSurf_EGFP^{TRUN} using 5 moi and harvested 3 dpi, the expression levels were slightly higher and also resulted in double bands (Figure 4.6B top panel).

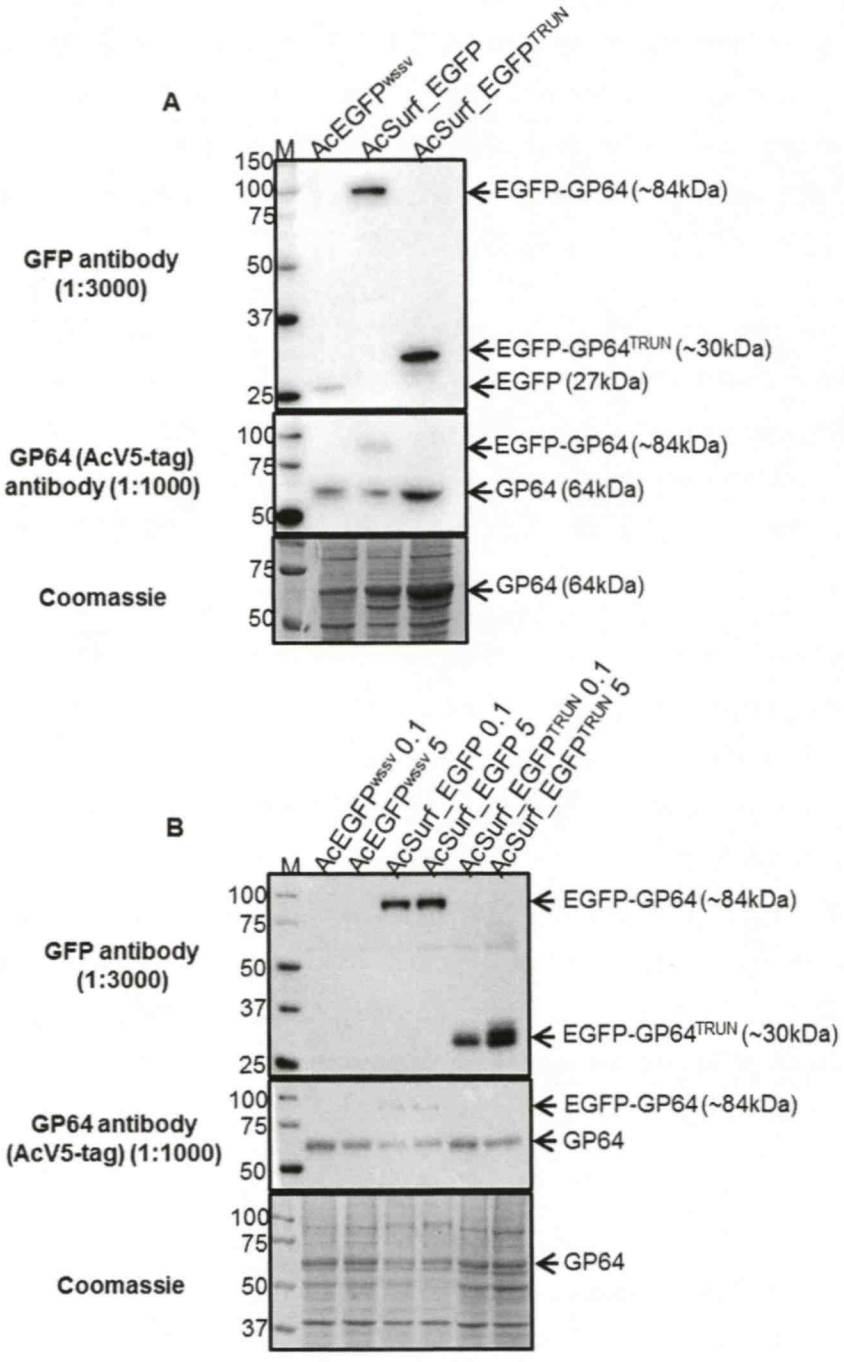


Figure 4.6 Characterization of AcSurf_EGFP and AcSurf_EGFP^{TRUN} by western blotting and Coomassie staining

Analysis of EGFP-GP64 and EGFP-GP64^{TRUN} production in pelleted (A) and purified (B) budded virus particles using EGFP-specific (top), AcV5-tag GP64-specific (middle) antibodies and Coomassie staining (bottom). M: Precision plus protein WesternC standard. AcEGFP^{wssv} was used as a negative control for surface display.

A: P1 virus stocks of AcSurf_EGFP, AcSurf_EGFP^{TRUN} and AcEGFP^{wssv} were pelleted and run on 10% SDS-PAGE gel ($1x10^8$ pfu/well).

B: Sf9 cell cultures (50ml at $2x10^6$ cells/ml) were infected with 0.1 or 5 moi of AcSurf_EGFP, AcSurf_EGFP^{TRUN} and AcEGFP^{wssv}. 0.1 moi cultures were harvested 5 dpi and 5 moi cultures were harvested 3 dpi. Budded virus particles were purified using 10%-50% (w/v) sucrose gradient, titrated by QPCR and run on SDS-PAGE ($2.8x10^7$ pfu/well).

The fluorescent characteristics of EGFP also enabled the examination of chimeric protein production using microscopy imaging. In order to do this, Sf9 ($1x10^6$ cells/dish) and TnHi5 ($0.5x10^6$ cells/dish) cells were infected with AcSurf_EGFP or AcSurf_EGFP^{TRUN} using 5 moi. Mock-infected cells for each cell line were used as a negative control in this analysis. At 72 hpi, cells were imaged using a Zeiss fluorescent microscope (Axiovert 135). The majority of Sf9 cells were fluorescent when infected with either AcSurf_EGFP or AcSurf_EGFP^{TRUN}. However, only a small population of TnHi5 cells were fluorescent when infected with AcSurf_EGFP, whereas the majority of cells infected with AcSurf_EGFP^{TRUN} showed fluorescence (Figure 4.7).

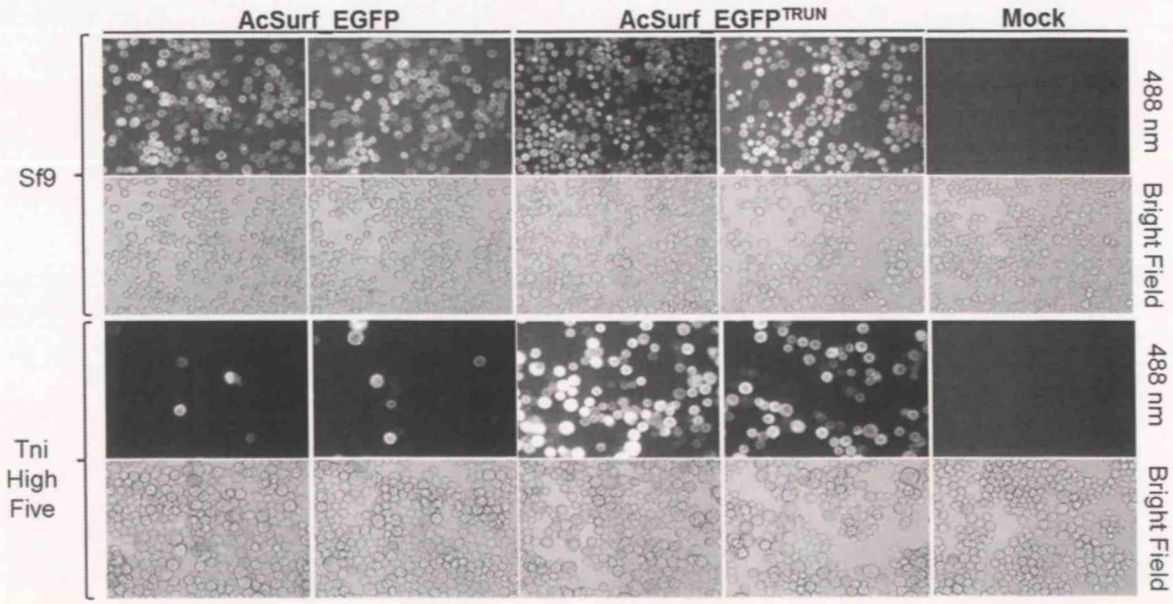


Figure 4.7 Characterization of AcSurf_EGFP and AcSurf_EGFP^{TRUN} by fluorescence microscopy

Analysis of EGFP-GP64 and EGFP-GP64^{TRUN} production in Sf9 (top) and TnHi5 (bottom) cells using fluorescence microscopy. Sf9 ($1x10^6$ cells/well) and TnHi5 ($0.5x10^6$ cells/well) cells were infected using 5 moi of AcSurf_EGFP and AcSurf_EGFP^{TRUN}. At 72 hpi, the cells were visualized and imaged at 100x magnification using a Zeiss Axiovert 135 fluorescent microscope (488 wavelength). Mock: non-infected cells as negative control.

In order to investigate the reason why only a small population of TnHi5 cells were fluorescent after infection with AcSurf_EGFP, a repeat infection was set up in both Sf9 and TnHi5 cells using 5 moi. However, this time the cells were visualized and imaged over a time course using confocal microscopy at 24, 46 and 68 hpi. Analysis over a time-course would enable understanding of whether the spread of infection is delayed or defective; which results in only a small population of fluorescent cells at the time of imaging.

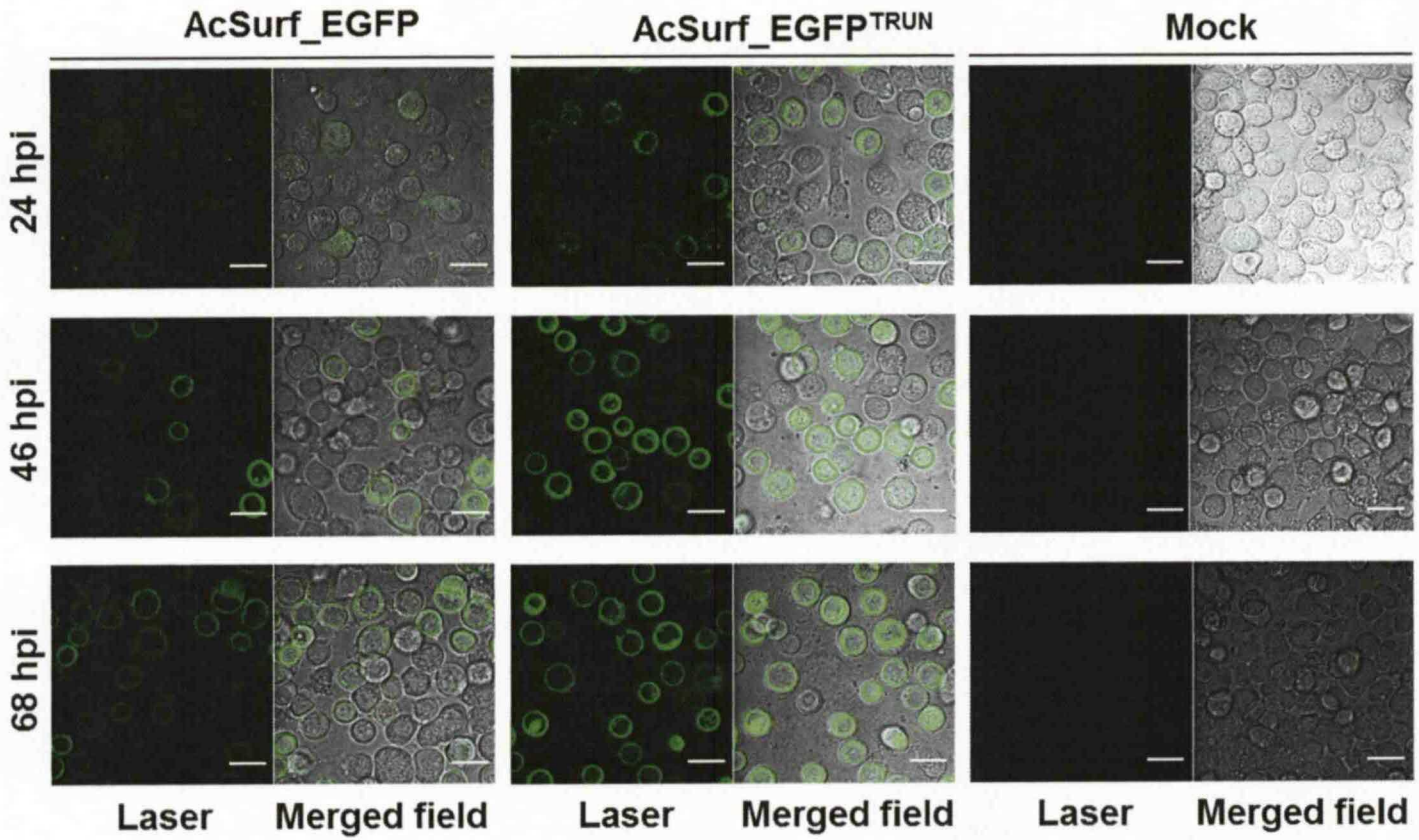


Figure 4.8A Characterization of AcSurf_EGFP and AcSurf_EGFP^{TRUN} in Sf9 cells by Confocal microscopy

Analysis of EGFP-GP64 and EGFP-GP64^{TRUN} production in Sf9 cells using a confocal microscope over a time course. Sf9 cells ($1x10^6$ cells/well) were infected using 5 moi of AcSurf_EGFP and AcSurf_EGFP^{TRUN}. At 24, 46 and 68 hpi, live cells were visualized and imaged using a confocal microscope (488 wavelength). Mock: non-infected cells as negative control. The images shown are representative of the majority of the cells. Scale bars represent 20 µm.

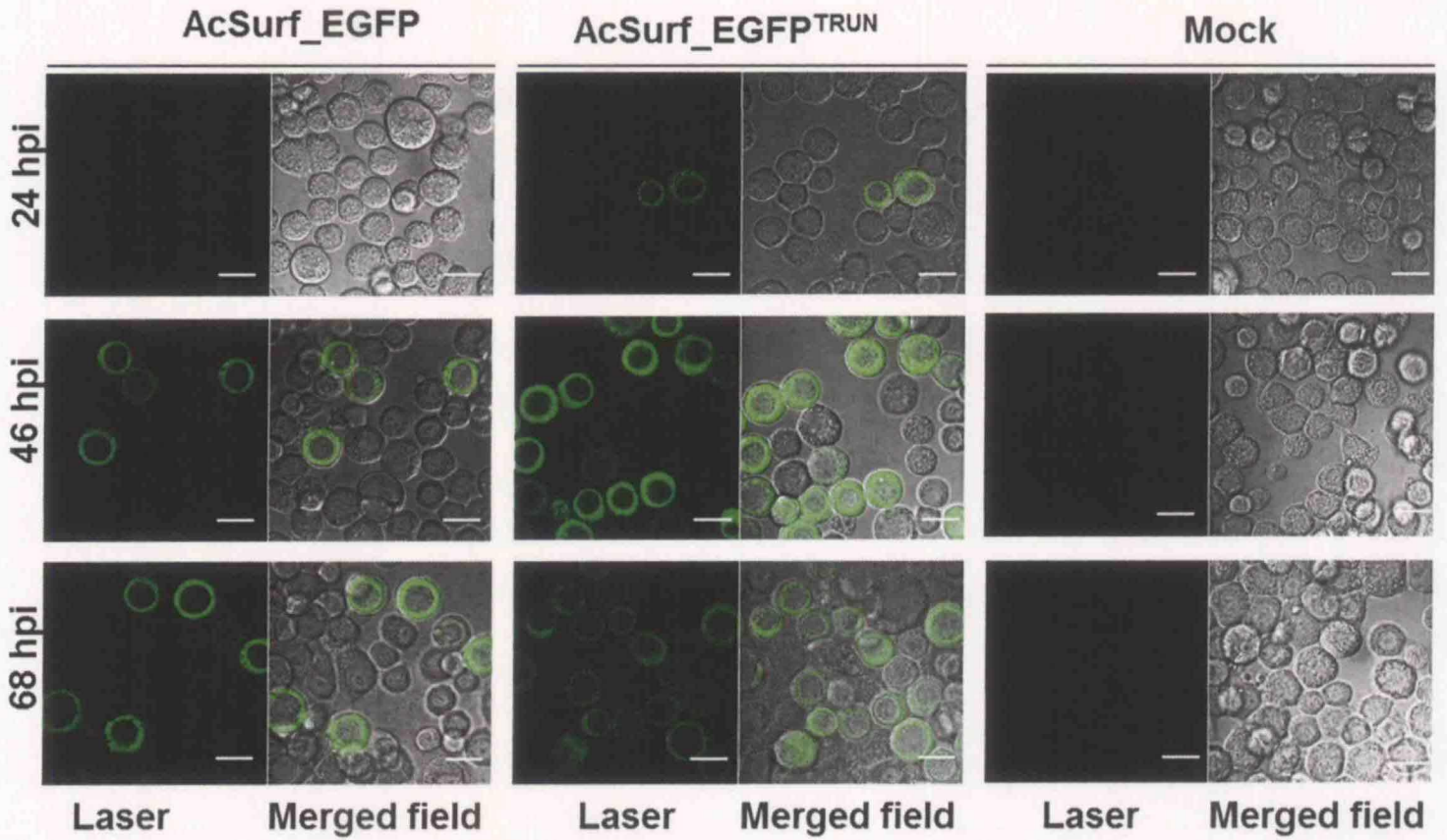


Figure 4.8B Characterization of AcSurf_EGFP and AcSurf_EGFPTRUN in TnHi5 cells by Confocal microscopy

Analysis of EGFP-GP64 and EGFP-GP64^{TRUN} production in TniHi5 cells using confocal microscope over a time course. TnHi5 cells ($0.5x10^6$ cells/well) were infected using 5 moi of AcSurf_EGFP and AcSurf_EGFP^{TRUN}. At 24, 46 and 68 hpi, live cells were visualized and imaged using a confocal microscope (488 wavelength). Mock: non-infected cells as negative control. The images shown are representative of the majority of the cells. Scale bars represent 20 µm.

A gradual increase was observed in the number of fluorescent Sf9 cells from 24 to 68 hpi when infected with AcSurf_EGFP^{TRUN}, as would be expected with the spread of viral infection over the time-course (Figure 4.8A). In the case of AcSurf_EGFP-infected Sf9 cells, the distinct fluorescent cells were detected at 46 hpi and the population of fluorescent cells had increased by 68 hpi (Figure 4.8A).

A very similar profile was observed with AcSurf_EGFP^{TRUN}-infected TnHi5 cells, where the population of fluorescent cells increased from 24 to 68 hpi (Figure 4.8B). However, compared to Sf9 cells, fewer fluorescent cells were detected especially at 24 hpi. In the case of AcSurf_EGFP-infected TnHi5 cells, the fluorescence was first detected at 46 hpi, however, the population of fluorescent cells did not increase by 68 hpi; unlike Sf9 cells (Figure 4.8B). These results supported the findings from Figure 4.7 and suggested that there is a defect in the spread of virus, mainly in TnHi5 cells, when a recombinant protein is displayed on the budded virus envelope as a fusion to the full-length GP64.

Once AcSurf_EGFP and AcSurf_EGFP^{TRUN} were characterized and the chimeric protein production was confirmed by western blotting and microscopy analysis, a quantitative analysis was carried out using a fluorescent plate reader. This would allow a comparison between two viruses based on the amount of chimeric protein production. In order to do this, a 96-well plate was seeded with Sf9 ($0.2x10^6$ cells/well) and TnHi5 ($0.1x10^6$ cells/well) cells. Each cell line was infected with twelve replicates of AcSurf_EGFP, AcSurf_EGFP^{TRUN} or AcVP2$^{HIS/N}$ using 5 moi. AcVP2$^{HIS/N}$-infected and mock-infected cells were used as negative controls in this analysis. At 72 hpi, the EGFP fluorescence was read at an excitation wavelength of 485 nm using a fluorescent plate reader (Infinite® 200 PRO).

The sample data were normalized against mock-infected cells within each cell line. The fluorescence from AcSurf_EGFP-infected Sf9 cells was 2216 relative fluorescence unit (rfu), which was lower than the fluorescence detected from AcSurf_EGFP^{TRUN}-infected Sf9 cells at 5487 rfu (Figure 4.9A) . In the case of TnHi5 cells, fluorescence detected from AcSurf_EGFP- and AcSurf_EGFP^{TRUN}-infected cells was 6049 rfu and 8470 rfu, respectively (Figure 4.9B). An unpaired t-test was used to compare the fluorescence values from the EGFP-producing viruses using GraphPad software. It was shown that the P value from Sf9 cells was less than 0.0001 and it was equal to 0.0008 from TnHi5 cells, suggesting that the difference between two viruses was extremely statistically significant within each cell line. In addition, more chimeric protein was produced from both viruses in TnHi5 cells compared to Sf9 and this difference was found to be extremely statistically significant using an unpaired t-test (P value < 0.0001 for both viruses). Overall, these results suggested that truncating the GP64 improved the chimeric GFP production in both Sf9 and TnHi5 cells.

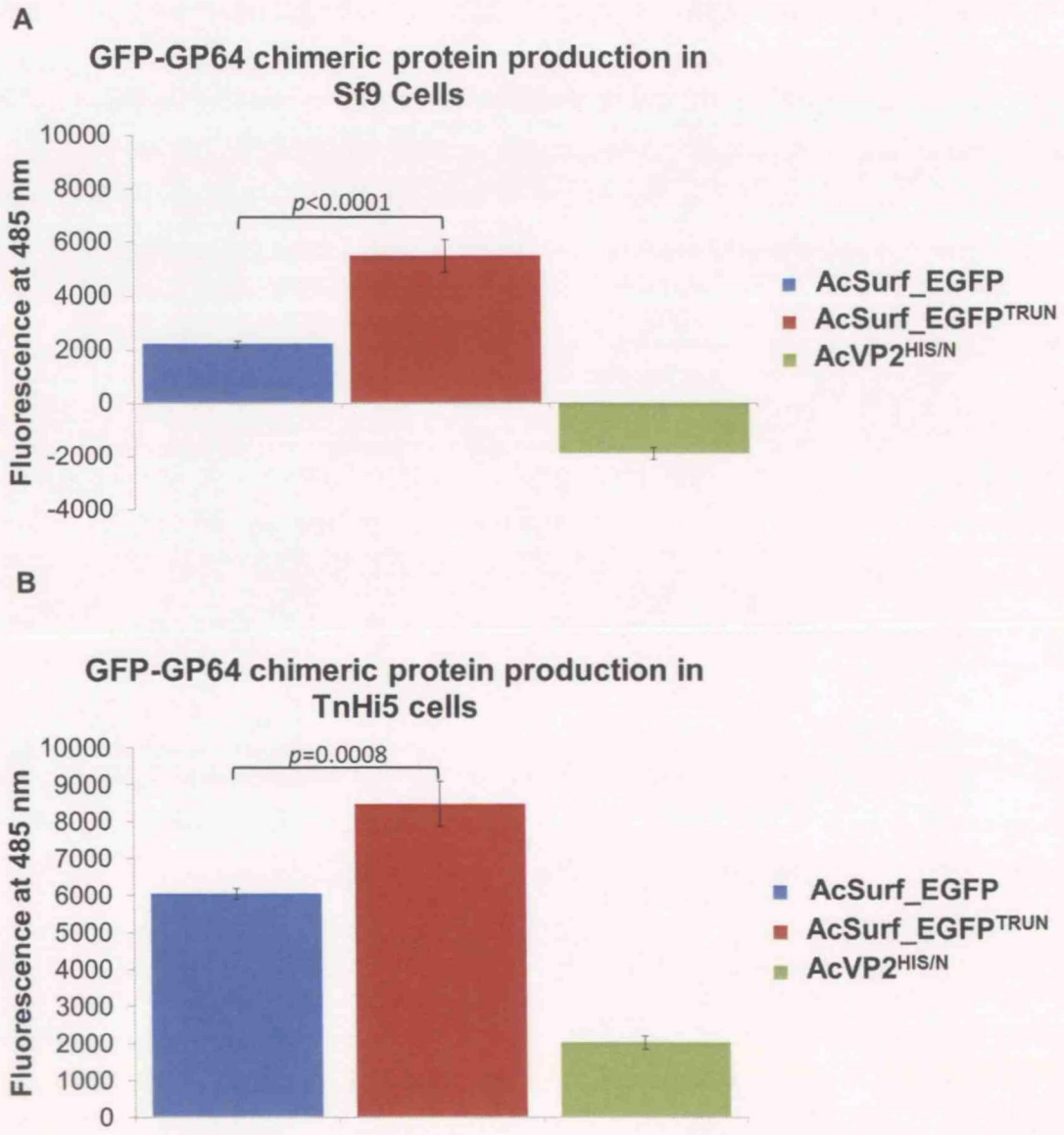


Figure 4.9 Quantitative analysis of EGFP chimeric protein production in Sf9 and TnHi5 cells

Sf9 ($0.2x10^6$ cells/well) and TnHi5 ($0.1x10^6$ cells/well) cells seeded in a 96- well plate (48 wells/cell line) were infected with AcSurf_EGFP, AcSurf_EGFP^{TRUN} or AcVP2$^{HIS/N}$ using 5 moi. EGFP fluorescence was read at an excitation wavelength of 485 nm using a fluorescent plate reader (Infinite® 200 PRO) at 72 hpi. AcVP2$^{HIS/N}$ was used as a negative control. Each sample had 12 replicates on the assay plate. Graphs were generated using the mean fluorescence data of virus samples after removing the mean fluorescence data obtained with the non-infected mock cells. Error bars indicate the standard error of each sample. An unpaired t-test was carried out using GraphPad software to compare chimeric GFP production from AcSurf_EGFP, AcSurf_EGFP^{TRUN} in both cell lines. Sf9 AcSurf_EGFP/AcSurf_EGFP^{TRUN} t-test $p<0.0001$, TnHi5 Acsurf_EGFP/AcSurf_EGFP^{TRUN} t-test $p=0.0008$. Unpaired t-test was also carried out to compare the two cell lines for the production of chimeric proteins from each virus, $p<0.0001$. Raw data can be found in Appendix 3.

4.10 Construction of pBACsurf-1_VP2$^{GP64/F463}$ and pBACsurf-1_VP2-H$^{GP64/F463}$

It was shown in this project that truncating the GP64 improved chimeric protein production and enhanced infectivity/spread compared to the viruses with chimeric proteins using the full-length GP64. Therefore, it was decided to test whether this would allow the surface display of full-length AHSV4-VP2 and improve the fragment H subdomain chimeric protein production.

Previously amplified PCR products for non-tagged VP2 (3.1 kbp) and fragment H (500bp) from Figure 4.2C and D (top), respectively, were ligated into pBACsurf-1$^{GP64/F463}$ using *Pst*I and *Xma*I restriction enzymes. Following ligation and transformation of *E.coli* (Sections 2.4.4, 2.3.2 and 2.3.3), restriction digest analysis was carried out on plasmids from several colonies using the latter restriction enzymes. *Pst*I and *Xma*I digestion resulted in two fragments corresponding the fragment H (500bp) and the remaining pBACsurf-1$^{GP64/F463}$ (8040bp), confirming the successful construction of pBACsurf-1_VP2-H$^{GP64/F463}$ in Figure 4.10A. On the other hand, four out of five plasmids digested contained the full-length VP2 (3.1kbp), confirming the successful generation of pBACsurf-1_VP2$^{GP64/F463}$ transfer vector (Figure 4.10B). Double bands resulted due to the presence of undigested pBACsurf-1_VP2$^{GP64/F463}$ plasmid in the sample (Figure 4.10B).

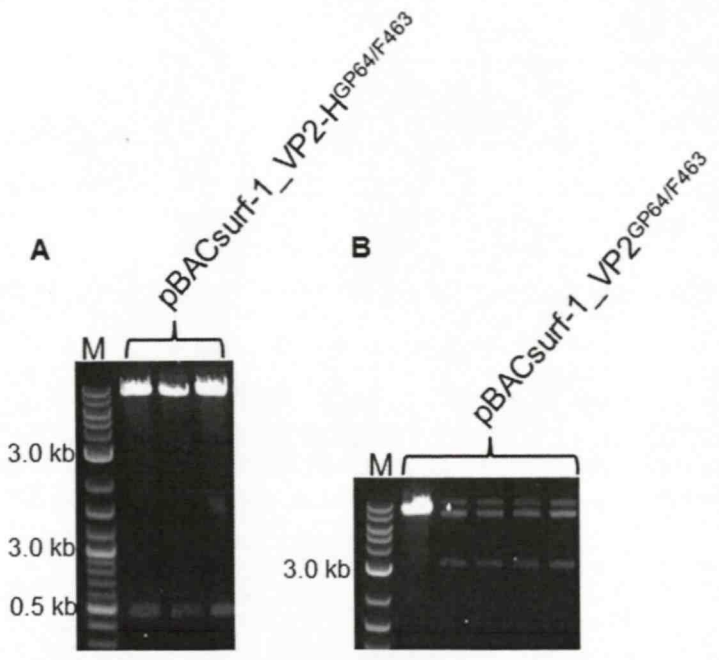


Figure 4.10 Restriction digest analysis of pBACsurf-1_VP2$^{GP64/F463}$ and pBACsurf-1_VP2-H$^{GP64/F463}$

2µl of pBACsurf-1_VP2-H$^{GP64/F463}$ (A) and pBACsurf-1_VP2$^{GP64/F463}$ (B) plasmids purified from several colony picks were digested using *Pst*I and *Xma*I restriction enzymes for 2 hours at 37°C. Digested plasmids were then run in a 1% agarose gel. M: 2-log ladder.

4.11 Generation of AcSurf_VP2^{TRUN} and AcSurf_VP2-H^{TRUN}

Following the construction of transfer vectors in section 4.10, recombinant baculoviruses were generated using the *flash*BACULTRA system (section 2.2.3) to display full-length VP2 and fragment H on the baculovirus envelope surface as a fusion to truncated GP64. After virus seed stocks were generated, 50ml P1 virus stocks were amplified in Sf9 insect cells and titrated by QPCR following the protocols from sections 2.2.2 and 2.2.4, respectively. Titres for P1 virus stocks were $1.8x10^8$ pfu/ml and $1.6x10^8$ pfu/ml for Acsurf_VP2^{TRUN} and Acsurf_VP2-H^{TRUN}, respectively.

4.12 Characterization of AcSurf_VP2^{TRUN} and AcSurf_VP2-H^{TRUN} by SDS-PAGE

Initial analysis of VP2 (VP2-GP64^{TRUN}) and fragment H (Fragment H-GP64^{TRUN}) chimeric protein production was carried out on pelleted budded virus particles. P1 stocks for each virus were pelleted to a final amount of $2.4x10^8$ pfu on a table-top centrifuge at 13000 rpm for 30 minutes. Pelleted virus particles were separated on SDS-PAGE and analysed by Coomassie staining and western blotting using VP2- and GP64- specific antibodies. Fragment H-GP64^{TRUN} chimeric protein was detected by VP2-specific antibody at the predicted size of 22.4 kDa (data not shown). However, no bands were detected for VP2-GP64^{TRUN}, suggesting that full-length VP2 could not be produced even after truncating the GP64 (data not shown).

In order to do a direct comparison between fragment H-GP64 and fragment H-GP64^{TRUN} production that are associated with baculoviruses, $1.1x10^9$ pfu of budded virus particles from the P1 virus stocks of AcSurf_VP2-H and AcSurf_VP2-H^{TRUN} were pelleted based on QPCR titres. Pelleted virus particles were equally loaded in SDS-PAGE gels (10%) and analysed by Coomassie staining and western blotting using VP2- and GP64-specific antibodies. AcEGFP^{WSSV} was used as a negative control for surface display in this analysis. Detection of native GP64 by Coomassie staining and western blotting using the GP64-specific antibody confirmed the pelleted samples to be the budded virus particles (Figure 4.11, middle and bottom panels). On the other hand, VP2-specific antibody detected the fragment H-GP64 and fragment H-GP64^{TRUN} chimeric proteins at their expected sizes of 75 kDa and 22.4 kDa, respectively. When the band intensities from this western blot were compared, it was concluded that more chimeric protein was produced from the Acsurf_VP2-H^{TRUN} (Figure 4.11, top panel).

The same larger band from Figure 4.3, which was suggested to be a dimer of fragment H-GP64 chimeric protein, was also observed in Figure 4.11 top panel for the pelleted

AcSurf_VP2-H sample. Furthermore, a similar profile was observed with the AcSurf_VP2-H^{TRUN}, where a larger band was observed that could be the dimer form of fragment H-$GP64^{TRUN}$ chimeric protein, based on its size (Figure 4.11, top panel).

4.12.1 Difference of plaque profile between AcSurf_VP2-H and AcSurf_VP2-H^{TRUN}

It was shown by previous analysis in this project that the spread of surface display virus infection across a cell monolayer was different depending on the length of the GP64. In order to investigate this further, a plaque assay was set-up using AcSurf_VP2-H and AcSurf_VP2-H^{TRUN} following the protocol from section 2.2.4a. $AcVP2^{HIS/N}$ and AcVP2-$H^{HIS/N}$ were also included in the plaque assay as non-surface display virus controls. Plaques generated by Acsurf_VP2-H were observed to be smaller than the plaques formed by AcSurf_VP2-H^{TRUN}. The plaques formed by the latter were similar to the non-surface display recombinant viruses (Figure 4.12A). Following this observation, plaque dimensions were measured using ImageJ software to obtain a semi-quantitative data. For each sample, 32 plaques from two wells (16 plaques/well) were measured and the average plaque sizes were used for the analysis (Figure 4.12B). An unpaired t-test has shown that the difference of plaque size between AcSurf_VP2-H (1.98mm) and AcSurf_VP2-H^{TRUN} (1.15mm) was statistically significant ($P<0.0001$).

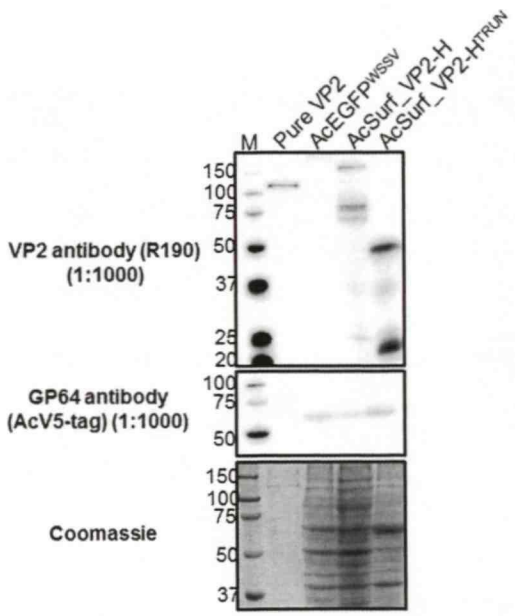
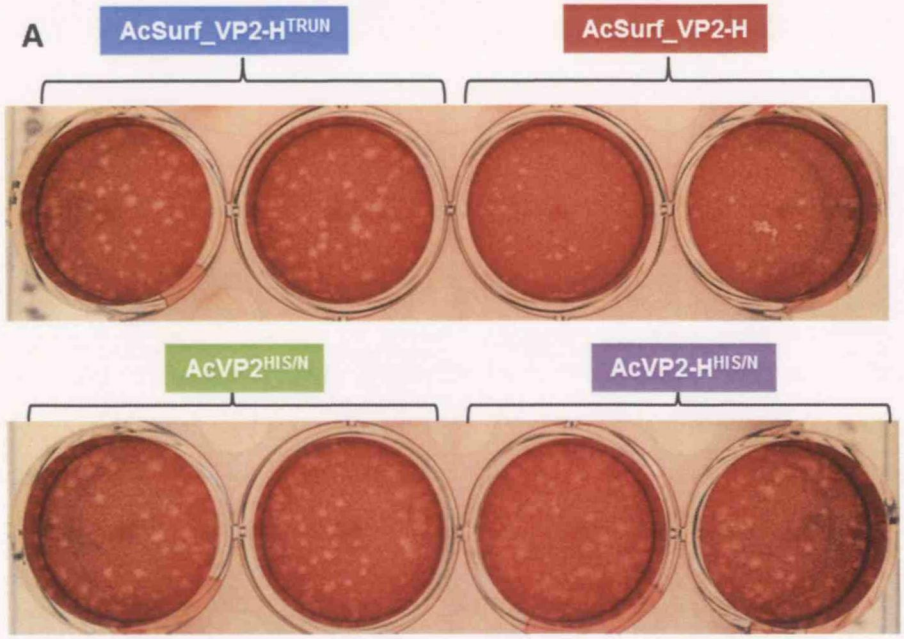


Figure 4.11 Characterization of Acsurf_VP2-H and Acsurf_VP2-H^{TRUN} by SDS-PAGE

P1 virus stocks of Acsurf_VP2-H and Acsurf_VP2-H^{TRUN} were pelleted to $1.1x10^9$ pfu on a table-top centrifuge at 13000 rpm for 30 minutes. Pelleted virus particles were separated on 10% SDS-PAGE and analysed by western blotting using VP2- (top) and GP64-specific (middle) antibodies and Coomassie staining (bottom). Pure VP2: purified VP2 from chapter 3 as positive control on the blot. $AcEGFP^{WSSV}$: negative control virus for surface display. M: Precision plus protein WesternC standard.



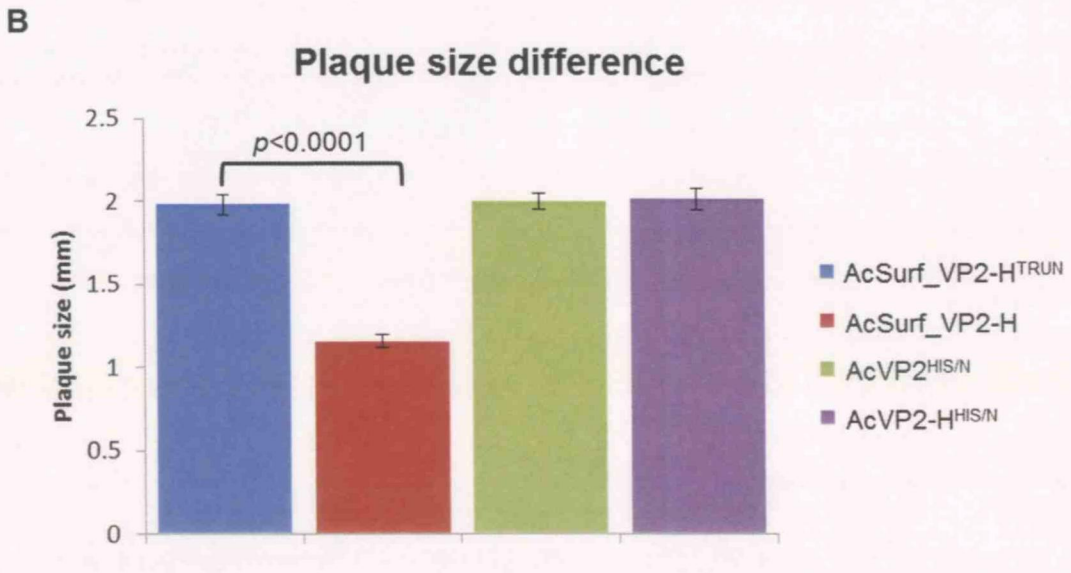


Figure 4.12 Plaque formation analyses of AcSurf_VP2-H and AcSurf_VP2-H^{TRUN}

AcSurf_VP2-H and AcSurf_VP2-H^{TRUN} were analysed by plaque assay in Sf21 cells. AcVP2$^{HIS/N}$ and AcVP2-H$^{HIS/N}$ were used as controls as non-surface display viruses.

A: Photographed image of the plaque assay results.

B: Plaque sizes of each virus were counted using ImageJ software. In total 32 plaques for each sample from 2 wells were counted (16 plaques/well). Graph was created using the mean values of the plaque sizes. Error bars represent the standard error of each sample. An un-paired t-test was carried out using GraphPad software to compare the plaque sizes of AcSurf_VP2-H and AcSurf_VP2-H^{TRUN}, t-test $p<0.0001$. Raw data can be found in Appendix 4.

4.13 Discussion

Baculovirus expression vectors have been widely used for the high-yield production of correctly-folded, complex proteins such as human beta interferon (Smith *et al.*, 1983b), influenza virus hemagglutinin and neuraminidase (Margine *et al.*, 2013) and plasmodium falciparum EBA-140 ligand (Rydzak *et al.*, 2015). Baculovirus-infected insect cells provide post-translational modifications for proteins to fold correctly, which made baculovirus expression vectors more advantageous in other platforms as well, such as surface display systems to study protein-protein interactions. The vector for displaying recombinant proteins on the baculovirus envelope surface was developed first by Boublik *et al.* (1995). The way recombinant proteins were displayed on the baculovirus envelope surface was found to be very similar to the phage display system. In both platforms, the recombinant proteins are displayed on the surface as a fusion to the viral attachment proteins (Smith, 1985, Boublik *et al.*, 1995).

It was identified by Boublik *et al.* (1995) that the gene of interest should be inserted into the baculovirus genome inbetween the GP64 signal peptide and the TMD to be displayed on the envelope surface by forming a chimeric protein with GP64. However, it was shown that Vesicular Stomatitis Virus G Gylcoprotein could be displayed on baculovirus envelope surface using its own transmembrane domain for membrane anchorage (Barsoum *et al.*, 1997). In the following years, it was discovered that baculovirus surface display of recombinant proteins could also be achieved by using other membrane glycoproteins for anchorage such as VSV-G (Chapple and Jones, 2002), influenza hemagglutinin (HA) (Ernst *et al.*, 1998) and neuraminidase (NA) (Borg *et al.*, 2004).

Proteins to be displayed on the baculovirus envelope surface in this project are from the outer capsid of a non-enveloped virus (Burrage *et al.*, 1993). Therefore unlike the VSV-G protein from the study by Barsoum *et al* (1997), they were required to be displayed on the surface by using the membrane anchorage of another glycoprotein. Use of the baculovirus GP64 signal peptide and transmembrane domain for membrane anchorage and surface display was the most established method used by several studies (Boublik *et al.*, 1995, Tami *et al.*, 2004, Xu *et al.*, 2011). Therefore, the latter was decided to be the method in this project to display the proteins of interest using the commercial baculovirus transfer vector, pBACsurf-1. However, initially several analyses were carried out to achieve the optimum conditions for the display of recombinant proteins using this vector.

pBACsurf-1 vector harbours the recombinant gene expression under the control of the very late *polh* promoter. As the budded virus particles starts to bud from the cells between early and late phases of the infection cycle, promoters that are active at these phases

(*gp64* and *p6.9*) were also tested (Friesen, 1997, Lu and Miller, 1997). These promoters were compared by testing the expression levels of the AHSV4 full-length VP2 and the fragment H subdomain. Moreover, the addition of 6xhis tag to the amino terminus of proteins was tested for any effects on baculovirus surface display.

It was very difficult to clone the full-length VP2 gene into the pBACsurf-1 transfer vectors containing three different promoters and only pBACsurf-1_*p6.9*_VP2^{HIS} and pBACsurf-1_*gp64*_VP2 were successfully generated (Figure 4.2 F). Several protocol variations were tested to enable the generation of the remaining full-length VP2 transfer vectors, but all proved unsuccessful. The reason behind this was not investigated any further but it could be suggested that the full-length VP2 DNA structure was toxic to the *E.coli* cells, inhibiting the efficient amplification of recombinant DNA. On the other hand, both 6xhis-tagged and non-tagged versions of fragment H were successfully cloned in between the GP64 signal peptide and the TMD in pBACsurf-1 transfer vectors under the control of three promoters. Following the transfer vector construction, eight recombinant baculoviruses were generated.

When the chimeric protein production was characterized from the surface display viruses in Table 4.1, it was found out that fragment H-GP64 could only be detected after the virus particles were amplified in Sf9 cells, and purified using 10-50% sucrose gradient (Figure 4.3). However, VP2-GP64 chimeric protein was not detected even after virus purification (data not shown).

Full-length VP2 is a large protein itself (124 kDa) and when it is fused to the GP64 for display on the surface, the protein size increases to around 180 kDa. However, the failure of VP2-GP64 incorporation into the baculovirus envelope surface could not be due to the large size of the protein. This is because a larger, complex protein such as HIV-1 gp120 was successfully displayed on baculovirus envelope surface previously (Boublik *et al.*, 1995). However, it should be noted that HIV-1 gp120 is an envelope glycoprotein whose nature is to be displayed on viral envelope surface whereas AHSV VP2 is a capsid protein of a non-enveloped virus. In addition, another study has shown that a capsid protein, foot and mouth disease virus (FMDV) VP1, was also failed to be displayed on baculovirus envelope surface (Peralta *et al.*, 2013). Peralta *et* al. (2013) has investigated this further and tried to display FMDV VP1 protein on baculovirus envelope surface by fusion to the VSV G transmembrane domain, but this also proved unsuccessful. In contrast, VP1 capsid protein of human enterovirus 71 was shown to be successfully displayed on baculovirus envelope surface as a fusion to GP64 in another study (Meng *et al.*, 2011).

Different types of proteins from diverse organisms such as mouse functional antibody Fab fragments (Takada *et al.*, 2015), rodent malaria *Plasmodium berghei* circumsporozoite

protein (PbCSP) (Yoshida *et al.*, 2003), different viral capsid (Lin *et al.*, 2008, Meng *et al.*, 2011) and envelope glycoproteins (Boublik *et al.*, 1995, Peralta *et al.*, 2007) were successfully displayed on baculovirus envelope surface. Therefore, it could be suggested that the failure to be displayed on baculovirus envelope surface is most probably due to individual protein characteristics. The surface display problem could be related to chimeric protein production, localization in the cell or incorporation into the baculovirus envelope during the budding process. VP2-GP64 chimeric protein in this project could not be detected within the crude Sf9 cell lysates throughout a time course of 24, 48 and 72 hpi, suggesting that the problem was probably due to the initial production of the chimeric protein. However, this was not investigated any further as the fragment H subdomain of VP2 was associated with purified budded virus particles (Figure 4.3). On the other hand, Peralta *et al.* (2013) has shown that GP64-VP1 chimeric protein was produced in infected cells as detected by western blotting, but failed to reach to the plasma membrane as shown by their confocal microscopy analysis.

Regarding fragment H-GP64 production, double bands were observed around the expected size region, which could be due to post-translational modifications or failure of signal peptide cleavage. Further analysis was carried out in chapter five to test whether the double bands were due to post-translational modifications. In addition, a larger band was also observed in samples specific to fragment H-GP64, whose size suggested that it could be a dimer form of the chimeric protein. SDS-PAGE was carried out under denaturing conditions and it was not expected to see any oligomers. However, a SDS-stable dimer of a RNA-binding protein was identified in a previous study after running on SDS-PAGE (Lico *et al.*, 2015). Therefore, it is possible that fragment H-GP64 could also form SDS-stable dimers.

When the fragment H-GP64 expression levels were compared based on the band intensities on the western blot from Figure 4.3, it was shown that *polh* promoter gave the highest expression, which was followed by the *gp64* promoter and very little expression was observed from the *p6.9* promoter. It was interesting that *gp64* promoter, which drives the expression of the native GP64 envelope glycoprotein resulted in lower yield of the fragment H-GP64 chimeric protein compared to the very late *polh* promoter. However, based on the analysis, it was decided to take the *polh* promoter forward for future constructs. Grabherr *et al.* (1997) investigated a similar case where they compared the levels of chimeric protein production from *polh* and *gp64* promoters. They showed that the protein yields in infected cells were considerably lower from *gp64* promoter compared to the *polh* promoter but were similar on the viral surface when they checked the purified budded virus particles (Grabherr *et al.*, 1997).

Although 6xhis-tagged versions of the chimeric proteins were generated and the presence of 6xhis tag was confirmed by gene sequencing at the cloning stage, the chimeric proteins from purified budded virus particles could not be detected using the histidine antibody. A similar problem was encountered and discussed in chapter three of this thesis and in another study, where it was suggested that this could be due to the specificity of his-tag antibody or the location and the length of his-tag on the protein of interest (Debeljak *et al.*, 2006). There is a difference in this case that the histidine tag was added to a chimeric protein, which was targeted to be displayed on baculovirus envelope surface instead of an individual protein to be produced in the cells. However, this should not prevent his-tag from detection as it was shown by a previous study that his-tagged chimeric proteins was detected by western blotting in infected cells and on the envelope surface of purified baculoviruses using both histidine- and target protein-specific antibodies (Xu *et al.*, 2011). Considering the possibility that fragment H-GP64 forms SDS-stable dimers as discussed above, it is likely that the histidine-tag stayed buried within the protein structure despite denaturing conditions of SDS-PAGE, which prevented antibody binding. In addition, the band intensities on the western blot (Figure 4.3) from 6xhis-tagged constructs were lower than the non his-tagged, therefore it was decided to not add a 6xhis-tag to the future surface display constructs.

It was shown in chapter three of this thesis that the production of full-length VP2 and the subdomains thereof were favoured in TnHi5 cells. Therefore, it was investigated to see whether VP2-GP64 chimeric protein could be produced and the fragment H-GP64 production could be improved in TnHi5 cells. However, this proved unsuccessful as no VP2-GP64 chimeric protein could be detected from either pelleted or purified virus particles (data not shown). In the case of fragment H-GP64 chimeric protein, very faint band was observed under the control of *polh* promoter from pelleted samples but no bands were detected from the purified virus particles (data not shown). It is known that about 100-fold less virus particles are produced from TnHi5 compared to Sf9 cells (Wilde *et al.*, 2014). It could be suggested that the absence of fragment H-GP64 chimeric protein on the western blot from purified viruses was due to small amount of virus particles present in the samples.

Previous studies have shown that truncating the majority of the GP64 and fusing the proteins to only the membrane anchorage at the carboxy terminus could be more efficient for the display of proteins on baculovirus envelope surface (Grabherr *et al.*, 1997, Lin *et al.*, 2008). A similar approach was investigated in this thesis to try and improve baculovirus surface display of the full-length VP2 and its subdomains. Initial analysis and comparison was carried out by generating constructs to display a reporter protein, EGFP, on the baculovirus envelope surface. Western blot analysis of pelleted and sucrose-

gradient-purified virus particles has shown that both EGFP-GP64 and EGFP-GP64^{TRUN} chimeric proteins were successfully produced (Figure 4.6).

Chimeric protein production was analysed from both Sf9 and TnHi5 cells using fluorescent microscopy. It was shown that majority of AcSurf_EGFP- and AcSurf_EGFP^{TRUN}-infected Sf9 cells were fluorescent at 72 hpi. However, this wasn't the case in TnHi5 cells, where only a very small population of cells that were infected with AcSurf_EGFP was fluorescent (Figure 4.7). In order to investigate this further, the experiment was repeated and this time the cells were visualized and imaged throughout a time-course of 24, 46 and 68 hpi using a con-focal microscope. Both in Sf9 and TnHi5 cells, there was a gradual increase in the number of fluorescent cells from 24 to 68 hpi when the cells were infected with AcSurf_EGFP^{TRUN}, as would be expected with the spread of virus over the time-course (Figure 4.8 A&B). On the other hand, a delay was observed with the AcSurf_EGFP infection in both Sf9 and TnHi5 cells, where the fluorescent cells were first detected at 46 hpi. While the infection in Sf9 cells spread increasing the number of fluorescent cells by 68 hpi, the population of fluorescent TnHi5 cells remained very little at 68 hpi, suggesting a defect in virus spread (Figure 4.8 A&B).

The delay in virus spread using AcSurf_EGFP was observed in both cell lines, however it became more prevalent over time in TnHi5 cells, which could be related to the amount of virus particles produced in each cell line. It was shown that 100-fold more virus particles are produced in Sf9 cells (Wilde *et al.*, 2014), which could contribute in overcoming the defect of virus infectivity. It would be interesting to investigate later time-points during infection of AcSurf_EGFP in TnHi5 cells to find out whether the virus would eventually spread across the monolayer. If the infection wouldn't spread to the monolayer even at later stages during the infection, it could then be suggested that there is a defect in virus formation, binding or entry. However, truncating the GP64 was found to overcome this problem; therefore, for the interest of this project no further investigations were carried out to pinpoint this defect.

Following microscopy analysis, chimeric protein production was further investigated using a fluorescent plate reader to obtain quantitative data. It was shown that the AcSurf_EGFP^{TRUN}-infected Sf9 and TnHi5 cells produced more chimeric protein than the AcSurf_EGFP-infected cells. In addition, chimeric protein yield was a lot higher in TnHi5 cells compared to Sf9 (Figure 4.9).

The ratio between the amount of virus particles and the chimeric protein production is found to be opposite in Sf9 and TnHi5 cells. The fact that there were more chimeric proteins produced in TnHi5 cells increases the chances of incorporation onto baculovirus envelope surface. So if the amount of chimeric protein incorporation was causing the

defect in the virus, this could explain why it became more prevalent in TnHi5 cells. On the other hand less chimeric proteins and more budded virus particles were produced in Sf9 cells, which could make it easier to counter the defect and spread the virus infection across the monolayer. However, further investigations are required to confirm this, such as electron microscopy imaging of purified virus particles.

It is known that the native GP64 envelope protein of baculovirus budded viruses can oligomerize into trimers (Volkman and Goldsmith, 1984). It could be suggested that oligomerization of GP64 could also play a role in the defective phenotype of the virus infection with full-length chimeric GP64. It was shown by Boublik *et al.* that the full-length chimeric GP64 formed heterotrimers with the native GP64. Therefore, it could be suggested that there is a competition in forming trimers between the native and the chimeric GP64, which might decrease the virus infectivity. On the other hand, truncated GP64 lacks majority of the mature protein, which is likely incapable of forming heterotrimers, hence there is no competition. This enables the native GP64 to form the native functional homotrimers and might explain how the virus infectivity was recovered when the truncated GP64 constructs were used. However, further analysis is required to draw any conclusions.

Once it was identified that truncating the GP64 improved EGFP chimeric protein production and incorporation to budded virus particles, it was decided to test whether this would also be valid for the full-length VP2 and fragment H. Western blot analysis of pelleted virus particles has confirmed that fragment H-GP64^{TRUN} chimeric protein production was improved (Figure 4.11). In addition, a larger band, which was about double the size of the predicted, was detected. The fact that both constructs resulted in two bands strengthens the suggestions that fragment H-GP64 chimeric protein forms SDS-stable dimers. On the other hand, VP2-GP64^{TRUN} could not be produced.

Furthermore, AcSurf_VP2-H and AcSurf_VP2-H^{TRUN} were analysed by plaque assay to investigate whether there was a defect in virus spread and plaque formation. It was shown that statistically smaller plaques were formed by AcSurf_VP2-H whereas the plaques formed by AcSurf_VP2-H^{TRUN} were similar to ones formed by non-surface display recombinant viruses; AcVP2$^{HIS/N}$ and AcVP2-H$^{HIS/N}$ (Figure 4.12). All the results obtained for the comparison of two different surface display constructs were in parallel and the effects had been observed in three different cell lines. Although further investigations are required for a better understanding, it could be suggested that the surface display constructs using the full-length GP64 has a defect affecting their infectivity.

4.14 Conclusion

Overall from this chapter, it has been shown that the fragment H subdomain but not the full-length VP2 could form chimeric proteins with GP64 to be incorporated into the budded virus particles. Among the three gene promoters tested, *polh* has driven the highest expression levels and histidine tagging the genes was shown to be not beneficial. Furthermore, it was shown that truncating the GP64 improved chimeric protein production and recovered virus infectivity. Therefore, these optimum conditions were taken forward to display all VP2 subdomains on BV surface in chapter five of this thesis.

Chapter 5 Displaying VP2 Subdomains on BV surface

5.1 Introduction

As VP2, the major outercapsid protein of AHSV, is associated in generating virus neutralizing antibodies (VNAbs) (Burrage *et al.*, 1993), it is important to investigate its antigenic structure hence more efficient and safe vaccines can be developed. Previous research has identified that the amino-terminal half of the protein is more antigenic than the carboxy-terminal part (Martinez-Torrecuadrada and Casal, 1995). In addition, Manole *et* al. (2012) suggested that the central domain of VP2, which assembles into trimers, (see Figure 3.2A) forms an independent structural subdomain that contains most of the linear immunogenic peptides of VP2 defined so far.

Based on this information, ten VP2 subdomains were chosen to be expressed by recombinant baculoviruses, as described in chapter three of this thesis (Figure 3.2B). When the full-length VP2 and subdomains were produced in insect cells individually, it was found that only the full-length VP2 was produced in sufficient quantities to be successfully purified by poly-histidine tag affinity purification. Therefore, another approach, the display of recombinant proteins on the baculovirus BV envelope surface, was explored. Chapter four of this thesis demonstrated that the use of a very late *polh* promoter to drive expression of a chimeric protein comprising VP2 subdomain and transmembrane domain (TMD) of truncated GP64 were the optimum conditions for effective baculovirus surface display.

The aim of this chapter was, therefore, to generate ten VP2 subdomain surface display constructs, using the optimal conditions. The hypothesis was that increasing the stability of the subdomains by fusing them to the GP64 TMD should help them to fold correctly and improve their yield. In addition, being a part of the viral envelope surface might display the antigenic epitopes of the protein correctly compared to production of individual proteins. The surface display viruses will also help investigate the biological function of specific VP2 subdomains, including antigenic structure, by using the recombinant viruses in various biological assays. VP2 subdomain surface display constructs could also serve to investigate their immunogenic properties by means of vaccination experiments.

5.2 Constructing surface display transfer vectors for VP2 subdomains

The overall cloning strategy for inserting VP2 subdomains into pBACsurf-1$^{GP64/F463}$ is illustrated in Figure 5.1A; using the example of fragment A. Nucleotide sequences encoding each individual VP2 subdomain were PCR-amplified from the template vector pSC11-AHSV-4-VP2 using gene specific primers (Figure 5.1B-E). Start and stop codons were removed to enable fusion to GP64 and 5' *Pst*I and 3' *Xma*I restriction sites were added during the amplification. Fragments A, B, C, D, E and F shared the same forward

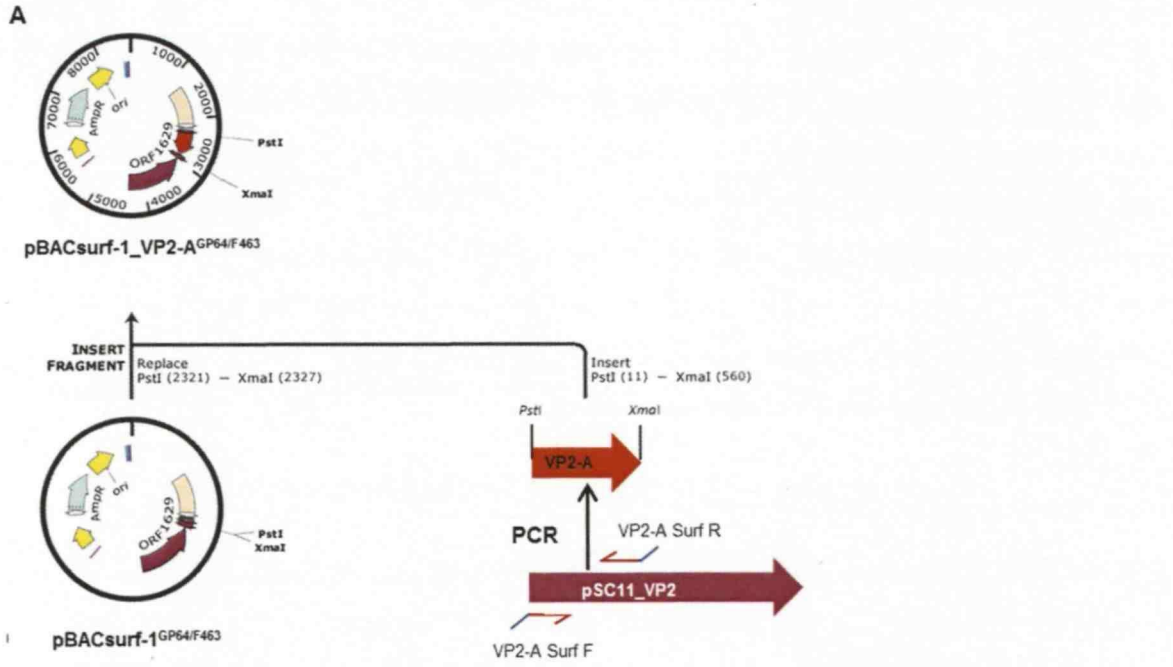
primer, with individual reverse primers, as all started from the same 5' nucleotide sequence (Table 2.5). Once the PCR products were amplified, they were ligated into the pBACsurf-1$^{GP64/F463}$ vector using the *Pst*I-*Xma*I restriction sites (section 2.4.4). Following ligation and transformation of *E.coli* (section 2.3.2), plasmids were purified from several colonies and screened using *Pst*I-*Xma*I restriction enzymes. Restriction digest analysis resulted in two fragments for each VP2 subdomain of the expected sizes confirming their successful cloning into the pBACsurf-1$^{GP64/F463}$ (Figure 5.1F&G). Recombinant plasmids were also analysed by Sanger sequencing using appropriate primers (Table 2.5), which also confirmed the presence of inserts in the right orientation.

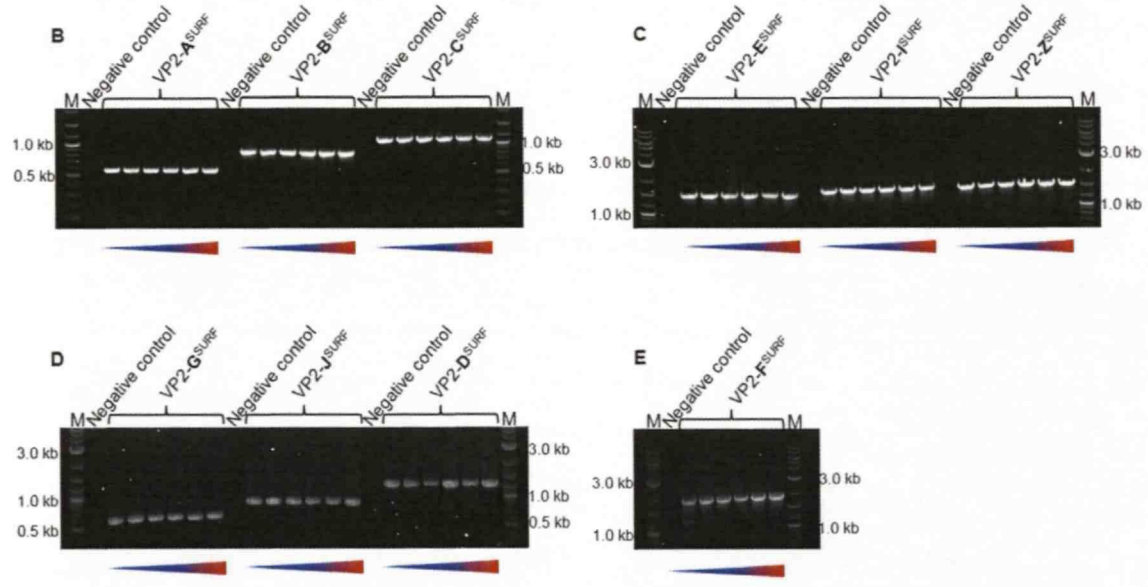
5.3 Generating VP2 subdomain surface display viruses

Following the construction of the surface display transfer vectors containing individual VP2 subdomains (section 5.2), ten recombinant surface display baculoviruses were generated using the *flash*BACULTRA system (section 2.2.3). After the generation of recombinant virus seed stocks, 50ml P1 virus stocks were amplified in Sf9 insect cells and titrated by QPCR (sections 2.2.2 and 2.2.4, respectively). A summary of these viruses is shown in Table 5.1.

Table 5.1: Summary of VP2 subdomain surface display viruses

Target	Virus Name	P1 virus stock titre (pfu/ml)	Predicted chimeric protein size (kDa)
Fragment A	Acsurf_VP2-A^{TRUN}	$1.4x10^8$	25.5
Fragment B	Acsurf_VP2-B^{TRUN}	$2.1x10^8$	36.4
Fragment C	Acsurf_VP2-C^{TRUN}	$1.2x10^8$	45.7
Fragment D	Acsurf_VP2-D^{TRUN}	$1x10^8$	51.9
Fragment E	Acsurf_VP2-E^{TRUN}	$7.4x10^7$	58.8
Fragment F	Acsurf_VP2-F^{TRUN}	$1x10^8$	78.1
Fragment G	Acsurf_VP2-G^{TRUN}	$9.1x10^7$	27
Fragment H	Acsurf_VP2-H^{TRUN}	$1.6x10^8$	22.4
Fragment I	Acsurf_VP2-I^{TRUN}	$3.3x10^8$	62.7
Fragment J	Acsurf_VP2-J^{TRUN}	$1.6x10^8$	35.5
Fragment Z	Acsurf_VP2-Z^{TRUN}	$1.6x10^8$	61.8


A
pBACsurf-1_VP2-A GP64/F463
INSERT FRAGMENT
Replace
PstI (2321) – XmaI (2327)
Insert
PstI (11) – XmaI (560)
PstI
XmaI
VP2-A
PCR
VP2-A Surf R
pSC11_VP2
VP2-A Surf F
pBACsurf-1 GP64/F463


B
Negative control
VP2-A SURF
Negative control
VP2-B SURF
Negative control
VP2-C SURF
M
1.0 kb
0.5 kb
C
Negative control
VP2-E SURF
Negative control
VP2-I SURF
Negative control
VP2-Z SURF
3.0 kb
1.0 kb
D
Negative control
VP2-G SURF
Negative control
VP2-J SURF
Negative control
VP2-D SURF
E
Negative control
VP2-F SURF

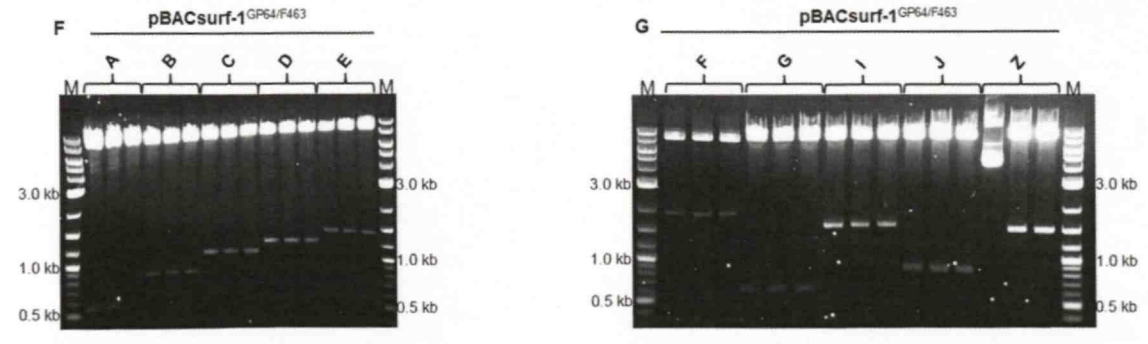

F
pBACsurf-1 GP64/F463
A
B
C
D
E
G
F
G
I
J
Z
3.0 kb
1.0 kb
0.5 kb

Figure 5.1 Constructing surface display transfer vectors for VP2 subdomains

A: Schematic representation of cloning strategy generated by the Snapgene® software, using the example of fragment A. The same approach was used for the cloning of all the remaining VP2 subdomains. In this case, fragment A was PCR-amplified from the template vector pSC11_VP2 using the primers: VP2-A Surf F and VP2-A Surf R. The final PCR product was ligated into pBACsurf-1$^{GP64/F463}$ using *Pst*I and *Xma*I restriction enzymes, which generated pBACsurf-1_VP2-A$^{GP64/F463}$.

B-E: Analysis of VP2 subdomain PCR amplification in 1% agarose gels. Panel B: fragments A, B and C, respectively. Panel C: fragments E, I and Z respectively. Panel D: fragments G, J and D, respectively. Panel E: Fragment F. For the amplification of each subdomain, a gradient of 6 temperatures was used at the annealing stage of the PCR and the products from all the gradient samples were run on these gels with the order of lowest to highest temperature from left to right, respectively.

F&G: Restriction digest analysis of VP2 subdomain surface display transfer vectors in 1% agarose gels. 2µl of plasmids purified from different colonies (3 colonies/construct) were digested with *Pst*I and *Xma*I enzymes for 2 hours at 37°C, prior to analysis.

Coloured arrows beneath the gel images in panels B-E indicate increasing temperature gradient.

5.4 Characterizing VP2 subdomain surface display viruses

Initial analysis of chimeric protein production was carried out on concentrated budded virus particles. Virus stocks (P1) were pelleted to a final amount of $1.1x10^8$ pfu using a bench-top centrifuge at 13000 rpm for 30 minutes. Concentrated virus particles were separated on 10% SDS-PAGE gels and analysed by Coomassie staining and western blotting using GP64- and VP2-specific antibodies. Although the native GP64 protein was clearly detected both by the Coomassie staining and western blotting using GP64-specific antibody, none of the recombinant chimeric proteins for VP2 subdomains were detected using the VP2-specific antibody on a western blot or by Coomassie staining (data not shown).

As the chimeric protein production could not be detected in concentrated budded viruses, the next step was to confirm production within insect cells. In order to do this, Sf9 and TnHi5 cells seeded in 6-well plates were infected with the viruses from Table 5.1 using 5 MOI. At 72hpi, alongside crude cell lysates, budded virus particles were also harvested from the culture medium (section 2.5.1). Proteins from both the crude cell lysates and the BV particles were separated on 10% SDS-PAGE gels and analysed by Coomassie staining and western blotting using GP64- and VP2-specific antibodies (section 2.5.2, 2.5.2a/b). It should be noted that chimeric proteins could only be detected by VP2-specific antibody as the target of the GP64-specific antibody, AcV5-tag, was removed from the constructs when GP64 was truncated (section 4.6).

Acsurf_VP2-A^{TRUN}, Acsurf_VP2-B^{TRUN} and Acsurf_VP2-G^{TRUN} samples were loaded only onto the Coomassie gels as the VP2-specific antibody does not recognize the position of

these subdomains (Section 3.2 and Figure 3.2B). Acsurf_VP2-H^{TRUN} was used as a positive control for the preparation of surface display samples; AcVP2-$H^{HIS/N}$ was used as a negative control for the surface display constructs, but as a positive control for the detection of recombinant proteins from crude cell lysates using the VP2-specific antibody. Acsurf_$EGFP^{TRUN}$, wild-type AcMNPV and mock-infected cells were used as negative controls and purified VP2 was included in the analysis as positive control for the VP2-specific antibody. Native GP64 was detected in all the virus-infected samples, crude cell lysates and pelleted BV from both Sf9 and TnHi5 cells, as expected, using GP64-specific antibody (Figure 5.2A-D). Due to the amount of protein, GP64 bands in the crude cell lysate blots were merged across the lanes.

A crude cell lysate from AcVP2-$H^{HIS/N}$-infected TnHi5 cells were included in the Sf9 blot as a positive control; as fragment H had not been previously detected in Sf9 crude cell lysates (section 3.5). The same was observed in this analysis, where 6xhis-tagged fragment H could only be detected in the TnHi5 crude cell lysate sample (Figure 5.2E). A non-specific band was observed in all the Sf9 crude cell lysate samples when the VP2-specific antibody was used. This was most likely a cell-type specific cellular protein as it was not observed in the purified VP2 sample or in the AcVP2-$H^{HIS/N}$ sample from TnHi5 cells (Figure 5.2E). Apart from fragment Z, all the VP2 subdomain chimeric proteins were detected in Sf9 crude cell lysates, at their expected sizes, using the VP2-specific antibody (Figure 5.2E). However, no distinctive bands could be detected for these chimeric proteins by Coomassie staining, suggesting their yield to be low (data not shown). In addition, chimeric proteins could not be detected in the concentrated BV neither by western blotting or Coomassie staining, which is consistent with the initial results (data not shown).

An improvement was observed in TnHi5 cells, where the chimeric proteins could be clearly detected in both the concentrated BV samples (Figure 5.2F) and the crude cell lysates (Figure 5.2G) using VP2-specific antibody. It should be noted that TnHi5 crude cell lysate samples had to be diluted (1 in 3) in comparison to the Sf9 crude cell lysate samples so that a clear western blot image could be obtained, suggesting the protein yield to be much higher in TnHi5 cells. Fragment H from AcVP2-$H^{HIS/N}$ could not be detected on the blot following this dilution (Figure 5.2G), however, it could be clearly detected from the same sample, analysed on the Sf9 crude cell lysate blot prior to dilution (Figure 5.2E).

In addition, all the chimeric proteins including fragments A, B and G (but not H) were clearly detected in the TnHi5 crude cell lysates analysed by Coomassie staining (Figure 5.2I). Even though no VP2-specific antibodies were available to detect fragments A, B and G, the Coomassie staining confirmed that these chimeric proteins were successfully produced in TnHi5 cells. Furthermore, it could be suggested that apart from fragment H, all the remaining chimeric proteins were produced to high yields as they were strongly

detected by Coomassie staining. However, no distinctive bands were detected from the Coomassie staining of the concentrated BV samples of TnHi5 cells (data not shown). A summary of these results are listed in Table 5.2.

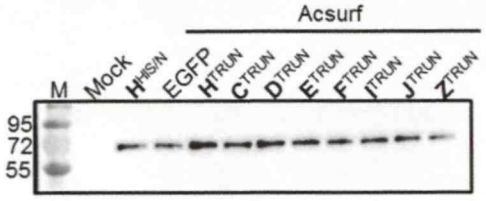
In order to confirm that the chimeric proteins detected in Figure 5.2 were incorporated into the virus particles, larger scale infections were set-up both in TnHi5 and Sf9 cells to amplify and purify the BV particles. Shake cultures (80ml) of Sf9 and TnHi5 cells were infected with 0.1 moi of VP2 subdomain surface display viruses from Table 5.1. Fragments A, B and G were not included in the analysis as they were not recognized by VP2-spcefic antibody to be analysed on a western blot. Acsurf_VP2-H^{TRUN} from chapter four was also included in the analysis. Amplified viruses were purified on a 10-50% (w/v) sucrose gradient (section 2.2.5). Purified BV particles were then separated on 10% SDS-PAGE gels and analysed by western blotting using GP64- and VP2-specific antibodies (sections 2.5.2 and 2.5.2b). Purified VP2 was included in the gels as positive control for the VP2-specific antibody.

Native GP64 was detected in all the virus samples amplified in both Sf9 (Figure 5.3A lower panel) and TnHi5 cells (Figure 5.3B lower panel), confirming the purified materials to be BV particles. All the analysed chimeric proteins were detected in the purified BV particles using VP2-specific antibody, which confirmed incorporation into BV particles. Although the chimeric proteins were detected in BV particles amplified from both cell lines, TnHi5 cell-produced BV resulted in clearer and stronger bands (Figure 5.3). The summary of these results are included in Table 5.2.

In addition, double bands with a very small size difference were also observed especially with fragments H, C, D, E and F, which could suggest post-translational modifications (Figure 5.3B upper panel). In the case of fragment H-GP64^{TRUN}, the possible SDS-stable dimer at around 50kDa (Figure 4.11) was also observed in these blots using the VP2-specific antibody (Figure 5.3). Furthermore, when the VP2-specific antibody was used, sample-specific small bands were observed mainly from fragments C, D and E purified from Sf9 cells, suggesting that some of the proteins may be cleaved (Figure 5.3A upper panel).

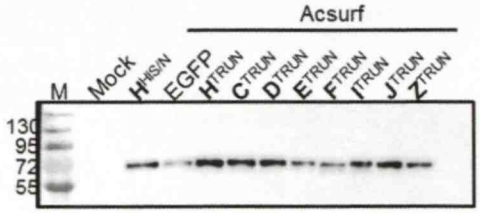
A

Sf9 BV pellet
GP64 antibody (AcV5-tag, 1:1000)



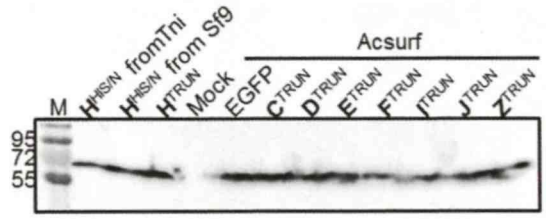
B

TnHi5 BV pellet
GP64 antibody (AcV5-tag, 1:1000)



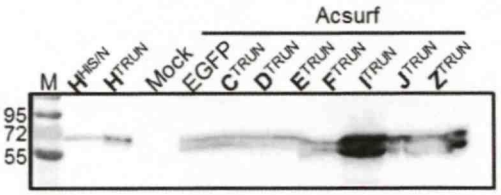
C

Sf9 crude cell lysates
GP64 antibody (AcV5-tag, 1:1000)



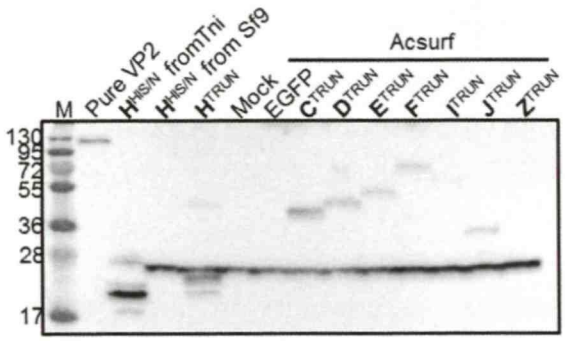
D

TnHi5 crude cell lysates
GP64 antibody (AcV5-tag, 1:1000)



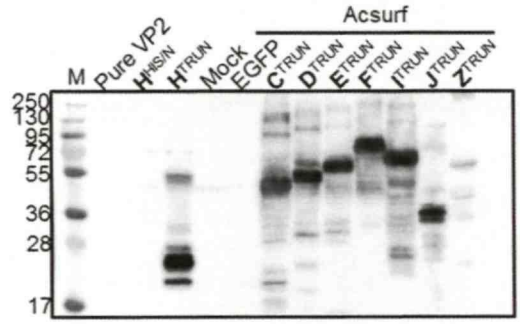
E

Sf9 crude cell lysates
VP2 antibody (R190, 1:1000)



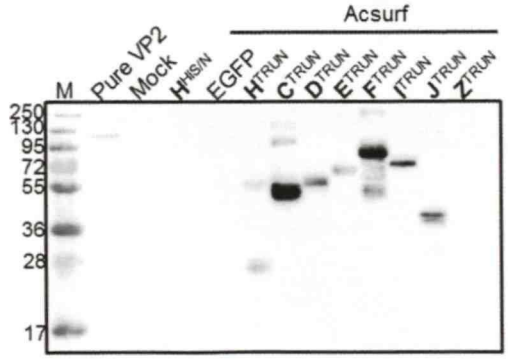
G

TnHi5 crude cell lysates
VP2 antibody (R190, 1:1000)



F

TnHi5 BV pellet
VP2 antibody (1:1000)



I

TnHi5 crude cell lysates
Coomassie

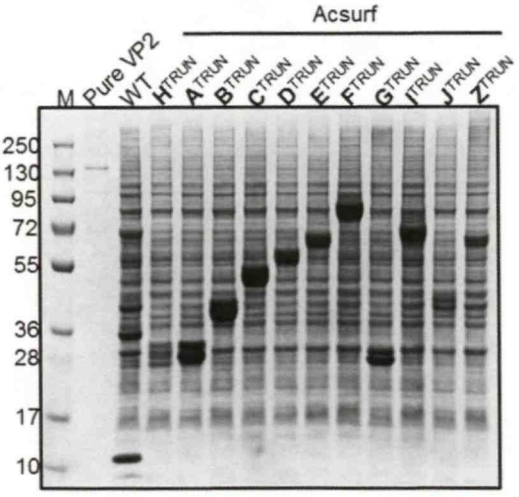


Figure 5.2 Characterizing VP2 subdomain surface display viruses by SDS-PAGE

Sf9 ($1x10^6$ cells/well) and TnHi5 cells ($0.5x10^6$ cells/well) were infected with the VP2 subdomain surface display viruses from Table 5.1, in a 6-well plate format using 5moi. At 72 hpi, the crude cell lysates and budded virus (BV) particles from the culture supernatant were harvested by centrifugation. Proteins were separated on SDS-PAGE gels and analysed by Coomassie staining and western blotting using GP64- and VP2-specific antibodies. M: PageRuler plus prestained protein ladder. Non-infected mock cells, Acsurf_EGFP, AcVP2-$H^{HIS/N}$, Acsurf_VP2-H^{TRUN}, wild-type AcMNPV (WT) and purified VP2 (chapter 3) were used as positive/negative controls during the analysis.

A&B: Concentrated BV particles from Sf9 (**A**) and TnHi5 (**B**) cells were separated on 10 % SDS-PAGE gels and analysed by western blotting using GP64-specific antibody (AcV5-tag, 1:1000).

C&D: Proteins from crude cell lysates of Sf9 (**C**) and TnHi5 (**D**) cells were separated on 10% SDS-PAGE gels and analysed by western blotting using GP64-specific antibody (AcV5-tag, 1:1000).

E&G: Proteins from crude cell lysates of Sf9 (**E**) and TnHi5 (**G**) cells were separated on 10% SDS-PAGE gels and analysed by western blotting using VP2-specific antibody (R190, 1:1000).

F: Concentrated BV particles from TnHi5 cells were separated on 10% SDS-PAGE gel and analysed by western blotting using VP2-specific antibody (R190, 1:1000).

I: Proteins from crude cell lysates of TnHi5 cells were separated on a 4-20% precast SDS-PAGE gel (Biorad) and analysed by Coomassie staining. WT (wild-type) AcMNPV-infected crude cell lysate sample was used as a negative control.

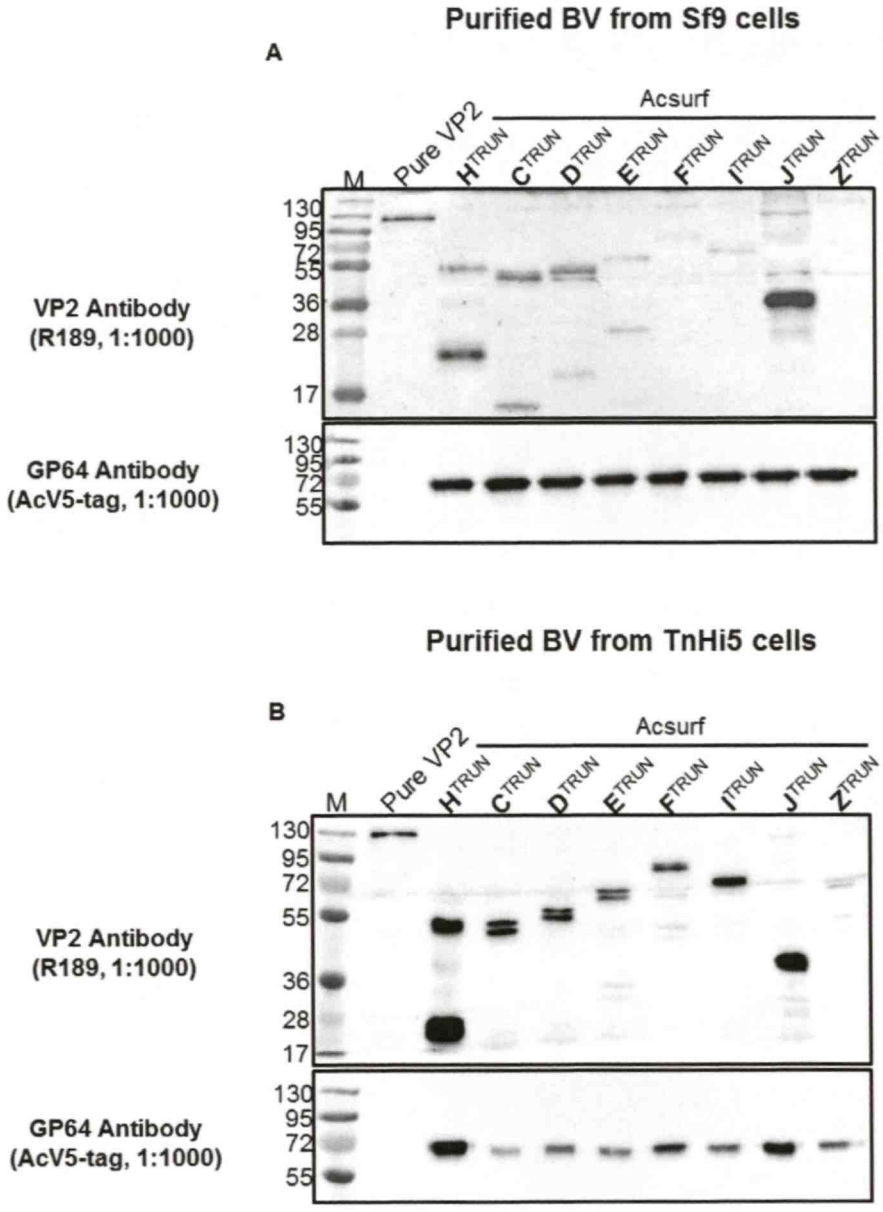


Figure 5.3 Characterizing purified VP2 subdomain surface display viruses by western blotting

VP2 subdomain surface display viruses from Table 5.1 apart from fragments A, B and G were amplified in 80ml shake cultures of Sf9 ($2x10^6$ cells/ml) and TnHi5 ($1x10^6$ cells/ml) using 0.1 moi. Amplified viruses were harvested from the culture media 5 dpi. Budded virus particles were then pelleted using high-speed centrifugation and purified on a 10-50% (w/v) sucrose gradient. Purified virus particles were than separated on 10% SDS-PAGE gels and analysed by western blotting using GP64- and VP2-specific antibodies. M: PageRuler plus prestained protein ladder. Pure VP2: purified VP2 from chapter 3 as appositive control for VP2-specific antibody.

A: Western blot analysis of purified VP2 subdomain surface display viruses amplified in Sf9 cells using VP2-specific antibody (**upper**) and GP64-specific antibody (**lower panel**).

B: Western blot analysis of purified VP2 subdomain surface display viruses amplified in TnHi5 cells using VP2-specific antibody (**upper**) and GP64-specific antibody (**lower panel**).

Table 5.2 Summary of chimeric protein expression results

VP2 subdomains	Sample type	Sf9 cells		TnHi5 cells	
		WB (R190)	*Coomassie*	*WB (R190)*	*Coomassie*
A^{TRUN}	*Concentrated BV*	n/a	x	n/a	x
	Crude cell lysates	n/a	x	n/a	✓
	Purified BV	n/a	x	n/a	x
B^{TRUN}	*Concentrated BV*	n/a	x	n/a	x
	Crude cell lysates	n/a	x	n/a	✓
	Purified BV	n/a	x	n/a	x
C^{TRUN}	*Concentrated BV*	x	x	✓	x
	Crude cell lysates	✓	x	✓	✓
	Purified BV	✓	x	✓	x
D^{TRUN}	*Concentrated BV*	x	x	✓	x
	Crude cell lysates	✓	x	✓	✓
	Purified BV	✓	x	✓	x
E^{TRUN}	*Concentrated BV*	x	x	✓	x
	Crude cell lysates	✓	x	✓	✓
	Purified BV	✓	x	✓	x
F^{TRUN}	*Concentrated BV*	x	x	✓	x
	Crude cell lysates	✓	x	✓	✓
	Purified BV	✓	x	✓	x
G^{TRUN}	*Concentrated BV*	n/a	x	n/a	x
	Crude cell lysates	n/a	x	n/a	✓
	Purified BV	n/a	x	n/a	x
I^{TRUN}	*Concentrated BV*	x	x	✓	x
	Crude cell lysates	✓	x	✓	✓
	Purified BV	✓	x	✓	x
J^{TRUN}	*Concentrated BV*	x	x	✓	x
	Crude cell lysates	✓	x	✓	✓
	Purified BV	✓	x	✓	x
Z^{TRUN}	*Concentrated BV*	x	x	x	x
	Crude cell lysates	x	x	✓	✓
	Purified BV	✓	x	✓	x
H^{TRUN}	*Concentrated BV*	x	x	✓	x
	Crude cell lysates	✓	x	✓	x
	Purified BV	✓	x	✓	x

✓ indicates the detection of chimeric proteins, x indicates that the chimeric proteins were not detected and n/a refers that there was no antibody binding site in the protein

5.5 Post-translational modification analysis of VP2 subdomain chimeric proteins

It is possible that post-translational modification could have accounted for the doublet bands observed in Figure 5.3B (upper panel). Hence, an online prediction tool was used to check for potential glycosylation sites of full-length VP2. Four glycosylation sites were predicted for asparagines at positions; 301, 498, 624 and 1016, which are present in majority of the subdomains (NetNGlyc 1.0 Server). Therefore, in order to investigate whether the doublet bands observed were due to glycosylation of the chimeric proteins, purified virus particles were treated with two glycosidases: PNGase F and Endo H. While Endo H removes only the high mannose and some hybrid types of N-linked carbohydrates, PNGase F removes the majority of all types of N-linked glycosylation (New England Biolabs (NEB)). For the initial analysis, only fragments C, D and E were tested as the doublets observed from these samples were the most apparent (Figure 5.3B lower panel). WT AcMNPV was used as a control.

Purified BV particles (200µl) prepared from TnHi5 cells were used in duplicate for each enzyme treatment. One set of samples was treated with PBS as a negative control for de-glycosylation and the other set was treated with PNGase or Endo H (section 2.5.4). After the treatment, all the samples were analysed by SDS-PAGE, followed by western blotting using VP2- and GP64- specific antibodies. Native GP64 protein has been previously shown to contain N-linked glycosylation (Jarvis *et al.*, 1998), therefore it served as a positive control in the de-glycosylation analysis. A very clear size difference was observed between the enzyme- and PBS-treated GP64 proteins, which showed the removal of carbohydrates confirming the successful enzyme reaction (Figure 5.4A&B, upper panels). However, when the VP2-specific antibody was used, enzyme-treated samples resulted in the same profile as the PBS treated; where the double bands were still present (Figure 5.4A&B lower panels), indicating that N-linked glycans did not account for size differences.

In order to investigate the doublet bands further, an online prediction tool was used to check for any potential phosphorylation sites for the chimeric proteins. It was found that there were several possible phosphorylation sites present (data not shown). Therefore, purified budded virus particles were treated with Lambda protein phosphatase (Lambda P P) (NEB), which is used to remove phosphate groups from proteins. When the samples were analysed by western blotting post Lambda P P treatment, the doublets were still present (data not shown). However, there was no available positive control to be used for this assay, therefore it cannot be concluded for sure that phosphorylation does not account for the size difference.

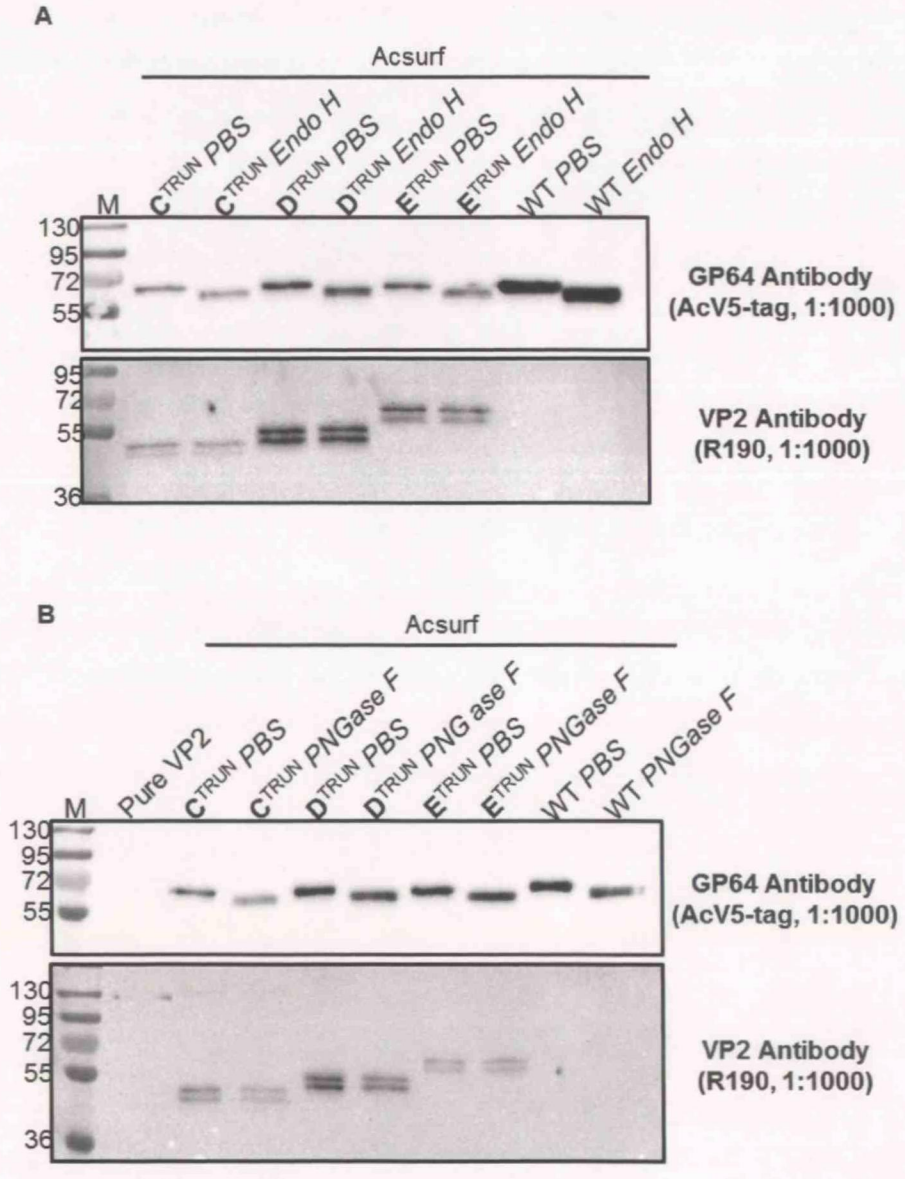


Figure 5.4 De-glycosylation of fragments C, D and E-GP64^{TRUN} chimeric proteins

Purified BV particles from TnHi5 cells (200µl) were pelleted on a bench-top centrifuge at 13000 rpm, for 30 minutes. For each enzyme treatment, samples were pelleted in duplicate; one to be used as a control with PBS and the other one as the actual test with the enzyme. Test samples were then treated with Endo H (**A**) and PNGase F (**B**) enzymes using the supplier's protocol (NEB). Following the enzyme reactions, the samples were separated on SDS-PAGE gels (10%) and analysed by western blotting using GP64- (**A&B, upper panels**) and VP2-specific (**A&B, lower panels**) antibodies. M: PageRuler plus prestained protein ladder. WT AcMNPV: negative control for the VP2 antibody. Purified VP2 (Chapter 3): positive control for the VP2 antibody (only in panel B).

5.6 Budded virus fractionation analysis

The incorporation of VP2 subdomains into the recombinant baculoviruses was confirmed by detecting the chimeric proteins from purified BV particles (Figure 5.3). As the VP2 subdomains are fused to the GP64 TMD, the chimeric proteins are therefore expected to present in the envelope fraction of recombinant BV. In order to confirm this, BV fractionation was carried out (section 2.2.6) with four of the constructs: Acsurf_VP2-E^{TRUN}, Acsurf_VP2-F^{TRUN}, Acsurf_VP2-H^{TRUN} and Acsurf_VP2-J^{TRUN}. Following the fractionation, envelope fraction (Env) was collected from the top of the glycerol gradient and analysed by western blotting using GP64- (BV envelope protein), VP39- (BV capsid protein) and VP2-specific antibodies (section 2.5.2b). Non-fractionated purified BV particles for each sample was included in the western blot analysis as positive control for antibodies.

Native GP64 envelope protein was detected both from the BV virus particles and the envelope fractions of each construct using GP64-specific antibody as expected. The baculovirus capsid protein, VP39, was only detected from the purified BV particles and not from the envelope fractions using VP39-specific antibody, as expected. These results confirmed that the fractionation has successfully worked and the envelope was separated from the nucleocapsid. However, when the VP2-specific antibody was used, unexpectedly chimeric proteins were only detected from the purified virus particles and not from the envelope fraction.

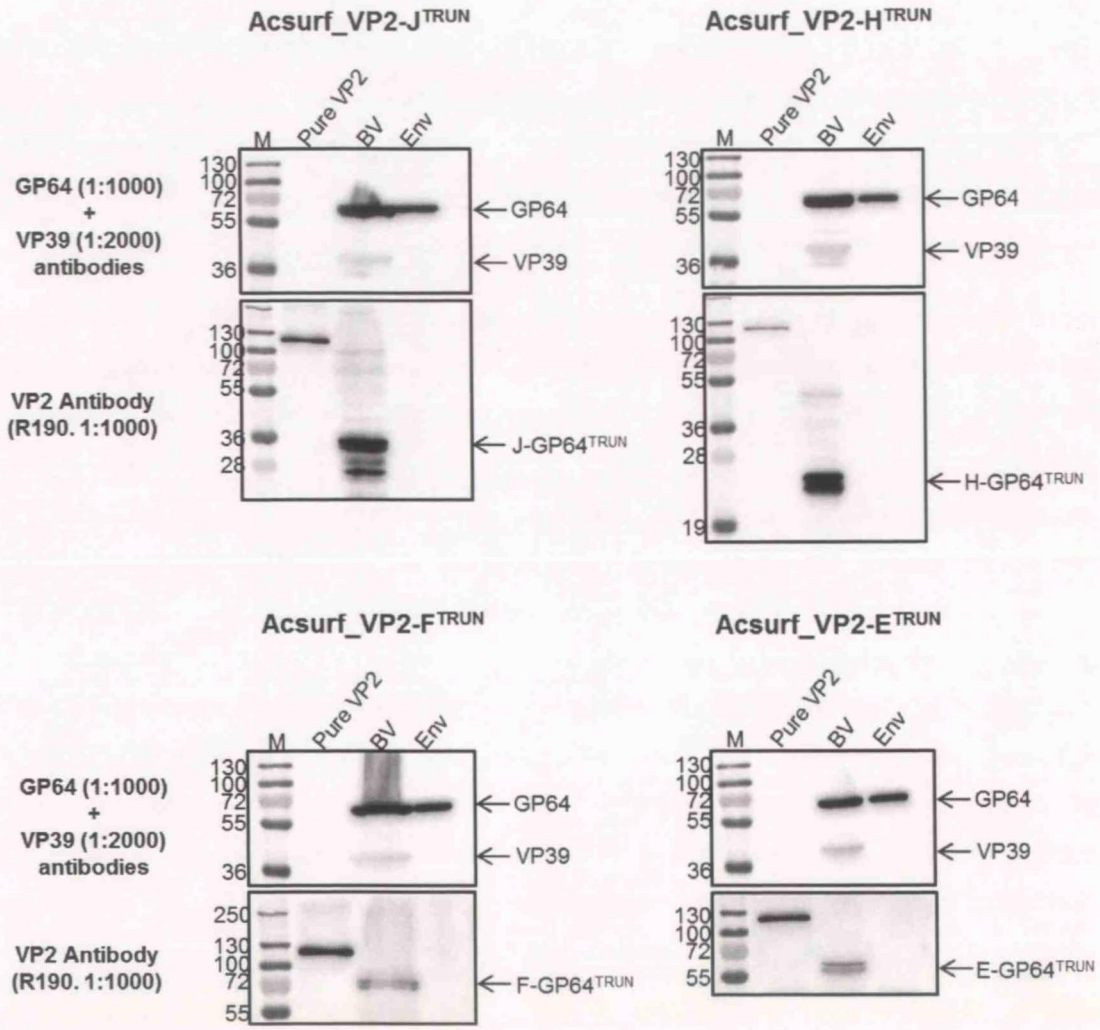


Figure 5.5 Budded virus fractionation of Acsurf_VP2-E^{TRUN}, Acsurf_VP2-F^{TRUN}, Acsurf_VP2-H^{TRUN} and Acsurf_VP2-J^{TRUN}

Purified budded virus particles (200µg) were fractionated on 30-70% (v/v) continuous glycerol gradient after treatment with 1% NP40. Envelope fraction (Env) was recovered from the top of the gradient, separated on 10% SDS-PAGE and analysed by western blotting using GP64-, VP39- (**upper panels)** and VP2-specific (**lower panels)** antibodies. Purified budded virus particles (BV) were used as controls. Purified VP2 was used a positive control for VP2-specific antibody. M: PageRuler plus prestained protein ladder.

5.7 Discussion

The main focus of this chapter was to display the ten VP2 subdomains on the baculovirus budded virus envelope surface, which were otherwise produced in low yields as shown in Chapter 3 of this thesis. In addition to the hypothesis of improving the yield of these subdomains, these surface display recombinant viruses will also be used as tools for studying the antigenicity of VP2 and serve as potential vaccine candidates for AHSV.

After the successful generation of ten recombinant baculoviruses to display VP2 subdomains on their envelope surface, an initial characterization of protein production was carried out on concentrated BV particles from P1 virus stocks. However, none of the VP2 subdomain proteins were detected in a western blot using VP2-specific antibodies (data not shown). Following this, protein production was investigated in both Sf9 and TnHi5 cells by analysing the crude cell lysates and the BV particles from infected culture medium. Acsurf_VP2-A, Acsurf_VP2-B and Acsurf_VP2-G viruses were only included in the Coomassie staining analysis as the antibody used is not specific to domains within these proteins (Section 3.2, Figure 3.2B). The results showed that fragments H, C, D, E, F, I and J were detected in Sf9 crude cell lysates by western blotting (Figure 5.2E) but not by Coomassie staining, suggesting a low yield. However, this was an improvement as the subdomains were not detected at all from Sf9 cells when they were produced individually in Chapter three. On the other hand, they were still not detected in BV particles pelleted from the infected culture medium, which could also be due to the low production within the cells.

There was, however, a considerable improvement in protein yield within TnHi5 cells. The crude cell lysates were diluted (1 in 3) more than the Sf9 samples and still resulted in darker bands in the western blot using VP2-specific antibody (Figure 5.2E&G). Improved protein yield was also confirmed by the detection of distinct chimeric protein bands by Coomassie staining in TnHi5 crude cell lysates (Figure 5.2I), unlike with Sf9 samples. This Coomassie staining also confirmed the successful production of fragments A, B and G as chimeric proteins, which otherwise could not be analysed by western blotting. The improved protein yield also reflected to the detection of these chimeric proteins from the BV particles produced in TnHi5 cells (Figure 5.2F). Overall, when the two cell lines were compared, the results were consistent with Chapter three, where TnHi5 cells were favoured for the production of these chimeric proteins. The possible reasons for this difference between the two cell lines were discussed in detail in Chapter three therefore they will not be discussed further in this chapter.

It was very clear from these results that our hypothesis of improving the VP2 subdomains yield by using surface display constructs was confirmed. There could be several reasons

why such an improvement was achieved. But the addition of GP64 signal peptide is highly likely to be one of the most important. GP64 is the envelope protein of baculoviurses whose target destination in the cells is the plasma membrane. Proteins to be secreted or to be located in the plasma membrane traffic through the secretory pathway, which is triggered by the presence of a signal peptide at the amino terminus (Cooper, 2000, Lodish and Zipursky, 2000). Proteins that enter the secretory pathway go through the endoplasmic reticulum (ER), which provides a quality control system for protein synthesis (Ellgaard and Helenius, 2003). The molecular chaperones found in the ER assist correct folding of the proteins and prevent their aggregation and subsequent degradation (Hartl and Hayer-Hartl, 2002, Ellgaard and Helenius, 2003). Therefore, it is suggested that by trafficking through the secretory pathway, VP2 subdomains were folded correctly and not targeted for degradation, enabling the accumulation of correctly folded proteins and so improving the yield. It was also recorded in the literature that up to 20-fold increase in the yield and secretion of HIV-1 gp120 protein was observed when its signal peptide was replaced with BV GP64 signal peptide (Murphy *et al.*, 1993). In addition, high- yield production of both secretory and membrane-bound forms of T1 receptor was achieved in insect cells by using baculovirus GP64 signal peptide (Rupp *et al.*, 1995).

Although the role of signal peptide in the improved yield of proteins is more apparent as discussed above, it is unknown whether membrane anchorage of proteins achieved by the GP64 TMD had any contributions to the high protein yield. This could be investigated by removing the TMD from the constructs, and carrying out a quantitative analysis to compare the protein yields. However, as the aim in this thesis chapter was to display VP2 subdomains on BV envelope surface, the presence of GP64 TMD in the constructs was crucial for membrane anchorage.

In order to confirm the incorporation of chimeric proteins into the BV envelope, further protein analysis was carried out on sucrose gradient-purified BV generated from both Sf9 and TnHi5 cells. Western blot analysis using VP2-specific antibody confirmed that these chimeric proteins were incorporated into baculovirus BV particles (Figure 5.3). Furthermore, the level of protein production within each insect cell line also reflected the amount of protein being incorporated into BV particles, as the detection of chimeric proteins was clearer and stronger from TnHi5 cell-generated BV particles.

It was also observed that fragments H, C, D, E and F resulted in doublet bands around the expected size of each chimeric protein using VP2-specific antibody (Figure 5.3). It is known that insect cells provide a range of post-translational modifications (Klenk, 1996, Harrison and Jarvis, 2006) and that the ER is shown to harbour the initial stages of protein glycosylation (Cooper, 2000, Harrison and Jarvis, 2006). In addition, the native baculovirus GP64 envelope protein was previously shown to have N-linked glycosylation

(Jarvis *et al.*, 1998). Therefore, it was possible that the chimeric proteins produced from the surface display constructs could have been post-translationally modified. In order to investigate whether glycosylation was responsible for the doublet bands, purified BV particles of fragments C, D and E were treated with glycosidases: Endo H and PNGase F. Post-treatment western blot analysis including successful positive controls suggested that N-linked glycosylation did not account for the size differences observed (Figure 5.4). Previous studies investigated the glycosylation of various baculovirus-expressed recombinant proteins by using tunicamycin, which is an antibiotic that prevents N-glycosylation during protein synthesis, unlike glycosidases used in this study, which removes the N-linked glycans post synthesis (Hericourt *et al.*, 2000, Faburay *et al.*, 2013). Therefore it would be also useful to carry out a tunicamycin assay in the future to confirm with a different experimental approach that glycosylation is not responsible for the double bands observed in the case of VP2 subdomain chimeric proteins.

A similar double-band profile was also observed by Hericourt *et al.* (2000), when turnip yellow mosaic virus RNA-dependent RNA polymerase was expressed by baculoviurses. They investigated glycosylation by using a tunicamycin assay and phosphorylation by using Lambda P P and also with [^{32}P]orthophosphate in *vivo* labelling. They concluded that the double-band profile was due to phosphorylation as Lambda P P treatment of the purified protein removed the higher band on a western blot and ^{32}P-labelled proteins were visible by autoradiography (Hericourt *et al.*, 2000). Lambda P P treatment was inconclusive in this study due to the lack of positive control, but another factor could be due to using purified virus particles and not individual proteins, which might have prevented access to the phosphate groups. [^{32}P]orthophosphate labelling could not be carried out as the required facilities were not available. Therefore, there is still a possibility that the doublet profile observed for VP2 subdomain chimeric proteins could be as a result of phosphorylation.

Although an online prediction tool for signal peptide cleavage (Signal P) identified a relevant site within the constructs, there is a possibility that the doublet profile of the chimeric proteins could be due to the presence of non-cleaved signal peptides. This could be investigated by carrying out protein sequencing using SDS-PAGE and mass spectrometry, which would confirm the presence/absence of the signal peptide. In addition, new constructs could be generated, where VP2 subdomains are only fused to the GP64 signal peptide and not the transmembrane domain. By this way, proteins will be targeted for secretion and the analysis of culture medium and cell pellets would reveal the efficiency of signal peptide cleavage.

The results obtained so far strongly suggested that the chimeric proteins were displayed on the baculovirus envelope surface. Furthermore, microscopy analysis were carried out

with the polyclonal antibodies used in western blotting and ELISA to have a visual confirmation of these chimeric proteins on cell plasma membrane and BV envelope surface, however, they proved unsuccessful (data not shown). Therefore, BV fractionation was carried out as an alternative method to confirm the presence of these chimeric proteins on the baculovirus envelope surface. Using antibodies specific for baculovirus envelope protein, GP64, and capsid protein, VP39, confirmed the successful separation of envelope and nucleocapsid fractions in a western blot. However, unlike the native GP64 protein, VP2 subdomain-GP64^{TRUN} chimeric proteins could only be detected from the whole virus particles and not the envelope fraction (Figure 5.5). This was unexpected, as the constructs were designed for the chimeric proteins to reach the plasma membrane in the same way as the native GP64, so they could be incorporated into the baculovirus envelope surface.

There could be a number of possible reasons to why the VP2 subdomain-GP64^{TRUN} chimeric proteins were absent from the envelope fraction. For example, the proteins could have become unstable and degraded after detaching from the membrane as a result of detergent treatment. It is also possible that they could precipitate into higher density fractions. Therefore, it would be beneficial to use protease inhibitors to minimize any possible degradation and also analyse higher density fractions from the fractionation experiment. In addition, the ratio of native GP64 and chimeric proteins incorporated into the envelope of each baculovirus particle is unknown; hence the amount of virus particles used for fractionation might not be sufficient for the detection of chimeric proteins. Carrying out larger scale fractionation analysis would therefore show whether insufficient amount of proteins was responsible for this outcome. Overall, further investigations are required to be carried out to draw any conclusions for the absence of VP2 subdomain chimeric proteins in BV envelope fraction. Acquiring antibodies that will work in con-focal and electron microscopy imaging will be very valuable in analysing the localization of chimeric proteins in cells and virus particles.

5.8 Conclusion

In conclusion, it was shown in this chapter that the production of VP2 subdomains were greatly improved by using the baculovirus surface display approach and TnHi5 remained the favoured cell line for the protein production. Incorporation of VP2 subdomain-GP64^{TRUN} chimeric proteins into the baculovirus BV particles were proven but the localization in the envelope surface is yet to be confirmed. However, these constructs provided sufficient material to analyse the antigenic nature of these subdomains as described in chapter six.

Chapter 6 Antigenic characterization of VP2 subdomains

6.1 Introduction

Baculovirus expression of viral antigens has been used as vaccine strategy for human and animal arboviruses such as dengue virus (Staropoli *et al.*, 1997), Japanese encephalitis virus (Kuwahara and Konishi, 2010) and Bluetongue virus (Roy *et al.*, 1994a, Stewart *et al.*, 2010). In addition, baculovirus-expressed recombinant VP2 of AHSV4 (Roy *et al.*, 1996), AHSV5 (Scanlen *et al.*, 2002) and more recently of all nine serotypes (Kanai *et al.*, 2014) were shown to induce protective immune responses in horses. Therefore, in this thesis, the baculovirus expression system was used to produce various VP2 subdomains (section 3.2) to further study the antigenic structure of AHSV4-VP2. The aim of this analysis was therefore to try and define/map the virus neutralizing (VN) epitopes of the protein and also determine whether any of the subdomains produced by baculoviruses could mimic these VN epitopes.

Poly-histidine-tagged VP2 was successfully produced and purified to high concentrations in Chapter three of this thesis and was shown to be antigenically similar to the native AHSV capsid protein. However, only low yields of the VP2 subdomains were obtained and these were unable to be purified due to insolubility, therefore, their antigenic analysis could not be carried out. The production of VP2 subdomains was, however, greatly improved in Chapter five by the use of a baculovirus surface display approach. Therefore, the aims of this chapter were to analyse the antigenic nature of the VP2 subdomains from the baculovirus surface display constructs (Chapter 5). In order to do this; ELISA, immunoblotting with AHSV4-VP2-specific antibodies and *in vivo* immunisation experiments in mice were used.

6.2 Binding of VP2 subdomains to AHSV4-VP2-specific monoclonal antibodies

A panel of MAbs previously shown to bind the polyhistidine tag-purified recombinant VP2 (Figure 3.11) and AHSV4 virions (Martinez-Torrecuadrada *et al.*, 1996) was used in an indirect ELISA (section 2.7) to test their binding to VP2 subdomains. This would help understand whether the subdomains generated in Chapter 5 form epitopes that are structurally similar to those present in the full-length VP2. It was shown in Figure 5.2 that very high yields of VP2 subdomains were produced in TnHi5 crude cell lysates. Therefore, an indirect ELISA was conducted in which the wells of a 96-well plate were coated with infected TnHi5 crude cell lysates to be analysed by the panel of MAbs. Briefly, TnHi5 cells seeded in large cell culture dishes ($1.7x10^7$cells/dish) were infected with different baculoviruses displaying specific VP2 subdomains on their surface (Table 5.1) using an MOI of 5. Cell pellets harvested at 72 hpi were lysed by osmotic shock and used to coat

the wells of the assay plate. From this point onwards, the indirect ELISA protocol from section 2.7 was followed. AcVP2$^{HIS/N}$-infected crude cell lysates, expressing full-length VP2, were also included in the analysis alongside positive (15ng/well affinity purified VP2) and negative (Acsurf^{TRUN}-infected crude cell lysates)[1] controls.

The results of the indirect ELISA showing the binding of MAbs to VP2 subdomains are summarized in Table 6.1 and Figure 6.1. The positive threshold for the assay was set to OD ≥ 0.1 at 450nm, after normalizing the raw absorbance data by subtracting the background O.D. obtained with the negative control. The antigenic binding site of these MAbs was determined by Martinez-Torrecuadrada *et al.* (1996) through competition ELISA experiments. The data from the indirect ELISA tests done in this thesis showed that the majority of MAbs belonging to antigenic sites I (8DF1), II (8AE7), III (8BG10, 10BE7, 10BG7) IV (10AH5, 6DF4, 6DG2, 6AF2) and VI (8CH7) did not bind to any of the VP2 subdomains but strongly bound to purified VP2. This suggested that the subdomains on their own do not mimic the epitopes recognized by these antibodies (Table 6.1, Figure 6.1) but that those epitopes are somehow present in the full length VP2. Binding of the same MAbs to non-purified recombinant VP2 was comparable, albeit weaker, than to the purified VP2, which could be due to the amount of protein present in the samples.

On the other hand, MAbs that belong to antigenic site V (8BB1, 8BC2, 8BF2, 8CE4, 8AE6, 8DB11) strongly bound to fragment H and majority of the subdomains overlapping its sequence, suggesting these subdomains do mimic the epitope(s) recognised by these antibodies (Table 6.1). Additionally, the overlapping sequence of the subdomains suggested that majority of antigenic site V antibodies recognize epitopes within the amino acid region 253-357 (Figure 6.1). Among these MAbs, 8AE6, 8CB11 and 8DB11 also weakly bound to subdomains that do not overlap this region such as fragments A, G or Z suggesting the latter MAbs bind conformational epitopes that comprise the amino acid region 253-357 and those other distant domains contained in fragments A, G and Z (Figure 6.1).

One of the neutralizing MAbs, 8DH3, was shown to bind all the VP2 subdomains apart from fragments A and G. Based on the overlapping sequences of these subdomains, it could be suggested that 8DH3 recognizes an epitope within the amino acid region 253-276 (Figure 6.1). However, it also weakly bound to fragment Z that is outside this region, hence also binding to amino acid regions 566-760 and/or 955-1060. On the other hand, a reversed profile was observed with another neutralizing MAb, SMAA, which only weakly reacted with fragments A and G but none of the other subdomains.

[1]Acsurf^{TRUN} virus was generated as a negative control for vaccination studies by using an empty transfer vector (pBACsurf-1$^{GP64/F463}$), therefore no recombinant protein is displayed on BV envelope surface.

In the case of 10BC12, which is also a neutralizing antibody, fragments E, H, G and Z were detected (Table 6.1) however, these four subdomains do not contain a common overlapping sequence. Instead, fragments E and H overlaps in the amino terminal half of the protein (aa 253-414) whereas fragments G and Z overlaps at the carboxy terminus (aa 760-955; Figure 6.1) suggesting the epitope recognized by 10BC12 to be discontinuous.

As mentioned above, these MAbs belong to different antigenic sites and some were suggested to recognize linear epitopes while others were suggested to recognize non-linear epitopes of VP2 (Martinez-Torrecuadrada *et al.*, 1996). However, it was important to confirm this binding pattern to be the same for full-length VP2 generated in this study. Hence, a better interpretation of epitopes formed by VP2 subdomains could be achieved. In order to investigate this, four MAbs from different antigenic sites were chosen and tested on a western blot under denaturing conditions for their binding against full-length VP2. It was shown that 8DH3 neutralizing antibody from antigenic site III, 8DB11 from antigenic site V and 8BG9 from antigenic site IV, which detected most of the subdomains in the ELISA (Table 6.1), also detected full-length VP2 under denaturing conditions (Figure 6.2), suggesting these epitopes to be linear. On the other hand, 6AF2 from antigenic site IV that only bound to the full-length VP2 but none of the subdomains in the ELISA, did not recognize full-length VP2 under denaturing conditions in the western blot (Figure 6.2), suggesting the epitopes of this MAb to be strongly conformational.

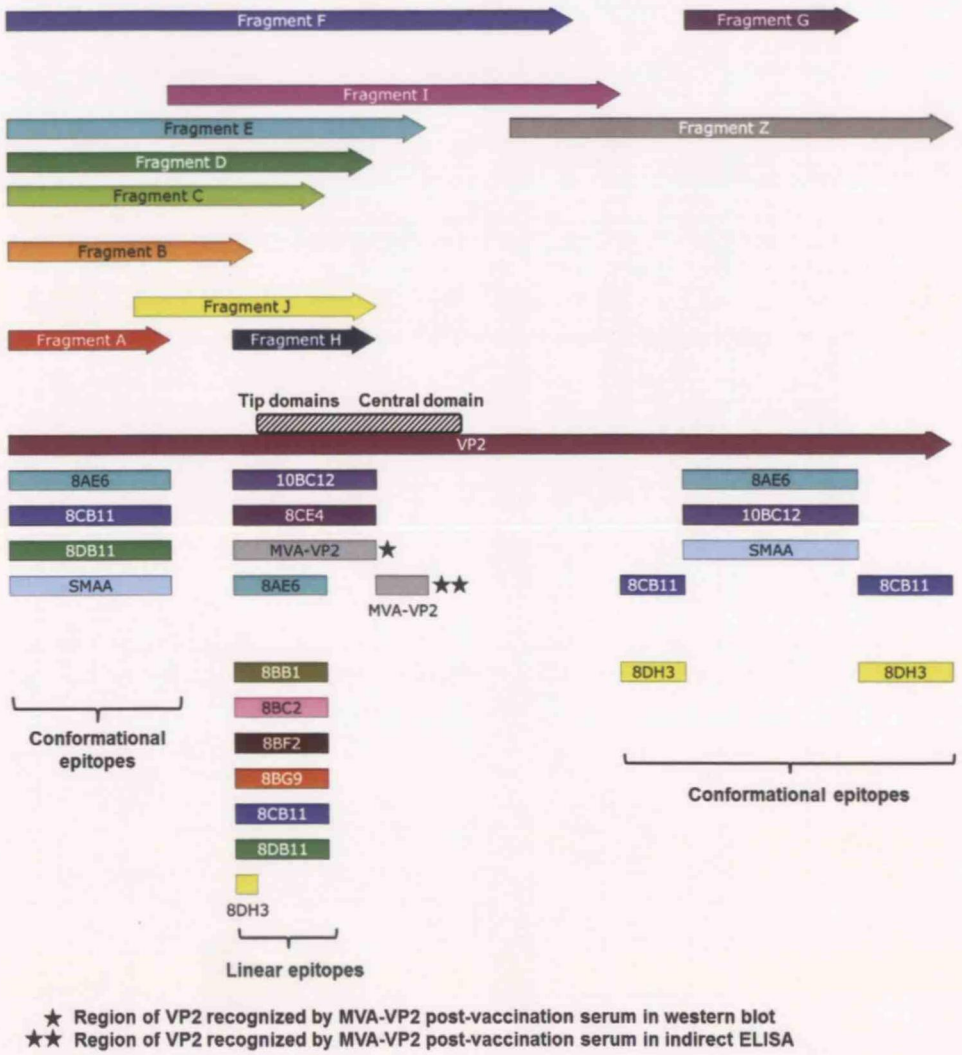


Figure 6.1 Schematic representation of monoclonal antibody binding sites within VP2

This diagram is generated by the Snapgene® software based on the results of this thesis. Full-length VP2 is represented in the middle of the diagram (purple arrow). Above VP2 is the location of all the subdomains in relation to their position in the protein. Below are the mapped binding regions for the monoclonal antibodies based on the analysis of overlapping sequences of subdomains and the results of the indirect ELISA. Central and tip domains marked on the full-length VP2 are the regions indicated by Manole *et al.*, (2012).

Table 6.1 Summary of VP2 subdomain binding to AHSV4-VP2-specific MAbs in an indirect ELISA

	8AF8	8DF1	8AE7	8CG1	8BG10	8DH3*	10BE7*	10BG7*	10BC12*	10AH5*	6DF4	6DG2	6AF2	8BG9	8BB1	8BC2	8BF2	8CE4	8AE6	8DB11	8CB11	SMAA*	8CH7*	8DA6
A	-0.2	-0.3	-0.4	-0.2	-0.6	0.0	-0.4	-0.5	-0.2	0.0	-0.1	0.0	-0.1	0.0	-0.1	0.0	0.0	-0.4	0.2	0.2	0.2	0.3	0.0	0.1
B	-0.2	-0.3	-0.5	-0.1	-0.6	0.1	-0.4	-0.6	-0.1	-0.1	-0.1	0.0	-0.2	-0.1	-0.2	0.0	0.0	-0.8	0.0	0.0	-0.2	0.0	0.0	-0.1
C	-0.2	-0.2	-0.4	-0.1	-0.7	0.3	-0.3	-0.5	-0.2	-0.1	-0.1	0.0	-0.2	0.1	0.8	0.8	0.6	-0.3	0.5	0.8	0.4	0.0	0.0	0.0
D	-0.1	-0.2	-0.5	-0.2	-0.7	0.2	-0.4	-0.6	-0.2	-0.1	-0.1	0.0	-0.2	0.0	0.3	0.5	0.4	-0.5	0.0	0.2	0.0	-0.3	0.0	-0.2
E	0.0	-0.1	-0.4	0.0	-0.3	0.4	-0.1	-0.5	0.1	0.0	-0.1	0.0	-0.3	0.2	0.7	1.1	0.7	0.1	0.7	0.7	0.2	0.0	0.0	-0.1
F	0.1	-0.2	-0.4	0.0	-0.4	0.2	0.0	-0.6	0.0	0.0	-0.1	0.0	-0.3	0.1	0.9	0.9	0.6	-0.1	0.5	0.7	0.2	-0.1	0.0	-0.1
I	-0.2	-0.2	-0.5	-0.1	-0.4	0.2	-0.3	-0.7	-0.4	-0.1	-0.1	0.0	-0.2	0.1	0.9	1.4	0.8	0.6	0.7	0.8	0.2	-0.2	0.0	-0.2
J	-0.1	-0.2	-0.3	-0.1	-0.6	0.1	-0.2	-0.8	-0.4	-0.1	-0.1	0.0	-0.3	0.1	0.4	0.9	0.6	0.2	0.4	0.5	0.1	-0.4	0.0	-0.2
G	-0.1	-0.3	-0.4	-0.1	-0.3	0.0	-0.3	-0.2	0.2	-0.1	-0.1	0.0	-0.2	-0.1	-0.1	0.0	0.0	-0.8	0.1	-0.1	-0.2	0.1	0.0	-0.1
H	0.0	0.0	-0.2	0.1	0.0	0.7	0.0	-0.3	0.5	0.0	0.0	0.0	-0.1	0.3	1.3	1.7	1.1	0.6	1.1	1.2	0.5	-0.1	0.0	0.2
Z	0.0	-0.2	-0.2	0.0	-0.4	0.2	0.0	-0.3	0.5	0.0	0.0	0.0	-0.1	0.0	-0.2	-0.1	0.0	-0.9	0.2	0.0	0.1	-0.2	0.0	0.0
VP2 lysate	0.0	0.3	-0.1	0.4	-0.7	-0.1	-0.1	-0.3	0.4	0.1	0.1	0.1	0.2	0.0	-0.1	-0.1	0.0	-0.3	-0.2	-0.1	-0.1	0.0	0.0	-0.1
VP2 purified	2.6	2.3	2.0	1.7	2.1	1.3	1.0	1.4	2.6	0.9	0.6	1.2	2.2	1.1	1.9	1.9	0.7	2.4	2.8	1.8	2.6	1.9	0.1	0.6
Antigenic sites defined by Martinez-Torrecuadrada *et al.*, 1996)		I		II			III				IV				V							VI		VII

* MAb with neutralization capacity

OD values: ≤0.0 | 0.1 ≤0.4 | 0.5≤1.0 | ≥1.0

An indirect ELISA was set-up where the wells of a 96-well plate were coated with virus-infected crude cell lysates. Duplicate samples were included in the assay for each subdomain/antibody sample. Null virus-infected crude cell lysates were used as a negative control for each MAb. The OD values represented in the table are obtained after the mean OD of null virus-infected samples was subtracted from the mean OD of each corresponding MAb sample. Raw data can be found in Appendix 5

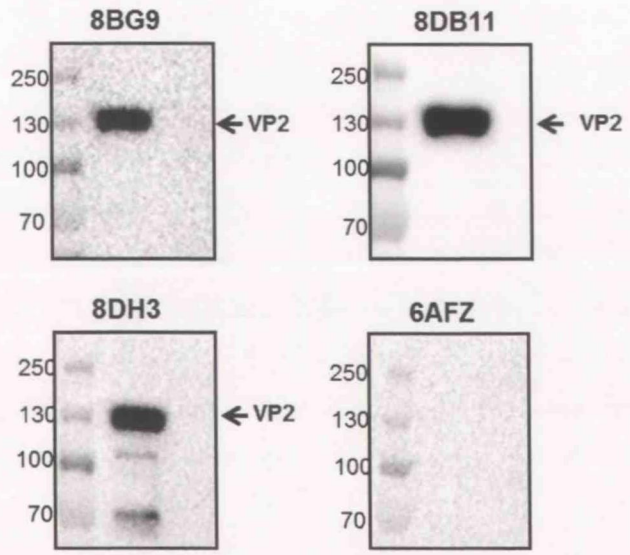


Figure 6.2 Western blot analyses of full-length VP2 using AHSV4-specific monoclonal antibodies

Polyhistidine-tag affinity-purified VP2 was separated by SDS-PAGE (4-20% gradient gel) and analysed by western blotting under denaturing conditions using AHSV4-specific MAbs; 8BG9, 8DB11, 8DH3 and 6AF2.

6.3 Binding of VP2 subdomains to antibodies from MVA-VP2 post-vaccination serum

After analysing the binding of VP2 subdomains to AHSV4-VP2-specific MAbs (section 6.2), the antigenic reactivity of each of the VP2 subdomains with virus neutralising equine antiserum from MVA-VP2 post-vaccination (obtained from The Pirbright Institute) was tested. This serum was shown to neutralise AHSV4 infectivity (personal communication with Dr Javier Castillo-Olivares). A similar protocol to that described in section 6.2 was followed to coat the wells of ELISA plates with infected TnHi5 crude cell lysates. An indirect ELISA was carried out using the protocol from section 2.7 with a 1 in 100 dilution of the MVA-VP2 post vaccination serum. AcVP2$^{HIS/N}$-infected crude cell lysate was also included in the analysis. In addition, purified VP2 (15ng/well) was used as a positive control and Acsurf^{TRUN}-infected cell lysate was used as a negative control. Furthermore, pre-immunization equine serum was also included in the analysis as a negative control and the raw data was normalized by removing the background values obtained with this serum.

High background values obtained with the pre-immunization serum from crude cell lysate samples suggested non-specific binding to virus-infected cellular proteins. However, after the background was subtracted, antibodies in the VN serum were shown to bind fragments E, F (very weakly) and also fragment I, whereas binding to whole length VP2

was very strong suggesting that VP2 epitopes are highly conformational and very difficult to mimic by each of the VP2 subdomains (Figure 6.3). No positive binding was detected with any of the remaining subdomains. When the overlapping sequences of the detected subdomains were analysed, it could be suggested that the antibodies bound very weakly to the amino acid region 413-472 (Figure 6.1). This could suggest that the epitopes on VP2 require the interaction of various subdomains of VP2 and that those subdomains only interact with each other when the full length protein is present. It is also possible that the purity and high concentration of VP2 in the purified preparation is an important factor in the results observed since VP2 from crude cell lysates appear not to have reacted with the equine MVA-VP2 post vaccination serum.

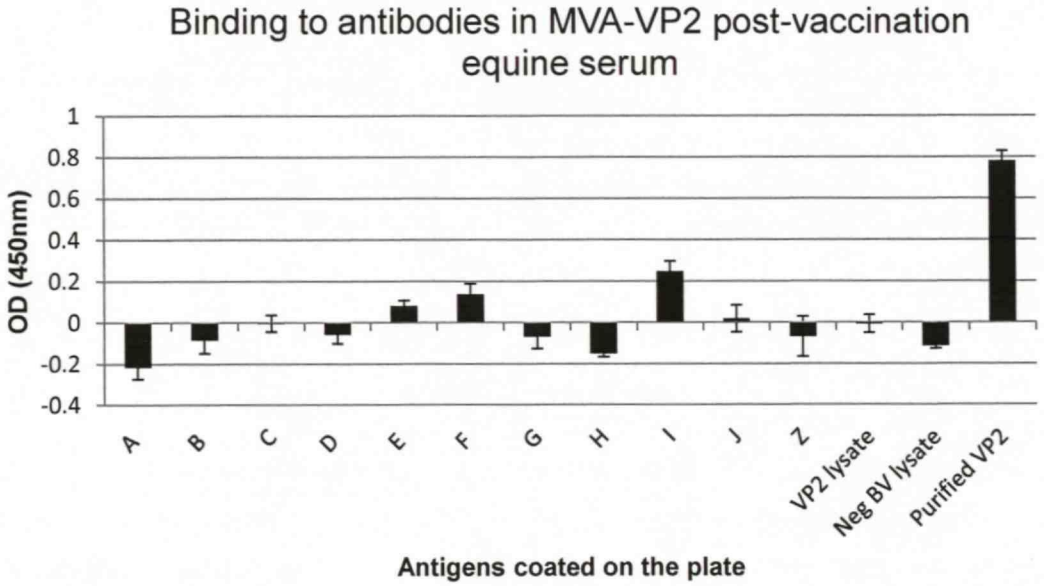


Figure 6.3 Binding of antibodies from MVA-VP2 post-vaccination serum to VP2 subdomains

Large cell culture dishes seeded with TnHi5 cells ($1.7x10^7$cells/dish) were infected with $AcVP2^{HIS/N}$ and VP2 subdomain surface display constructs from Table 5.1 using 5 MOI. The cell pellets harvested at 72 hpi were lysed by osmotic shock using 25mM $NaHCO_3$ and were diluted in carbonate/bicarbonate buffer (1 in 100) to coat the wells of assay plates for indirect ELISA. Equine MVA-VP2 post-vaccination serum (obtained from the Pirbright Institue) was used with 1 in 100 dilution at the primary antibody stage, which was followed by 1 in 15000 dilution of HRP-conjugated anti-horse antibody. Following the antibody incubations, 50µl of TMB substrate and sulfuric acid stop solution were added respectively and absorbance was measured at 450nm with a microplate reader (LT-4500). Purified VP2 (15ng/well) was used as a positive control and $Acsurf^{TRUN}$ (Neg BV lysate) was used as a negative control. The graph was generated using the mean OD of duplicate samples after subtracting the mean OD obtained with the pre-immunization equine serum for each corresponding sample. Error bars indicate the standard error of each sample. Raw data can be found in Appendix 6.

Following the antigenic analysis of the VP2 subdomains using ELISA, the presence of linear antigenic domains was explored under denaturing conditions by immunoblotting. In order to do this, TnHi5 crude cell lysates infected with the VP2 subdomain surface display

baculoviruses (Table 5.1) were analysed by western blotting using MVA-VP2 post vaccination serum. Wild-type AcMNPV-infected crude cell lysates and purified VP2 were used in the analysis as negative and positive controls, respectively. It was shown that antibodies in the MVA-VP2 post-vaccination serum distinctively bound to purified VP2 and fragments H, E, F, I and J with varying intensities under denaturing conditions. This suggested the presence of linear antigenic epitopes within these subdomains that could be recognized by antibodies produced against MVA-VP2 vaccination in the equine host (Figure 6.4). These results are consistent with previous data suggesting the presence of linear epitopes in this region of VP2. Whether these epitopes are neutralising or not could not be determined by this experiment.

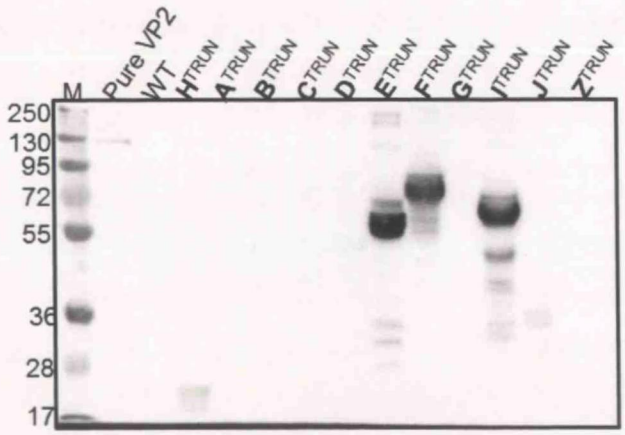


Figure 6.4 Western blot analysis of VP2 subdomains with MVA-VP2 post vaccination serum

TnHi5 cells seeded in a 6-well plate ($0.5x10^6$cells/well) were infected with VP2 subdomain surface display viruses from Table 5.1 using 5 MOI. At 72hpi, the cells were harvested and proteins from the crude cell lysates were analysed by SDS-PAGE (10% gel) and western blotting using MVA-VP2 post vaccination equine serum obtained from the Pirbright Institute (1 in 800 dilution).

6.4 Vaccination studies

Previous studies have indicated the use of baculovirus surface display to be a successful approach for immunogenicity analysis of proteins such as σC and σB proteins of avian reovirus (Lin *et al.*, 2008) and *Neospora caninum* antigens (Kato *et al.*, 2015). Furthermore, recombinant baculovirus-infected Sf9 insect cells have been shown to be highly immunogenic, inducing protective levels of target-specific VNAbs in animals, such as food and mouth disease virus antigens (Tami *et al.*, 2004). In order to examine the antigenic structure of VP2 and whether baculovirus surface display approach could improve the correct protein folding of VP2 epitopes potentially present in VP2 subdomains, a vaccination study was conducted. Hence, basic information about the

factors that influence the immunogenicity of this type of vaccines could be obtained and whether immunisation with baculovirus surface display constructs could induce VP2-specific antibody responses and furthermore whether these antibodies were capable of neutralising virus infectivity could be analysed.

It was shown in the *in vitro* antigenicity analysis that fragments E, F and I were recognized by antibodies from MVA-VP2 post vaccination serum both in an ELISA (Figure 6.3) and western blot under denaturing conditions (Figure 6.4). These subdomains were the most reactive with the panel of AHSV4-specific MAbs in an ELISA, suggesting that as individual subdomains, they still represent similar structure of the full-length VP2 protein (Table 6.1, Figure 6.1). Considering these results and the fact that this region has been identified by several studies as the most antigenic, it was important to examine whether correct folding of these subdomains could be achieved by displaying them in the surface of baculoviruses. The way of testing this hypothesis was to conduct a vaccination experiment and analyse the antisera from vaccinated animals for their capacity to neutralise AHSV-4 infectivity.

Initially, only one of the subdomains, Fragment E, was taken forward to be used in a pilot vaccination study for proof of concept. Fragment E was used as an antigen by incorporation to budded virus particles (baculovirus surface display) and also as an expressed protein from TnHi5 cells infected with the recombinant baculovirus. Full-length VP2 both in the form of polyhistidine tag affinity-purified protein and AcVP2$^{HIS/N}$-infected TnHi5 cells was also included in the immunizations. These served as positive controls in the analysis as baculovirus-expressed full-length VP2 was previously shown to induce protective levels of VNAbs (Roy *et al.*, 1996, Scanlen *et al.*, 2002, Kanai *et al.*, 2014). Acsurf^{TRUN} was used as a negative control both in the form of purified virus particles and infected TnHi5 cells. A simplified schematic representation of antigen types used in this thesis can be found in Figure 6.5.

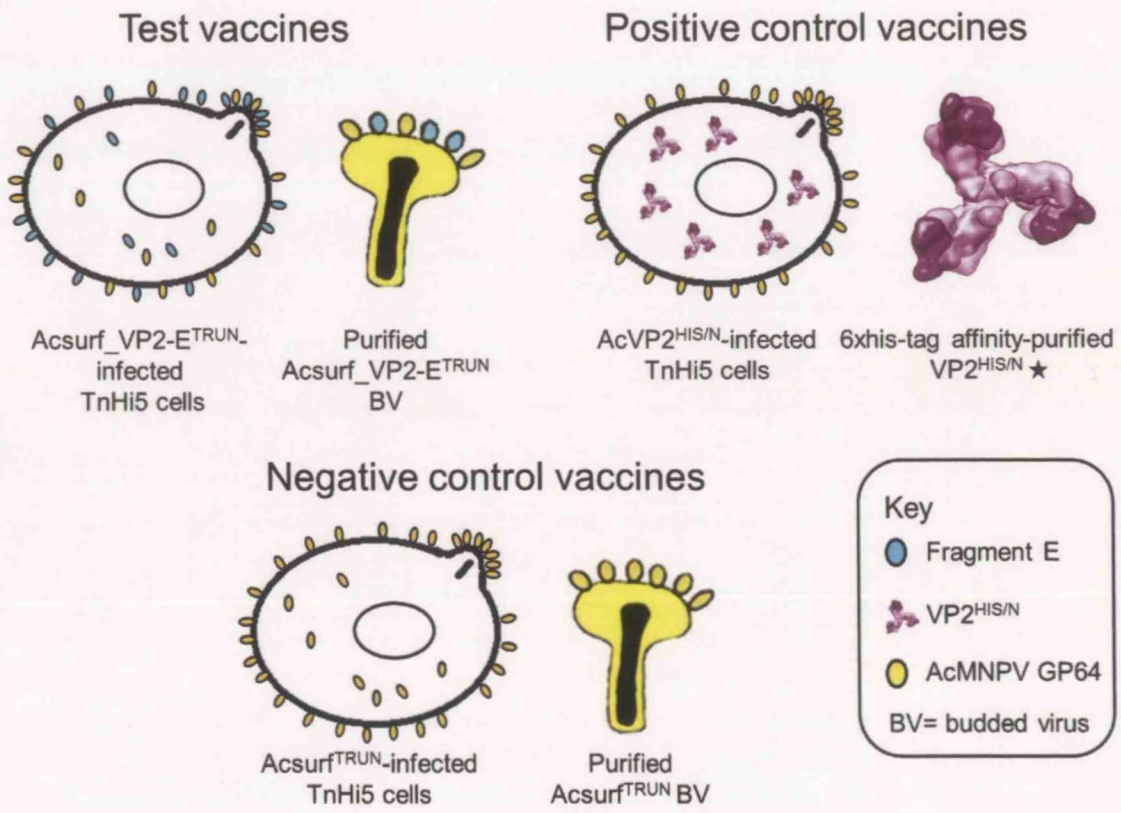


Figure 6.5 Schematic representation of antigens used in the pilot vaccination

The pilot vaccination study contained six different antigen groups where they were categorized as the test, positive and negative control vaccines, accommodating two antigen types per category. Acsurf_VP2-E^{TRUN}-infected TnHi5 cells and purified Acsurf_VP2-E^{TRUN} BV particles were used as the test vaccines to study the immunogenicity of fragment E VP2 subdomain. Control vaccines contained $AcVP2^{HIS/N}$-infected TnHi5 cells, where the $VP2^{HIS/N}$ was produced in the cells, and 6xhis-tag affinity purified $VP2^{HIS/N}$ protein. Negative control vaccines were $Acsurf^{TRUN}$-infected TnHi5 cells and the corresponding purified BV particles.

★ It is yet unknown whether the VP2 produced in this study is in the form of trimers.

6.4.1 Antigen preparation

Heretofore, an MOI of 5 was used for successful protein production in cells of adherent cultures in this thesis. However, if 0.1 MOI and cells in shake cultures can be used instead, antigen production for pilot vaccination would become more time and cost-effective, as a single virus amplification will provide both the infected cells and BV material for the vaccination. In order to compare protein production levels from 0.1 and 5 MOI-infected cells, a test expression was carried out in 20ml shake cultures of TnHi5 cells (section 2.5.1). The proteins from infected cell lysates were separated by SDS-PAGE and analysed by Coomassie staining (Sections 2.5.2 and 2.5.2a). Wild-type virus was included in the analysis as a negative control. Fragment E-$GP64^{TRUN}$ chimeric protein was detected

from both MOI samples at the expected size of 58.8kDa and no distinctive difference was observed between the two samples when the band intensities were compared (Figure 6.6). As the Coomassie staining showed that the samples were equally loaded on the gel, it was suggested that 0.1 MOI can be used for sufficient protein production in the antigen preparation.

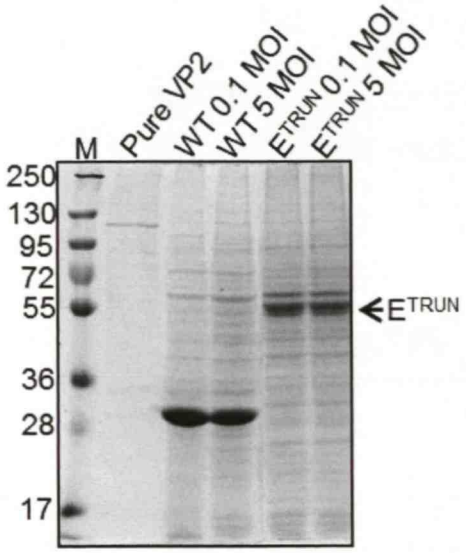


Figure 6.6 SDS-PAGE analysis of fragment E-GP64^{TRUN} production from TnHi5 cells infected with 0.1 vs 5 MOI

20ml shake cultures of TnHi5 cells (1x10^{6}cells/ml) were infected with Acsurf_VP2-E^{TRUN} virus using 0.1 or 5 MOI. The cultures infected with 0.1 MOI were harvested at 5 dpi and the cultures infected with 5 MOI were harvested at 3 dpi. Proteins from infected TnHi5 cell lysates were analysed by SDS-PAGE (10% gel) and Coomassie staining. Wild-type virus was used as a negative control in the analysis. M: PageRuler plus prestained protein ladder.

6.4.1a Preparation of test and negative control vaccine antigens

TnHi5 cells (1x10^{6}cells/ml) were infected with Acsurf_VP2-E^{TRUN} and Acsurf^{TRUN} viruses using an MOI of 0.1. After five days incubation at 28°C, culture medium from each virus infection was divided into 2x500ml tubes and was clarified by centrifuging at 3000 rpm for 15 minutes. Prior to centrifugation 1ml aliquots were taken to count the cells. In total 1x10^9 (tube 1), 8x10^8 (tube 2) cells for Acsurf_VP2-E^{TRUN} and 9x10^8 (tube 1), 1.2x10^9 (tube 2) cells for Acsurf^{TRUN} were pelleted. The cell pellets were washed with 1x PBS, re-pelleted at 3000 rpm for 10 minutes and frozen at -80°C until immunization. On the other hand, clarified culture media were processed further for the purification of BV particles following the protocol on section 2.2.5. After purification, BV particles were titrated using QPCR

(section 2.2.4) and the titres were; Acsurf_VP2-E^{TRUN}: 3.9x10^{8}pfu/ml and Acsurf^{TRUN}: 7.8x10^{8}pfu/ml.

Sucrose-gradient purified BV particles were prepared to a final amount of 1x10^7 or 1x10^{8}pfu/well and analysed on SDS-PAGE followed by western blotting using GP64- and VP2-specific antibodies. In addition to confirming the presence of antigens in the purified BV particles, western blot profiles were also used to help determine the antigen dose to be used in the immunizations. Native GP64 protein was detected from all samples, as expected, and the bands from 1x10^{8}pfu/well samples were thicker and darker (Figure 6.7 upper panel). Fragment E-GP64^{TRUN} chimeric protein was only detected from the corresponding virus sample as anticipated and the band was stronger from 1x10^{8}pfu/well sample (Figure 6.7 lower panel). Therefore, 1x10^{8}pfu was taken forward as the antigen dose to be used for purified BV antigens in immunization.



Figure 6.7 Western blot analyses of purified Acsurf^{TRUN} and Acsurf_VP2-E^{TRUN}

BV produced in one litre culture of TnHi5 cells (1x10^{6}cells/ml) were purified using 10-50% sucrose gradient. Purified BV particles (1x10^7 or 1x10^{8}pfu/well) were analysed on SDS-PAGE followed by western blotting using GP64- (upper panel) and VP2-specific (lower panel) antibodies. M: PageRuler plus prestained protein ladder.

6.4.1b Preparation of positive control vaccine antigens

TnHi5 cells seeded in 20x large cell culture dishes (1.7x10^{7}cells/dish) were infected with AcVP2$^{HIS/N}$ using 5 MOI (Section 2.5.1). After 72hpi at 28ºC, infected cells were harvested (10dishes/tube; total 250ml/tube) by centrifuging at 3000rpm for 15 minutes. Prior to centrifuging 2x1ml aliquots were taken from each tube for cell counting and SDS-PAGE analysis. The pelleted cells were washed with 1xPBS, re-pelleted at 3000rpm for 10 minutes and frozen at -80ºC until immunization. The cell counts were: 1.25x10^8 (tube 1)

and $1x10^8$ (tube 2). The protein production was confirmed by western blotting using VP2-specific antibody (section 2.5.2b), suggesting the successful preparation of $AcVP2^{HIS/N}$-infected TnHi5 cells vaccine antigen (Figure 6.8).

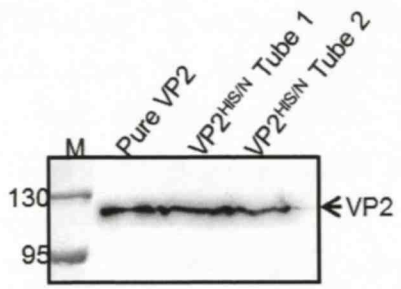


Figure 6.8 Western blot analysis of $AcVP2^{HIS/N}$-infected TnHi5 cells vaccine antigen

1ml aliquots collected from each tube of $AcVP2^{HIS/N}$-infected TnHi5 cells were pelleted by centrifuging at 4000rpm for 5 minutes. Proteins from whole cell lysates were analysed on SDS-PAGE (6% gel) followed by western blotting using VP2-specific antibody (R190, 1:1000). Pure VP2 (Chapter 3) was used as a positive control. M: PageRuler plus prestained protein ladder.

In order to prepare the purified $VP2^{HIS/N}$ vaccine antigen, TnHi5 cells seeded in 40x large cell culture dishes ($1.7x10^7$cells/dish) were infected with $AcVP2^{HIS/N}$ using 5 MOI (section 2.5.1). Infected cells were harvested at 72hpi, lysed by 1%NP40 buffer and $VP2^{HIS/N}$ was purified following the protocol from section 2.6. At the final stage of purification, 8x1ml eluate samples were collected and all fractions from the purification were analysed on SDS-PAGE followed by Coomassie staining and western blotting using VP2-specific antibody (section 2.5.2). Purified $VP2^{HIS/N}$ was detected from all eluate samples with decreasing band intensities using VP2-specific antibody (Figure 6.9, upper panel). On the other hand, $VP2^{HIS/N}$ was detected from the first four eluates samples on the Coomassie staining, suggesting lower protein concentration in the remaining eluate samples (Figure 6.9, lower panel).

The total protein concentration of all eluate samples were measured using the BCA assay from section 2.5.3a and specific VP2 protein concentration was determined by band densitometry using Coomassie stained gel. $VP2^{HIS/N}$ concentration from eluate one was estimated to be 318µg/ml and was taken forward for immunization.

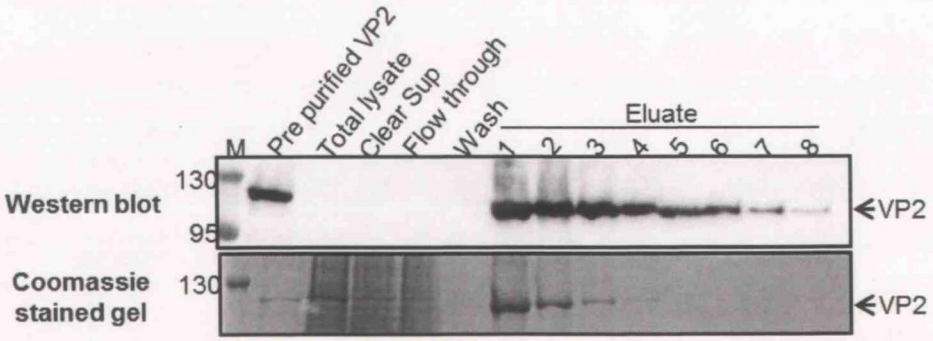


Figure 6.9 SDS-PAGE analysis of purified VP2$^{HIS/N}$ vaccine antigen

All purification fractions were separated on 6% SDS-PAGE gels and analysed by Coomassie staining (lower panel) and western blotting using VP2-specific antibody (upper panel, R190, 1:1000). Pre-purified VP2 (Chapter 3) was used as positive control on the gels. M: PageRuler plus prestained protein ladder.

6.4.2 Immunization of mice

Immunization of mice and the analysis of serum post-vaccination were carried out by Dr Eva Calvo at CISA-INIA (Research Centre for Animal Health) in Valdeolmos, Spain through collaboration with The Pirbright Institute.

Six groups of mice, each accommodating five female, six week-old BALB/c mice were immunized subcutaneously (200µl), using the antigens prepared in section 6.4.1. The antigen doses used in the immunization are listed in Table 6.2. Antigens were administered in the presence of 1:1 Imject Alum adjuvant (Thermo Fisher). At 21 days post vaccination (dpv), blood samples were collected by venepuncture for ELISA analysis of serum antibodies, which was followed by a booster immunization using the same antigens/doses from Table 6.2. Two weeks after the booster immunization (35dpv), blood samples were collected for ELISA and virus neutralization assays.

Table 6.2 Antigens and doses used for mice immunization

Group	Antigen	Dose/mouse	Number of mice
1	Purified VP2$^{HIS/N}$	10ug	5
2	AcVP2$^{HIS/N}$-infected TnHi5 cells	5x10^6 cells	5
3	Purified Acsurf_VP2-E^{TRUN} BV	1x10^8 pfu	5
4	Acsurf_VP2-E^{TRUN}-infected TnHi5 cells	5x10^6 cells	5
5	Purified Acsurf^{TRUN} BV	1x10^8 pfu	5
6	Acsurf^{TRUN}-infected TnHi5 cells	5x10^6 cells	5

The volume of injected material was absorbed by all mice with no signs of adverse effects one day post-vaccination. However, as time passed, a very small nodule of inflammation developed in mice from groups two, four and six, which became apparent around 20dpv. The inflammation was localized to the site of inoculation and the mice were otherwise healthy, not showing any signs of illness. The inflammation was suggested to be due to the nature of the inoculum, as these groups were injected with the whole-cell antigens, which contained cellular and viral proteins as well as other cellular debris. Therefore, the booster vaccination was injected at a different site by a sub-cutaneous route. Similar inflammation was observed around two weeks post-booster-injection.

6.4.3 Analysis of post-vaccination serum antibodies by ELISA

Serum antibodies were analysed from the blood collected on 21 and 35dpv using indirect ELISA. Group two, AcVP2$^{HIS/N}$-infected TnHi5 cells, resulted in the highest OD value (0.74), which was followed by group one, purified VP2$^{HIS/N}$, with an OD value of 0.41 on 21dpv (Figure 6.10A). Fragment E antigen groups (three and four) resulted in lower values than the full-length VP2 antigens, however, the OD values were significantly higher when compared to values obtained from their corresponding negative control antigen groups (Groups three/five t-test p=0.0014; Groups four/six t-test p=0.0120, Figure 6.10A).

When the serum antibodies from 35dpv were analysed by ELISA, a significant increase was observed in the OD values of groups one and two (1.42 and 1.28, respectively, Figure 6.10B). However, it was noticed that the background values from negative control groups (5 and 6) also increased after the booster vaccination. Therefore, OD value from group three, purified Acsurf_VP2-E^{TRUN} BV, was found to be not statistically different than the value of its corresponding negative control antigen group five (t-test p=0.3804). On the other hand, even though the value from group four was low, it was still statistically higher than its corresponding negative control antigen group six (t-test p=0.0128). Overall, these results showed that full-length VP2 antigen groups induced high levels of AHSV4-VP2-specific antibodies whereas fragment E antigens especially from group three were poor immunogens.

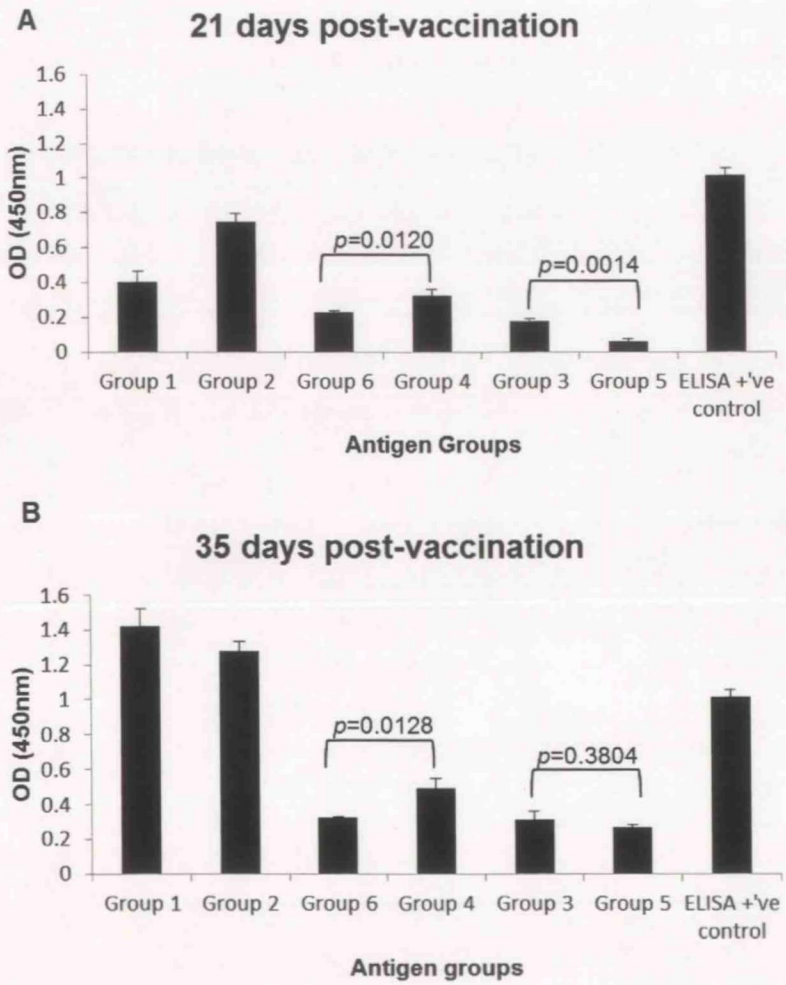


Figure 6.10 Analysis of post-vaccination serum antibodies by ELISA

Raw data for this figure was kindly generated by Dr Eva Calvo at CISA-INIA in Valdeolmos, Spain and the generation of graphs and the statistical analysis were carried out by the author of this thesis.

An indirect ELISA was carried out to analyse the AHSV4-VP2-specific antibodies generated in mice 21 **(A)** and 35dpv **(B).** Each antigen group is represented by the average OD obtained from five group-specific mice. Group 1: Purified $VP2^{HIS/N}$, Group 2: $AcVP2^{HIS/N}$-infected TnHi5 cells, Group 3: Purified Acsurf_VP2-E^{TRUN} BV, Group 4: Acsurf_VP2-E^{TRUN}-infected TnHi5 cells, Group 5: Purified $Acsurf^{TRUN}$ BV, Group 6: $Acsurf^{TRUN}$-infected TnHi5 cells, ELISA positive (+'ve) control is serum from MVA-VP2 vaccinated mice. The graph was generated using the mean OD of group-specific mice after subtracting the mean OD of blank from each sample. Error bars represent the standard error of each group. An unpaired t-test was carried out to compare each group of antigen to its corresponding negative control group. Groups three/five t-test p=0.0014 **(A)**, t-test p=0.3804 **(B)**; Groups four/six t-test p=0.0120 **(A)**, t-test p=0.0128 **(B)**. Raw data can be found in Appendix 7.

6.4.4 Analysing the virus neutralization capacity of post-vaccination serum antibodies by plaque reduction neutralization test

In order to test the capability of post-vaccination serum antibodies to neutralize AHSV4, a plaque reduction neutralization test (PRNT) was carried out by Dr Eva Calvo at CISA-INIA

in Valdeolmos, Spain. This assay has been widely used to measure the neutralisation capacity of target specific antibodies for several viruses including AHSV (Kanai *et al.*, 2014) and Dengue viruses (Thomas *et al.*, 2009). Briefly, a series of 35dpv serum dilutions (60µl) were incubated with 100pfu of AHSV4 (60µl) overnight at 4°C. The next day serum/virus mix was inoculated onto VERO cells (50-70% confluent) for 1 hour, which was followed by the medium/agar overlay. After five days incubation at 37◦C, live cells were stained by crystal violet and clear plaques were counted. Virus only samples were used as a negative control and serum from MVA-VP2 vaccinated mice was used as a positive control. The average plaque number obtained from five mice in each group was calculated by the author (Table 6.3).

Table 6.3 Average plaque count from each antigen group

Antigen Groups	Serum dilutions				
	1/10	1/20	1/40	1/80	1/160
Group 1	2	6	7	8	12
Group 2	2	5	6	9	15
Group 3	54	55	58	57	56
Group 4	46	48	50	55	56
Group 5	60	54	59	57	57
Group 6	57	53	58	61	60
Positive serum	n/a	n/a	7	10	16

*Average plaque count for virus only sample was 59

**Positive serum: mouse antiserum from MVA-VP2 post vaccination

Percentage neutralization capacity of antibodies from each group (Table 6.4) was calculated by the author using the following formula below:

=100-(Test plaque count*100/virus only plaque count)

The data were interpreted based on the standard 50% neutralisation potency estimate hence the values above 50% were accepted as positive for their capability in virus neutralisation.

Table 6.4 Virus plaque reduction percentages of pooled post-vaccination serum samples from vaccinated mice

Antigen Groups	Serum Dilutions				
	1/10	1/20	1/40	1/80	1/160
Group 1	96	90	89	86	80
Group 2	96	92	89	84	75
Group 3	8	6	1	4	5
Group 4	22	18	15	7	5
Group 5	-2	8	0	3	3
Group 6	3	10	2	-3	-2
Positive serum	n/a	n/a	88	83	73

Post-vaccination serum antibodies from groups one and two were shown to have a very high neutralizing capacity for AHSV4 (Table 6.4). On the other hand group three showed no neutralization capacity, which was similar to the levels observed by negative control antigen groups (five and six). This correlated with the ELISA data from Figure 6.10, suggesting that purified Acsurf_VP2-E^{TRUN} BV is a poor immunogen and the antibodies generated have no neutralizing capacity against AHSV4. In the case of antibodies generated by group four antigens (Acsurf_VP2-E^{TRUN}-infected TnHi5 cells), up to 22% neutralization capacity was observed, however values below 50% were not considered as significant.

6.5 Discussion

The importance of VNAbs to provide complete protection against AHSV was extensively reported in both mice and horses using several experimental MVA- (Chiam *et al.*, 2009, Castillo-Olivares *et al.*, 2011, Alberca *et al.*, 2014), baculovirus- (Roy *et al.*, 1996, Scanlen *et al.*, 2002, Kanai *et al.*, 2014) and DNA-based (Romito *et al.*, 1999) vaccines. However, the possible role of cell-mediated immunity was also raised by a number of studies, where a specific $CD8^+$ T-cell response was generated after vaccination with recombinant canarypox AHSV vaccine (El Garch *et al.*, 2012), live-attenuated AHSV vaccine (Pretorius *et al.*, 2012), and recombinant MVA-based vaccine (de la Poza *et al.*, 2013). Furthermore, a more recent study by Calvo-Pinilla *et al.* (2015) investigated the possible roles of humoral and cell-mediated immunity in an AHSV mouse model after passive immunization with antiserum or splenocytes from MVA-VP2 vaccinated mice. It was shown that mice immunized with antiserum (VNAb) were highly protected against clinical symptoms and viremia whereas the survival rate of mice immunized with splenocytes were only 40%. This suggested that cell-mediated immunity does not play a critical role in the clinical protection against AHSV when MVA-VP2 vaccines are used (Calvo-Pinilla *et al.*, 2015). As the role of VNAbs is more extensively reported in the literature, investigation of antigen-specific VNAb production was the target interest in this thesis.

The main focus of this chapter was therefore to investigate the antigenicity of VP2 subdomains produced in chapter five, so that the VN epitopes of VP2 could be mapped and the capability of VP2 subdomains to mimic these epitopes could be determined. This was carried out by testing the binding of a range of AHSV4-VP2-specific antibodies *in vitro*, which was followed by a pilot vaccination experiment *in vivo* in mice.

The reliable expression of various VP2 subdomains using baculovirus surface display constructs enabled the investigation of their relative contribution to the formation of different epitopes, including those involved in virus neutralisation. Initially an indirect

ELISA was carried out to test the binding of a panel of AHSV4-VP2 specific MAbs. It was confirmed that all these antibodies bind to baculovirus-expressed full-length VP2 (Figure 3.11). More importantly the panel of MAbs were shown previously to bind AHSV4 virions (Martinez-Torrecuadrada *et al.*, 1996), which would suggest that subdomains detected by these MAbs should represent similar epitopes.

6.5.1 Analysis with non-neutralising monoclonal antibodies

Analysis by indirect ELISA suggested that MAbs belonging to antigenic site V, which according to Martinez-Torrecuadrada *et al.* (1996) contains linear epitopes of VP2, recognized epitopes within the amino acid region 253-357 (Figure 6.1, Table 6.1). This was in line with previous findings where *E. coli*-expressed VP2 fragments within the amino acid region of 200-413 were also detected with these antigenic site V MAbs (Martinez-Torrecuadrada and Casal, 1995). While none of the *E.coli*-expressed VP2 fragments outside this region was detected by these antibodies, 8AE6, 8DB11 and 8CB11 were shown to weakly bind subdomains A (amino acids 1-182), G (amino acids 760-955) and Z (566-1060). Although these antibodies are suggested to recognize linear epitopes, it might be possible for them to have a weak affinity to epitopes with similar properties at distant locations or that these linear domains are part of larger conformational epitope together with other distant domains of VP2; however, this requires further investigation.

The majority of MAbs belonging to antigenic sites I, II, IV and VI only bound to the full-length VP2 but not to the subdomains in the indirect ELISA (Table 6.1). According to Martinez-Torrecuadra *et al.* (1996), these sites are considered as non-linear epitopes of VP2. This was further supported by the western blot analysis in this thesis, which resulted in 6AF2 MAb (antigenic site IV) not detecting full-length VP2 under denaturing conditions (Figure 6.2). Therefore, the fact that these MAbs did not bind to any of the VP2 subdomains in the indirect ELISA strongly suggests that these conformational epitopes were not mimicked by individual subdomains.

Although 8BG9 MAb belongs to antigenic site IV, expected to recognize non-linear epitopes, it was interesting to observe that it presented weak binding to fragments C, E, F, I, J and H in the indirect ELISA as well as the full-length VP2 (Figure 6.1, Table 6.1). This raised the question of whether 8BG9 does actually belong to antigenic site V instead of IV or as suggested above there are epitopes formed by linear subdomains in the central region and additional distant subdomains of VP2. In order to investigate this further, a western blot analysis was carried out, which resulted in the detection of VP2 using 8BG9 under denaturing conditions. These results strongly suggested 8BG9 to recognize linear

epitopes of VP2 hence possibly binding to antigenic site V and antigenic site IV simultaneously.

6.5.2 Analysis with neutralising monoclonal antibodies

In the case of MAbs with virus neutralisation capacity; 10BE7, 10BG7, 10AH5 and 8CH7 did not bind to any of the subdomains in the ELISA, while strongly binding to full-length VP2 (Table 6.1). On the other hand, 8DH3, SMAA and 10BC12 detected subdomains that are distant from each other including subdomains in the carboxy terminus, which are located outside the previously identified antigenic domain of AHSV4-VP2 (aa 200 to 413, Martinez-Torrecuadrada and Casal, 1995). A previous study also showed SMAA to bind epitopes that were in distant regions from each other during a PEPSCAN analysis of AHSV4-VP2. The same PEPSCAN analysis identified only a single peptide for 8DH3 antibody, which overlaps with one of the regions identified for 8DH3 binding in this study. However, it should be noted that the PEPSCAN analysis was only carried out between the amino acid region 199-689 and not the whole protein sequence (Martinez-Torrecuadrada *et al.*, 2001).

Interestingly, antibodies raised in rabbits against the peptide identified by 8DH3 in the PEPSCAN, were shown not to neutralise AHSV4 infectivity. This is contradicting with the results of an earlier study by Martinez-Torrecuadrada *et al.* (1996), where they have shown 8DH3 antibody itself to neutralise the infectivity of AHSV4 virions. All this information could suggest that a single peptide is not sufficient to generate VN antibodies and other parts of the protein are required for successful display of VN epitopes. More importantly, this could suggest that fragment Z region of the carboxy terminus detected by 8DH3 in the indirect ELISA (Figure 6.1, Table 6.1) may play a crucial role in the formation of VN epitopes recognized by 8DH3.

8DH3 was also shown to recognize full-length VP2 under denaturing conditions on a western blot, which could suggest these epitopes to be linear. However, the fact that 8DH3 recognizes additional epitopes in the carboxy terminus, suggests that the linear epitopes detected in the western blot constitutes to the formation of a larger conformational epitope.

The possible involvement of carboxy terminus was also reported in the literature for another AHSV serotype when Bentley *et al.* (2000) studied the antigenic structure of AHSV3-VP2 using a phage display library. Although the main antigenic determinants were mapped to be in the amino terminal half of the protein, a neutralising MAb was shown to detect residues in the carboxy terminus (Bentley *et al.*, 2000). Altogether, these results suggest that neutralising epitopes of AHSV-VP2 are most likely discontinuous and are

assembled after conformational folding of the protein. More importantly this raises the question whether important neutralising epitopes of AHSV-VP2 lay outside the central (aa 368-483) and tip (279-368) domains of the VP2 triskelion that was suggested by Manole *et al.* (2012) and that carboxy terminus plays an important role for the display of VP2 antigenic epitopes.

6.5.3 Analysis with MVA-VP2 post-vaccination equine serum

Overall, the analysis using AHSV4-VP2-specific MAbs suggested that the linear epitopes of VP2 could be successfully mimicked by the subdomains expressed using baculovirus surface display constructs. However, it is more difficult to mimic conformational epitopes with individual subdomains. Therefore, it would be interesting to test the binding pattern of these subdomains to antibodies in equine VN serum obtained from MVA-VP2 post vaccination. Initial analysis with this serum using an indirect ELISA showed that only fragments E, F and I were detected weakly that share a common amino acid region (aa 413-472), which is not overlapped by any of the other subdomains produced in this thesis (Figure 6.1). Thus, this region could be mapped as important for detection with antibodies from MVA-VP2 post vaccination serum. When the same serum was used in the western blot under denaturing conditions, additional subdomains were detected suggesting the presence of linear epitopes, most likely within the amino acid region 253-414.

It is important to remark that even though fragment H and other subdomains overlapping its region were detected by several MAbs in the ELISA (Table 6.1) and by MVA-VP2 post-vaccination serum in the western blot, the majority of these subdomains were not detected by this serum in the indirect ELISA. This could suggest that antibodies produced in mouse and horses may recognize different epitopes. This possibility was also reported by a previous study, where they have shown that fragment H (aa 253-414) induced VNAbs both in mice and rabbits but did not block the activity of VNAbs from naturally-infected horses (Martinez-Torrecuadrada and Casal, 1995).

Therefore, the amino acid region 413-472 identified in this thesis (Figure 6.1), could contain a potential antigenic epitope of AHSV4-VP2 that is important for recognition by antibodies produced in horses. However, it should be noted that the equine VN serum used in this thesis was from animals vaccinated with MVA-VP2 hence further analysis is required using serum from naturally-infected horses to test the importance of this region.

6.5.4 Analysis of post-vaccination serum from mice

6.5.4a Immunogenicity of full-length VP2

It should be noted that the epitopes recognized by antibodies from VN serum does not necessarily correlate with virus neutralisation as the serum comprises a heterogeneous mix of polyclonal VP2-specific antibodies, some of which are neutralising and some of which are not. It was, therefore, important to move forward with *in vivo* vaccination experiments in mice, which would provide better understanding of the biological functions of the antigen. The analysis of post-vaccination serum antibodies showed that both affinity-purified VP2 and VP2 from crude TnHi5 cell lysates were capable of inducing high levels of VNAbs in mice. This is consistent with previous findings where recombinant full-length VP2 was found to be very efficacious in generating VNAbs (Roy *et al.*, 1996, Scanlen *et al.*, 2002, Kanai *et al.*, 2014).

Martinez Torrecuadrada *et al.* (1996) used a similar vaccination strategy as in this thesis where they immunized horses either with purified VP2 or infected Sf9 cells containing VP2. Interestingly, both forms of the protein were reported to be poor immunogens unlike the results of this thesis. They have shown that clinical protection against lethal AHSV4 was conferred only when VP2 was injected together with other capsid proteins, VP5 and VP7. However, this was only achieved with non-purified proteins as when purified forms of VP2, VP5 and VP7 were used together, only partial protection was achieved where the horse survived a lethal virus challenge but viremia was observed. As it was discussed in detail in chapter three of this thesis, their purification method using antibody affinity chromatography could have altered the structure of VP2, which resulted in poor immunogenicity they observed in their vaccination study. In this thesis however, poly-histidine tag affinity purification was used and this purified VP2 was shown to represent the native viral protein as it was detected by AHSV4-specific MAbs (Figure 3.11). In addition, generation of AHSV4-specific VNAb in mice (Figure 6.10, Table 6.4) confirmed that poly-histidine tag affinity purification retained the biological function of the protein.

On the other hand, using the same baculovirus construct as Martinez-Torrecuadrada *et al.* (1996), Roy *et al.* (1996) has reported that soluble VP2 on its own from Sf9 cell extracts was capable of generating protective levels of VNAbs in horses. The reason for these conflicting results might be due to the amount of soluble VP2 present in the inoculation prepared by Martinez-Torrecuadrada *et al.* (1996). In a different study, Du Plessis *et al.* (1998) reported partial protection (survival with severe AHS symptoms) in horses when they were inoculated with VP2 in crude Sf9 cell lysates. Their further investigation of the inoculum revealed that only 10% of the VP2 produced in Sf9 cells was soluble. Follow-up

experiments in guinea pigs using soluble and aggregated VP2 showed that presence of soluble proteins in the inoculum was crucial for generating VNAb (Du Plessis *et al.*, 1998). In addition, high immunogenicity of soluble VP2 was also proven in horses, where a complete clinical protection was observed (Scanlen *et al.*, 2002). In this thesis however, use of TnHi5 cells eliminated the problems encountered by previous studies using Sf9 cells for the production of VP2.

6.5.4b Immunogenicity of fragment E

Post-vaccination serum analysis showed that both forms of fragment E antigens were poor immunogens and the antibodies generated were incapable of neutralising AHSV4 infectivity in a monolayer protection assay. A number of technical points should be taken into consideration before a final conclusion could be drawn. For instance, in the case of group three antigens, the amount of fragment E incorporated into purified BV particles was unknown therefore; insufficient levels of antigens delivered by this strategy might be the reason for the outcome. On the other hand, both fragment E antigens were presented as membrane-bound proteins, which made them insoluble. Considering the fact that solubility of VP2 from Sf9 cells was shown to be crucial for the generation of VNAbs, (Du Plessis *et al.*, 1998), it could be suggested that insolubility was responsible for the poor immunogenicity observed from fragment E antigens in this thesis. Therefore, it would be very useful to test the capability of solubilized fragment E to generate VNAbs in future analysis.

Furthermore, Du Plessis *et al.* (1998) showed that initially doing a single booster immunization in horses with recombinant baculovirus-infected Sf9 cell lysates containing 50µg VP2 did not induce significant titres of VNAbs, which were then raised by a second booster with an increased amount of antigen. Therefore, it would be interesting to investigate this with fragment E antigens, to test whether their immunogenicity could be enhanced with a second booster immunization.

All these technical points discussed above could eventually improve the results of fragment E immunogenicity. However, it should be noted that the binding of AHSV4-specific MAbs to VP2 subdomains demonstrated the difficulty of representing VP2 conformational epitopes as well as those involved in virus neutralisation, using individual subdomains. Hence, poor immunogenicity could be due to fragment E being insufficient at mimicking VN epitopes of the protein on its own and that highly conformational structure of the full-length protein is required for virus neutralisation. However, the immunogenicity of all the remaining constructs, especially fragments F and I are required to be tested, before a solid conclusion could be drawn.

6.6 Conclusion

In conclusion, this chapter has shown with the use of AHSV4-specific MAbs that VP2 subdomains expressed by baculovirus surface display constructs (aa 253-413) can mimic linear epitopes of VP2. On the other hand, it was demonstrated that mimicking of VP2 conformational epitopes using individual subdomains is more difficult. However, analysis by MAbs suggested a possible role of carboxy terminus, which could be important in the formation of conformational epitopes, including those involved in virus neutralisation. In addition, a potential antigenic epitope (aa 413-472) that could be important for recognition by equine antibodies was proposed after testing with MVA-VP2 post-vaccination serum, however further analysis is required using antibodies generated from natural infection to understand the importance of this region.

Due to time limitations, immunogenicity of only one subdomain, fragment E, could be tested in the *in vivo* immunization experiments in mice, however the results were inconclusive. As the binding pattern of neutralising MAbs demonstrated the importance of VP2 conformational epitopes, it could be suggested that it might be difficult to represent VP2 VN epitopes using individual subdomains. However, further analysis is required to initially test other individual VP2 subdomains such as fragments F and I but more importantly multiple subdomains simultaneously to see whether VN epitopes could be represented with the combination of different epitopes. By this way, we could have a better understanding of VP2 antigenic structure.

In the case of full-length VP2, this chapter has shown for the first time in literature that poly-histidine tag affinity-purified VP2 elicits AHSV4-specific VNAbs in mice. Furthermore, use of infected-TnHi5 cells was shown to be a viable platform for the delivery of antigens in immunization studies of mice.

Chapter 7
Final Discussion and Future Work

7.1 Introduction

The disease caused by AHSV is lethal for horses and prevention is mainly dependent on an efficient vaccination regime. However, currently available vaccines are live-attenuated viruses and are not considered safe for use in disease-free regions. The safety concerns are mainly due to the risk of reversion to virulence and the risk of re-assortment between the vaccine and the wild-type viruses and the sub-sequent generation of novel strains of unpredictable biological characteristics. For these reasons, alternative vaccination strategies for AHS have been pursued for the last three decades.

Sub-unit protein vaccines developed using baculoviruses are an option for generating safe vaccines, as shown by the approval of baculovirus-generated commercial vaccines such as Cervarix (Harper *et al.*, 2004, Paavonen *et al.*, 2007, Monie *et al.*, 2008) and Flublok (Wang *et al.*, 2006, Cox *et al.*, 2008, McPherson, 2008, Cox and Hollister, 2009). These subunit vaccines could be in the form of purified proteins (McPherson, 2008), virus-like particles (VLPs, Paavonen *et al.*, 2007) or as baculovirus BV particles displaying the recombinant proteins on their envelope surface, which has also been shown to be a promising vaccine approach (Tami *et al.*, 2004, Lin *et al.*, 2008, Xu *et al.*, 2011).

Although BV cannot replicate in mammalian cells, there are reports indicating that BV on itself can have an immunogenic effect in mice (Gronowski *et al.*, 1999, Abe *et al.*, 2003, Abe *et al.*, 2005). Moreover, BV were shown to have strong adjuvant characteristics in mice, inducing target-specific, robust humoral and CD8 T-cell adaptive responses when target antigen and BV were administered simultaneously (Hervas-Stubbs *et al.*, 2007). Hence, using baculovirus surface display as a vaccine approach could have an added advantage over using individual purified proteins.

As AHSV is transmitted by *Culicoides* species, it replicates in the cells and tissues of its arthropod vector before it can be transmitted to a mammalian host. Therefore, the use of baculovirus-insect cell expression increases the chances of producing AHSV proteins, which mimic the natural folding of the viral capsid protein before infecting the mammalian host. AHSV-VP2 is a good target to be used for subunit vaccine studies, as it has been shown to be the major viral protein carrying virus neutralizing epitopes (Ranz *et al.*, 1992, Burrage *et al.*, 1993).

The overall aim of this thesis was to investigate further the antigenic structure of AHSV4-VP2 and define better the nature of VN epitopes. This was carried out by the expression of full-length VP2 and eleven subdomains thereof using the baculovirus expression and surface display approaches. Furthermore, the capability of VP2 subdomains to mimic VN

epitopes would be determined. Understanding the antigenic structure of the protein is very valuable for generating more effective vaccines in future.

7.2 Discussion of results and future work

7.2.1 Analysis of full-length VP2

Recombinant VP2 produced by baculoviruses was previously shown to be immunogenic both in guinea pigs (Du Plessis *et al.*, 1998, Kanai *et al.*, 2014) and horses (Roy *et al.*, 1996, Scanlen *et al.*, 2002). In this thesis modifications from this technology were investigated and resulted in improved AHSV-VP2 antigen preparation, which translated into higher yields and increased immunogenicity. Previous studies encountered low-yield insoluble protein production in Sf9 cells (Martinez-Torrecuadrada *et al.*, 1994, Du Plessis *et al.*, 1998), which in some cases was slightly improved by the co-expression of VP5 capsid protein (Martinez-Torrecuadrada *et al.*, 1994). However, this thesis has demonstrated that high-yields of VP2 can be achieved when expressed in adherent cultures in an alternative insect cell line (TnHi5 cells; Chapter three). Du Plessis *et al.* (1998) reported that only 10% of the VP2 protein produced in Sf9 cells was soluble. As the soluble VP2 produced in TnHi5 cells in this thesis was sufficient for purification and downstream analysis, the ratio of soluble/insoluble protein was not determined. However, it would be interesting to investigate this in the future so that the benefits of TnHi5 cells for the production of recombinant VP2 can be demonstrated quantitatively.

It is also important to highlight that by using polyhistidine-tag affinity purification in this thesis, AHSV-VP2 immunisation resulted in the induction of high VNAb titres. This contradicts with previous findings because Martinez-Torrecuadrada *et al.* (1996) previously demonstrated that antibody-affinity-purified VP2 was poorly recognized by AHSV4-specific MAbs and did not induce VNAbs in horses. It is hypothesised that perhaps the purification method used in those studies (affinity chromatography with polyclonal AHSV4 antisera) altered the structure of AHSV-VP2. Alternatively, it is possible, as demonstrated in this thesis, that the increased immunogenicity of both polyhistidine tag-purified VP2 and non-purified recombinant VP2 produced in TnHi5 cells, is directly related to the expression levels achieved in this system (Chapter six). Further studies aimed at testing the stability and immunogenicity of affinity purified VP2, are warranted as this system could result in improved manufacturability of this type of vaccines. Martinez-Torrecuadrada *et al.* (1996) reported that the purified VP2 in their study was relatively unstable after seven-month's storage at -20°C. In this thesis, purified VP2 that had been stored at 4°C for at least ten months was found to be stable for *in vitro* analyses such as ELISA and western blotting. Therefore, it will be useful to determine the

stability of its biological functionality *in vivo*. Having a stable purified protein would be very beneficial for using in vaccines.

Native VP2 is known to form trimers on the outer capsid layer of AHSV (Manole *et al.*, 2012). Confirmation of whether trimer formation is preserved in baculovirus-expressed VP2 remains to be determined as this could be a critical factor of its immunogenicity. This could be achieved by analysing VP2 on native PAGE under non-denaturing conditions; hence any oligomerization can be visualized. Trimerisation has been shown to play an important role in the immunogenicity of other viral surface proteins such as influenza virus HA (Wei *et al.*, 2008) and human immunodeficiency virus GP140 (Kovacs *et al.*, 2012), when compared to their monomeric forms. Further studies are therefore warranted to determine whether VP2 trimerisation is critical for VNAb epitope formation. Analysing this for VP2 will greatly contribute to unrevealing the antigenic structure of the protein. Additionally, VP2 subdomains (section 7.2.2) could be optimized based on this information to try and mimic the domains potentially brought together by trimerisation.

As the full-length VP2 was shown to be successfully purified in biologically active form using polyhistidine-tag affinity purification, it will be interesting to take this forward for crystallographic analysis. If the crystal structure of VP2 could be solved, then immunogenic epitopes of the protein would be better-understood, leading to the design of more effective vaccines. Furthermore, if the molecular structure of the protein is known, its interactions with other viral capsid proteins such as VP5 and VP7 as well as host cell surface receptors will be better understood, which will contribute to the knowledge of this protein's role in the overall virus replication.

Finally, attempts were made to display the full-length AHSV-VP2 on the baculovirus envelope surface as a fusion to the transmembrane domain of GP64, however, the production of a fusion protein could not be detected, unlike with subdomains of VP2, in the cells at any time post-infection (Chapter 4). The underlying reason for this was not investigated at the time, but it would be interesting to carry out a reverse transcription (RT-) PCR to understand whether the problem was at the gene expression stage. Otherwise, it could be suggested that the protein is synthesised but at such low levels that it could not be detected, or it was not stable in the cells and targeted for degradation.

7.2.2 Analysing VP2 subdomains

7.2.2a Production of VP2 subdomains

AHSV4-VP2 has been shown to be the main antigenic determinant carrying VN epitopes. Although the amino terminal half of the protein was found to be more antigenic (Martinez-

Torrecuadrada and Casal, 1995), the VN epitopes of the protein are yet to be defined. Hence, this thesis aimed at gaining further understanding of VN epitopes by expressing subdomains of the protein. These subdomains were chosen mainly from the amino-terminal half of the protein based on the previous findings (Martinez-Torrecuadrada and Casal, 1995). However, additional subdomains covering the carboxy terminus were also included in this thesis so that the whole protein was covered.

When these subdomains were produced individually with a histidine tag, their expression could only be detected in TnHi5 cells and yields were very low and the proteins largely insoluble. Regardless of treatments with guanidinium hydrochloride and urea, the solubility could not be improved sufficiently and hence these subdomains were not taken forward for further study as purified proteins (Chapter three). This problem could be addressed in the future by the use of alternative fusion/purification tags such as SUMO or GST, which have been shown to improve protein solubility and purification (reviewed by Costa *et al.*, 2014).

In this thesis, the yield of VP2 subdomains was greatly enhanced when produced as a chimeric protein with GP64 in the surface display constructs. In order to pin point whether the improved protein yield was due to the presence of the GP64 signal peptide or the TMD, additional studies including constructs which only contain a signal peptide could be done in the future. This would help understand better whether trafficking through the secretory pathway due to signal peptide or anchorage in the plasma membrane through the TMD is responsible for the enhanced yield of the subdomains. Additionally, these constructs would show whether the subdomains could be secreted into the culture medium. If that were the case and the yields were high, this would be very advantageous as the subdomains could be isolated from the culture medium by using centrifugal filter concentrators, which would remove lower molecular weight protein contaminants and they could be used in immunization studies. Alternatively, purification tags could be added to purify the proteins, however, this would require the generation of additional recombinant baculovirus constructs.

It will also be worth carrying out native PAGE to check whether the currently produced subdomains form oligomers. In the case of fragment H, a possible SDS-resistant dimer was detected in the western blots (Chapters four and five). The information obtained from this analysis might indicate the domains involved in overall VP2 trimerisation.

Regarding the baculovirus surface display of the VP2 subdomains, this thesis has provided evidence of their incorporation into BV as proteins could be clearly detected in sucrose-gradient purified virus particles. However, their display on the BV envelope

surface is yet to be confirmed as the chimeric proteins could not be detected in the envelope fraction, following BV fractionation analysis (Chapter five). As discussed previously, this could be due to several reasons including, protein degradation upon detergent treatment or low protein yield. This could be analysed by carrying out a larger scale fractionation assay including protein inhibitors to prevent degradation. However, the best way to reveal the localization of the proteins would be the use of target-specific antibodies in immuno-gold electron microscopy imaging as previously used for the detection of avian reovirus capsid proteins (Lin *et al.*, 2008) and envelope glycoprotein of Japanese encephalitis virus (Xu *et al.*, 2011) on BV envelope surface.

This thesis investigated the use of different promoters and cell lines for surface display constructs and shown that the use of *polh* promoter (Chapter four) and TnHi5 (Chapter five) cells were the optimum conditions for the production of AHSV4-VP2 subdomain chimeric proteins. However, currently the ratio of chimeric protein to native GP64 incorporated into the BV envelope is unknown. Hence, if these constructs would be taken forward either as vaccines or for studying protein-protein interactions, it would be very beneficial to maximise the amount of chimeric proteins incorporated into BV particles. This could be approached by generating GP64-null viruses, which would only enable the display of recombinant proteins on envelope surface. However, a crucial step for this approach to be viable would be the generation of GP64 complementing cell line hence the virus stocks could be propagated in these cells. Otherwise the viruses lacking native GP64 will be incapable of replication. This should be achievable as recovering the infectivity of GP64-null virus with GP64 from a complementing cell line was previously established (Monsma *et al.*, 1996). However, anecdotal evidence (personal communication with RD Possee) suggests that genes can be restored to the virus genome when a null-virus is propagated in a cell line complementing the gene that was deleted.

An alternative approach would be to use small interfering RNA (siRNA) to knock down native GP64. In this case, the same surface display constructs described in this thesis would be used and at the final stage, the amplification of virus particles would be carried out in cells treated with siRNA, targeting the knock-down of native GP64. Hence, the chimeric protein incorporation into BV could potentially be maximised.

7.2.2b Characterization of VP2 subdomains

In respect to the antigenicity of the VP2 subdomains, it has been shown that linear antigenic epitopes of VP2 could be expressed using baculovirus surface display constructs. However, it was shown to be more difficult to mimic the conformational

epitopes of the protein using individual subdomains. Some of the MAbs such as 10BC12 with neutralisation capacity detected subdomains both in the amino terminal half and the carboxy terminus of the protein. This strongly suggested that these epitopes are discontinuous, which are brought together after conformational folding of the protein or formation of VP2 trimers. Although the main antigenic domain of AHSV4-VP2 was mapped to the amino terminal half (aa 253-413), the results from this thesis (chapter 6) indicated that the carboxy terminus could also have a role in the formation of important antigenic epitopes; which might explain why it is difficult to represent the conformational epitopes of the protein using individual subdomains.

Due to time limitations, only one of the subdomains, Fragment E could be tested in mice for its capability to induce VNAbs. Although fragment E was recognized by several MAbs including those with virus neutralisation capacity *in vitro*, it was found to be a poor immunogen, not generating VNAbs in mice. Technical issues such as insufficient immunization dose or insolubility could be responsible for this outcome as discussed previously (chapter six) however, it should be noted that Fragment E was only one of the eleven subdomains produced in this study. Thus the remaining subdomains, especially fragments F and I should be tested in mice for their immunogenicity.

The possible role of carboxy terminus in the formation of important antigenic epitopes and the difficulty of mimicking the conformational epitopes of the protein raises the question whether AHSV neutralisation is a multifunctional, synergistic process. It could be that the binding of some antibodies causes a conformational change in the virus structure, which then exposes other epitopes enabling a more potent neutralization in the host. Furthermore, Manole *et al.* (2012) proposed that central domain of VP2 triskelion (aa 368-483) could be the possible target for cleavage by horse serum proteases, which might also alter the conformation of the protein. Hence it would be very interesting to use multiple VP2 subdomains and analyse the effect of their combination on representing VN epitopes. In a previous study, rabbit immunizations carried out with the combination of two antigenic peptides was shown to enhance the neutralizing activity (Martinez-Torrecuadrada *et al.*, 2001).

In a different approach, BV particles displaying VP2 subdomains could also be used to study other roles of VP2 in virus life cycle such host cell binding and virus internalization. This could be tested by altering the surface display constructs to contain a reporter gene, ie; EGFP, under a mammalian promoter such as cytomegalovirus immediate early one promoter (CMV *ie1*). This would allow the interaction of subdomains with host cell surface receptors to be studied and could identify the domains of the protein responsible for cell attachment and virus internalization. The reporter gene will serve as an indicator for virus

internalization. It should be noted that these constructs should be generated as GP64-null viruses as GP64 is known to mediate mammalian cell entry (Kataoka *et al.*, 2012).

7.3 Concluding remarks

There is still a substantial room for exploring and understanding the antigenic structure of this highly conformational, complex protein and resolving its molecular structure by crystallography would be very advantageous in answering these questions. This thesis has concluded that the use of subdomains is not sufficient to mimic VN epitopes, whereas the full-length VP2 was shown to be an efficacious vaccine target.

References

ABE, T., HEMMI, H., MIYAMOTO, H., MORIISHI, K., TAMURA, S., TAKAKU, H., AKIRA, S. & MATSUURA, Y. (2005). Involvement of the Toll-like receptor 9 signaling pathway in the induction of innate immunity by baculovirus. *J Virol,* 79**,** 2847-58.

ABE, T., TAKAHASHI, H., HAMAZAKI, H., MIYANO-KUROSAKI, N., MATSUURA, Y. & TAKAKU, H. (2003). Baculovirus induces an innate immune response and confers protection from lethal influenza virus infection in mice. *J Immunol,* 171**,** 1133-9.

AFRICAN HORSE SICKNESS TRUST. (2016a). *African Horse Sickness Movement Policy* [Online]. Available: http://www.africanhorsesickness.co.za/Documents/doc_55.pdf [Accessed 29 November 2016].

AFRICAN HORSE SICKNESS TRUST. (2016b). *AHS Control information pamphlet, including maps of the control zones* [Online]. Available: http://www.africanhorsesickness.co.za/Documents/AHS%20Control%20Circular%20Aug%2020031.pdf [Accessed 29 November 2016].

ÅGREN, E., BURGIN, L., LEWERIN, S. S., GLOSTER, J. & ELVANDER, M. (2010). Possible means of introduction of bluetongue virus serotype 8 (BTV-8) to Sweden in August 2008: comparison of results from two models for atmospheric transport of the Culicoides vector. *Veterinary Record: Journal of the British Veterinary Association,* 167.

AGUERO, M., GOMEZ-TEJEDOR, C., ANGELES CUBILLO, M., RUBIO, C., ROMERO, E. & JIMENEZ-CLAVERO, A. (2008). Real-time fluorogenic reverse transcription polymerase chain reaction assay for detection of African horse sickness virus. *J Vet Diagn Invest,* 20**,** 325-8.

AIRENNE, K. J., HU, Y. C., KOST, T. A., SMITH, R. H., KOTIN, R. M., ONO, C., MATSUURA, Y., WANG, S. & YLA-HERTTUALA, S. (2013). Baculovirus: an insect-derived vector for diverse gene transfer applications. *Mol Ther,* 21**,** 739-49.

ALBERCA, B., BACHANEK-BANKOWSKA, K., CABANA, M., CALVO-PINILLA, E., VIAPLANA, E., FROST, L., GUBBINS, S., URNIZA, A., MERTENS, P. & CASTILLO-OLIVARES, J. (2014). Vaccination of horses with a recombinant modified vaccinia Ankara virus (MVA) expressing African horse sickness (AHS) virus major capsid protein VP2 provides complete clinical protection against challenge. *Vaccine,* 32**,** 3670-4.

ALEXANDER, K., KAT, P., HOUSE, J., HOUSE, C., O'BRIEN, S., LAURENSON, M., MCNUTT, J. & OSBURN, B. (1995). African horse sickness and African carnivores. *Vet Microbiol,* 47**,** 133-140.

ALEXANDER, R. A. & DU TOIT, P. J. (1934). The immunization of horses and mules against Horsesickness by means of the neurotropic virus of mice and guinea-pigs.

AYRES, M. D., HOWARD, S. C., KUZIO, J., LOPEZ-FERBER, M. & POSSEE, R. D. (1994). The complete DNA sequence of Autographa californica nuclear polyhedrosis virus. *Virology,* 202**,** 586-605.

BACHANEK-BANKOWSKA, K., MAAN, S., CASTILLO-OLIVARES, J., MANNING, N. M., MAAN, N. S., POTGIETER, A. C., DI NARDO, A., SUTTON, G., BATTEN, C. & MERTENS, P. P. (2014). Real time RT-PCR assays for detection and typing of African horse sickness virus. *PLoS One,* 9**,** e93758.

BARNARD, B. (1998). Epidemiology of African horse sickness and the role of the zebra in South Africa. *African Horse Sickness.* Springer.

BARNARD, B., BENGIS, R. G., KEET, D. & DEKKER, E. (1994). Epidemiology of African horsesickness: duration of viraemia in zebra (Equus burchelli).

BARRAL, J. M., BROADLEY, S. A., SCHAFFAR, G. & HARTL, F. U. (2004). Roles of molecular chaperones in protein misfolding diseases. *Semin Cell Dev Biol,* 15**,** 17-29.

BARSOUM, J., BROWN, R., MCKEE, M. & BOYCE, F. M. (1997). Efficient transduction of mammalian cells by a recombinant baculovirus having the vesicular stomatitis virus G glycoprotein. *Hum Gene Ther,* 8**,** 2011-8.

BELHOUCHET, M., MOHD JAAFAR, F., FIRTH, A. E., GRIMES, J. M., MERTENS, P. P. & ATTOUI, H. (2011). Detection of a fourth orbivirus non-structural protein. *PLoS One,* 6**,** e25697.

BENTLEY, L., FEHRSEN, J., JORDAAN, F., HUISMANS, H. & DU PLESSIS, D. H. (2000). Identification of antigenic regions on VP2 of African horsesickness virus serotype 3 by using phage-displayed epitope libraries. *J Gen Virol,* 81, 993-1000.

BETA. (2016). *National Equestrian Survey 2015* [Online]. British Equestrian Trade Association. Available: http://www.beta-uk.org/pages/industry-information/market-information.php [Accessed 29 December 2016].

BINEPAL, V., WARIRU, B., DAVIES, F., SOI, R. & OLUBAYO, R. (1992). An attempt to define the host range for African horse sickness virus (Orbivirus, Reoviridae) in East Africa, by a serological survey in some Equidae, Camelidae, Loxodontidae and Carnivore. *Vet Microbiol,* 31, 19-23.

BLANCHARD, P., MAHE, D., CARIOLET, R., KERANFLEC'H, A., BAUDOUARD, M. A., CORDIOLI, P., ALBINA, E. & JESTIN, A. (2003). Protection of swine against post-weaning multisystemic wasting syndrome (PMWS) by porcine circovirus type 2 (PCV2) proteins. *Vaccine,* 21, 4565-75.

BLISSARD, G. W. & WENZ, J. R. (1992). Baculovirus gp64 envelope glycoprotein is sufficient to mediate pH-dependent membrane fusion. *J Virol,* 66, 6829-35.

BODER, E. T. & WITTRUP, K. D. (1997). Yeast surface display for screening combinatorial polypeptide libraries. *Nat Biotechnol,* 15, 553-7.

BONNING, B. C. & HAMMOCK, B. D. (1992). Development and potential of genetically engineered viral insecticides. *Biotechnol Genet Eng Rev,* 10, 455-89.

BOORMAN, J., MELLOR, P., PENN, M. & JENNINGS, M. (1975). The growth of African horse-sickness virus in embryonated hen eggs and the transmission of virus byCulicoides variipennis Coquillett (Diptera, Ceratopogonidae). *Archives of virology,* 47, 343-349.

BORG, J., NEVSTEN, P., WALLENBERG, R., STENSTROM, M., CARDELL, S., FALKENBERG, C. & HOLM, C. (2004). Amino-terminal anchored surface display in insect cells and budded baculovirus using the amino-terminal end of neuraminidase. *J Biotechnol,* 114, 21-30.

BOSMAN, P., BRÜCKNER, G. & FAUL, A. (1995). African horse sickness surveillance systems and regionalisation/zoning: the case of South Africa. *Revue scientifique et technique (International Office of Epizootics),* 14, 645-653.

BOUAYOUNE, H., TOUTI, J., EL HASNAOUI, H., BAYLIS, M. & MELLOR, P. (1998). The Culicoides vectors of African horse sickness virus in Morocco: distribution and epidemiological implications. *African Horse Sickness.* Springer.

BOUBLIK, Y., DI BONITO, P. & JONES, I. M. (1995). Eukaryotic virus display: engineering the major surface glycoprotein of the Autographa californica nuclear polyhedrosis virus (AcNPV) for the presentation of foreign proteins on the virus surface. *Biotechnology (N Y),* 13, 1079-84.

BREMER, C. (1976). A gel electrophoretic study of the protein and nucleic acid components of African horsesickness virus. *The Onderstepoort journal of veterinary research,* 43, 193-199.

BREMER, C. W., HUISMANS, H. & VAN DIJK, A. A. (1990). Characterization and cloning of the African horsesickness virus genome. *J Gen Virol,* 71 (Pt 4), 793-9.

BROOKES, S. M., HYATT, A. D. & EATON, B. T. (1993). Characterization of virus inclusion bodies in bluetongue virus-infected cells. *Journal of general virology,* 74, 525-530.

BUHRMANN, G. (2016). *Veterinary Services Animal Health* [Online]. Western Cape Government. Available: http://www.savc.org.za/pdf_docs/Procedure%20for%20Blanket%20AHS%20Movement%20Ban%20Feb%202016.pdf [Accessed 29 November 2016].

BURRAGE, T. G. & LAEGREID, W. W. (1994). African horsesickness: pathogenesis and immunity. *Comp Immunol Microbiol Infect Dis,* 17, 275-85.

BURRAGE, T. G., TREVEJO, R., STONE-MARSCHAT, M. & LAEGREID, W. W. (1993). Neutralizing epitopes of African horsesickness virus serotype 4 are located on VP2. *Virology,* 196, 799-803.

CALVO-PINILLA, E., DE LA POZA, F., GUBBINS, S., MERTENS, P. P., ORTEGO, J. & CASTILLO-OLIVARES, J. (2014). Vaccination of mice with a modified Vaccinia Ankara (MVA) virus expressing the African horse sickness virus (AHSV) capsid protein VP2 induces virus neutralising antibodies that confer protection against AHSV upon passive immunisation. *Virus Res,* 180, 23-30.

CALVO-PINILLA, E., DE LA POZA, F., GUBBINS, S., MERTENS, P. P. C., ORTEGO, J. & CASTILLO-OLIVARES, J. (2015). Antiserum from mice vaccinated with modified vaccinia Ankara virus expressing African horse sickness virus (AHSV) VP2 provides protection when it is administered 48h before, or 48h after challenge. *Antiviral research,* 116, 27-33.

CARPENTIER, D. C., GRIFFITHS, C. M. & KING, L. A. (2008). The baculovirus P10 protein of Autographa californica nucleopolyhedrovirus forms two distinct cytoskeletal-like structures and associates with polyhedral occlusion bodies during infection. *Virology,* 371, 278-91.

CASTILLO-OLIVARES, J., CALVO-PINILLA, E., CASANOVA, I., BACHANEK-BANKOWSKA, K., CHIAM, R., MAAN, S., NIETO, J. M., ORTEGO, J. & MERTENS, P. P. (2011). A modified vaccinia Ankara virus (MVA) vaccine expressing African horse sickness virus (AHSV) VP2 protects against AHSV challenge in an IFNAR -/- mouse model. *PLoS One,* 6, e16503.

CHAPPLE, S. D. & JONES, I. M. (2002). Non-polar distribution of green fluorescent protein on the surface of Autographa californica nucleopolyhedrovirus using a heterologous membrane anchor. *J Biotechnol,* 95, 269-75.

CHARLTON, C. A. & VOLKMAN, L. E. (1986). Effect of tunicamycin on the structural proteins and infectivity of budded Autographa californica nuclear polyhedrosis virus. *Virology,* 154, 214-8.

CHIAM, R., SHARP, E., MAAN, S., RAO, S., MERTENS, P., BLACKLAWS, B., DAVIS-POYNTER, N., WOOD, J. & CASTILLO-OLIVARES, J. (2009). Induction of antibody responses to African horse sickness virus (AHSV) in ponies after vaccination with recombinant modified vaccinia Ankara (MVA). *PLoS One,* 4, e5997.

CHUMA, T., LE BLOIS, H., SANCHEZ-VIZCAINO, J. M., DIAZ-LAVIADA, M. & ROY, P. (1992). Expression of the major core antigen VP7 of African horsesickness virus by a recombinant baculovirus and its use as a group-specific diagnostic reagent. *J Gen Virol,* 73 (Pt 4), 925-31.

COETZER, J. & GUTHRIE, A. (2005). African horsesickness. *Infectious Diseases of Livestock.* Second ed. Cape Town: Oxford University Press.

COOPER, G. M. (2000). The endoplasmic reticulum. *The cell: A Molecular Approach.* 2nd ed. Sunderland (MA): Sinauer Associates.

COSTA, S., ALMEIDA, A., CASTRO, A. & DOMINGUES, L. (2014). Fusion tags for protein solubility, purification and immunogenicity in Escherichia coli: the novel Fh8 system. *Front Microbiol,* 5, 63.

COSTA, S., SASTRE, P., PEREZ, T., TAPIA, I., BARRANDEGUY, M., SANCHEZ-VIZCAINO, J. M., SANCHEZ-MATAMOROS, A., WIGDOROVITZ, A., SANZ, A. & RUEDA, P. (2016). Development and evaluation of a new lateral flow assay for simultaneous detection of antibodies against African Horse Sickness and Equine Infectious Anemia viruses. *J Virol Methods,* 237, 127-131.

COX, M. M. (2012). Recombinant protein vaccines produced in insect cells. *Vaccine,* 30, 1759-66.

COX, M. M. & HOLLISTER, J. R. (2009). FluBlok, a next generation influenza vaccine manufactured in insect cells. *Biologicals,* 37, 182-9.

COX, M. M., PATRIARCA, P. A. & TREANOR, J. (2008). FluBlok, a recombinant hemagglutinin influenza vaccine. *Influenza Other Respir Viruses,* 2, 211-9.

DE LA POZA, F., CALVO-PINILLA, E., LOPEZ-GIL, E., MARIN-LOPEZ, A., MATEOS, F., CASTILLO-OLIVARES, J., LORENZO, G. & ORTEGO, J. (2013). Ns1 is a key protein in the vaccine composition to protect Ifnar(-/-) mice against infection with multiple serotypes of African horse sickness virus. *PLoS One,* 8, e70197.

DE WAAL, P. J. & HUISMANS, H. (2005). Characterization of the nucleic acid binding activity of inner core protein VP6 of African horse sickness virus. *Arch Virol,* 150, 2037-50.

DEBELJAK, N., FELDMAN, L., DAVIS, K. L., KOMEL, R. & SYTKOWSKI, A. J. (2006). Variability in the immunodetection of His-tagged recombinant proteins. *Anal Biochem,* 359, 216-23.

DIOUF, N., ETTER, E., LO, M., LO, M. & AKAKPO, A. (2013). Outbreaks of African horse sickness in Senegal, and methods of control of the 2007 epidemic. *Vet Rec,* 172, 152.

DOBSON, C. M. (2004). Principles of protein folding, misfolding and aggregation. *Semin Cell Dev Biol,* 15, 3-16.

DU PLESSIS, M., CLOETE, M., AITCHINSON, H. & VAN DIJK, A. (1998). Protein aggregation complicates the development of baculovirus-expressed African horsesickness virus serotype 5 VP2 subunit vaccines. *The Onderstepoort journal of veterinary research,* 65, 321.

DU PLESSIS, M. & NEL, L. (1997). Comparative sequence analysis and expression of the M6 gene, encoding the outer capsid protein VP5, of African horsesickness virus serotype nine. *Virus Res,* 47, 41-49.

DU TOIT, R. (1944). The transmission of bluetongue and horse sickness by Culicoides. *Onderstepoort J. Vet. Sci. Anim. Ind,* 19, 16.

EHN. (2016). *Horse Industry's Econmic Impact* [Online]. European Horse Network. Available: http://www.europeanhorsenetwork.eu/the-horse-industry/economic-impact/ [Accessed 29 December 2016].

EL GARCH, H., CRAFFORD, J. E., AMOUYAL, P., DURAND, P. Y., EDLUND TOULEMONDE, C., LEMAITRE, L., COZETTE, V., GUTHRIE, A. & MINKE, J. M. (2012). An African horse sickness virus serotype 4 recombinant canarypox virus vaccine elicits specific cell-mediated immune responses in horses. *Vet Immunol Immunopathol,* 149, 76-85.

ELBERS, A., KOENRAADT, C. & MEISWINKEL, R. (2015). Mosquitoes and Culicoides biting midges: vector range and the influence of climate change. *Rev. Sci. Tech. Off. Int. Epiz,* 34, 123-137.

ELLGAARD, L. & HELENIUS, A. (2003). Quality control in the endoplasmic reticulum. *Nat Rev Mol Cell Biol,* 4, 181-91.

ERNST, W., GRABHERR, R., WEGNER, D., BORTH, N., GRASSAUER, A. & KATINGER, H. (1998). Baculovirus surface display: construction and screening of a eukaryotic epitope library. *Nucleic Acids Res,* 26, 1718-23.

FABURAY, B., WILSON, W., MCVEY, D. S., DROLET, B. S., WEINGARTL, H., MADDEN, D., YOUNG, A., MA, W. & RICHT, J. A. (2013). Rift Valley fever virus structural and nonstructural proteins: recombinant protein expression and immunoreactivity against antisera from sheep. *Vector Borne Zoonotic Dis,* 13, 619-29.

FACHINGER, V., BISCHOFF, R., JEDIDIA, S. B., SAALMULLER, A. & ELBERS, K. (2008). The effect of vaccination against porcine circovirus type 2 in pigs suffering from porcine respiratory disease complex. *Vaccine,* 26, 1488-99.

FAULKNER, P., KUZIO, J., WILLIAMS, G. V. & WILSON, J. A. (1997). Analysis of p74, a PDV envelope protein of Autographa californica nucleopolyhedrovirus required for occlusion body infectivity in vivo. *J Gen Virol,* 78 (Pt 12), 3091-100.

FEDERICI, B. A. (1997). Baculovirus pathogenesis. *The baculoviruses.* Springer.

FEENSTRA, F., VAN GENNIP, R. G., MARIS-VELDHUIS, M., VERHEIJ, E. & VAN RIJN, P. A. (2014). Bluetongue virus without NS3/NS3a expression is not virulent and protects against virulent bluetongue virus challenge. *Journal of general virology,* 95, 2019-2029.

FELBERBAUM, R. S. (2015). The baculovirus expression vector system: A commercial manufacturing platform for viral vaccines and gene therapy vectors. *Biotechnol J,* 10, 702-14.

FERNANDEZ-PINERO, J., FERNANDEZ-PACHECO, P., RODRIGUEZ, B., SOTELO, E., ROBLES, A., ARIAS, M. & SANCHEZ-VIZCAINO, J. M. (2009). Rapid and sensitive detection of African horse sickness virus by real-time PCR. *Res Vet Sci,* 86, 353-8.

FIEDLER, K. & SIMONS, K. (1995). The role of N-glycans in the secretory pathway. *Cell,* 81, 309-12.

FIRTH, A. E. (2008). Bioinformatic analysis suggests that the Orbivirus VP6 cistron encodes an overlapping gene. *Virology journal,* 5, 1.

FOWLER, V. L., HOWSON, E. L., FLANNERY, J., ROMITO, M., LUBISI, A., AGUERO, M., MERTENS, P., BATTEN, C. A., WARREN, H. R. & CASTILLO-OLIVARES, J. (2016). Development of a Novel Reverse Transcription Loop-Mediated Isothermal Amplification Assay for the Rapid Detection of African Horse Sickness Virus. *Transbound Emerg Dis.*

FRASER, M. (1986). Ultrastructural observations of virion maturation in Autographa californica nuclear polyhedrosis virus infected Spodoptera frugiperda cell cultures. *Journal of ultrastructure and molecular structure research,* 95, 189-195.

FRENCH, T. & ROY, P. (1990). Synthesis of bluetongue virus (BTV) corelike particles by a recombinant baculovirus expressing the two major structural core proteins of BTV. *J Virol,* 64, 1530-1536.

FRIESEN, P. D. (1997). Regulation of Baculovirus Early Gene Expression. *In:* MILLER, L. K. (ed.) *The Baculoviruses.* New York: Plenum Press.

FUNK, C. J., BRAUNAGEL, S. C. & ROHRMANN, G. F. (1997). Baculovirus structure. *In:* MILLER, L. K. (ed.) *The Baculoviruses.* New York: Plenum Press.

GAUDET, D., METHOT, J., DERY, S., BRISSON, D., ESSIEMBRE, C., TREMBLAY, G., TREMBLAY, K., DE WAL, J., TWISK, J., VAN DEN BULK, N., SIER-FERREIRA, V. & VAN DEVENTER, S. (2013). Efficacy and long-term safety of alipogene tiparvovec (AAV1-LPLS447X) gene therapy for lipoprotein lipase deficiency: an open-label trial. *Gene Ther,* 20, 361-9.

GEISLER, C. & JARVIS, D. (2009). Insect cell glycosylation patterns in the context of biopharmaceuticals. *Post-translational Modification of Protein Biopharmaceuticals,* 165-191.

GRABHERR, R., ERNST, W., DOBLHOFF-DIER, O., SARA, M. & KATINGER, H. (1997). Expression of foreign proteins on the surface of Autographa californica nuclear polyhedrosis virus. *Biotechniques,* 22, 730-5.

GREWAR, J. D., WEYER, C. T., GUTHRIE, A. J., KOEN, P., DAVEY, S., QUAN, M., VISSER, D., RUSSOUW, E. & BUHRMANN, G. (2013). The 2011 outbreak of African horse sickness in the African horse sickness controlled area in South Africa. *J S Afr Vet Assoc,* 84, e1-7.

GRIMES, J. M., BURROUGHS, J. N., GOUET, P., DIPROSE, J. M., MALBY, R., ZIENTARA, S., MERTENS, P. P. & STUART, D. I. (1998). The atomic structure of the bluetongue virus core. *Nature,* 395, 470-8.

GRONOWSKI, A. M., HILBERT, D. M., SHEEHAN, K. C., GAROTTA, G. & SCHREIBER, R. D. (1999). Baculovirus stimulates antiviral effects in mammalian cells. *J Virol,* 73, 9944-51.

GUTHRIE, A. J., QUAN, M., LOURENS, C. W., AUDONNET, J. C., MINKE, J. M., YAO, J., HE, L., NORDGREN, R., GARDNER, I. A. & MACLACHLAN, N. J. (2009). Protective immunization of horses with a recombinant canarypox virus vectored vaccine co-expressing genes encoding the outer capsid proteins of African horse sickness virus. *Vaccine,* 27, 4434-8.

HAHN, T. J., WEBB, B., KUTNEY, J., FIX, E., NIDEL, N., WONG, J., JENDREK, D., BAULA, C., LICHAA, J. & SOWERS, M. (2015). Rapid Manufacture and Release of a GMP Batch of Zaire Ebolavirus Glycoprotein Vaccine Made Using Recombinant Baculovirus-Sf9 Insect Cell Culture Technology. *BioProcessing Journal,* 14.

HARPER, D. M., FRANCO, E. L., WHEELER, C., FERRIS, D. G., JENKINS, D., SCHUIND, A., ZAHAF, T., INNIS, B., NAUD, P., DE CARVALHO, N. S., ROTELI-MARTINS, C. M., TEIXEIRA, J., BLATTER, M. M., KORN, A. P., QUINT, W. & DUBIN, G. (2004). Efficacy of a bivalent L1 virus-like particle vaccine in prevention of infection with human papillomavirus types 16 and 18 in young women: a randomised controlled trial. *Lancet,* 364, 1757-65.

HARRISON, R. L. & JARVIS, D. L. (2006). Protein N-Glycosylation in the Baculovirus–Insect Cell Expression System and Engineering of Insect Cells to Produce "Mammalianized" Recombinant Glycoproteins. *Advances in virus research,* 68, 159-191.

HARTL, F. U. & HAYER-HARTL, M. (2002). Molecular chaperones in the cytosol: from nascent chain to folded protein. *Science,* 295, 1852-8.

HASSAN, S. H., WIRBLICH, C., FORZAN, M. & ROY, P. (2001). Expression and functional characterization of bluetongue virus VP5 protein: role in cellular permeabilization. *J Virol,* 75, 8356-67.

HAWTIN, R. E., ARNOLD, K., AYRES, M. D., ZANOTTO, P. M., HOWARD, S. C., GOODAY, G. W., CHAPPELL, L. H., KITTS, P. A., KING, L. A. & POSSEE, R. D. (1995). Identification and preliminary characterization of a chitinase gene in the Autographa californica nuclear polyhedrosis virus genome. *Virology,* 212, 673-85.

HAWTIN, R. E., ZARKOWSKA, T., ARNOLD, K., THOMAS, C. J., GOODAY, G. W., KING, L. A., KUZIO, J. A. & POSSEE, R. D. (1997). Liquefaction of Autographa californica nucleopolyhedrovirus-infected insects is dependent on the integrity of virus-encoded chitinase and cathepsin genes. *Virology,* 238, 243-53.

HEIMPEL, A., THOMAS, E., ADAMS, J. & SMITH, L. (1973). The presence of nuclear polyhedrosis viruses of Trichoplusia ni on cabbage from the market shelf. *Environmental Entomology,* 2, 72-75.

HERICOURT, F., BLANC, S., REDEKER, V. & JUPIN, I. (2000). Evidence for phosphorylation and ubiquitinylation of the turnip yellow mosaic virus RNA-dependent RNA polymerase domain expressed in a baculovirus-insect cell system. *Biochem J,* 349, 417-25.

HERNIOU, E. A., OLSZEWSKI, J. A., CORY, J. S. & O'REILLY, D. R. (2003). The genome sequence and evolution of baculoviruses. *Annu Rev Entomol,* 48, 211-34.

HERVAS-STUBBS, S., RUEDA, P., LOPEZ, L. & LECLERC, C. (2007). Insect baculoviruses strongly potentiate adaptive immune responses by inducing type I IFN. *J Immunol,* 178, 2361-9.

HITCHMAN, R. B., LOCANTO, E., POSSEE, R. D. & KING, L. A. (2011). Optimizing the baculovirus expression vector system. *Methods,* 55, 52-7.

HITCHMAN, R. B., POSSEE, R. D., CROMBIE, A. T., CHAMBERS, A., HO, K., SIATERLI, E., LISSINA, O., STERNARD, H., NOVY, R., LOOMIS, K., BIRD, L. E., OWENS, R. J. & KING, L. A. (2010a). Genetic modification of a baculovirus vector for increased expression in insect cells. *Cell Biol Toxicol,* 26, 57-68.

HITCHMAN, R. B., POSSEE, R. D. & KING, L. A. (2007a). Improved Baculovirus Expression Vectors. In: Methods Express: Expression Systems, Eds. Dyson, MR and Durocher, Y pp. 147-167. Scion Publishing Ltd, Oxford. .

HITCHMAN, R. B., POSSEE, R. D. & KING, L. A. (2009). Baculovirus expression systems for recombinant protein production in insect cells. *Recent Pat Biotechnol,* 3, 46-54.

HITCHMAN, R. B., POSSEE, R. D., SIATERLI, E., RICHARDS, K. S., CLAYTON, A. J., BIRD, L. E., OWENS, R. J., CARPENTIER, D. C., KING, F. L., DANQUAH, J. O., SPINK, K. G. & KING, L. A. (2010b). Improved expression of secreted and membrane-targeted proteins in insect cells. *Biotechnol Appl Biochem,* 56, 85-93.

HITCHMAN, R. B., SIATERLI, E. A., NIXON, C. P. & KING, L. A. (2007b). Quantitative real-time PCR for rapid and accurate titration of recombinant baculovirus particles. *Biotechnology and bioengineering,* 96, 810-814.

HODGSON, J. J., ARIF, B. M. & KRELL, P. J. (2011). Interaction of Autographa californica multiple nucleopolyhedrovirus cathepsin protease progenitor (proV-CATH) with insect baculovirus chitinase as a mechanism for proV-CATH cellular retention. *J Virol,* 85, 3918-29.

HOHMANN, A. W. & FAULKNER, P. (1983). Monoclonal antibodies to baculovirus structural proteins: determination of specificities by Western blot analysis. *Virology,* 125, 432-44.

HORSETALK. (2013). *African Horse Sickness* [Online]. Available: http://horsetalk.co.nz/2012/04/29/african-horse-sickness/#axzz2XQJcqwaY [Accessed 12.5.2013.

HOUSE, C., MIKICIUK, P. E. & BERNINGER, M. L. (1990). Laboratory diagnosis of African horse sickness: comparison of serological techniques and evaluation of storage methods of samples for virus isolation. *J Vet Diagn Invest,* 2, 44-50.

HOWELL, P. G. (1960). The 1960 epizootic of African horsesickness in the Middle East and S.W. Asia. *Journal of the South African Veterinary Medical Association,* 31, 329-334.

HUISMANS, H. & ELS, H. J. (1979). Characterization of the tubules associated with the replication of three different orbiviruses. *Virology,* 92, 397-406.

IDRISSI, B. S., FASSI, F. O., EL HARRAK, M. & FASSI, F. M. (1999). [Use of the immunoenzyme test ELISA-NS3 to distinguish horses infected by African horsesickness virus from vaccinated horses]. *Revue scientifique et technique (International Office of Epizootics),* 18, 618-626.

IWATA, H., YAMAGAWA, M. & ROY, P. (1992). Evolutionary relationships among the gnat-transmitted orbiviruses that cause African horse sickness, bluetongue, and epizootic hemorrhagic disease as evidenced by their capsid protein sequences. *Virology,* 191, 251-61.

JARVIS, D. L. & GARCIA, A., JR. (1994). Biosynthesis and processing of the Autographa californica nuclear polyhedrosis virus gp64 protein. *Virology,* 205, 300-13.

JARVIS, D. L., WILLS, L., BUROW, G. & BOHLMEYER, D. A. (1998). Mutational analysis of the N-linked glycans on Autographa californica nucleopolyhedrovirus gp64. *J Virol,* 72, 9459-69.

JE, Y. H., CHANG, J. H., CHOI, J. Y., ROH, J. Y., JIN, B. R., O'REILLY, D. R. & KANG, S. K. (2001). A defective viral genome maintained in Escherichia coli for the generation of baculovirus expression vectors. *Biotechnol Lett,* 23, 575-582.

JOOSTE, B. (2016). *African Horse Sickness Movement Restrictions Lifted* [Online]. Western Cape Government. Available: https://www.westerncape.gov.za/news/african-horse-sickness-movement-restrictions-lifted-0 [Accessed 29 November 2016].

KABA, S. A., SALCEDO, A. M., WAFULA, P. O., VLAK, J. M. & VAN OERS, M. M. (2004). Development of a chitinase and v-cathepsin negative bacmid for improved integrity of secreted recombinant proteins. *J Virol Methods,* 122, 113-8.

KANAI, Y., VAN RIJN, P. A., MARIS-VELDHUIS, M., KANAME, Y., ATHMARAM, T. N. & ROY, P. (2014). Immunogenicity of recombinant VP2 proteins of all nine serotypes of African horse sickness virus. *Vaccine,* 32, 4932-7.

KATAOKA, C., KANAME, Y., TAGUWA, S., ABE, T., FUKUHARA, T., TANI, H., MORIISHI, K. & MATSUURA, Y. (2012). Baculovirus GP64-mediated entry into mammalian cells. *J Virol,* 86, 2610-20.

KATO, T., OTSUKI, T., YOSHIMOTO, M., ITAGAKI, K., KOHSAKA, T., MATSUMOTO, Y., IKE, K. & PARK, E. Y. (2015). Bombyx mori nucleopolyhedrovirus displaying Neospora caninum antigens as a vaccine candidate against N. caninum infection in mice. *Mol Biotechnol,* 57, 145-154.

KIMPLE, M. E., BRILL, A. L. & PASKER, R. L. (2013). Overview of affinity tags for protein purification. *Current Protocols in Protein Science,* 9.9. 1-9.9. 23.

KING, L. A., HITCHMAN, R. & POSSEE, R. D. (2007). Recombinant baculovirus isolation. *Methods Mol Biol,* 388, 77-94.

KING, L. A. & POSSEE, R. D. (1992). *The Baculovirus Expression System. A Laboratory Guide.* London: Chapman & Hall.

KITTS, P. A., AYRES, M. D. & POSSEE, R. D. (1990). Linearization of baculovirus DNA enhances the recovery of recombinant virus expression vectors. *Nucleic Acids Res,* 18, 5667-72.

KITTS, P. A. & POSSEE, R. D. (1993). A method for producing recombinant baculovirus expression vectors at high frequency. *Biotechniques,* 14, 810-7.

KLENK, H.-D. (1996). Post-translational modifications in insect cells. *Insect Cell Culture: Fundamental and Applied Aspects.* Springer.

KNEBEL, D., LUBBERT, H. & DOERFLER, W. (1985). The promoter of the late p10 gene in the insect nuclear polyhedrosis virus Autographa californica: activation by viral gene products and sensitivity to DNA methylation. *EMBO J,* 4, 1301-6.

KOST, T. A., CONDREAY, J. P. & JARVIS, D. L. (2005). Baculovirus as versatile vectors for protein expression in insect and mammalian cells. *Nat Biotechnol,* 23, 567-75.

KOVACS, J. M., NKOLOLA, J. P., PENG, H., CHEUNG, A., PERRY, J., MILLER, C. A., SEAMAN, M. S., BAROUCH, D. H. & CHEN, B. (2012). HIV-1 envelope trimer elicits more potent neutralizing antibody responses than monomeric gp120. *Proc Natl Acad Sci U S A,* 109, 12111-6.

KRAMMER, F., SCHINKO, T., PALMBERGER, D., TAUER, C., MESSNER, P. & GRABHERR, R. (2010). Trichoplusia ni cells (High Five) are highly efficient for the production of influenza A virus-like particles: a comparison of two insect cell lines as production platforms for influenza vaccines. *Mol Biotechnol,* 45, 226-34.

KRISTENSEN, C. S., BAADSGAARD, N. P. & TOFT, N. (2011). A meta-analysis comparing the effect of PCV2 vaccines on average daily weight gain and mortality rate in pigs from weaning to slaughter. *Preventive veterinary medicine,* 98, 250-258.

KUWAHARA, M. & KONISHI, E. (2010). Evaluation of extracellular subviral particles of dengue virus type 2 and Japanese encephalitis virus produced by Spodoptera frugiperda cells for use as vaccine and diagnostic antigens. *Clinical and Vaccine Immunology,* 17, 1560-1566.

KWEON, C. H., KWON, B. J., KO, Y. J. & KENICHI, S. (2003). Development of competitive ELISA for serodiagnosis on African horsesickness virus using baculovirus expressed VP7 and monoclonal antibody. *J Virol Methods,* 113, 13-18.

LAVIADA, M., BABIN, M., DOMINGUEZ, J. & SANCHEZ-VIZCAINO, J. (1992). Detection of African horsesickness virus in infected spleens by a sandwich ELISA using two monoclonal antibodies specific for VP7. *J Virol Methods,* 38, 229-242.

LAVIADA, M. D., ROY, P., SÁNCHEZ-VIZCAÍNO, J. & CASAL, J. I. (1995). The use of African horse sickness virus NS3 protein, expressed in bacteria, as a marker to differentiate infected from vaccinated horses. *Virus Res,* 38, 205-218.

LELLI, R., MOLINI, U., RONCHI, G. F., ROSSI, E., FRANCHI, P., ULISSE, S., ARMILLOTTA, G., CAPISTA, S., KHAISEB, S., DI VENTURA, M. & PINI, A. (2013). Inactivated and adjuvanted vaccine for the control of the African horse sickness virus serotype 9 infection: evaluation of efficacy in horses and guinea-pig model. *Vet Ital,* 49, 89-98.

LICO, D. T., LOPES, G. S., BRUSCO, J., ROSA, J. C., GOULD, R. M., DE GIORGIS, J. A. & LARSON, R. E. (2015). A novel SDS-stable dimer of a heterogeneous nuclear ribonucleoprotein at presynaptic terminals of squid neurons. *Neuroscience,* 300, 381-92.

LIN, Y. H., LEE, L. H., SHIH, W. L., HU, Y. C. & LIU, H. J. (2008). Baculovirus surface display of sigmaC and sigmaB proteins of avian reovirus and immunogenicity of the displayed proteins in a mouse model. *Vaccine,* 26, 6361-7.

LODISH, H. & ZIPURSKY, S. (2000). Section 17.3, Overview of the secretory pathway. *Molecular cell biology. 4th ed. New York: WH Freeman.*

LONG, M. T. & GUTHRIE, A. J. (2014). AHS. *In:* SELLON, D. C. & LONG, M. (eds.) *Equine Infectious Diseases.* 2nd ed. Philadelphia: Elsevier Health Sciences.

LU, A. & MILLER, L. K. (1997). Regulation of Baculovirus Late and Very Late Gene Expression. *In:* MILLER, L. K. (ed.) *The Baculoviruses.* New York: Plenum Press.

LUBROTH, J. (Year) Published. African Horsesickness and the epizootic in Spain, 1987. Proceedings of the annual convention of the American Association of Equine Practitioners (USA), 1988.

LUCKOW, V. A., LEE, S. C., BARRY, G. F. & OLINS, P. O. (1993). Efficient generation of infectious recombinant baculoviruses by site-specific transposon-mediated insertion of foreign genes into a baculovirus genome propagated in Escherichia coli. *J Virol,* 67, 4566-79.

LUCKOW, V. A. & SUMMERS, M. D. (1988). Trends in the Development of Baculovirus Expression Vectors. *Nature biotechnology,* 6, 47-55.

LULLA, V., LULLA, A., WERNIKE, K., AEBISCHER, A., BEER, M. & ROY, P. (2016). Assembly of Replication-Incompetent African Horse Sickness Virus Particles: Rational Design of Vaccines for All Serotypes. *J Virol,* 90, 7405-14.

MADHAN, S., PRABAKARAN, M. & KWANG, J. (2010). Baculovirus as vaccine vectors. *Curr Gene Ther,* 10, 201-13.

MANOLE, V., LAURINMAKI, P., VAN WYNGAARDT, W., POTGIETER, C. A., WRIGHT, I. M., VENTER, G. J., VAN DIJK, A. A., SEWELL, B. T. & BUTCHER, S. J. (2012). Structural insight into African horsesickness virus infection. *J Virol,* 86, 7858-66.

MAREE, F. F. & HUISMANS, H. (1997). Characterization of tubular structures composed of nonstructural protein NS1 of African horsesickness virus expressed in insect cells. *J Gen Virol,* 78 (Pt 5), 1077-82.

MAREE, S., DURBACH, S. & HUISMANS, H. (1998). Intracellular production of African horsesickness virus core-like particles by expression of the two major core proteins, VP3 and VP7, in insect cells. *Journal of general virology,* 79, 333-337.

MAREE, S., MAREE, F. F., PUTTERILL, J. F., DE BEER, T. A., HUISMANS, H. & THERON, J. (2016). Synthesis of empty african horse sickness virus particles. *Virus Res,* 213, 184-94.

MAREE, S. & PAWESKA, J. T. (2005). Preparation of recombinant African horse sickness virus VP7 antigen via a simple method and validation of a VP7-based indirect ELISA for the detection of group-specific IgG antibodies in horse sera. *J Virol Methods,* 125, 55-65.

MARGINE, I., PALESE, P. & KRAMMER, F. (2013). Expression of functional recombinant hemagglutinin and neuraminidase proteins from the novel H7N9 influenza virus using the baculovirus expression system. *J Vis Exp,* e51112.

MARSHALL, J. J. & ROY, P. (1990). High level expression of the two outer capsid proteins of bluetongue virus serotype 10: their relationship with the neutralization of virus infection. *Virus Res,* 15, 189-195.

MARTINEZ-TORRECUADRADA, J. L. & CASAL, J. I. (1995). Identification of a linear neutralization domain in the protein VP2 of African horse sickness virus. *Virology,* 210, 391-9.

MARTINEZ-TORRECUADRADA, J. L., DIAZ-LAVIADA, M., ROY, P., SANCHEZ, C., VELA, C., SANCHEZ-VIZCAINO, J. M. & CASAL, J. I. (1996). Full protection against African horsesickness (AHS) in horses induced by baculovirus-derived AHS virus serotype 4 VP2, VP5 and VP7. *J Gen Virol,* 77 (Pt 6), 1211-21.

MARTINEZ-TORRECUADRADA, J. L., DIAZ-LAVIADA, M., ROY, P., SANCHEZ, C., VELA, C., SANCHEZ-VIZCAINO, J. M. & CASAL, J. I. (1997). Serologic markers in early stages of African horse sickness virus infection. *J Clin Microbiol,* 35, 531-5.

MARTINEZ-TORRECUADRADA, J. L., IWATA, H., VENTEO, A., CASAL, I. & ROY, P. (1994). Expression and characterization of the two outer capsid proteins of African horsesickness virus: the role of VP2 in virus neutralization. *Virology,* 202, 348-59.

MARTINEZ-TORRECUADRADA, J. L., LANGEVELD, J. P., MELOEN, R. H. & CASAL, J. I. (2001). Definition of neutralizing sites on African horse sickness virus serotype 4 VP2 at the level of peptides. *J Gen Virol,* 82, 2415-24.

MARTÍNEZ-TORRECUADRADA, J. L., LANGEVELD, J. P., VENTEO, A., SANZ, A., DALSGAARD, K., HAMILTON, W. D., MELOEN, R. H. & CASAL, J. I. (1999). Antigenic profile of African horse sickness virus serotype 4 VP5 and identification of a neutralizing epitope shared with bluetongue virus and epizootic hemorrhagic disease virus. *Virology,* 257, 449-459.

MATSUO, E., CELMA, C. C., BOYCE, M., VIAROUGE, C., SAILLEAU, C., DUBOIS, E., BREARD, E., THIERY, R., ZIENTARA, S. & ROY, P. (2011). Generation of replication-defective virus-based vaccines that confer full protection in sheep against virulent bluetongue virus challenge. *J Virol,* 85, 10213-21.

MATSUO, E., CELMA, C. C. & ROY, P. (2010). A reverse genetics system of African horse sickness virus reveals existence of primary replication. *FEBS Lett,* 584, 3386-91.

MCCAFFERTY, J., GRIFFITHS, A. D., WINTER, G. & CHISWELL, D. J. (1990). Phage antibodies: filamentous phage displaying antibody variable domains. *Nature,* 348, 552-4.

MCPHERSON, C. E. (2008). Development of a novel recombinant influenza vaccine in insect cells. *Biologicals,* 36, 350-3.

MEISWINKEL, R. (1998). The 1996 outbreak of African horse sickness in South Africa—the entomological perspective. *African Horse Sickness.* Springer.

MEISWINKEL, R., BAYLIS, M. & LABUSCHAGNE, K. (2000). Stabling and the protection of horses from Culicoides bolitinos (Diptera: Ceratopogonidae), a recently identified vector of African horse sickness. *Bull Entomol Res,* 90, 509-15.

MEISWINKEL, R. & PAWESKA, J. (2003). Evidence for a new field Culicoides vector of African horse sickness in South Africa. *Preventive veterinary medicine,* 60, 243-253.

MELLOR, P. (1993). African horse sickness: transmission and epidemiology. *Vet Res,* 24, 199-212.

MELLOR, P., BOORMAN, J. & JENNINGS, M. (1975). The multiplication of African horse-sickness virus in two species ofCulicoides (Diptera, Ceratopogonidae). *Archives of virology,* 47, 351-356.

MELLOR, P. S., BONED, J., HAMBLIN, C. & GRAHAM, S. (1990). Isolations of African horse sickness virus from vector insects made during the 1988 epizootic in Spain. *Epidemiol Infect,* 105, 447-54.

MELLOR, P. S., BOORMAN, J. & BAYLIS, M. (2000). Culicoides biting midges: their role as arbovirus vectors. *Annu Rev Entomol,* 45, 307-40.

MELLOR, P. S. & HAMBLIN, C. (2004). African horse sickness. *Vet Res,* 35, 445-66.

MENG, T., KOLPE, A. B., KIENER, T. K., CHOW, V. T. & KWANG, J. (2011). Display of VP1 on the surface of baculovirus and its immunogenicity against heterologous human enterovirus 71 strains in mice. *PLoS One,* 6, e21757.

MERTENS, P., MAAN, S., SAMUEL, A. & ATTOUI, H. (2005). Orbivirus, reoviridae. *Virus Taxonomy,* 21.

MERTENS, P. P. & DIPROSE, J. (2004). The bluetongue virus core: a nano-scale transcription machine. *Virus Res,* 101, 29-43.

MERTENS, P. P., DIPROSE, J., MAAN, S., SINGH, K. P., ATTOUI, H. & SAMUEL, A. R. (2004). Bluetongue virus replication, molecular and structural biology. *Vet Ital,* 40, 426-37.

MIRCHAMSY, H. & TASLIMI, H. (1968). Inactivated African horse sickness virus cell culture vaccine. *Immunology,* 14, 81-8.

MIZUKOSHI, N., SAKAMOTO, K., IWATA, A., TSUCHIYA, T., UEDA, S., WATANABE, T., KAMADA, M. & FUKUSHO, A. (1992). The complete sequence of African horsesickness virus serotype 4 (vaccine strain) RNA segment 5 and its predicted polypeptide compared with NS1 of bluetongue virus. *J Gen Virol,* 73 (Pt 9), 2425-8.

MOHD JAAFAR, F., BELHOUCHET, M., VITOUR, D., ADAM, M., BREARD, E., ZIENTARA, S., MERTENS, P. P. & ATTOUI, H. (2014). Immunisation with bacterial expressed VP2 and VP5 of bluetongue virus (BTV) protect alpha/beta interferon-receptor knock-out (IFNAR(-/-)) mice from homologous lethal challenge. *Vaccine,* 32, 4059-67.

MOLINI, U., MARUCCHELLA, G., MASEKE, A., RONCHI, G. F., DI VENTURA, M., SALINI, R., SCACCHIA, M. & PINI, A. (2015). Immunization of horses with a polyvalent live-attenuated African horse sickness vaccine: Serological response and disease occurrence under field conditions. *Trials in Vaccinology,* 4, 24-28.

MONACO, F., POLCI, A., LELLI, R., PINONI, C., DI MATTIA, T., MBULU, R. S., SCACCHIA, M. & SAVINI, G. (2011). A new duplex real-time RT-PCR assay for sensitive and specific detection of African horse sickness virus. *Mol Cell Probes,* 25, 87-93.

MONIE, A., HUNG, C. F., RODEN, R. & WU, T. C. (2008). Cervarix: a vaccine for the prevention of HPV 16, 18-associated cervical cancer. *Biologics,* 2, 97-105.

MONSMA, S. A., OOMENS, A. G. & BLISSARD, G. W. (1996). The GP64 envelope fusion protein is an essential baculovirus protein required for cell-to-cell transmission of infection. *J Virol,* 70, 4607-16.

MONTILLA, R. D. & MARTÍ, P. (1967). [Epizootiology of equine plague in Spain]. *Bulletin-Office international des épizooties,* 68, 705-714.

MOORMANN, R. J., BOUMA, A., KRAMPS, J. A., TERPSTRA, C. & DE SMIT, H. J. (2000). Development of a classical swine fever subunit marker vaccine and companion diagnostic test. *Vet Microbiol,* 73, 209-19.

MURPHY, C. I., MCINTIRE, J. R., DAVIS, D. R., HODGDON, H., SEALS, J. R. & YOUNG, E. (1993). Enhanced expression, secretion, and large-scale purification of recombinant HIV-1 gp120 in insect cell using the baculovirus egt and p67 signal peptides. *Protein Expr Purif,* 4, 349-57.

NEVILL, E. & ANDERSON, D. (1972). Host preferences of Culicoides midges (Diptera: Ceratopogonidae) in South Africa as determined by precipitin tests and light trap catches. *Onderstepoort Journal of Veterinary Research.*

NOTOMI, T., OKAYAMA, H., MASUBUCHI, H., YONEKAWA, T., WATANABE, K., AMINO, N. & HASE, T. (2000). Loop-mediated isothermal amplification of DNA. *Nucleic Acids Res,* 28**,** E63.

O'HARA, R. S., MEYER, A. J., BURROUGHS, J. N., PULLEN, L., MARTIN, L. A. & MERTENS, P. P. (1998). Development of a mouse model system, coding assignments and identification of the genome segments controlling virulence of African horse sickness virus serotypes 3 and 8. *Arch Virol Suppl,* 14**,** 259-79.

OBP. (2016). *African horse sickness vaccine for horses, mules and donkeys* [Online]. South Africa: Onderstepoort Biological Products. Available: http://www.obpvaccines.co.za/Cms_Data/Contents/OBPDB/Folders/Product/~contents/4AR2ZW46HZAJAFDB/2063_AHS_PI.pdf [Accessed 29 November 2016].

OELLERMANN, R. (1970). Plaque formation by African horsesickness virus and characterization of its RNA.

OELLERMANN, R., ELS, H. & ERASMUS, B. (1970). Characterization of African horsesiekness virus. *Archiv für die gesamte Virusforschung,* 29**,** 163-174.

OIE, T. M. (2016). *African horse sickness* [Online]. France: OIE. Available: http://www.oie.int/fileadmin/Home/eng/Health_standards/tahm/2.05.01_AHS.pdf [Accessed 30 November 2016].

OKER-BLOM, C., AIRENNE, K. J. & GRABHERR, R. (2003). Baculovirus display strategies: Emerging tools for eukaryotic libraries and gene delivery. *Brief Funct Genomic Proteomic,* 2**,** 244-53.

OLDHAM, R. K. (2012). Principles of Cancer Biotherapy. Third ed. Netherlands: Kluwer academic publishers.

OOMENS, A. G. & BLISSARD, G. W. (1999). Requirement for GP64 to drive efficient budding of Autographa californica multicapsid nucleopolyhedrovirus. *Virology,* 254**,** 297-314.

OXFORD EXPRESSION TECHNOLOGIES LTD. (2016). *flashBAC time line compared to other baculovirus expression vector systems* [Online]. Available: https://oetltd.com/wp-content/uploads/2016/01/flashBAC%E2%84%A2-time-comparison.pdf [Accessed November 2016].

PAAVONEN, J., JENKINS, D., BOSCH, F. X., NAUD, P., SALMERON, J., WHEELER, C. M., CHOW, S. N., APTER, D. L., KITCHENER, H. C., CASTELLSAGUE, X., DE CARVALHO, N. S., SKINNER, S. R., HARPER, D. M., HEDRICK, J. A., JAISAMRARN, U., LIMSON, G. A., DIONNE, M., QUINT, W., SPIESSENS, B., PEETERS, P., STRUYF, F., WIETING, S. L., LEHTINEN, M. O. & DUBIN, G. (2007). Efficacy of a prophylactic adjuvanted bivalent L1 virus-like-particle vaccine against infection with human papillomavirus types 16 and 18 in young women: an interim analysis of a phase III double-blind, randomised controlled trial. *Lancet,* 369**,** 2161-70.

PAIN, R. H. (2000). *Mechanisms of protein folding.* New York: Oxford University Press Inc.

PANAVAS, T., SANDERS, C. & BUTT, T. R. (2009). SUMO fusion technology for enhanced protein production in prokaryotic and eukaryotic expression systems. *Methods Mol Biol,* 497**,** 303-17.

PAWESKA, J. T., PRINSLOO, S. & VENTER, G. J. (2003). Oral susceptibility of South African Culicoides species to live-attenuated serotype-specific vaccine strains of African horse sickness virus (AHSV). *Med Vet Entomol,* 17**,** 436-47.

PERALTA, A., MARONICHE, G. A., ALFONSO, V., MOLINARI, P. & TABOGA, O. (2013). VP1 protein of Foot-and-mouth disease virus (FMDV) impairs baculovirus surface display. *Virus Res,* 175**,** 87-90.

PERALTA, A., MOLINARI, P., CONTE-GRAND, D., CALAMANTE, G. & TABOGA, O. (2007). A chimeric baculovirus displaying bovine herpesvirus-1 (BHV-1) glycoprotein D on its surface and their immunological properties. *Appl Microbiol Biotechnol,* 75**,** 407-14.

PHIZICKY, E. M. & FIELDS, S. (1995). Protein-protein interactions: methods for detection and analysis. *Microbiol Rev,* 59**,** 94-123.

PIERCE, C. M., BALASURIYA, U. B. & MACLACHLAN, N. J. (1998). Phylogenetic analysis of the S10 gene of field and laboratory strains of bluetongue virus from the United States. *Virus Res,* 55**,** 15-27.

PITCHFORD, N. & THEILER, A. (1903). Investigations into the nature and causes of horsesickness. *Agricultural Journal of the Cape of Good Hope,* 23, 153-156.

PORTAS, M., BOINAS, F., SOUSA, J. O. E. & RAWLINGS, P. (1999). African horse sickness in Portugal: a successful eradication programme. *Epidemiol Infect,* 123, 337-346.

POSSEE, R. D., GRIFFITHS, C. M., HITCHMAN, R. B., CHAMBERS, A., MURGUIA-MECA, F., DANQUAH, J., JESHTADI, A. & KING, L. A. (2010). Baculoviruses: biology, replication and exploitation. In: Asgari, S and Johnson, K Insect Virology. Great Britain: Caister Academic Press. p35-58.

POSSEE, R. D., HITCHMAN, R. B., RICHARDS, K. S., MANN, S. G., SIATERLI, E., NIXON, C. P., IRVING, H., ASSENBERG, R., ALDERTON, D., OWENS, R. J. & KING, L. A. (2008). Generation of baculovirus vectors for the high-throughput production of proteins in insect cells. *Biotechnol Bioeng,* 101, 1115-22.

POSSEE, R. D. & HOWARD, S. C. (1987). Analysis of the polyhedrin gene promoter of the Autographa californica nuclear polyhedrosis virus. *Nucleic Acids Res,* 15, 10233-48.

POSSEE, R. D., THOMAS, C. J. & KING, L. A. (1999). The use of baculovirus vectors for the production of membrane proteins in insect cells. *Biochem Soc Trans,* 27, 928-32.

POTGIETER, A. C., CLOETE, M., PRETORIUS, P. J. & VAN DIJK, A. A. (2003). A first full outer capsid protein sequence data-set in the Orbivirus genus (family Reoviridae): cloning, sequencing, expression and analysis of a complete set of full-length outer capsid VP2 genes of the nine African horsesickness virus serotypes. *J Gen Virol,* 84, 1317-26.

PRETORIUS, A., VAN KLEEF, M., VAN WYNGAARDT, W. & HEATH, J. (2012). Virus-specific CD8+ T-cells detected in PBMC from horses vaccinated against African horse sickness virus. *Vet Immunol Immunopathol,* 146, 81-86.

RADFORD, S. E. (2000). Protein folding: progress made and promises ahead. *Trends Biochem Sci,* 25, 611-8.

RAMADEVI, N., BURROUGHS, N. J., MERTENS, P. P., JONES, I. M. & ROY, P. (1998). Capping and methylation of mRNA by purified recombinant VP4 protein of bluetongue virus. *Proc Natl Acad Sci U S A,* 95, 13537-42.

RANZ, A. I., MIGUET, J. G., ANAYA, C., VENTEO, A., CORTES, E., VELA, C. & SANZ, A. (1992). Diagnostic methods for African horsesickness virus using monoclonal antibodies to structural and non-structural proteins. *Vet Microbiol,* 33, 143-53.

RAWLINGS, P. & MELLOR, P. (1994). African horse sickness and the overwintering of Culicoides spp. in the Iberian peninsula. *Revue scientifique et technique (International Office of Epizootics),* 13, 753-761.

ROBIN, M., PAGE, P., ARCHER, D. & BAYLIS, M. (2016). African horse sickness: The potential for an outbreak in disease-free regions and current disease control and elimination techniques. *Equine Vet J,* 48, 659-69.

RODRIGUEZ-SANCHEZ, B., FERNANDEZ-PINERO, J., SAILLEAU, C., ZIENTARA, S., BELAK, S., ARIAS, M. & SANCHEZ-VIZCAINO, J. M. (2008). Novel gel-based and real-time PCR assays for the improved detection of African horse sickness virus. *J Virol Methods,* 151, 87-94.

RODRIGUEZ, M., HOOGHUIS, H. & CASTAÑO, M. (1992). African horse sickness in Spain. *Vet Microbiol,* 33, 129-142.

ROHRMANN, G. F. (2008). Baculovirus Molecular Biology. [e-book] Bethesda (MD): National Center for Biotechnology Information (US): NCBI <http://www.ncbi.nlm.nih.gov/books/NBK1736/> (Accessed 2010). .

ROMANOWSKI, V. (2013). Marcelo F. Berretta, M. Leticia Ferrelli, Ricardo Salvador, Alicia Sciocco and.

ROMITO, M., DU PLESSIS, D. & VILJOEN, G. (1999). Immune responses in a horse inoculated with the VP2 gene of African horsesickness virus. *The Onderstepoort journal of veterinary research,* 66, 139.

ROY, P., BISHOP, D. H., HOWARD, S., AITCHISON, H. & ERASMUS, B. (1996). Recombinant baculovirus-synthesized African horsesickness virus (AHSV) outer-capsid protein VP2 provides protection against virulent AHSV challenge. *J Gen Virol,* 77 (Pt 9), 2053-7.

ROY, P., BISHOP, D. H., LEBLOIS, H. & ERASMUS, B. J. (1994a). Long-lasting protection of sheep against bluetongue challenge after vaccination with virus-like particles: evidence for homologous and partial heterologous protection. *Vaccine,* 12, 805-811.

ROY, P., MERTENS, P. P. & CASAL, I. (1994b). African horse sickness virus structure. *Comp Immunol Microbiol Infect Dis,* 17, 243-73.

ROY, P., URAKAWA, T., VAN DIJK, A. A. & ERASMUS, B. J. (1990). Recombinant virus vaccine for bluetongue disease in sheep. *J Virol,* 64, 1998-2003.

RUPP, B., ROSSLER, U., LOWEL, M. & WERENSKIOLD, A. K. (1995). High level expression of the IL-1 receptor related T1 receptor in insect cells. *Biochem Biophys Res Commun,* 216, 595-601.

RYDZAK, J., KACZMAREK, R., CZERWINSKI, M., LUKASIEWICZ, J., TYBOROWSKA, J., SZEWCZYK, B. & JASKIEWICZ, E. (2015). The baculovirus-expressed binding region of *Plasmodium falciparum* EBA-140 ligand and its glycophorin C binding specificity. *PLoS One,* 10, e0115437.

SAILLEAU, C., HAMBLIN, C., PAWESKA, J. T. & ZIENTARA, S. (2000). Identification and differentiation of the nine African horse sickness virus serotypes by RT-PCR amplification of the serotype-specific genome segment 2. *J Gen Virol,* 81, 831-7.

SANCHEZ-MATAMOROS, A., BECK, C., KUKIELKA, D., LECOLLINET, S., BLAISE-BOISSEAU, S., GARNIER, A., RUEDA, P., ZIENTARA, S. & SANCHEZ-VIZCAINO, J. M. (2016a). Development of a Microsphere-based Immunoassay for Serological Detection of African Horse Sickness Virus and Comparison with Other Diagnostic Techniques. *Transbound Emerg Dis,* 63, e270-e277.

SANCHEZ-MATAMOROS, A., NIETO-PELEGRIN, E., BECK, C., RIVERA-ARROYO, B., LECOLLINET, S., SAILLEAU, C., ZIENTARA, S. & SANCHEZ-VIZCAINO, J. M. (2016b). Development of a Luminex-Based DIVA Assay for Serological Detection of African Horse Sickness Virus in Horses. *Transbound Emerg Dis,* 63, 353-9.

SCANLEN, M., PAWESKA, J. T., VERSCHOOR, J. A. & VAN DIJK, A. A. (2002). The protective efficacy of a recombinant VP2-based African horsesickness subunit vaccine candidate is determined by adjuvant. *Vaccine,* 20, 1079-88.

SELLERS, R., PEDGLEY, D. & TUCKER, M. (1977). Possible spread of African horse sickness on the wind. *Journal of Hygiene,* 79, 279-298.

SIMON, O., WILLIAMS, T., CABALLERO, P. & POSSEE, R. D. (2008). Effects of Acp26 on in vitro and in vivo productivity, pathogenesis and virulence of Autographa californica multiple nucleopolyhedrovirus. *Virus Res,* 136, 202-5.

SINCLAIR, M., BUHRMANN, G. & GUMMOW, B. (2006). An epidemiological investigation of the African horsesickness outbreak in the Western Cape Province of South Africa in 2004 and its relevance to the current equine export protocol. *J S Afr Vet Assoc,* 77, 191-6.

SLACK, J. & ARIF, B. M. (2006). The Baculoviruses Occlusion-Derived Virus: Virion Structure and Function *Advances in Virus Research,* 69, 99-165

SLACK, J. M., KUZIO, J. & FAULKNER, P. (1995). Characterization of v-cath, a cathepsin L-like proteinase expressed by the baculovirus Autographa californica multiple nuclear polyhedrosis virus. *J Gen Virol,* 76 (Pt 5), 1091-8.

SMALL, E. J., FRATESI, P., REESE, D. M., STRANG, G., LAUS, R., PESHWA, M. V. & VALONE, F. H. (2000). Immunotherapy of hormone-refractory prostate cancer with antigen-loaded dendritic cells. *J Clin Oncol,* 18, 3894-903.

SMITH, G. E., FRASER, M. J. & SUMMERS, M. D. (1983a). Molecular Engineering of the Autographa californica Nuclear Polyhedrosis Virus Genome: Deletion Mutations Within the Polyhedrin Gene. *J Virol,* 46, 584-93.

SMITH, G. E., SUMMERS, M. D. & FRASER, M. J. (1983b). Production of human beta interferon in insect cells infected with a baculovirus expression vector. *Mol Cell Biol,* 3, 2156-65.

SMITH, G. E., VLAK, J. M. & SUMMERS, M. D. (1983c). Physical Analysis of Autographa californica Nuclear Polyhedrosis Virus Transcripts for Polyhedrin and 10,000-Molecular-Weight Protein. *J Virol,* 45, 215-25.

SMITH, G. P. (1985). Filamentous fusion phage: novel expression vectors that display cloned antigens on the virion surface. *Science,* 228, 1315-7.

STAROPOLI, I., FRENKIEL, M.-P., MÉGRET, F. & DEUBEL, V. (1997). Affinity-purified dengue-2 virus envelope glycoprotein induces neutralizing antibodies and protective immunity in mice. *Vaccine,* 15, 1946-1954.

STASSEN, L., HUISMANS, H. & THERON, J. (2011). Membrane permeabilization of the African horse sickness virus VP5 protein is mediated by two N-terminal amphipathic alpha-helices. *Arch Virol,* 156, 711-5.

STÄUBER, N., MARTINEZ-COSTAS, J., SUTTON, G., MONASTYRSKAYA, K. & ROY, P. (1997). Bluetongue virus VP6 protein binds ATP and exhibits an RNA-dependent ATPase function and a helicase activity that catalyze the unwinding of double-stranded RNA substrates. *J Virol,* 71, 7220-7226.

STEWART, M., BHATIA, Y., ATHMARAN, T., NOAD, R., GASTALDI, C., DUBOIS, E., RUSSO, P., THIÉRY, R., SAILLEAU, C. & BRÉARD, E. (2010). Validation of a novel approach for the rapid production of immunogenic virus-like particles for bluetongue virus. *Vaccine,* 28, 3047-3054.

STILES, B., WOOD, H. & HUGHES, P. (1983). Effect of tunicamycin on the infectivity of Autographa californica nuclear polyhedrosis virus. *Journal of Invertebrate Pathology,* 41, 405-408.

STOLTZ, M. A., VAN DER MERWE, C. F., COETZEE, J. & HUISMANS, H. (1996). Subcellular localization of the nonstructural protein NS3 of African horsesickness virus. *Onderstepoort J Vet Res,* 63, 57-61.

STONE-MARSCHAT, M. A., MOSS, S. R., BURRAGE, T. G., BARBER, M. L., ROY, P. & LAEGREID, W. W. (1996). Immunization with VP2 is sufficient for protection against lethal challenge with African horsesickness virus Type 4. *Virology,* 220, 219-22.

STUART, D., GOUET, P., GRIMES, J., MALBY, R., DIPROSE, J., ZIENTARA, S., BURROUGHS, J. & MERTENS, P. (1998). Structural studies of orbivirus particles. *African Horse Sickness.* Springer.

SUMMERS, M. D. (2006). Milestones leading to the genetic engineering of baculoviruses as expression vector systems and viral pesticides. *Adv Virus Res,* 68, 3-73.

TAKADA, S., OGAWA, T., MATSUI, K., SUZUKI, T., KATSUDA, T. & YAMAJI, H. (2015). Baculovirus display of functional antibody Fab fragments. *Cytotechnology,* 67, 741-7.

TAMI, C., PERALTA, A., BARBIERI, R., BERINSTEIN, A., CARRILLO, E. & TABOGA, O. (2004). Immunological properties of FMDV-gP64 fusion proteins expressed on SF9 cell and baculovirus surfaces. *Vaccine,* 23, 840-5.

THOMAS, C. J., BROWN, H. L., HAWES, C. R., LEE, B. Y., MIN, M. K., KING, L. A. & POSSEE, R. D. (1998). Localization of a baculovirus-induced chitinase in the insect cell endoplasmic reticulum. *J Virol,* 72, 10207-12.

THOMAS, S. J., NISALAK, A., ANDERSON, K. B., LIBRATY, D. H., KALAYANAROOJ, S., VAUGHN, D. W., PUTNAK, R., GIBBONS, R. V., JARMAN, R. & ENDY, T. P. (2009). Dengue plaque reduction neutralization test (PRNT) in primary and secondary dengue virus infections: How alterations in assay conditions impact performance. *Am J Trop Med Hyg,* 81, 825-33.

TURNBULL, P. J., CORMACK, S. B. & HUISMANS, H. (1996). Characterization of the gene encoding core protein VP6 of two African horsesickness virus serotypes. *J Gen Virol,* 77 (Pt 7), 1421-3.

UC DAVIS CENTER. (2008). *Emerging Equine Diseases* [Online]. The Horse Media Group. Available: http://www.thehorse.com/articles/21626/emerging-equine-disease-four-diseases-syndromes-to-watch [Accessed 4 December 2016].

UITENWEERDE, J., THERON, J., STOLTZ, M. & HUISMANS, H. (1995). The multimeric nonstructural NS2 proteins of bluetongue virus, African horsesickness virus, and epizootic hemorrhagic disease virus differ in their single-stranded RNA-binding ability. *Virology,* 209, 624-632.

URAKAWA, T., RITTER, D. G. & ROY, P. (1989). Expression of largest RNA segment and synthesis of VP1 protein of bluetongue virus in insect cells by recombinant baculovirus: association of VP1 protein with RNA polymerase activity. *Nucleic Acids Res,* 17, 7395-401.

VAIL, P. (Year) Published. Cross infectivity of a nuclear polyhedrosis virus isolated from the alfalfa looper Autographa californica. Proceedings, 4th International Colloquium Insect Pathology., 1971. 297-304.

VAN DE WATER, S. G., VAN GENNIP, R. G., POTGIETER, C. A., WRIGHT, I. M. & VAN RIJN, P. A. (2015). VP2 Exchange and NS3/NS3a Deletion in African Horse Sickness Virus (AHSV) in Development of Disabled Infectious Single Animal Vaccine Candidates for AHSV. *J Virol,* 89, 8764-72.

VAN DEN BOUT, J. I. (2005). Characterization of VP4, a minor core protein of African horse sickness virus with putative capping enzyme activity.

VAN NIEKERK, M., SMIT, C. C., FICK, W. C., VAN STADEN, V. & HUISMANS, H. (2001). Membrane association of African horsesickness virus nonstructural protein NS3 determines its cytotoxicity. *Virology,* 279, 499-508.

VAN OERS, M. M., PIJLMAN, G. P. & VLAK, J. M. (2015). Thirty years of baculovirus-insect cell protein expression: from dark horse to mainstream technology. *J Gen Virol,* 96, 6-23.

VAN SITTERT, S. J., DREW, T. M., KOTZE, J. L., STRYDOM, T., WEYER, C. T. & GUTHRIE, A. J. (2013). Occurrence of African horse sickness in a domestic dog without apparent ingestion of horse meat. *Journal of the South African Veterinary Association,* 84, 1-5.

VAN STADEN, V. & HUISMANS, H. (1991). A comparison of the genes which encode non-structural protein NS3 of different orbiviruses. *J Gen Virol,* 72 (Pt 5), 1073-9.

VAN STADEN, V., STOLTZ, M. A. & HUISMANS, H. (1995). Expression of nonstructural protein NS3 of African horsesickness virus (AHSV): evidence for a cytotoxic effect of NS3 in insect cells, and characterization of the gene products in AHSV infected Vero cells. *Arch Virol,* 140, 289-306.

VANDENBERGH, S. (2010). " The story of a disease": African horsesickness and its direct influence on the necessary development of veterinary science in South Africa c. 1890s-1920s. *Historia,* 55, 243-262.

VAUGHN, J. L., GOODWIN, R. H., TOMPKINS, G. J. & MCCAWLEY, P. (1977). The establishment of two cell lines from the insect Spodoptera frugiperda (Lepidoptera; Noctuidae). *In Vitro,* 13, 213-7.

VENTER, G. J. & MEISWINKEL, R. (1994). The virtual absence of Culicoides imicola (Diptera: Ceratopogonidae) in a light-trap survey of the colder, high-lying area of the eastern Orange Free State, South Africa, and implications for the transmission of arboviruses.

VERMAAK, E., CONRADIE, A. M., MAREE, F. F. & THERON, J. (2016). African horse sickness virus infects BSR cells through macropinocytosis. *Virology,* 497, 217-32.

VERWOERD, D., HUISMANS, H. & ERASMUS, B. (1979). Orbiviruses. *Comprehensive virology.* Springer.

VERWOERD, D. W. (2012). History of orbivirus research in South Africa. *Journal of the South African Veterinary Association,* 83, 01-06.

VLAK, J. M., KLINKENBERG, F. A., ZAAL, K. J., USMANY, M., KLINGE-ROODE, E. C., GEERVLIET, J. B., ROOSIEN, J. & VAN LENT, J. W. (1988). Functional studies on the p10 gene of Autographa californica nuclear polyhedrosis virus using a recombinant expressing a p10-beta-galactosidase fusion gene. *J Gen Virol,* 69 (Pt 4), 765-76.

VLAK, J. M., SCHOUTEN, A., USMANY, M., BELSHAM, G. J., KLINGE-ROODE, E. C., MAULE, A. J., VAN LENT, J. W. & ZUIDEMA, D. (1990). Expression of cauliflower mosaic virus gene I using a baculovirus vector based upon the p10 gene and a novel selection method. *Virology,* 179, 312-20.

VOLKMAN, L. E. & GOLDSMITH, P. A. (1984). Budded Autographa californica NPV 64K protein: Further biochemical analysis and effects of postimmunoprecipitation sample preparation conditions. *Virology,* 139, 295-302.

VOLKMAN, L. E., GOLDSMITH, P. A., HESS, R. T. & FAULKNER, P. (1984). Neutralization of budded Autographa californica NPV by a monoclonal antibody: identification of the target antigen. *Virology,* 133, 354-62.

VOLKMAN, L. E., SUMMERS, M. D. & HSIEH, C. H. (1976). Occluded and nonoccluded nuclear polyhedrosis virus grown in Trichoplusia ni: comparative neutralization comparative infectivity, and in vitro growth studies. *J Virol,* 19, 820-32.

VON TEICHMAN, B. F., DUNGU, B. & SMIT, T. K. (2010). In vivo cross-protection to African horse sickness Serotypes 5 and 9 after vaccination with Serotypes 8 and 6. *Vaccine,* 28, 6505-17.

VREEDE, F. & HUISMANS, H. (1998). Sequence analysis of the RNA polymerase gene of African horse sickness virus. *Archives of virology,* 143, 413-419.

WADE-EVANS, A., WOOLHOUSE, T., O'HARA, R. & HAMBLIN, C. (1993). The use of African horse sickness virus VP7 antigen, synthesised in bacteria, and anti-VP7 monoclonal antibodies in a competitive ELISA. *J Virol Methods,* 45, 179-188.

WAHID. (2016). *World Animal Health* [Online]. France: OIE. Available: http://www.oie.int/wahis_2/public/wahid.php/Countryinformation/Countryreports [Accessed 4 December 2016].

WANG, K., HOLTZ, K. M., ANDERSON, K., CHUBET, R., MAHMOUD, W. & COX, M. M. (2006). Expression and purification of an influenza hemagglutinin--one step closer to a recombinant protein-based influenza vaccine. *Vaccine,* 24, 2176-85.

WANG, Q., BOSCH, B. J., VLAK, J. M., VAN OERS, M. M., ROTTIER, P. J. & VAN LENT, J. W. (2016). Budded baculovirus particle structure revisited. *J Invertebr Pathol,* 134, 15-22.

WATERS, R. A., FOWLER, V. L., ARMSON, B., NELSON, N., GLOSTER, J., PATON, D. J. & KING, D. P. (2014). Preliminary validation of direct detection of foot-and-mouth disease virus within clinical samples using reverse transcription loop-mediated isothermal amplification coupled with a simple lateral flow device for detection. *PLoS One,* 9, e105630.

WEI, C. J., XU, L., KONG, W. P., SHI, W., CANIS, K., STEVENS, J., YANG, Z. Y., DELL, A., HASLAM, S. M., WILSON, I. A. & NABEL, G. J. (2008). Comparative efficacy of neutralizing antibodies elicited by recombinant hemagglutinin proteins from avian H5N1 influenza virus. *J Virol,* 82, 6200-8.

WESTERLUND-WIKSTROM, B., TANSKANEN, J., VIRKOLA, R., HACKER, J., LINDBERG, M., SKURNIK, M. & KORHONEN, T. K. (1997). Functional expression of adhesive peptides as fusions to Escherichia coli flagellin. *Protein Eng,* 10, 1319-26.

WEYER, C. T., GREWAR, J. D., BURGER, P., ROSSOUW, E., LOURENS, C., JOONE, C., LE GRANGE, M., COETZEE, P., VENTER, E., MARTIN, D. P., MACLACHLAN, N. J. & GUTHRIE, A. J. (2016). African Horse Sickness Caused by Genome Reassortment and Reversion to Virulence of Live, Attenuated Vaccine Viruses, South Africa, 2004-2014. *Emerg Infect Dis,* 22, 2087-2096.

WHITFORD, M., STEWART, S., KUZIO, J. & FAULKNER, P. (1989). Identification and sequence analysis of a gene encoding gp67, an abundant envelope glycoprotein of the baculovirus Autographa californica nuclear polyhedrosis virus. *J Virol,* 63, 1393-9.

WICKHAM, T. J., DAVIS, T., GRANADOS, R. R., SHULER, M. L. & WOOD, H. A. (1992). Screening of insect cell lines for the production of recombinant proteins and infectious virus in the baculovirus expression system. *Biotechnol Prog,* 8, 391-6.

WICKHAM, T. J. & NEMEROW, G. R. (1993). Optimization of growth methods and recombinant protein production in BTI-Tn-5B1-4 insect cells using the baculovirus expression system. *Biotechnol Prog,* 9, 25-30.

WILDE, M., KLAUSBERGER, M., PALMBERGER, D., ERNST, W. & GRABHERR, R. (2014). Tnao38, high five and Sf9--evaluation of host-virus interactions in three different insect cell lines: baculovirus production and recombinant protein expression. *Biotechnol Lett,* 36, 743-9.

WILLIAMS, C. F., INOUE, T., LUCUS, A.-M., PAOLO, M. D. A. & ROY, P. (1998). The complete sequence of four major structural proteins of African horse sickness virus serotype 6: evolutionary relationships within and between the orbiviruses. *Virus Res,* 53, 53-73.

WILLIAMS, G. V., ROHEL, D. Z., KUZIO, J. & FAULKNER, P. (1989). A cytopathological investigation of Autographa californica nuclear polyhedrosis virus p10 gene function using insertion/deletion mutants. *J Gen Virol,* 70 (Pt 1), 187-202.

WILSON, A., MELLOR, P. S., SZMARAGD, C. & MERTENS, P. P. (2009). Adaptive strategies of African horse sickness virus to facilitate vector transmission. *Vet Res,* 40**,** 16.

WILSON, M. E., MAINPRIZE, T. H., FRIESEN, P. D. & MILLER, L. K. (1987). Location, transcription, and sequence of a baculovirus gene encoding a small arginine-rich polypeptide. *J Virol,* 61**,** 661-6.

WONG, S. S. & WEBBY, R. J. (2013). Traditional and new influenza vaccines. *Clin Microbiol Rev,* 26**,** 476-92.

WONG, T. K., NIELSEN, L. K., GREENFIELD, P. F. & REID, S. (1994). Relationship between oxygen uptake rate and time of infection of Sf9 insect cells infected with a recombinant baculovirus. *Cytotechnology,* 15**,** 157-67.

XU, X. G., WANG, Z. S., ZHANG, Q., LI, Z. C., ZHAO, H. N., LI, W., TONG, D. W. & LIU, H. J. (2011). Baculovirus surface display of E envelope glycoprotein of Japanese encephalitis virus and its immunogenicity of the displayed proteins in mouse and swine models. *Vaccine,* 29**,** 636-43.

YOSHIDA, S., KONDOH, D., ARAI, E., MATSUOKA, H., SEKI, C., TANAKA, T., OKADA, M. & ISHII, A. (2003). Baculovirus virions displaying Plasmodium berghei circumsporozoite protein protect mice against malaria sporozoite infection. *Virology,* 316**,** 161-70.

ZIENTARA, S., SAILLEAU, C., MOULAY, S. & CRUCIERE, C. (1994). Diagnosis of the African horse sickness virus serotype 4 by a one-tube, one manipulation RT-PCR reaction from infected organs. *J Virol Methods,* 46**,** 179-88.

ZIENTARA, S., WEYER, C. T. & LECOLLINET, S. (2015). African horse sickness. *Rev Sci Tech,* 34**,** 315-27.

ZWART, L., POTGIETER, C. A., CLIFT, S. J. & VAN STADEN, V. (2015). Characterising Non-Structural Protein NS4 of African Horse Sickness Virus. *PLoS One,* 10**,** e0124281.

Appendix

Appendix 1: Raw data for Figure 3.11

Sample Name	Raw data OD (duplicates)		Mean OD	Standard Deviation (±1)	Standard Deviation (±3)
8AF8	1.9885	1.7259	1.8572	0.1857	0.5571
8DF1	1.8456	1.9219	1.88375	0.0540	0.1619
8EA7	1.5369	1.6691	1.603	0.0935	0.2804
8CG1	1.4324	1.6609	1.54665	0.1616	0.4847
8BG10	2.7881	2.8338	2.81095	0.0323	0.0969
8DH3	2.0497	2.1637	2.1067	0.0806	0.2418
10BE7	0.627	0.5662	0.5966	0.0430	0.1290
10BG7	0.7764	0.7199	0.74815	0.0400	0.1199
10BC12	1.535	1.5998	1.5674	0.0458	0.1375
10AH5	0.9533	0.9871	0.9702	0.0239	0.0717
6DF4	0.525	0.4067	0.46585	0.0837	0.2510
6DG2	0.701	0.693	0.697	0.0057	0.0170
6AFZ	0.8265	0.9788	0.90265	0.1077	0.3231
8BG9	0.9068	0.9716	0.9392	0.0458	0.1375
8BB1	2.1834	2.2236	2.2035	0.0284	0.0853
8BC2	3.3121	2.5912	2.95165	0.5098	1.5293
8BF2	1.0867	1.0624	1.07455	0.0172	0.0515
8CE4	2.7264	2.7797	2.75305	0.0377	0.1131
8EA6	3.1191	3.0796	3.09935	0.0279	0.0838
8DB11	2.2465	2.4192	2.33285	0.1221	0.3664
8CB11	2.8911	2.6595	2.7753	0.1638	0.4913
SMAA	1.9392	2.488	2.2136	0.3881	1.1642
8CH7	0.5223	0.5214	0.52185	0.0006	0.0019
8DA6	1.0098	1.1063	1.05805	0.0682	0.2047
Neg Control	0.0343	0.0342	0.03425	0.0001	0.0002

Appendix 2: Raw data for Figure 3.12

Sample	Raw data OD (+ serum)				Raw data OD (- serum)				Mean OD (+)	Mean OD (-)	Normalised mean OD	Standard deviation	Standard error
50ng	0.3739	0.4319	0.4899	0.4319	0.1269	0.2021	0.0944	0.1118	0.4319	0.1338	0.2981	0.0474	0.0237
100ng	0.2137	0.2309	0.2412	0.1996	0.1151	0.1143	0.1196	0.1114	0.2214	0.1151	0.1063	0.0184	0.0092
200ng	0.1174	0.1164	0.1931	0.1612	0.1158	0.1125	0.0748	0.0939	0.1470	0.0993	0.0478	0.0371	0.0186
400ng	0.1448	0.1382	0.1483	0.1518	0.1507	0.1080	0.1350	0.0887	0.1458	0.1206	0.0252	0.0058	0.0029
Serum Only	0.7753	0.7578	0.5190	0.6469	0.1845	0.1329	0.1272	0.1428	0.6748	0.1469	0.5279	0.1184	0.0592

Appendix 3: Raw data for Figure 4.9

Sf9	Raw Data (12 replicates)												Mean	Normalised (-Mock)	Standard deviation	Standard error
AcSurf_EGFP	30550	30399	30560	30341	31259	31335	31026	31243	31464	31534	31129	31230	31006	2216	426	123
AcSurf_EGFP^{TRUN}	36452	33268	32788	32606	33350	32945	34465	32892	33543	34444	34778	39796	34277	5487	2059	594
AcVP2$^{HIS/N}$	25032	27048	27308	27392	27324	27110	27337	27252	27281	27014	27294	25340	26894	-1896	809	234
Mock	26698	29107	29046	29103	29103	29067	29406	29376	29276	29320	29229	26751	28790			
TnHi5																
AcSurf_EGFP	16853	17511	17510	18132	18253	18064	18561	18467	18254	18624	18503	17964	18058	6049	529	153
AcSurf_EGFP^{TRUN}	24005	18548	19059	19759	18520	21302	19851	20024	19623	20259	19530	25267	20479	8470	2098	606
AcVP2$^{HIS/N}$	12857	14065	14513	13100	14270	13974	14417	14183	14603	14693	14336	13329	14028	2020	608	175
Mock	11887	11952	12083	12088	11681	11948	12134	11947	12066	12228	12302	11789	12009			

Appendix 4: Raw data for Figure 4.12

	AcSurf_VP2-H^{TRUN}	AcSurf_VP2-H	AcVP2$^{HIS/N}$	AcVP2-H$^{HIS/N}$
	2.103	1.102	2.229	2.354
	1.632	0.789	1.92	1.782
	1.132	1.479	1.669	1.632
	1.761	1.025	2.267	1.739
	1.979	1.233	2.065	1.57
	1.968	1.055	1.963	2.36
	2.034	1.478	1.87	2.232
	2.002	0.519	1.694	3.145
	2.261	1.218	1.847	1.397
	1.69	1.211	2.189	1.92
	1.508	1.296	2.756	2.106
	1.871	1.247	1.632	1.579
	1.77	1.335	2.44	2.281
	1.335	1.277	2.171	2.224
Raw data Plaque sizes	1.968	1.025	2.447	2.296
(32 plaques/virus)	2.11	1.063	2.083	2.482
	1.75	1.168	1.806	2.224
	1.673	0.882	2.19	2.359
	2.913	1.435	1.983	1.467
	1.944	1.069	1.776	2.293
	1.915	1.626	1.757	2.155
	1.979	1.168	1.467	2.086
	2.46	1.045	2.148	1.911
	2.468	1.277	1.986	2.293
	1.88	1.039	1.648	1.489
	2.083	1.195	2.132	2.034
	1.742	1.322	2.04	1.752
	2.341	0.9	2.09	1.679
	2.313	1.277	1.774	1.801
	2.399	0.989	1.729	1.529
	1.974	1.039	2.09	2.162
	2.406	1.174	2.171	2.156
Mean	1.980	1.155	2.000	2.015
Standard deviation	0.357	0.217	0.276	0.380
Standard error	0.063	0.038	0.049	0.067

Appendix 5: Raw data for Table 6.1

	Raw data (OD)																							
	8AF8	8DF1	8EA7	8CG1	8BG10	8DH3	10BE7	10BG7	10BC12	10AH5	6DF4	6DG2	6AFZ	8BG9	8BB1	8BC2	8BF2	8CE4	8EA6	8DB11	8CB11	SMAA	8CH7	8DA6
A surf	0.928	0.566	0.829	0.704	2.275	0.944	0.837	1.167	2.724	0.417	0.223	0.103	0.502	0.384	0.684	0.840	0.164	1.947	2.569	1.092	2.145	2.446	0.254	0.945
	1.024	0.529	0.861	0.703	2.357	0.965	0.816	0.979	2.608	0.475	0.218	0.095	0.538	0.337	0.674	0.832	0.125	1.981	2.373	0.987	1.954	2.235	0.232	0.905
B surf	0.917	0.526	0.739	0.738	2.288	0.995	0.856	1.001	2.778	0.396	0.220	0.090	0.449	0.281	0.589	0.763	0.108	1.440	2.385	0.914	1.586	2.007	0.207	0.784
	0.982	0.509	0.778	0.714	2.293	1.078	0.833	1.015	2.626	0.411	0.212	0.092	0.448	0.277	0.554	0.731	0.103	1.711	2.059	0.934	1.850	2.083	0.229	0.705
C surf	0.972	0.688	0.871	0.816	2.356	1.354	0.974	1.168	2.751	0.455	0.217	0.093	0.471	0.568	1.589	1.629	0.794	2.206	2.896	1.816	2.216	2.096	0.250	0.858
	1.053	0.542	0.767	0.739	1.943	1.155	0.846	0.954	2.479	0.405	0.198	0.077	0.383	0.485	1.540	1.506	0.727	1.923	2.605	1.503	2.293	1.923	0.218	0.787
D surf	0.974	0.505	0.795	0.667	2.171	1.161	0.820	0.974	2.651	0.391	0.200	0.104	0.365	0.323	1.062	1.426	0.419	1.776	2.161	1.039	1.803	1.785	0.171	0.643
	1.112	0.664	0.764	0.715	2.168	1.150	0.845	1.001	2.622	0.407	0.231	0.148	0.419	0.429	1.078	1.210	0.572	1.929	2.270	1.046	1.963	1.767	0.189	0.641
E surf	1.193	0.654	0.898	0.841	2.651	1.401	1.133	1.168	3.226	0.451	0.222	0.104	0.369	0.568	1.440	2.050	0.914	2.548	2.931	1.499	2.154	2.168	0.203	0.770
	1.178	0.739	0.833	0.842	2.499	1.343	1.075	1.087	2.697	0.481	0.217	0.116	0.341	0.523	1.417	1.693	0.737	2.502	2.935	1.681	2.061	1.963	0.186	0.724
F surf	1.130	0.659	0.829	0.850	2.469	1.267	1.187	1.028	2.777	0.424	0.234	0.095	0.395	0.503	1.686	2.160	0.804	2.213	2.827	1.735	2.127	1.967	0.201	0.687
	1.397	0.675	0.925	0.854	2.562	1.081	1.218	0.930	2.930	0.457	0.225	0.102	0.356	0.426	1.635	1.329	0.653	2.435	2.622	1.485	1.993	1.949	0.191	0.709
I surf	1.032	0.665	0.854	0.749	2.618	1.239	0.987	0.903	2.602	0.433	0.191	0.080	0.408	0.514	1.760	2.692	1.108	2.935	2.915	1.799	2.242	1.806	0.182	0.688
	1.037	0.615	0.741	0.737	2.298	1.041	0.876	0.762	2.156	0.393	0.182	0.093	0.365	0.477	1.633	1.763	0.785	2.937	2.860	1.532	2.028	1.781	0.157	0.640
J surf	1.052	0.668	0.939	0.749	2.324	1.100	1.023	0.826	2.539	0.408	0.190	0.085	0.377	0.506	1.228	1.852	0.685	2.469	2.542	1.359	2.081	1.629	0.155	0.676
	1.094	0.651	0.897	0.723	2.259	1.125	0.967	0.805	2.223	0.373	0.200	0.146	0.381	0.447	1.144	1.448	0.759	2.639	2.763	1.418	1.837	1.644	0.185	0.677
G surf	1.173	0.552	0.868	0.826	2.489	0.960	0.864	1.423	3.111	0.445	0.244	0.098	0.442	0.304	0.606	0.753	0.169	1.500	2.165	0.794	1.815	2.096	0.196	0.770
	1.061	0.535	0.859	0.778	2.614	1.078	0.975	1.274	2.964	0.400	0.229	0.101	0.423	0.276	0.675	0.835	0.146	1.587	2.417	0.686	1.678	2.107	0.212	0.769
H surf	1.169	0.799	1.051	0.914	2.956	1.828	1.228	1.257	3.361	0.527	0.315	0.125	0.520	0.786	1.914	2.634	1.101	3.009	3.361	2.205	2.479	2.131	0.250	1.028
	1.199	0.754	1.100	0.980	2.854	1.533	1.152	1.282	3.349	0.518	0.278	0.130	0.519	0.692	2.109	2.331	1.287	3.048	3.224	2.037	2.420	1.779	0.263	1.020
Z surf	1.003	0.708	1.142	0.842	2.511	1.207	1.255	1.260	3.361	0.495	0.273	0.146	0.549	0.330	0.568	0.828	0.136	1.577	2.665	0.895	2.062	1.838	0.262	0.854
	1.278	0.599	0.914	0.816	2.469	1.072	1.176	1.218	3.367	0.544	0.278	0.137	0.481	0.350	0.549	0.641	0.121	1.388	2.268	0.828	1.865	1.833	0.214	0.838
VP2 lysate	1.018	1.131	1.172	1.234	2.268	0.874	1.149	1.331	3.323	0.574	0.343	0.163	0.806	0.339	0.739	0.632	0.145	2.018	1.998	0.730	1.766	2.060	0.179	0.765
	1.286	1.135	1.245	1.383	2.170	0.899	1.111	1.240	3.168	0.573	0.364	0.169	0.945	0.368	0.569	0.763	0.166	2.046	2.023	0.765	1.787	2.030	0.196	0.771
Purified VP2	2.680	2.373	2.063	1.693	2.166	1.374	1.085	1.579	2.654	0.900	0.698	1.232	2.137	1.028	2.014	1.883	0.685	2.425	2.906	1.829	2.581	1.935	0.124	0.603
	2.587	2.291	2.009	1.720	2.061	1.217	0.944	1.208	2.480	0.803	0.540	1.191	2.311	1.214	1.806	1.853	0.743	2.303	2.760	1.686	2.531	1.810	0.158	0.566
Null virus	1.148	0.836	1.155	0.886	2.825	0.957	1.219	1.620	2.691	0.513	0.280	0.115	0.696	0.405	0.860	0.835	0.135	2.415	2.170	0.912	1.879	1.971	0.215	0.870
	1.228	0.799	1.368	0.847	2.922	1.015	1.210	1.538	2.964	0.468	0.302	0.097	0.562	0.375	0.660	0.759	0.127	2.342	2.287	0.841	1.920	2.084	0.215	0.811

Appendix 5: Raw data for Table 6.1 continued

Mean OD																								
A surf	0.976	0.547	0.845	0.704	2.316	0.955	0.826	1.073	2.666	0.446	0.221	0.099	0.520	0.360	0.679	0.836	0.145	1.964	2.471	1.039	2.049	2.340	0.243	0.925
B surf	0.949	0.517	0.758	0.726	2.291	1.037	0.845	1.008	2.702	0.403	0.216	0.091	0.448	0.279	0.571	0.747	0.105	1.575	2.222	0.924	1.718	2.045	0.218	0.745
C surf	1.013	0.615	0.819	0.778	2.150	1.254	0.910	1.061	2.615	0.430	0.208	0.085	0.427	0.527	1.564	1.568	0.760	2.064	2.751	1.659	2.255	2.009	0.234	0.823
D surf	1.043	0.584	0.780	0.691	2.169	1.156	0.832	0.987	2.636	0.399	0.215	0.126	0.392	0.376	1.070	1.318	0.495	1.853	2.216	1.042	1.883	1.776	0.180	0.642
E surf	1.186	0.697	0.865	0.842	2.575	1.372	1.104	1.127	2.962	0.466	0.219	0.110	0.355	0.546	1.428	1.871	0.826	2.525	2.933	1.590	2.107	2.065	0.194	0.747
F surf	1.263	0.667	0.877	0.852	2.516	1.174	1.202	0.979	2.854	0.440	0.230	0.098	0.375	0.464	1.661	1.744	0.729	2.324	2.725	1.610	2.060	1.958	0.196	0.698
I surf	1.034	0.640	0.798	0.743	2.458	1.140	0.932	0.832	2.379	0.413	0.186	0.087	0.387	0.496	1.696	2.228	0.946	2.936	2.888	1.666	2.135	1.793	0.170	0.664
J surf	1.073	0.659	0.918	0.736	2.292	1.112	0.995	0.816	2.381	0.391	0.195	0.116	0.379	0.477	1.186	1.650	0.722	2.554	2.652	1.388	1.959	1.637	0.170	0.676
G surf	1.117	0.544	0.863	0.802	2.552	1.019	0.919	1.349	3.037	0.423	0.236	0.099	0.433	0.290	0.641	0.794	0.157	1.544	2.291	0.740	1.747	2.101	0.204	0.770
H surf	1.184	0.776	1.075	0.947	2.905	1.680	1.190	1.270	3.355	0.523	0.297	0.128	0.519	0.739	2.012	2.483	1.194	3.028	3.292	2.121	2.449	1.955	0.256	1.024
Z surf	1.141	0.654	1.028	0.829	2.490	1.139	1.216	1.239	3.364	0.520	0.276	0.141	0.515	0.340	0.559	0.735	0.129	1.483	2.467	0.862	1.964	1.835	0.238	0.846
VP2 lysate	1.152	1.133	1.209	1.309	2.219	0.887	1.130	1.285	3.245	0.573	0.353	0.166	0.875	0.354	0.654	0.697	0.155	2.032	2.011	0.747	1.776	2.045	0.187	0.768
Purified VP2	2.633	2.332	2.036	1.707	2.114	1.295	1.014	1.394	2.567	0.852	0.619	1.211	2.224	1.121	1.910	1.868	0.714	2.364	2.833	1.758	2.556	1.873	0.141	0.585
Null virus	1.188	0.818	1.261	0.866	2.873	0.986	1.215	1.579	2.827	0.490	0.291	0.106	0.629	0.390	0.760	0.797	0.131	2.378	2.228	0.876	1.899	2.028	0.215	0.840
Normalized OD (-null virus OD)																								
A surf	-0.212	-0.270	-0.417	-0.163	-0.557	-0.032	-0.388	-0.506	-0.161	-0.045	-0.070	-0.007	-0.109	-0.030	-0.081	0.039	0.013	-0.414	0.243	0.163	0.150	0.313	0.029	0.084
B surf	-0.239	-0.300	-0.503	-0.140	-0.583	0.051	-0.370	-0.571	-0.126	-0.087	-0.075	-0.015	-0.181	-0.111	-0.188	-0.050	-0.026	-0.803	-0.006	0.047	-0.181	0.018	0.003	-0.095
C surf	-0.175	-0.203	-0.442	-0.089	-0.723	0.268	-0.304	-0.518	-0.213	-0.060	-0.083	-0.021	-0.202	0.137	0.805	0.771	0.629	-0.314	0.523	0.783	0.355	-0.018	0.019	-0.018
D surf	-0.145	-0.233	-0.482	-0.175	-0.704	0.170	-0.382	-0.592	-0.191	-0.092	-0.076	0.020	-0.237	-0.014	0.310	0.521	0.364	-0.526	-0.012	0.166	-0.017	-0.252	-0.035	-0.198
E surf	-0.002	-0.121	-0.396	-0.025	-0.298	0.386	-0.111	-0.452	0.134	-0.025	-0.072	0.004	-0.274	0.156	0.669	1.075	0.695	0.147	0.705	0.714	0.208	0.038	-0.020	-0.093
F surf	0.075	-0.150	-0.384	-0.014	-0.357	0.188	-0.012	-0.600	0.027	-0.050	-0.061	-0.007	-0.254	0.074	0.901	0.948	0.597	-0.054	0.497	0.734	0.161	-0.069	-0.018	-0.142
I surf	-0.154	-0.178	-0.464	-0.124	-0.416	0.154	-0.283	-0.747	-0.448	-0.077	-0.105	-0.019	-0.243	0.106	0.937	1.431	0.815	0.558	0.659	0.789	0.236	-0.234	-0.045	-0.176
J surf	-0.115	-0.158	-0.343	-0.130	-0.582	0.126	-0.219	-0.763	-0.446	-0.100	-0.096	0.010	-0.250	0.087	0.426	0.853	0.591	0.175	0.424	0.512	0.060	-0.391	-0.045	-0.164
G surf	-0.071	-0.274	-0.398	-0.064	-0.322	0.033	-0.295	-0.230	0.210	-0.068	-0.055	-0.007	-0.197	-0.100	-0.119	-0.003	0.026	-0.835	0.063	-0.136	-0.153	0.074	-0.011	-0.071
H surf	-0.004	-0.041	-0.186	0.081	0.032	0.694	-0.025	-0.310	0.528	0.032	0.006	0.022	-0.110	0.349	1.252	1.686	1.063	0.650	1.064	1.245	0.550	-0.072	0.042	0.183
Z surf	-0.048	-0.164	-0.234	-0.037	-0.383	0.153	0.001	-0.340	0.537	0.029	-0.015	0.035	-0.114	-0.050	-0.201	-0.062	-0.002	-0.896	0.238	-0.015	0.064	-0.192	0.023	0.006
VP2 lysate	-0.036	0.316	-0.053	0.442	-0.654	-0.099	-0.085	-0.294	0.418	0.083	0.062	0.060	0.246	-0.036	-0.106	-0.099	0.024	-0.346	-0.218	-0.129	-0.123	0.018	-0.028	-0.073

Appendix 6: Raw data for Figure 6.3

Sample	Raw data (D42)		Raw data (D0)		Mean OD (D42)	Mean OD (D0)	Normalized	Standard deviation	Standard Error
A	0.5066	0.6252	0.8369	0.7246	0.5659	0.7808	-0.2149	0.0839	0.0593
B	0.5231	0.6550	0.7928	0.5524	0.5891	0.6726	-0.0835	0.0933	0.0659
C	0.7294	0.6491	0.6577	0.7295	0.6893	0.6936	-0.0043	0.0568	0.0402
D	0.7213	0.6331	0.7524	0.7188	0.6772	0.7356	-0.0584	0.0624	0.0441
E	0.8777	0.8263	0.6783	0.8640	0.8520	0.7712	0.0809	0.0363	0.0257
F	0.9187	0.8160	0.6361	0.8243	0.8674	0.7302	0.1372	0.0726	0.0514
G	0.7332	0.6164	0.7360	0.7504	0.6748	0.7432	-0.0684	0.0826	0.0584
H	1.0023	1.0356	1.2307	1.1093	1.0190	1.1700	-0.1511	0.0235	0.0167
I	1.0074	0.9118	0.6540	0.7692	0.9596	0.7116	0.2480	0.0676	0.0478
J	1.0154	0.8842	0.9116	0.9532	0.9498	0.9324	0.0174	0.0928	0.0656
Z	0.8418	0.6471	0.8378	0.7879	0.7445	0.8129	-0.0684	0.1377	0.0973
VP2 lysate	0.9101	0.8240	0.8677	0.8825	0.8671	0.8751	-0.0081	0.0609	0.0431
Null BV lysate	0.7847	0.7585	0.8250	0.9457	0.7716	0.8854	-0.1138	0.0185	0.0131
Purified VP2	0.8614	0.9573	0.1268	0.1332	0.9094	0.1300	0.7794	0.0678	0.0480

Appendix 7: Raw data for Figure 6.10A

Day 21 post vaccination raw data	Mice				
	1	2	3	4	5
Group 1	0.322	0.488	0.685	0.506	0.438
Group 2	0.930	0.768	0.658	0.874	0.900
Group 3	0.193	0.296	0.287	0.276	0.237
Group 4	0.353	0.370	0.502	0.366	0.462
Group 5	0.102	0.116	0.16	0.185	0.139
Group 6	0.316	0.335	0.306	0.291	0.309
blank	0.101	0.122	0.051	0.082	0.0549
C + sera	0.888	0.987	1.114	1.05	

Day 21	OD from each mice after normalization (- mean OD of Blank)							
	1	2	3	4	5	Mean OD of all mice	Standard deviation	Standard error
Group 1	0.2398	0.4058	0.6028	0.4238	0.3558	0.4056	0.1315	0.0588
Group 2	0.8478	0.6858	0.5758	0.7918	0.8178	0.7438	0.1120	0.0501
Group 3	0.1108	0.2138	0.2048	0.1938	0.1548	0.1756	0.0426	0.0191
Group 4	0.2708	0.2878	0.4198	0.2838	0.3798	0.3284	0.0670	0.0300
Group 5	0.0198	0.0338	0.0778	0.1028	0.0568	0.0582	0.0333	0.0149
Group 6	0.2338	0.2528	0.2238	0.2088	0.2268	0.2292	0.0160	0.0072
ELISA +'ve cont	0.8880	0.9870	1.1140	1.0500		1.0098	0.0963	0.0431
Blank	0.1010	0.1220	0.0510	0.0820	0.0549			
Mean Blank	0.0822							

Appendix 7: Raw data for Figure 6.10B

Day 35 post vaccination raw data	Mice				
	1	2	3	4	5
Group 1	1.47	1.86	1.27	1.35	1.56
Group 2	1.32	1.36	1.58	1.26	1.28
Group 3	0.34	0.29	0.35	0.42	0.57
Group 4	0.56	0.58	0.77	0.54	0.43
Group 5	0.38	0.37	0.38	0.30	0.31
Group 6	0.40	0.43	0.40	0.38	0.42

Day 35	OD from each mice after normalization (-mean OD of Blank)							
	1	2	3	4	5	Mean OD off all mice	Standard deviation	Standard error
Group 1	1.3908	1.7738	1.1888	1.2648	1.4788	1.4194	0.2275	0.1017
Group 2	1.2398	1.2758	1.4978	1.1798	1.1938	1.2774	0.1289	0.0577
Group 3	0.2598	0.2048	0.2668	0.3358	0.4838	0.3102	0.1076	0.0481
Group 4	0.4758	0.4998	0.6838	0.4608	0.3458	0.4932	0.1219	0.0545
Group 5	0.2938	0.2908	0.2998	0.2138	0.2228	0.2642	0.0421	0.0188
Group 6	0.3148	0.3458	0.3198	0.3018	0.3338	0.3232	0.0171	0.0076